

Validating the accuracy and repeatability of transition analysis for age estimation in

South Africa

By

Nicolene Jooste

Submitted in fulfilment of the requirements for the degree of

MASTER OF SCIENCE

In the

FACULTY OF HEALTH SCIENCES

Department of Anatomy

University of Pretoria

2014

The financial assistance of the National Research Foundation (NRF) towards this research is hereby acknowledged. Opinions expressed and conclusions arrived at, are those of the author and are not necessarily to be attributed to the NRF.

Declaration

I, Nicolene Jooste, hereby declare that this research dissertation is my own work. It is being submitted for the degree of Master of Science in Anatomy at the University of Pretoria. It has not been submitted before for any degree or examination at this or any other University.

Signed:

Ethics



UNIVERSITEIT VAN PRETORIA
UNIVERSITY OF PRETORIA
YUNIBESITHI YA PRETORIA

Faculty of Health Sciences Research Ethics Committee

3/10/2012

Number : S179/2012

Title : Validating the accuracy and repeatability of transition analysis for age estimation in South Africa

Investigator : Nicolene Jooste, Department of Anatomy, University of Pretoria
(SUPERVISOR: Prof. M. Steyn)

Sponsor : National Research Foundation (NRF) bursary

Study Degree: MSc.

This Student Protocol was reviewed by the Faculty of Health Sciences, Student Research Ethics Committee, University of Pretoria on 2/10/2012 and found to be acceptable. The approval is valid for a period of 3 years.

Prof M J Bester BSc (Chemistry and Biochemistry); BSc (Hons)(Biochemistry); MSc (Biochemistry); PhD (Medical Biochemistry)

Prof R Delpont (female)BA et Scien, B Curationis (Hons) (Intensive care Nursing), M Sc (Physiology), PhD (Medicine), M Ed Computer Assisted Education

Dr NK Likibi MBB HM – (Representing Gauteng Department of Health) MPH

Dr MP Mathebula Deputy CEO: Steve Biko Academic Hospital

Prof A Nienaber (Female) BA (Hons) (Wits); LLB (Pretoria); LLM (Pretoria); LLD (Pretoria); PhD; Diploma in Datametrics (UNISA)

Prof L M Ntthe MBChB(Natal); FCS(SA)

Mrs M C Nzeku (Female) BSc(NUL); MSc Biochem(UCL,UK)

Snr Sr J. Phatoli (Female) BCur (Et.AI); BTech Oncology

Dr R Reynders MBChB (Pret), FCPaed (CMSA) MRCPCH (Lon) Cert Med. Onc (CMSA)

Dr T Rossouw (Female) MBChB.(cum laude); M.Phil (Applied Ethics) (cum laude), MPH (Biostatistics and Epidemiology (cum laude), D.Phil

Mr Y Sikweyiya MPH (Umea University Umea, Sweden); Master Level Fellowship (Research Ethics) (Pretoria and UKZN); Post Grad. Diploma in Health Promotion (Unitra); BSc in Health Promotion (Unitra)

Dr L Schoeman (Female) BPharm (NWU); BAHons (Psychology)(UP); PhD (UKZN); International Diploma in Research Ethics (UCT)

Dr R Sommers **Vice-Chair** (Female) - MBChB; MMed (Int); MPharMed.

Prof T J P Swart BChD, MSc (Odont), MChD (Oral Path), PGCHE

Prof C W van Staden **Chairperson** - MBChB; MMed (Psych); MD; FCPsych; FTCL; UPLM; Dept of Psychiatry

Student Ethics Sub-Committee

Prof R S K Apatu MBChB (Legon,UG); PhD (Cantab); PGDip International Research Ethics (UCT)

Mrs N Briers (female) BSc (Stell); BSc Hons (Pretoria); MSc (Pretoria); DHETP (Pretoria)

Prof M M Ehlers (female) BSc (Agric) Microbiology (Pret); BSc (Agric) Hons Microbiology (Pret); MSc (Agric) Microbiology (Pret); PhD Microbiology (Pret); Post Doctoral Fellow (Pret)

Dr R Leech (female) B.Art et Scien; BA Cur; BA (Hons); M (ECI); PhD Nursing Science

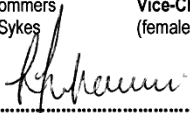
Mr S B Masombuka BA (Communication Science) UNISA; Certificate in Health Research Ethics Course (B compliant cc)

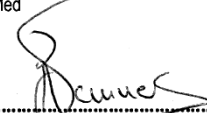
Dr S A S Olorunju BSc (Hons). Stats (Ahmadu Bello University –Nigeria); MSc (Applied Statistics (UKC United Kingdom); PhD (Ahmadu Bello University – Nigeria)

Dr L Schoeman CHAIRPERSON: (female) BPharm (North West); BAHons (Psychology)(Pretoria); PhD (KwaZulu-Natal); International Diploma in Research Ethics (UCT)

Dr R Sommers **Vice-Chair** (Female) MBChB; M.Med (Int); MPhar.Med

Prof L Sykes (female) BSc, BDS, MDent (Pros)


.....
DR L SCHOEMAN; BPharm, BA Hons (Psy), PhD;
Dip. International Research Ethics
CHAIRPERSON of the Faculty of Health Sciences
Student Research Ethics Committee, University of Pretoria


.....
DR R SOMMERS; MBChB; M.Med (Int); MPhar.Med.
VICE-CHAIR of the Faculty of Health Sciences Research
Ethics Committee, University of Pretoria

☎ 012 354 1677 ☎ 0866516047 ✉ deepeka.behari@up.ac.za 🌐 <http://www.healthethics-up.co.za>
✉ Private Bag X323, Arcadia, 0007 - 31 Bophelo Road, HW Snyman South Building, Level 2, Room 2.33, Gezina, Pretoria

Abstract

Transition analysis transforms skeletal traits with an invariant, unidirectional series of stages into a likelihood function with a maximum likelihood value and a 95% confidence interval. Boldsen *et al.* used transition analysis to develop an adult age estimation method employing components of the cranial sutures, pubic symphysis and ilial portion of the sacroiliac joint, used either in combination or individually. This validation study aimed to use the 36 transition analysis numerical, categorical scores for the anatomical features in conjunction with the ADBOU computer program to assess the accuracy and precision of the age estimates for 149 black individuals from the Pretoria Bone Collection. In addition, the effect of observer variability in scoring of these traits was assessed. Six age estimations were generated by the ADBOU computer program using 1) the cranial sutures only, 2) the pubic symphysis only, 3) the auricular surface of the ilium only, 4) all three features combined, 5) all three features combined and modified by a forensic prior distribution and 6) all three features combined and modified by an archaeological prior distribution. The six point estimate categories, calculated from the maximum likelihood values, were evaluated for accuracy using mean absolute values. The 95% confidence intervals were evaluated for range width and accuracy. Cohen's Kappa statistics were used to analyse repeatability of the scoring procedure through inter- and intra-observer agreement and Kruskal-Wallis ANOVA statistics to determine the effect of observer differences on the final age estimates. The usefulness of the age ranges were diminished by large widths encompassing up to 95 years. The accuracy for the point estimates fared better for the combined skeletal indicators and overall accuracy was improved by using the archaeological prior distribution. The archaeological prior distribution was also responsible for narrowing the age ranges, especially in the older ages (over 70 years). Age estimates did not differ significantly when using inter- and intra-observer scores, but experience with the method did seem to improve results. Overall, age ranges were too wide, but accuracy could potentially be improved by adding more skeletal components to the method and using a population-specific prior distribution. The method would need considerable adjustments to make it usable in a South African setting.

Abstrak

Oorgangsanalise verander skeletale eienskappe met 'n onafhanklike, eenrigting reeks fases in 'n waarskynlikheidsfunksie met 'n maksimum waarskynlikheid waarde en 'n 95% vertrouensinterval. Boldsen *et al.* het oorgang analise gebruik om 'n volwasse ouderdom beraming metode te ontwikkel deur komponente van die skedelnate, pubiese simfise en iliale gedeelte van die sakro-iliale gewrig óf gesamentlik óf individueel te gebruik. Hierdie valideringsstudie was daarop gemik om die 36 oorgangsanalise numeriese, kategorieëse tellings vir die anatomiese kenmerke in samewerking met die ADBOU rekenaarprogram te gebruik om die akkuraatheid en noukeurigheid van die ouderdomsberamings vir 149 swart individue van die Pretoria Been Versameling te evalueer. Die effek van waarnemer variasie in die tellings van hierdie eienskappe is ook ondersoek. Ses ouderdomsberamings is deur die ADBOU rekenaarprogram gegenereer deur die volgende te gebruik, 1) slegs die skedel nate, 2) slegs die pubiese simfise, 3) slegs die oovormige artikulasie vlak op die ilium, 4) al drie eienskappe gekombineer, 5) al drie eienskappe gekombineer en aangepas deur 'n forensiese a priori-verdeling en 6) al drie eienskappe gekombineer en aangepas deur 'n argeologiese a priori-verdeling. Vir die ses kategorieë van ouderdom puntberamings, bereken vanaf die maksimum waarskynlikheid waardes, was die akkuraatheid deur die gemiddelde absolute fout waardes geëvalueer. Die 95% vertroude ouderdomsinterval was vir die reeks breedte en akkuraatheid geëvalueer. Cohen se Kappa statistiek is gebruik om herhaalbaarheid van die telling proses te ontleed deur middel van inter-en intra-waarnemer ooreenkoms en Kruskal-Wallis ANOVA statistiek om die effek van waarnemer verskille op die finale ouderdom beramings te bepaal. Die nut van die reeks is verminder deur groot reikwydtes van tot 95 jaar. Die akkuraatheid van die punt skattings het beter gevaar vir die gekombineerde skeletale aanwysers en algehele akkuraatheid het verbeter deur gebruik te maak van die argeologiese a priori-verdeling. Die argeologiese a priori-verdeling was ook verantwoordelik vir die vernouing van die ouderdomsreeks, veral in die ouer ouderdomme (meer as 70 jaar). Ouderdomsberamings het nie aansienlik verskil met die gebruik van inter-of intra-waarnemer tellings nie, maar dit blyk of ervaring met die metode die resultate verbeter. Algeheel was die reikwydtes veels te groot en akkuraatheid kan potensieel verbeter word deur die toevoeging van meer skeletale komponente en die gebruik van 'n bevolkingsspesifieke a priori-verdeling. Die metode sal aansienlike moet aangepas word om dit bruikbaar te maak in 'n Suid-Afrikaanse omgewing.

Acknowledgements

The inspiration for this project are the original developers of the transition analysis age estimation method, Jesper L. Boldsen, George R. Milner, Lyle W. Konigsberg and James W. Wood, without whom this project would not have existed.

Secondly, Professor Maryna Steyn without whose guidance and reassurances this project would not have grown to completion.

All the staff at the University of Pretoria, who assisted with the project, including Ms Sophie Silinda and Ms Mamphuthi Mogola who provided me with articles from the Medical and BMS Libraries, Ms Stephany van der Walt who packed out endless rows of crania and os coxae and especially Professor Ericka L'abbé who scored the skeletal material that made the interobserver agreement portion of this dissertation possible.

Also Ms Samantha Pretorius, the math guru, who always knew exactly which statistics would be the most meaningful and created graphic representations of the results that guaranteed visual impact. I am truly grateful for your willingness to rehash explanations and confirm my understanding of the concepts.

I am grateful to my colleagues, in the Department of Anatomy and Physiology at the University of Johannesburg, who always had a supportive attitude and an encouraging word and never hesitated to lend an ear. A special thank you to my boss Mrs Elaine Swanepoel and my sounding board Mr Ryan Inkley.

Lastly and most emphatically, thank you to all my friends and family who mostly listened to me gripe and spew gobbledeygook. A special thank you to De Waal, who was always willing to listen and spent many late nights fixing Microsoft Word documents that went haywire. Most importantly, thank you to my Granny who is my inspiration and first sparked my interest in osteology pertaining to forensic medicine with many a shared murder mystery.

Table of Contents

Declaration	i
Ethics	ii
Abstract	iii
Abstrak	iv
Acknowledgements	v
List of Tables	viii
List of Figures.....	x
Chapter 1: Introduction	1
1.1. Introduction and problem statement	1
1.2. Aim	5
Chapter 2: Literature Review	6
2.1. Introduction.....	6
2.2. Age-at-death estimation in adult skeletal remains	7
2.2.1. Cranial sutures.....	8
2.2.2. Pubic symphysis	12
2.2.3. Auricular surface	17
2.3. Statistical considerations	20
2.3.1. The old age dilemma	21
2.3.2. Combination of skeletal indicators	21
2.3.3. Ability to repeat and compare methods.....	22
2.3.4. Impact of natural variation on age estimation	24
2.3.5. Reference sample mimicry	25
2.4. Transition analysis.....	26
2.4.1. Anatomical features	27
2.4.2. Statistical approach.....	28
2.4.3. Prior distributions	29
2.4.4. Success of transition analysis.....	30
Chapter 3: Materials and Methods	59
3.1. Materials.....	59
3.2. Methods.....	60
3.3. Statistical analysis	62
Chapter 4: Results.....	66

4.1. Introduction.....	66
4.2. Age estimations.....	67
4.2.1. Accuracy and precision of the age ranges.....	68
4.2.2. Accuracy of the point value.....	71
4.3. Observer agreement.....	73
4.3.1. Inter- and intra-repeatability of scores.....	74
4.3.2. Effect of score repeatability on age estimates.....	78
Chapter 5: Discussion.....	147
5.1. Introduction.....	147
5.2. The scoring procedure.....	147
5.3. Age estimations.....	148
5.3.1. Accuracy and precision of the age ranges.....	148
5.3.2. Accuracy and precision of the point estimate.....	151
5.4. Observer agreement.....	154
5.4.1. Inter- and intra-repeatability of scores.....	154
5.4.2. Effect of score repeatability on age estimates.....	156
5.5. The success of transition analysis in a South African population.....	158
5.6. Future research in transition analysis.....	159
Chapter 6: Conclusion.....	162
References.....	163
Appendix A.....	171
Appendix B.....	195

List of Tables

Table 2.1: Age categories with corresponding biological age indicators ⁴²	33
Table 2.2: Four category cranial suture scores ^{1,48,62}	33
Table 2.3: Five category cranial suture scores ^{10,26,61}	34
Table 2.4: Todd & Lyon's ²⁶ timing for endocranial suture closure in white males ...	35
Table 2.5: Sutures rejected by Meindl & Lovejoy ⁴⁸ due to restricted value	35
Table 2.6: Acsádi and Nemeskéri age estimation from suture closure ²⁷	35
Table 2.7: Todd's pubic symphyseal phases for white males ^{1,25,62}	36
Table 2.8: Todd's pubic symphyseal metamorphosis for age estimation of females ²³	37
Table 2.9: Acsádi-Nemeskéri pubic symphysis age estimation method ^{27,37}	38
Table 2.10: McKern and Stewart's component stages ¹⁰	39
Table 2.11: Gilbert & McKern's component stages ²³	40
Table 2.12: Suchey and Brook's ³⁷ phases for estimating age at death from the pubic symphysis, developed from the Todd method	41
Table 2.13: Meindl <i>et al.</i> 's ³¹ condensed Todd method for pubic symphyseal age estimation	42
Table 2.14: Description of auricular surface features ⁴⁴	42
Table 2.15: Phase description for auricular surface method of age estimation ⁴⁴	43
Table 2.16: Osborne's revised auricular surface age estimation ³³	44
Table 2.17: Stage descriptions for Buckberry and Chamberlain's method of age estimation from the auricular surface ²⁹	45
Table 3.1: Landis and Koch ¹¹¹ strength of agreement categories.....	64
Table 4.1: Factors influencing scoring ability and visibility	81
Table 4.2: Number and frequency of non-scorable features (n = 149)	81

Table 4.3: Number and percentage of known ages within estimated age range (n = 149)	82
Table 4.4: Range width	82
Table 4.5: Correlation between point value and known age	82
Table 4.6: Mean absolute error for point value	82
Table 4.7: Number and frequency of point estimate values represented by upper or lower terminal values	83
Table 4.8: Cohen's kappa statistics for determining intra- and interobserver agreement strength	84
Table 4.9: Number and magnitude of observer differences by features	85
Table 4.10: p-value from Kruskal-Wallis ANOVA indicating no significant difference in age estimation during different observations.....	86
Table 5.1: Comparison of the accuracy of the age range between Bethard's ¹⁰⁶ validation study and the current validation study	161
Table 5.2: Comparison of correlation between estimated age and actual age from different researchers.....	161

List of Figures

Figure 2.1:	Subdivision of the vault cranial sutures used in the McKern & Stewart method ^{10,62}	46
Figure 2.2:	Four sutures of the bony palate used in age estimation by Mann <i>et al.</i> ⁴³	47
Figure 2.3:	Pattern of suture obliteration for the bony palate as established by Mann <i>et al.</i> ⁴³	47
Figure 2.4:	Sutures retained by Meindl & Lovejoy for their age estimation method ⁴⁸	48
Figure 2.5:	Cranial suture segments selected by Perizonius ⁶¹ as relevant to indices for 20 - 49 year olds (a) and 50 - 99 year olds (b)	49
Figure 2.6:	Ventral view of female pubic bones (above) compared to male (below) ⁷⁸	50
Figure 2.7:	The difference of location and morphology of the ventral rampart (V) in the female (left) and the male (right) ⁷⁸	50
Figure 2.8:	The dorsal aspect of a male pubic bone (A) compared to the dorsal aspect of a female pubic bone (B) ⁷⁸	51
Figure 2.9:	Regions of the ilium used in auricular surface age estimation ^{29,44,110} ..	51
Figure 2.10:	Changes in combined age estimation (uniform prior distribution) confidence interval lengths with age from Milner and Boldsen's ¹⁴ validation study	52
Figure 2.11:	Changes in combined estimation (modified by an archaeological prior distribution) confidence interval lengths with age from Milner and Boldsen's ¹⁴ validation study	53

Figure 2.12: Typical prior distribution models ¹⁴. 54

Figure 2.13: Age-at-death distribution for Bethard's ¹⁰⁶ validation study sample ... 55

Figure 2.14: Cranial suture age estimation ranges and point values with true ages superimposed from Milner and Boldsen's ¹⁴ validation study 56

Figure 2.15: Pubic symphysis estimation age ranges and point values with true ages superimposed from Milner and Boldsen's ¹⁴ validation study 56

Figure 2.16: Auricular surface estimation age ranges and point values with true ages superimposed from Milner and Boldsen's ¹⁴ validation study 57

Figure 2.17: Combined estimation (uniform prior distribution) age ranges and point values with true ages superimposed from Milner and Boldsen's ¹⁴ validation study 57

Figure 2.18: Combined estimation (modified by archaeological prior distribution) age ranges and point values with true age superimposed from Milner and Boldsen's ¹⁴ validation study 58

Figure 3.1: Sample distribution by sex and age 64

Figure 3.2: Data capturing screen in the ADBOU computer program ³⁵ 65

Figure 3.3: Likelihood graphs for the three separate anatomical features, pubic symphysis (**pink**), auricular surface (**green**) and cranial sutures (**red**), as well as the combined graph (**black**) generated by the ADBOU computer program ³⁵. 65

Figure 4.1: Changes in cranial age estimation confidence interval length with age. 87

Figure 4.2: Changes in pubic symphysis age estimation confidence interval length with age 88

Figure 4.3: Changes in auricular surface age estimation confidence interval length with age	89
Figure 4.4: Changes in combined age estimation (uniform prior distribution) confidence interval lengths with age	90
Figure 4.5: Changes in combined age estimation (modified with forensic prior distribution) confidence interval lengths with age.....	91
Figure 4.6: Changes in combined age estimation (modified with an archaeological prior distribution) confidence interval lengths with age	92
Figure 4.7: Cranial suture estimated age ranges	93
Figure 4.8: Pubic symphysis estimated age ranges	94
Figure 4.9: Auricular surface estimated age ranges.....	95
Figure 4.10: Combined estimated age ranges (uniform prior distribution).....	96
Figure 4.11: Combined estimated age ranges (forensic prior distribution)	97
Figure 4.12: Combined estimated age ranges (archaeological prior distribution)....	98
Figure 4.13: Cranial suture age estimation point values.....	99
Figure 4.14: Pubic symphysis age estimation point values	100
Figure 4.15: Auricular surface age estimation point values	101
Figure 4.16: Combined age estimation (uniform prior distribution) point values....	102
Figure 4.17: Combined age estimation (forensic prior distribution) point values ...	103
Figure 4.18: Combined age estimation (archaeological prior distribution) point values	104
Figure 4.19: Observer agreement for coronal pterica left.....	105
Figure 4.20: Observer agreement for coronal pterica right.....	106
Figure 4.21: Observer agreement for sagittal obelica.....	107
Figure 4.22: Observer agreement for lambdoidal asterica left.....	108

Figure 4.23: Observer agreement for lambdoidal asterica right	109
Figure 4.24: Observer agreement for interpalatine.....	110
Figure 4.25: Observer agreement for zygomaxillary left.....	111
Figure 4.26: Observer agreement for zygomaxillary right.....	112
Figure 4.27: Observer agreement for symphyseal relief left.....	113
Figure 4.28: Observer agreement for symphyseal relief right.....	114
Figure 4.29: Observer agreement for symphyseal texture left.....	115
Figure 4.30: Observer agreement for symphyseal texture right	116
Figure 4.31: Observer agreement for superior apex left.....	117
Figure 4.32: Observer agreement for superior apex right.....	118
Figure 4.33: Observer agreement for ventral symphyseal margin left.....	119
Figure 4.34: Observer agreement for ventral symphyseal margin right.....	120
Figure 4.35: Observer agreement for dorsal symphyseal margin left.....	121
Figure 4.36: Observer agreement for dorsal symphyseal margin right.....	122
Figure 4.37: Observer agreement for superior demiface topography left.....	123
Figure 4.38: Observer agreement for superior demiface topography right.....	124
Figure 4.39: Observer agreement for inferior demiface topography left	125
Figure 4.40: Observer agreement for inferior demiface topography right.....	126
Figure 4.41: Observer agreement for superior surface morphology left	127
Figure 4.42: Observer agreement for superior surface morphology right.....	128
Figure 4.43: Observer agreement for middle surface morphology left	129
Figure 4.44: Observer agreement for middle surface morphology right	130
Figure 4.45: Observer agreement for inferior surface morphology left	131
Figure 4.46: Observer agreement for inferior surface morphology right.....	132
Figure 4.47: Observer agreement for inferior surface texture left.....	133

Figure 4.48: Observer agreement for inferior surface texture right.....	134
Figure 4.49: Observer agreement for superior posterior iliac exostoses left	135
Figure 4.50: Observer agreement for superior posterior iliac exostoses right	136
Figure 4.51: Observer agreement for inferior posterior iliac exostoses	137
Figure 4.52: Observer agreement for inferior posterior iliac exostoses right	138
Figure 4.53: Observer agreement for posterior exostoses left	139
Figure 4.54: Observer agreement for posterior exostoses right	140
Figure 4.55: Comparison of age distributions using inter- and intra-observer scores for cranial suture age estimation.....	141
Figure 4.56: Comparison of age distributions using inter- and intra-observer scores for pubic symphysis age estimation	142
Figure 4.57: Comparison of age distributions using inter- and intra-observer scores for auricular surface age estimation.....	143
Figure 4.58: Comparison of age distributions using inter- and intra-observer scores for uniform combined age estimation.....	144
Figure 4.59: Comparison of age distributions using inter- and intra-observer scores for combined age estimation modified with a forensic prior distribution	145
Figure 4.60: Comparison of age distributions using inter- and intra-observer scores for combined age estimation modified with an archaeological prior distribution	146

Chapter 1: Introduction

1.1. Introduction and problem statement

It is common practice to estimate age-at-death, along with sex, stature and population affinity, during an osteological investigation ¹. In an archaeological context these estimations are used to study population dynamics through mortuary practices, palaeopathology and palaeodemography, childhood and neonate mortality rates and size of breeding group ¹⁻⁵, while in a forensic context individual traits are established in order to narrow the field of investigation and make a personal identification ^{1,2,4,5}. Guidelines ensuring the relevance and reliability of the methods used to calculate these estimations exist, as represented by the Daubert guidelines ^{6,7}, for use in forensic context and the Rostock Manifesto ⁸ for research in palaeodemography.

The Daubert guidelines assist the legal system in assessing scientific testimony, ensuring that the analytical technique has been tested, that the potential error rate is quantifiable, that standards exist for the technique, that the technique has been peer reviewed and published and has been generally accepted within the scientific community ^{5,6,9}. The Daubert guidelines, although only pertinent to courts in the United States of America, can also be used to validate techniques used in other countries and other avenues of scientific enquiry such as archaeological analysis.

The Rostock Manifesto originated from a collaborative effort that provided a foundation for the improvement of age-at-death estimation in a palaeodemographic context. The main guidelines of the Rostock Manifesto are the development and validation of better age indicator stages in better documented reference samples, as well as the use of Bayes' theorem to calculate the probability of a certain age given a specific age indicator by making use of the mortality distribution of the target sample ⁸.

Before rigorous guidelines for the development of effective and reliable methods existed, skeletal information was garnered from anatomy textbooks with an oversimplification of facts stemming from the use of central tendencies and absolute values ¹⁰. Currently, osteological investigations compare skeletal features of

unknown individuals to a standard series of skeletal individuals with known age and sex ¹. The information generated from the standard series is then used to estimate the biological profile of individual unknown skeletons, with the assumption that the skeletal features follow uniform periodicity and morphology in both groups ^{1,11,12}. The standard series can be composed of radiographic material from living individuals, but as many surface features of bones are obscured in radiographs, skeletal collections are used most often. Coroner based samples are also being used increasingly when researching analytical methods ¹.

Suitable skeletal collections used to derive osteological standards should possess records of age, sex, and population affinity. Skeletal collections of this kind are found, for example, in the United States of America (the Hamann-Todd collection, the Korean War dead collection, the Terry collection ¹³, the Los Angeles County autopsy collection, the Cobb collection and the Bass Donated Collection ^{1,14}) ¹⁵, the United Kingdom (the St. Bride's and the Spitalfields collections ¹⁶) ¹⁵, Europe (the Leiden, Lisbon ¹⁷, Coimbra, Sassari, Bologna, Turin ¹⁸, Weisbach, Rainer, St. Petersburg and Virchow collections) ¹⁵, as well as South Africa (the Raymond A. Dart Collection of Human Skeletons ^{19,20} and the Pretoria Bone Collection ^{2,21}). The skeletal collection needs to be representative of the unidentified remains by taking into account the geographic variability, socio-economic class and secular changes that exist ²².

Most skeletal collections contain only adult skeletons, mostly over 25 years, but with advanced age being the norm ^{1,2}. If a majority of ages end in increments of five it can be assumed that these documented ages are based on ages estimated by the coroner or medical school ^{1,2,23,24}, rather than actual ages. Even ages reported by the deceased are sometimes found to be averages, as not everyone is aware of their actual age or willing to report an exact age ²⁴⁻²⁷. Biological ancestry is often confused with social terms referring to "race" and no acknowledgement is made for admixture ^{1,2}. Inaccuracy of the data accompanying the skeletal collection influences the success of the analytical methods developed using the skeletal collection ²⁸. The age distribution of the skeletal collection used to produce analytical methods, whether representative of individuals who died of old age or younger individuals who died during war, is mirrored when making use of that analytical method ^{12,29}.

Skeletons originating as dissection room samples often arise from low socio-economic status and individuals from non-Western subsistence practices are not often included in these skeletal collections ^{1,2}. The composition of the skeletal collection limit reliability of analytical methods developed on the skeletal collection when assessing samples with lifestyle differences ³⁰. The solution is frequently to eliminate individuals and restrict sample sizes when testing specific parameters and analytical methods ^{25,31}.

Skeletal collections from archaeological contexts are cemetery samples and can either reflect a natural population distribution or a social formation which can influence the distribution of sex and age in the sample ^{2,27,30,32}. The option of burial and the method used is influenced by cultural factors such as social and economic conditions and religious beliefs. This in turn can affect the physical conditions of the burial which may affect the remains ^{2,32}. Archaeological samples can be fragmentary and poorly preserved. These conditions, inherent in an archaeological sample, create additional bias ^{2,30,32}.

The abovementioned skeletal collections are used for continuous research in order to refine and validate techniques for collecting, capturing and interpreting data in an effort to increase accuracy, precision and reliability of analytical methods ¹ as is insisted upon by the Daubert guidelines ⁶ and Rostock Manifesto ⁸. Accuracy or validity is considered the degree to which an estimate conforms to reality and the degree of precision is the degree of refinement of the estimate ^{1,5,6,14,33}. Estimations with high accuracy and precision are considered successful relative to the specific aims and hypotheses of the investigation ¹, but it is important to balance high degree of accuracy with prediction intervals that are small enough to be practically helpful ^{10,14}. Reliability concerns the uncertainty in an estimate due to observation inconsistency and variation among individuals and populations ^{5,6}.

Adult age-at-death estimation has serious osteological and statistical problems which influence the accuracy, precision and reliability of the estimation. These problems include the mimicry of the reference sample structure, very few procedures that provide systematic combination of information from different anatomical structures, the inability to estimate ages after 50 years of age and a tendency to underestimate

these older ages, as well as fixed age interval lengths with no means of including age indicator consistency ^{4,14}.

Statistical applications used in past research were often inappropriate with small sample sizes and insufficient descriptive data for meaningful comparisons ³⁴. Boldsen *et al.* ⁴, have attempted to create a mathematically sound, adult age estimation method using a large research sample. The method reinvents traits to suit sophisticated statistics by transforming the skeletal traits into an invariant, unidirectional series of senescent stages. The timing of transition from one stage to the next will vary among individuals, but the direction of the sequence of stages is fixed. This timing of transition gives the method its name, transition analysis. Boldsen *et al.* ⁴ applied their transition analysis technique to components of the pubic symphysis, ilial portion of the sacroiliac joint and the cranial sutures, which have been reinvented from previous research on these anatomical units. Transition analysis provides both point estimates and age ranges, calculated by the ADBOU (Anthropological DataBase, Odense University) age estimation computer program ³⁵. The point estimates are calculated from maximum likelihood estimates and the age ranges are calculated from 95% confidence intervals. Additionally, transition analysis was developed for use with fragmentary remains. Thus, not all features are necessary in order for an age estimation to be calculated, but the range width will differ according to the combination of available traits ¹⁴.

Although transition analysis adheres to many of the Daubert and Rostock Manifesto guidelines, these guidelines insist on rigorous validation in a significantly different population, by a researcher other than the original developers. Accuracy, precision and reliability of the method need to be tested in a South African population, before the method can be used in a South African setting.

1.2. Aim

The aims of this study were to use scoring techniques for 36 features from the cranial sutures, pubic symphysis and auricular surface of the ilium (currently available in the “*Transition Analysis Age Estimation: Skeletal Scoring Manual*”³⁶), together with the ADBOU age estimation computer program³⁵, to estimate age in South Africans in order to:

- assess the ability of these scores to accurately estimate age when entered into the ADBOU age estimation computer program³⁵, developed by Boldsen *et al.*⁴;
- assess the repeatability of the scoring procedure through analysis of inter- and intra-observer error; and
- assess the effect of observer differences in scoring on the final age estimates

Chapter 2: Literature Review

2.1. Introduction

Two types of age can be distinguished, namely chronological age, which is the passage of time calculated from birth and biological age, which is growth, size and maturity as represented by the morphology and physiology of an individual^{1,2,5,11,27,30,37-39}. Age related morphology is used to create osteological age indicators. A relationship does exist between passage of time and osteological indicators^{4,27}, but they do not always progress in a synchronous and coordinated manner^{1,2,5,11,12,30,37-39}. This asynchronous progression is the result of genetic, environmental and lifestyle factors that influence the biological age. These influences are unique to each individual and accumulates with time^{5,12}. The observed variations are unique to each individual and may result in the biological appearance being younger or older than the chronological age. The accumulating effects of these unique characteristics result in broader age ranges with time progression. Thus, osteological indicators cannot always successfully predict chronological age, as there is not always good correlation between biological age and chronological age leading to age estimations rather than determinations^{1,2,5,11,14,30,33,37}.

For an osteological indicator to be suitable for the successful estimation of age, three characteristics are required. Firstly, with advancing age, the feature must display progressive, unidirectional change. Secondly, the morphological feature should provide reliable results, whether by phase classification (categorical data) or measurement (continuous data). Thirdly, the changes in morphology due to age progression should be relatively consistent throughout the species, with perhaps one or two divisions such as sex or geographical origin⁵.

Osteological age indicators in subadults experience developmental changes that include the appearance of bones and teeth as well as the formation and fusion of epiphyses^{1-5,25,27,40,41}. Subadult skeletons produce more precise age estimations with minimal bias, however, subadult development can occur in stops-and-starts with normal individual variation in rate and timing^{1,38}.

Biological adulthood is arguably recognised as 20 years of age, when the third molars have emerged and the bulk of the epiphyses have fused⁴². As adulthood progresses, skeletal modifications become degenerative at joint sites and teeth. These degenerative changes are influenced by health, lifestyle and repetitive tasks. As a result adult age estimation is less precise, more difficult and more variable^{1,4,5,25,41,43}. Death becomes increasingly prevalent during senescence as a result of incapacity to resist and adapt to external influences, even though mortality does not exclusively affect the senescent²⁷.

Although it is considered unwise to use socially defined arbitrary divisions of the continuum of growth, intervals of discrete and constant width are sometimes useful when drawing comparisons from different datasets^{1,42}. In these situations where it is deemed necessary to supplement strictly numerical age estimations with age categories, the descriptive terminology should be standardised as exemplified by Falys and Lewis (Table 2.1)⁴².

2.2. Age-at-death estimation in adult skeletal remains

In the adult skeleton there is a shift from developmental modification to maintenance and degeneration. An accumulation of extrinsic factors such as health, lifestyle and environment results in difficulties with analysing and reporting age. However, numerous techniques for estimating age from the adult skeleton have been documented since the 1920s with the most popular regions currently including the pubic symphysis^{5,10,23,25,31,37,39}, auricular surface^{29,33,44}, sternal rib ends^{45–47} and cranial sutures⁴⁸. Many other methods have been developed using anatomical features as varied as the medial clavicle⁴⁹, first rib^{12,50}, teeth^{51–54}, cortical bone histology^{55–58} and arthritic joints⁵⁹. Microscopic methods, which are destructive and require training, experience and equipment, are often dismissed in favour of macroscopic methods. The combination of several age indicators into a single method will theoretically improve the estimates. A successful combined method can only be as successful as the separate age indicators of which it is composed, whether microscopic or macroscopic in nature^{60,61}. Only the three regions relevant to the Boldsen *et al.* transition analysis technique, namely the cranial sutures, pubic symphysis and auricular surface⁴, will be discussed in more detail in this review.

2.2.1. Cranial sutures

Ancient scientists such as Hippocrates, Aristotle and Galen already expressed interest in the interlocking serrated joints of the skull. Early research concentrated specifically on the sutures' relationship with the shape of the cranium and the relationship of both these features with brain development and intelligence. Only later were these pursuits abandoned to concentrate on the significance of cranial sutures in estimating age ^{10,26,48,62}. Researchers mostly describe cranial sutures as unreliable, but nevertheless cranial suture closure is still frequently used to estimate age, because there is a great interest in the skull and it is the bone most often preserved and recovered ³.

The sphenoccipital synchondrosis or basilar suture has been found to be particularly useful in subadult age estimation. This synchondrosis between the occipital and sphenoid bones is an immovable, cartilaginous joint that ossifies gradually ^{63,64}. Previously thought to ossify between 18 and 25 years ^{10,62,65}, it is now widely accepted that the basilar suture of females fuse between 11 and 13 and males between 13 and 18 years ².

Twenty-four other cranial sutures from the calvaria and facial region are easily observable and are considered to be analogous to epiphyseo-diaphyseal planes ⁴⁸. Researchers frequently group these sutures according to location, phylogeny and development. Sutures of the vault include the sagittal, coronal and lambdoid sutures, as well as a persistent metopic suture. The spheno-temporal, squamous, parieto-mastoid and occipito-mastoid sutures are categorised as the circummeatal sutures. The accessory sutures consist of the spheno-frontal and spheno-parietal sutures ²⁶. The sutures of the calvaria and face show more variation than the sphenoccipital synchondrosis and according to Perizonius are only correlated with age between 20 - 49 years ⁶¹. Suture closure is scored between zero and three as in Table 2.2 ^{1,10,34,48,62} or between zero and four as illustrated in Table 2.3 ^{1,10,27,61,62}. Key ⁶⁶ found that only the first and last score is relevant in age estimation, with the scores in between retaining no significant difference from one another and accounting for much assessment error. A score of zero has nearly an equal probability of occurring in a 60 year old than in a 20 year old. Methods of age estimation from cranial sutures relied on mean closure scores rather than assessment of individual suture sites ⁶⁶

until Meindl and Lovejoy suggested using small lengths of sutures or specific sites of sutures to analyse instead of using the entire suture⁴⁸. Nawrocki also followed this method by using one centimetre portions of sutures or circles with a one centimetre radius at the juncture of sutures³⁴.

Researchers differ on the subject of onset time difference between ectocranial and endocranial sutures^{1,62}, as some state that suture closure begins endocranially and proceeds ectocranially²⁷ while others find no differences⁶⁷. Ectocranial sutures never attain the degree of closure that endocranial sutures achieve and do not show as much conformation to pattern and rate, leading Todd and Lyon to speculate that the cause of suture closure arises endocranially^{67,68}. This leads to the conclusion that a lack of ectocranial suture closure does not indicate youth, but rather that the presence of suture closure indicates old age^{43,48,66}.

Making use of endocranial suture closure does necessitate the sectioning of the skull in order to make these sutures visible^{44,62,66}, or peering through the foramen magnum with the aid of a light source^{27,61}, making ectocranial sutures easier to examine. However, most research indicates that lapsed union of sutures, a normal variation recognised by the piled-up appearance of the surrounding bone^{26,48,62,66}, occurs more frequently in ectocranial sutures, making the endocranial sutures more reliable as an age indicator^{26,48,62}. Lapsed union occurs especially in the sagittal and lambdoid sutures and has been likened to the persistent junction line between the epiphyses and shaft of a long bone²⁶. The endocranial sutures tend to be either completely open or completely closed, in contrast to the more gradual progression of the ectocranial sutures, which may contribute to the greater endocranial reliability through the minimising of error due to difficulty in distinguishing stages⁶⁶. Due to conflicting opinions about the reliability of endocranial and ectocranial sutures, some methods utilise endocranial sutures^{27,62}, others utilise ectocranial sutures⁴⁸ and some make use of both^{22,27,34,61}.

As with the rest of the skeleton, the age relationship of suture closure is very variable with some individuals showing accelerated closure and some showing retarded closure²⁶. In most cases ossification starts rapidly, but then slows down to progress more sedately^{26,27,67-69}. However, a pattern of suture closure exists to some degree with closure of the sagittal suture beginning in the first and fourth parts, the first part

of the lambdoid and the first and fourth parts of the coronal suture (Figure 2.1). The final stage of closure occurs in the first and second parts of the sagittal suture, the first or second part of the lambdoid and the first part of the coronal. Thus, in a general sense, the sagittal suture unites from anterior to posterior and the coronal and lambdoid sutures unite from medial to lateral and union commences in the order of sagittal, coronal and lambdoid^{26,62}. Commencement and termination of suture closure first occurs in the obelion and experiences a lagging effect in the pterion and asterion areas^{26,62}. Less denticular sutures close earlier^{1,62} and although asymmetries occur between right and left sides, no bias to either side was found^{1,26,27,34,61,62,66,67}. Todd and Lyon²⁶ did extensive research into commencement, progression and completion of the vault, circummeatal and accessory sutures of the cranium as summarised in Table 2.4.

The sutures of the bony palate also follow a general sequence of obliteration that is correlated with age, beginning at the incisive suture, followed by the posterior median palatine, transverse palatine and lastly the anterior median palatine (Figures 2.2 and 2.3)^{43,70}. The incisive suture begins obliteration in childhood, starting laterally and moving medially, and is completely obliterated from 25 years. From Figure 2.3 it is apparent that obliteration of the anterior median palatine suture and the transverse palatine suture occur in the upper age ranges. The transverse palatine suture begins obliteration in the greater palatine foramen⁷⁰. Some individuals show delayed closure in the maxillary sutures until the 7th and 8th decades⁴³.

In the vault the age range during which suture closure occurs is between 17 and 50 years, but the circummeatal sutures only achieve closure after 70 years of age. The circummeatal sutures could thus be used as an old age indicator. The squamous suture is rarely obliterated⁶². Facial sutures are considered more regular in their closure onset time, which occurs during the mid-twenties. Extrinsic determinants, such as muscle attachments, can influence suture closure⁶⁶. Some age estimation methods use only the coronal, sagittal and lambdoid sutures^{27,61}, but findings by McKern and Stewart¹⁰ suggest that using all of the sutures of the skull combined produce a higher correlation to age¹⁰.

Meindl and Lovejoy⁴⁸ found that some sutures have limited value when estimating age as these sutures have a low age correlation with no contributing age-related information, possess bilateral asymmetry, are difficult to observe or preserve post-mortem or increase the tendency of interobserver errors⁴⁸. These sutures listed in Table 2.5, should be rejected for estimation of age in favour of sutures correlated at least moderately with age as represented in Figure 2.4⁴⁸. The lambdoid suture, especially, has a high error of assessment⁶⁶. The sutures from the lateral and anterior portion of the skull have more value than those of the vault and as a result Meindl and Lovejoy developed separate methods to assess the vault and anterolateral facial area^{48,66}.

Once the sutures are scored according to degree of closure, different methods are used to obtain a practical age estimation. Acsádi and Nemeskéri²⁷ developed an endocranial closure index by averaging the scores for the three vault sutures with associated age ranges (Table 2.6). Perizonius⁶¹ continued the trend of obtaining averages of the vault sutures both endocranially and ectocranially by adding the scores and dividing the total by the number of scores obtained. Perizonius⁶¹ further refined the method by developing two different indices for use with age groups 20 - 49 and 50 - 99 respectively by using different suture portions, as illustrated in Figure 2.5, more closely correlated with the time period in question. Nawrocki³⁴ updated the cranial suture age estimation technique by utilising regression and analysis of variance techniques and making use of stepwise selection procedures to select landmarks most suitable from the palate and the endocranial and ectocranial vault area. From this research Nawrocki³⁴ developed 15 regression equations that factor in the availability of landmarks, population affinity and sex and obtained correlations with age of up to 0.93.

Research is conflicting on the matter of sex and interpopulation differences in suture closure^{1,62}. Some researchers found no differences in suture closure onset time for different sexes^{27,61,66} and populations,^{34,43,48,67-69} while others found suture closure to have a later onset in females with males having more advanced suture development at a given age^{3,34,43,48,66}. More suture closure sites are correlated with age in female individuals than in males, but female cranial sutures are much more variable with a tendency to remain open indefinitely or much later^{3,66}. The difference in opinion of researchers regarding the sex differences in suture closure could be an

indication of interpopulation differences in sexual dimorphism of cranial sutures⁶⁶. Galera *et al.*²² reported population differences in suture closure, which were more pronounced in the ectocranial sutures than the endocranial sutures²². Key *et al.*⁶⁶ also noticed a population difference between an American reference population and their Spitalfields sample, leading to an underestimation of age. Ectocranial sutures are also said to be more sensitive to interpopulation differences than endocranial sutures⁶⁶.

In conclusion it can be said that great individual variation exists in the amount of suture obliteration that occurs with age⁴³. Many authors agree that cranial sutures are only moderately related to age and are only a reliable age indicator in a broad sense with a standard error of ± 10 years^{3,25,26,48,66,71}, with the exception of the basilar sutures which completes closure before 20 years^{2,63}. Even though cranial sutures are of limited value when used singularly to estimate age, the sutures make an important contribution to multifactorial methods such as the Acsádi and Nemeskéri complex method and transition analysis where cranial suture closure is one of the components^{4,10,26,27,62,66}.

2.2.2. Pubic symphysis

Metamorphosis of the pubic symphysis is the most widely used adult age indicator as the symphysis continues to change throughout life, after other epiphyses have fused subsequent to achievement of full stature^{1,10,25,31}. The performance of the pubic symphysis as an age estimator is much better in younger individuals^{28,39}, and after age 40 - 55 the morphology of the pubic symphysis does not experience sufficient metamorphosis to be accurately and reliably used as an age estimator^{23,39,72,73}. Berg, for example, found estimate ranges to be very large around the point estimate for methods using the pubic symphysis⁷².

Todd²⁵ developed the first formal system of estimating age from morphological changes on the male pubic symphysis in 1920. Four basic parts of the oval symphyseal surface were identified namely, the ventral border or rampart, the dorsal border or rampart, the superior extremity and the inferior extremity. Todd considered the ventral rampart as an epiphyses and found changes to this section to be less reliable than changes to the pubic symphysis proper^{25,73-75}. Todd²⁵ recognized ten phases (Table 2.7) of pubic symphyseal age using surface features such as

billowing, ridging, ossific nodules and texture of each of the four identified parts
1,10,25,62.

The Todd²⁵ method was found to be more reliable between 20 - 40 years than in older skeletons. Todd suggested that other features of the pelvic bone, such as the ossification of tendons and ligaments, should be employed as compensation for the decrease in the reliability of the later phases²⁵. Todd²⁵ was adamant that the entire skeleton should be used in age estimation, when possible, in order to increase the success of the estimation^{1,62}. Later, Todd also developed four phases to be used with radiographic imaging to estimate age from the pubic symphysis, as well as a sequence of phases to be used with the female pubis illustrated in Table 2.8^{23,25,74,76}. Todd's⁷⁶ radiographic method gives only a very general impression but is not a replacement for the actual specimen.

Acsádi and Nemeskéri²⁷ developed an age estimation method in Europe, shortly after the Todd²⁵ method, which suggested using the pubic symphysis in conjunction with other parts of the skeleton. The other skeletal components suggested were the cranial sutures, as well as the internal structures of the humerus and femur. The five stages of pubic symphysis morphology (Table 2.9) are used as a starting point for the complex method, determining whether lower limits or upper limits are used for the other features²⁷.

The Todd²⁵ method was modified in 1957 by McKern and Stewart¹⁰, specifically in order to incorporate more natural variation¹⁰. The method was developed on an exclusively male skeletal collection^{1,10,62}, restricting the research sample severely²⁸. The symphyseal surface was divided into three independent components namely the dorsal demi-face and the ventral demi-face, separated by a longitudinal ridge or groove and the symphyseal rim. Five phases of development were recognised for each of the three components^{1,10,62}. These components were chosen to facilitate the visualisation of the morphological changes with chronological progression¹⁰, and the method is aided in this through a model cast system illustrating typical phases^{10,28}. As a developmental sequence exists between the three components of the McKern and Stewart method, the developmental stage of the dorsal rampart must always be further along or equal to the developmental stage of the ventral rampart and the development of the ventral rampart must always be further along or equal to the

development of the symphyseal rim⁶². The gradual unidirectional development of the three components from build-up to break-down can be attributed one of the quantitative scores listed in Table 2.10 on the basis of experience¹⁰. These individual scores are summed and the composite score provides a corresponding mean, standard deviation and observed range of age in tables supplied by McKern and Stewart^{10,77}. An accuracy of 90% has been achieved by an independent observer using this method, but differences of opinion regarding the allocation of stages can be expected by observers as the stages are interrelated and not easily distinguishable. This difference need not necessarily lead to an erroneous age estimation, but makes the method difficult to apply^{10,39,78}.

Gilbert and McKern²³ generated a component method, based on the method of McKern and Stewart¹⁰, for female pubic symphyses^{1,23}. Six stages of metamorphosis were recognised in each of the three components (the dorsal demi-face, the ventral rampart and the symphyseal rim; Table 2.11)²³. Once again the typical phases were illustrated through a cast system for ease of identification^{23,28}. In an effort to expedite the age estimation process and treat the data sets as a whole in order to obtain more accurate estimates, Snow developed four equations to be used with the composite scores of the McKern and Stewart¹⁰ and Gilbert and McKern²³ component method⁷⁷. Eight equations, four per sex, were also developed by Chen *et al.*^{79,80} to be used with scores modified from Hanihara and Suzuki⁸¹, McKern and Stewart¹⁰, Gilbert and McKern²³ and Brooks and Suchey³⁷.

Brooks and Suchey³⁷ as well as Katz and Suchey³⁹ investigated the success of existing methods of age estimation using the pubic symphysis, including those developed by Gilbert and McKern²³, McKern and Stewart¹⁰, Todd²⁵ and Acsádi and Nemeskéri²⁷. Brooks and Suchey³⁷ rejected the component method, due to the fact that the variability in the components are not independent of each other and that inaccuracy is high when judging whether the ventral rampart is in build-up or break-down phase^{23,37,62,78}. In addition to this, they argued that the complexities associated with the technique are unwarranted³⁷. The observation was made that many of the Todd's phases were not readily distinguishable from each other³⁹, but that overall, Todd's²⁵ method of using the total pattern visible on the pubic symphysis was found to be more accurate and easier to use than the later component methods^{37,39}. The Todd²⁵ method, which gives clear and comprehensive treatment of the maturational

stages of the symphysis, was reduced to a six phase method (Table 2.12) and expanded to include variability associated with a modern sample^{37,39,78}. Both the Todd²⁵ and Brooks and Suchey^{3,37} methods show high correlations between pubic face pattern and known age³. As Suchey and Brooks³⁷ used a larger more diverse sample the age estimate is reported with a larger range than compared to other methods²⁸. The use of a sex specific cast system is employed not only to familiarise one with the typical morphology of the maturational phases, but also to aid identification of specific phases in the two sexes^{28,37}. Berg⁷² subsequently found it necessary to add a phase VII category to the terminal end of the Suchey-Brooks phases.

Meindl *et al.*³¹ also concluded that the most reliable method, with the highest correlation between known age and estimated age, is the original Todd²⁵ method abbreviated to five phases of development, as seen in Table 2.13^{1,62}. The conclusion by Meindl *et al.*³¹ stemmed from the fact that the entire symphyseal phase contributed more strongly and accurately to age estimation than individual components. The method was developed on a large sample size of both sexes and with a greater age range than previously studied^{31,62}.

As with all skeletal biology much individual variation occurs in the morphology of the pubic symphysis^{72,78}. This variation can be seen in features such as the presence of the ossific nodule, the degree of ridge and furrow formation as well as the smoothness with which the symphyseal face will present and whether the ventral rampart will present with a hiatus and remain incomplete indefinitely^{25,75}. These variations are intimately associated with both the shape and the development of the pubic symphysis^{73,75}. Natural variation accumulates with time as can be seen by many of Todd's later phases (VI, VIII, IX and X) which are plagued by difficulties²⁵. Todd only described model phases representative of central tendencies and much natural variation went unaccounted for in the method^{3,10,39}. Todd did, however, draw attention to some of the variations that he originally thought to be pathological such as some rough or crenulated variations that can mistakenly lead to overestimation³. Hatchet-shaped variations provide inaccurate age estimations and should not be used according to Suchey and Katz⁷⁸, and Berg⁷². Extremely big pubic symphyses, especially in males and extremely narrow pubic symphyses are variations that can confuse the typical maturation pattern⁷². Differences between pubic symphyses of

the right and left side can also confound matters ^{25,82} and there is no clear guidelines in the literature to suggest whether to use the younger pattern or the older pattern ⁷⁸.

The use of population specific methods are suggested, as differences related to either genetics, environment or both have been observed ^{72,74,78-80}. Observations of population differences include overaging of a Japanese population using the Todd method ^{10,81} and underaging of individuals over 40 years in a Thai sample using the Suchey and Brooks method ⁸². Todd ⁷⁴ noticed increased variation in black individuals compared to white individuals at the pubic symphysis and as a result developed phases of metamorphosis specific to black individuals ^{73,74}.

Many authors ^{1,3,10,62,77} insist on a sex specific method for estimating age from the pelvis as the female pelvis is not only involved in bipedal locomotion, but also in parturition, causing differences in the morphology and rate of maturation at the female symphysis ^{23,28,31,78,83,84}. Female pelvises seem to have more variation than male pelvises including more movement prone joints ³⁹ paired with smaller articular areas ⁸⁵. Some researchers observe a difference in female pubic morphology, in the area between the symphyseal rim and the ventral arc, which displays age related changes unique to the female pelvis ³⁷. The ventral arc is a predominately female structure that modifies the pubic bone from the pubic crest to the subpubic concavity with a raised crest ⁸⁶⁻⁸⁸. The broadening of the pubic bone that occurs in the maturation of the female pelvis results in differing morphology of the ventral arc in females and males (Figure 2.6). In females the ventral rampart is between the pubic symphysis and the arc, while in males the ventral rampart and the dorsal demi-face are divided by an imaginary line illustrated in Figure 2.7 ⁷⁸. Therefore, in the female pubic symphysis the symphyseal rim divides the dorsal and ventral surfaces from each other, while in the male the symphyseal rim encloses and surrounds both the dorsal and ventral surfaces ^{23,78}.

Observed changes in the female pelvis due to parturition include the dorsal edge of the pubis (pitting and lipping modification of this area can be seen in Figure 2.8) ^{1,23,72,78}, the auricular surface and the preauricular area and the pubic tubercle ^{1,44,72,84,89}. Parity damage can also lead to confusion as to whether the dorsal demi-face and ventral rampart are in a stage of build-up or break down, once again possibly leading to overaging ³⁷. These structures, modified by parity, contain very

poor quality information regarding age that frequently lead to errors of estimation^{23,44,72,84,89}. Many of these modifications made during pregnancy and parturition are obliterated by old age⁸⁹ and some authors also argue that old age or body mass index can be responsible for dorsal pitting observed in nulliparous females and male individuals^{84,85,90}.

Postmenopausal and senile osteoporosis, more prevalent in females, can lead to overaging from as early as 35+ years, but only becomes apparent in males after 40 years⁷². Despite all of these sex differences on the pelvis, methods of age estimation such as the six Suchey-Brooks phases in Table 2.12 are able to focus on changes central to both sexes, but need to be assessed with separate cast models for the male and female pubic symphysis to ensure that the correct phase is allocated for the corresponding sex^{37,78}. Some authors, however, are not convinced that sex differences at the pelvis necessitate sex specific methods^{31,62}.

2.2.3. Auricular surface

The maturational changes on the bony and cartilaginous surfaces of the sacroiliac joint have been investigated since the early 1900s^{91–93}, but the use of the auricular surface of the pelvis in age estimation was only pioneered by Lovejoy *et al.*⁴⁴ in 1985 after they realised the advantages presented by this area^{1,82}. Advantages include the facts that this area is more robust and thus more likely to be preserved post-mortem, the method can be utilised without knowledge of sex or population affinity and changes to the feature occur well beyond age 50 enabling accurate age estimation past this decade, whereas the pubic symphysis is only helpful to the fourth decade of life^{1,33,44,82}. The articular area is divided into a superior and inferior demi-face. Posterior to this articular area is the retroauricular surface and anterior to the articular area is the apex (Figure 2.9).

The age related changes documented for the auricular surface include appearance of surface granulation, macroporosity, microporosity, transverse organisation, billowing and striations (Table 2.14)^{1,44}. No corresponding age related changes are found on the auricular surface of the sacrum, as the changes are most likely caused by cartilage on the ilial surface becoming fibrotic and thinning⁴⁴. According to Lovejoy *et al.*⁴⁴ the auricular surface is modified progressively and regularly with increasing age. The auricular surface modification is represented by eight

recognisable phases with corresponding age ranges as listed in Table 2.15^{1,44}. If the specimen under analysis does not correspond precisely to a single phase the best representation of the criteria, shown in italics in Table 2.15, should be used⁴⁴.

The Lovejoy *et al.*⁴⁴ method was found more useful in palaeodemographic analysis where skeletal seriation was possible. As a component of a combined skeletal analysis the auricular surface improved the overall reliability^{33,44}. The original research and subsequent tests indicate that the auricular surface method to estimate age has large estimation errors, possibly linked to the fact that investigators find the method difficult to master with many characteristics difficult to classify^{1,82}. Factors contributing to the difficulty with interpreting morphological stage include the lack of a delayed epiphysis as seen in the ventral rampart of the pubic symphysis and more complex, even though regular, changes⁴⁴.

Difficulty with mastering the method and confusion when assigning stages of development could be due to the overlap of the morphology between successive stages caused by the narrow age ranges that do not successfully account for individual variation^{29,33}. Some phases showed no significant difference between the mean ages, leading Osborne³³ to suggest that the original eight phases should be condensed to six phases (Table 2.16), in order to simplify the method, but still retaining the method's accuracy.

In order to rectify the large estimation errors occurring in the original method, Buckberry and Chamberlain²⁹ revised the method to record the features of the surface as separate components and then construct a composite score^{29,33}.

Buckberry and Chamberlain elected to exclude the retroauricular area and keep only transverse organization, surface texture, microporosity, macroporosity and apical changes as defined and described in Table 2.17. Each feature corresponds independently with age²⁹, indicating that the features could be used independently to estimate age, but the largest agreement with age is achieved when combining the individual components^{29,33}. The resultant method is considered both reliable and repeatable²⁹.

Schmitt⁹⁴ also developed a new scoring system with four separate morphological features, with the aim of simplifying the Lovejoy *et al.*⁴⁴ method and in doing so increase the reliability and accuracy achieved. Schmitt⁹⁴ found the morphological

features to be subject to prejudice and experience. In contrast, regression estimates using the Lovejoy *et al.* ⁴⁴ method were shown to be unbiased by Murray and Murray ⁹⁵, but the intervals were considered too large for use in forensic science ⁹⁵.

Igarashi *et al.* ⁹⁶ confirm that rough, granular and porous changes to the subchondral bone and scleroses and osteophytoses of the auxiliary area occur as a matter of degeneration with age and used the presence or absence of these features as part of a multiple regression analysis to estimate age. The Igarashi *et al.* ⁹⁶ method works particularly well as some of the features (wide groove, striation, flatness, smoothness and fine granularity) are representative of younger individuals while the remaining features (roughness, coarse granularity, sparse porosity, dense porosity and the hypertrophied bony structures) are representative of older individuals.

The sacroiliac diarthrosis, like the pubic symphysis, becomes increasingly moveable in the female pelvic girdle during pregnancy as a result of relaxin ⁴⁴. This sex difference does not influence the area ^{29,33,44,62,94,95}, with the exception of an accentuated preauricular area, consisting of the margin and apex of the articular surface in females. In the case of an accentuated preauricular sulcus, changes to the inferior margin and apex should be disregarded ^{29,33,44,62,94}. Also, the sacroiliac joint does have the tendency to synostose in males over 50 years ^{31,44,97}. These sex differences can be ascribed to a change in the ligaments at the onset of puberty which increase in thickness for added strength in males, but remain comparatively lax in females in order to increase mobility ⁹⁷. Igarashi *et al.* ⁹⁶ found female morphology at the auricular surface to be much more variable than that of males and considered this observation to be consistent with differing chronological changes between sexes at the auricular surface.

Population differences in this skeletal feature have been noticed by some ^{82,94}, although Murray and Murray ⁹⁵ found no population variations between a white and a black American population ⁹⁵.

The auricular surface age estimation method does not fare well when using single indicators only ³³ and should not be used to the exclusion of other methods ⁹⁵. Efforts to refine the auricular surface method, in order to improve age estimation, suggested using features from the acetabulum including the acetabular rim, the acetabular fossa, porosity of the lunate surface and apical activity ⁹⁸. As with all age estimation

methods, inaccuracy increases with increasing age³³. Symmetrical differences have also been noted^{29,82,94}.

2.3. Statistical considerations

The success of any age estimation technique is dependent not only on the osteological indicators, but also on numerous statistical considerations. Balance needs to be achieved between the amount of precision or uncertainty, as represented by the interval widths, and the accuracy represented by the proportion of the true ages which fall within the interval^{1,31}. Accuracy can also be a reference to the correlation of the point estimate (representing a single year) with true age or stated differently, inaccuracy is the measurement of the magnitude of deviation in years from true age, regardless of under- or overestimation^{1,14,33}. With regard to the consideration of the directionality of inaccuracy, the tendency of under- or overestimation is referred to as bias¹.

When using wider, more diverse reference samples the resultant age ranges are frequently wider, leading to more reliable results in forensic settings. However, the usefulness of wide ranges when narrowing down potential identifications is limited²⁸. The reliability of a technique refers to the consistency and repeatability of results and is an important consideration not only for the developer of the technique wishing to achieve consistent results, but especially when numerous different investigators employ the same technique⁹⁵.

Reliability of a technique can be decreased by error stemming from two sources. Firstly, chronological age which is not perfectly correlated to biological indicators produces error and necessitates the use of age ranges, often taking the form of standard deviations or more suitably a 95% confidence interval³⁴. Secondly, the degree of age-related information contained within specific skeletal traits is a source of error^{12,34}. Mistakes concerning sampling strategies and statistical methods used in the development of methods can also lead to erroneous conclusions¹². Six mistakes that plague methodology include mistakes with application of technique, interobserver error, intraobserver error, instrument errors, recording error and computer data error, all of which influence the reliability of a technique⁶.

Statistical concerns and possible solutions that are discussed here in more detail include problems with refining ranges after 50 years, combining as much relevant information from skeletal indicators into a single statistically valid method, development of repeatable and comparable techniques, minimizing mimicry of the reference sample collection and development of suitable standards that consider sex, population and individual variation.

2.3.1. The old age dilemma

Uncertainty, represented by the age range of an age estimate, does not increase linearly, but rather increases steadily until around 60 or 70 years of age, when it reaches a plateau, after which it decreases slightly (Figures 2.10 and 2.11)¹⁴. The decrease in these interval lengths in the elderly could partly be caused by the effect of selective mortality¹⁴, but there are some skeletal traits that can serve to narrow estimation ranges in the older ages, for example the break-down of the dorsal margin of the pubic symphysis and the appearance of exostoses on the posterior auricular surface⁴.

Recent improvements in the precision of age estimation in older individuals have improved the previous state of open-ended age categories of 50+ years^{4,12,41}, which would lump all individuals over 50 together in a single category and would ultimately skew demographic profiles toward seemingly younger ages-of-death^{12,14}. Age can still not be estimated with the same certainty throughout the lifespan and although it is now possible to refine older (above 70 years) age estimations the middle age category ($\pm 50/60$ years) is still riddled with uncertainty in the form of overly wide age ranges and open-ended estimates¹⁴.

2.3.2. Combination of skeletal indicators

It has long been recognised that it is best to use as many skeletal indicators as possible to improve age assessments^{10,12,24,25,27,29,44} in order to encompass all morphological variation found in the skeleton^{4,14,25,37,62,99}. However, very few techniques have formally combined more than one skeletal feature in a single age estimation method^{27,31,100}.

Combined methods can only perform as well as the single indicator methods used to compile them³³. Reliability of the various skeletal indicators used in combined

methods will vary and sometimes even be contradictory¹⁴. These techniques and features will still contribute additional data which will improve the accuracy and precision and decrease observer error of the estimation^{1,3,33,37,48,62,99}. However, with contradictory skeletal indicators the age ranges should be accordingly adjusted, resulting in very different and very individual age ranges even when the point estimates correspond¹⁴.

Combining multiple independent skeletal indicators into a single combined age estimation method should occur in an appropriate, systematic and statistically valid manner as the indicators are not independent of each other. An appropriate manner of combining single indicators takes into account the correlation of the indicators with each other, by using a correlation matrix, which unfortunately demands an enormous reference sample⁴.

The skeletal material available for analysis is influenced by both post-mortem and perimortem factors^{1,2,12,27,40,78,101} which in turn can influence the accuracy and precision of the estimate, as different features are more representative of different developmental stages and some will correspond more closely with chronological age^{1,2,27,40,101} and some will be influenced by sexual dimorphism, stature and population variation^{1,2,101}. Post- and perimortem modification that influences the endurance of the skeletal features are slow-soak maceration, boiling, embalming, burning and deterioration, cortical erosion, soil characteristics, animal activity and fragmentary recovery^{10,12,25,78,95}. Delicate bones, such as the pubic bone and the sternal rib ends, are more often impacted by taphonomic modification, rendering them useless during analysis^{10,12,25,95}.

2.3.3. Ability to repeat and compare methods

Whether making use of single skeletal features or a composite methodology, the analytical method is an important consideration in the success of estimation¹. The analytical method needs to be developed in such a way that results are reliable, by definition both correct and repeatable, as well as being easily comparable with results from other methods. Comparability of results are achieved through uniform methodology and dimensions, even when methods yield different degrees of reliability or are applicable to individuals or samples in different degrees^{1,99,102}. Consequently, comparisons of results reported in the form of standard deviations

can be problematic as the width of the standard deviation intervals differ across different analytical methods. A 95% confidence interval provides a better range for comparison, but should not merely be calculated from two standard deviations ²⁸.

Comparisons between analytical methods are flawed if individuals are eliminated from the reference sample during the development of the method. The elimination of individuals for whatever reason creates an artificial reduction in variability ³⁹, and ultimately causes bias in samples where the individuals with these characteristics have not been removed as well ⁴⁸. Another developmental flaw occurs if too many narrow morphological phases are recognised with too much overlap between the phases, causing error of assessment. The number of phases should be reduced in favour of broader ranges that are beneficial to forensic investigation in need of positive identification and also leads to a reduction in the probability of incorrect phase assignment ^{33,66}. When comparisons of the suitability and success of analytical methods are conducted, prejudice should be eliminated by using researchers independent of the original developers and a sample as biologically unique from the original reference sample as possible ^{4,28,33}.

Complexities existing in the analytical technique and identification of phases create difficulties for inexperienced investigators, which may influence the repeatability of a technique ³⁹. The investigator's skill at using the analytic method to estimate age and their familiarity with the method, as well as its limitations, should not be ignored. Notable improved results could be implying beneficial incorporation of age indicators outside those used in the estimation method ^{1,14,28,33,99}. The value of professional training and experience should not be ignored ⁹⁹, but using experience and intuition to estimate age can only exist in general terms without the accurate data support, statistical realities and acknowledgement of the limitations of the technique ²⁵. Regardless of experience with the analytical method, the fatigue factor may also play a role in repeatability and accuracy of age estimation ^{6,28}. Klepinger *et al.* found that missed estimates had a tendency to cluster in time possibly inferring a drain in concentration and energy ²⁸.

When making use of a linear model, with equally spaced intervals and a numerical score illustrating sequential progression of age, a single score difference can result in an age difference of ± 4 years ³⁹. In order to capture all possible morphological

variation expressed by an osteological feature it is important to optimise scoring for ease of use and repeatability⁴. The component methods seem to capture these changes occurring with age better than the classificatory schemes that analyse the structure in its entirety. Also with the component method the information from the feature is preserved regardless of any biological variation occurring between different features as they are analysed in different categories⁴. Thus, the key to replicating observations and results is the use of explicit trait definitions and the standardisation of methodology⁶.

2.3.4. Impact of natural variation on age estimation

Most standards used in analytical methods have been developed on European or North American skeletal series and do not apply equally to human populations from other contexts in space and time^{1,11}. However, a useful method needs to be equally applicable to all samples, whether forensic or archaeological in nature, and should be tested on a population distinct from the reference population^{1,14}. Ideally, every analytical method should be adapted to consider natural variation within individual remains, within populations and between populations as well as through spans of time with the aid of situation specific standards^{1,4,11,29,32,34,40}.

Causes of skeletal variation include life history, antemortem defects or pathologies, trauma and death^{3,10,25,27,29}. If nutritional or environmental conditions are the cause of skeletal variation, age estimates can be impacted at the individual level, at the population aggregate or the impact can even be delayed until later in life^{11,23,30,101}. These factors cause both underestimation and overestimation of age^{10,25,28,29,31,78}. Even in individuals with similar biological backgrounds and environmental conditions, individual variation causes different biological ages²⁹. Variation is also found within a single skeleton and can either be a general anomaly throughout the entire skeleton, can be restricted to a single anomalous structure (i.e. the pubic symphysis) or can form a mosaic of contradictory features in the skeleton⁷⁵. Distortions of age estimation due to malformations, trauma and pathologies should be prevented by using skeletal features that are not influenced by these changes¹⁰.

Variation at the population level is observed in different degrees between different parts of the skeleton¹⁰². Sometimes geographically related populations yield comparable results, but with modern populations becoming increasingly

homogenous clear population distinctions can no longer be made and instead an entire range of variability should be considered ¹⁰¹.

The most distinct variation to occur is between the sexes, where robusticity and size vary. Some skeletal features are especially sexually dimorphic. One bone that shows such marked differences is the pelvis, as the male pelvis is only structured for habitual bipedalism while the female pelvis also needs to facilitate birth ^{28,31,84}. Sexual variation becomes more accentuated after puberty, but sex differences are already observed where onset times of the fusion of epiphyses are concerned ⁴⁰. Sexual dimorphism in skeletal age indicators necessitates separate standards for males and females ^{23,37,39}, just as population differences necessitate separate standards for geographically and biologically distinct groups.

Much research has been conducted on variation, especially that concerning population differences, but in actual fact many of these differences are accounted for by the different age structures between the study populations (such as the reference collection and the sample) ²⁴. Many of these perceived differences can be eliminated by using large sample sizes.

2.3.5. Reference sample mimicry

When differences exist between the sample under investigation and the reference sample used to develop the technique bias will occur ¹⁰³, as age estimates produced from any analytical method will mimic the structure of the reference sample used to develop the method ^{4,28,33,60}. This reference sample mimicry occurs because an estimate of age for each trait value was obtained, leaving the values sensitive to the age composition of the reference sample ⁴. Reference sample mimicry often leads to the overestimation of young adults and the underestimation of old adults ¹⁴. Thus, it is imperative to find a method of avoiding reference sample mimicry. One method of eliminating reference sample mimicry is by evaluating the entire age distribution, in a large target sample, or making use of information independent of the target sample, in order to obtain an appropriate and informative prior distribution ⁴. This is problematic if no knowledge of the population age distribution exists ¹⁴ or if the target sample is too small to obtain a prior distribution. The only solution is then to use a uniform prior distribution, but this places disproportional weight on the extremely old, because a uniform prior distribution does not conform to the construct of the age

factor in a population that would account for the lack of survival past 90 years. In fact when using a uniform prior distribution the likelihood of age 70 is the same as that for age 90, 100 or 110 years. However, this is still preferable to an informative prior where the same information serves both to calculate the prior distribution and to estimate the age (the skeletal material) ⁴. Thus, any prior distribution making use of independent information from a real population mortality distribution will perform better than a uniform prior distribution, but the most satisfactory results will be obtained with relevant population information ¹⁴.

2.4. Transition analysis

Some statistical headway has been made in the field of age-at-death estimation, especially concerning the bias resulting from reference sample mimicry ^{12,96,103} and the problems associated with multifactorial age estimation. Transition analysis is a method of estimating age, developed by Boldsen *et al.*, in an attempt to address the difficulties with combining age estimates obtained from different estimation techniques ⁴. The transition analysis method is named for its methodology which works by estimating the timing of transition from one age-related stage to the next by treating each transition event as distinct ^{4,103}. Transition analysis focusses on the probability of an individual being in a specific anatomical stage as defined by age, instead of classifying an individual with a specific anatomical feature into a set age distribution as done with traditional methods ¹⁰³. The timing of the transition from one stage to the next will vary among individuals, but the direction and sequence of the transition remains fixed among all ⁴.

The technique focuses on adult age estimation, where limitations are greatest. The technique is applicable to individual skeletons and addresses the following four major analytical difficulties - avoiding the large uncertainty associated with age estimation; mimicry of the age distribution of the reference sample; effective combination of multiple skeletal indicators; and the development of methods that relate morphological changes to age ^{4,12}. Three skeletal features can be combined or used separately in the Boldsen *et al.* method, namely the cranial sutures, pubic symphysis and the sacroiliac joint, but the principle of transition analysis can be used with any feature that has an unchanging series of age-related stages ^{4,103}. Any

combination of scores obtained for the three skeletal features are entered into the ADBOU (Anthropological DataBase, Odense University) age estimation computer program, which calculates a maximum likelihood value, 95% confidence interval and a graphic representation of transition for each of the three features separately and combined ³⁵.

2.4.1. Anatomical features

The three osteological components, used in transition analysis, namely the pubic symphysis, iliac portion of the sacroiliac joint and segments of cranial sutures, are evaluated for likelihood of transition from one stage to the next ^{4,14}. A total of 36 observations are possible, five of which are from cranial suture segments, five components from the pubic symphysis and nine components from the sacroiliac joint. These components, with morphological changes relevant to each stage, are explained in detail in Appendix A. Cranial suture segments are scored on the ectocranial surface, similarly to existing methods, from open to closed ¹⁴. Cranial sutures were specifically included in this method as isolated crania are often found in both archaeological and forensic contexts; in these instances suture analysis can still provide some information even though cranial suture closure is not very reliable ⁴.

New scoring stages were developed for the pubic symphysis and auricular surface, mostly following morphological traits described in the literature prior to the mid-1990s ^{14,104}. The pubic symphysis and sacroiliac joint record both left and right sides separately. Three of the five components of the pubic symphysis refer to the characteristics on the symphyseal face, with the remaining two referring to the ventral and dorsal margins and immediately adjacent areas ¹⁴. These components resemble the method established by McKern and Stewart ^{10,14}. Six of the nine components of the sacroiliac joint describe aspects on the auricular-shaped articular surface of the ilium, while the remaining three components refer to different parts of the auxiliary retroauricular surface that serves as ligament attachment ¹⁴. The descriptions used for the sacroiliac joint resemble those developed by Lovejoy *et al.* ⁴⁴, but are divided into separately scored components as opposed to utilising the entire surface ¹⁴ as seen in Schmitt ⁹⁴ as well as Buckberry and Chamberlain ²⁹. The method was designed to accommodate fragmentary remains and thus does not require a complete set of observations to be available ^{4,14}.

In addition to developing new scoring techniques, two old age traits were also identified that make the method more successful when estimating age-at-death for older age ranges. The presence of these old age traits, namely the breakdown stage of the dorsal margin of the symphysis and the widely and thickly distributed exostoses on the retroauricular surface, are indicative of old age. However, the lack of these traits does not necessarily indicate a young individual. These two old age traits reportedly allow transition analysis to achieve the previously impossible; the estimation of ages from older individuals and provision of an age range that enables the quantification of uncertainty ^{4,104}.

2.4.2. Statistical approach

Transition analysis assumes that all features from the cranial sutures, the pubic symphysis and the sacroiliac joint are correlated only through age and thus are conditionally, with the elimination of age, independent of each other. It is expected, however, that neighbouring features might be correlated with each other independent of the effect of age ⁴. The conditional independence of a trait entering into a stage allows for a combined likelihood function to be formed from the three separate likelihood functions obtained from the three separate skeletal elements ^{4,14}. The likelihood based confidence interval is calculated from the Z-score of the natural logarithm ⁴. Thus, the method produces a point estimate from the maximum likelihood estimate and an age range, based on a 95% confidence interval. Both the point estimate and age range are dependent on the individual traits available to be scored ^{14,103,104}. Log distributions are specifically used as they eliminate the occurrence of extremely young ages-at-transition ²⁴. One cannot argue that conditional independence is reflected in the biology of all skeletal traits, especially those attributed to development, but even if the assumption of conditional independence is incorrect the method still produces asymptotically unbiased point estimates with only the confidence intervals effectively becoming narrower ^{4,14}. The narrow confidence intervals are corrected by widening the shape of the likelihood surfaces ¹⁴.

Each feature is scored according to separate individual components that follow an age-related trajectory of invariant, unidirectional, distinct and non-overlapping sequence of stages. If a feature has only two possible stages, it will be scored as a

binomial random variable with age as the only parameter. If a feature has more than two stages a binary contrast is constructed between individuals who have concluded the transition and those who have not. Each stage of morphology has a different average age, with a younger age at a lower stage, but the standard deviation is the same for all stages, even though developmental biology suggests that the standard deviation should increase with each stage. The method does not simply produce a point estimate of the most likely age-at-death, but rather produces a probability distribution of death occurring at each possible age, producing a better representation⁴. In a case where all component stages are in the terminal state or the beginning state, the point estimate will shift to the maximum or minimum likelihood for the range (15 or 110 years), respectively. This is usually observed when very few observable components are present and the actual point estimate is usually more central than the calculated likelihood value¹⁴. The consistency of the trait scores is evaluated to take note of unlikely combinations, possibly indicating commingling or observer error⁴.

2.4.3. Prior distributions

Prior distributions are model age-at-death distributions from the population at large that can be used to draw reasonable assumptions during age-at-death estimations²⁴. Prior distributions are usually obtained from mortality profiles from model reference samples or from independent documentary information. All death distribution information does not fit all contexts, for example, age-at-death information obtained from coroner records will be reasonable models for death from accident, suicide or homicide but would not provide helpful assumptions when dealing with deaths from wars or genocides²⁴.

When the age estimation is influenced by the age distribution of the reference sample, the reference sample is acting as a prior distribution²⁴. To negate the effect of the reference sample distribution, transition analysis makes use of either a uniform (uninformative) prior distribution or independent documentary information^{4,14}. Population patterns for age-at-death are not imposed on the data when using a uniform prior distribution, instead the likelihood of each age-at-death is equal, leading to overestimations at older ages^{4,14}. However, according to the Gompertz law of mortality the human death rate increases exponentially with age, realistically

making an age of 130 years less likely than that of 80 years ¹⁰⁵. An informative prior distribution represents the likelihood of each age-at-death by considering model population age-at-death patterns. An example of an informative prior distribution would be a Gompertz mortality graph representing age-at-death from a Danish population as seen in Figure 2.12. Relevant, independent population information makes for good prior distributions. Such information is incorporated into the transition analysis method and comes from an age-of-death distribution from 17th century Danish rural parish records for use in archaeological contexts and homicide data from 1996 USA for use in forensic contexts ^{4,14}.

Depending on the selection of skeletal features used with the method, there is not always a noticeable difference between the estimates using the uniform prior distribution contrasting with the informative prior distribution ⁴. Although the informative prior distribution sometimes produces better results, it also clouds population mortality rates when this is the goal of the analysis ¹⁴.

2.4.4. Success of transition analysis

The quality of the age estimates calculated with the transition analysis method has been evaluated by correlation with known age. Correlation with age for the pubic symphysis was 0.86, correlation for the sacroiliac joint 0.82, correlation for the cranial sutures 0.66 and correlation for the combination of all three skeletal features 0.88. Not only does the correlation with age improve with an increase in indicators, but also the quality of the age estimate is improved with multiple indicators ⁴. As with other methods of age estimation, transition analysis encounters a decrease in precision when estimating age ranges between 40 - 70 years, but age estimates are no longer open-ended, for example 50+ years. Poor 40 - 70 year age estimates are most likely linked to a lack of representative anatomical traits associated with this age period ^{14,104}. However, age estimates after 70 years become more successful with input from specifically the dorsal margin of the pubic symphysis and the exostoses on the posterior auricular surface making narrower age ranges possible ⁴.

Observations show conclusively that each collection of traits is unique and variable between individuals and variation in morphology occurs between sexes and populations. These variations could be due to genetics or lifestyle histories. Variation

is greater for a single component than the aggregate of the combined method. This variation identifies a need for the use of an appropriate reference sample ⁴.

This variation in morphology could be the cause of the poor results achieved by Bethard ¹⁰⁶ when testing transition analysis in the Bass Collection (Figure 2.13). Bethard ¹⁰⁶ achieved correlation coefficients as low as 0.173 for cranial sutures, 0.412 for the pubic symphysis and the auricular surface, 0.498 for the combined method with forensic prior distribution and 0.509 for the unmodified combined method during his test. As possible explanation for his poor success with the method Bethard ¹⁰⁶ stated the possibility that the transition analysis protocol was applied incorrectly, secular differences between the test sample and the reference sample and the inappropriateness of the prior distributions available with the ADBOU age estimation program.

Boldsen *et al.* ⁴ state the method's independence of mimicry from the reference sample as one of the significant advantages of transition analysis ^{103,104}. Thus, when Milner and Boldsen ¹⁴ conducted a validation study, they did so with a test sample they described as vastly different from the reference sample ¹⁴ (the same sample used by Bethard ¹⁰⁶ in his test). The reference sample contained individuals who lived mostly before World War II and who lived physically demanding lives with poor medical care and low socio-economic status. This contrasted with the test sample, which contained individuals who lived mostly after World War II and had a comparatively prosperous status. The research concluded that transition analysis can be successfully applied in samples other than the early 20th-century reference sample, but notably the age intervals provided were of such a wide nature that they were of little practical use as illustrated in Figures 2.14 to 2.18. In addition to this, the cranial suture segments displayed a tendency to underestimate individuals older than 40 years and not only produced very long interval lengths, but also often imposed point estimates of 110 years when all scores were in terminal stages (Figure 2.14). These attributes of the cranial suture segments have limited value and produce poor accuracy and precision. The sacroiliac joint also revealed a tendency to underestimate individuals in age categories older than 60 years (Figure 2.16). It is promising, however, that the combined procedure improves both accuracy and precision, although estimates calculated with both the uniform and Danish prior

distributions underestimated individuals in the 70 and older age ranges (Figures 2.17 and 2.18)¹⁴.

Another vastly different test sample, two Mexican skeletal collections, was used by Bullock *et al.*¹⁰⁷ to compare transition analysis to traditional age estimation methods. Although Bullock *et al.*¹⁰⁷ concluded that transition analysis fared better where older individuals were concerned and addressed the problem of reference sample mimicry, they were unsatisfied by the degree of accuracy and precision provided by transition analysis. Large differences between the population construct for the Mexican samples and the available prior distributions were also a concerning factor¹⁰⁷.

Despite conflicting results from the few validation studies, transition analysis has been used as the primary method of adult age estimation in some archaeological investigations^{108,109}. Although the primary goal of these investigations were respectively to determine the link between bone mineral density and multiparity¹⁰⁸ and the link between childhood stress and adult age mortality¹⁰⁹ and not a palaeodemography study, the use of transition analysis for age estimation played a prominent role in these determinations.

Table 2.1: Age categories with corresponding biological age indicators ⁴²

Age category	Age range	Biological indicators
Onset of adulthood	20 years	Third molars emerged; roots completed development; majority of epiphyses fused to metaphyses
Young adult	20 - 25 years	Sternum, iliac crest, ischial tuberosity and vertebral end plates fusing
Middle adult	25 - 35 years	Medial clavicle and first and second sacral vertebrae fusing; metamorphosis of pubic symphysis and auricular surface
Mature adult	35 - 45 years	All late fusing epiphyses fused; metamorphosis of pubic symphysis, auricular surface and sternal rib ends
Older adult	46+ years	Degeneration of pubic symphysis, auricular surface and sternal rib ends

Table 2.2: Four category cranial suture scores ^{1,48,62}

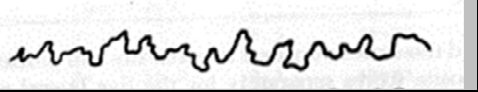
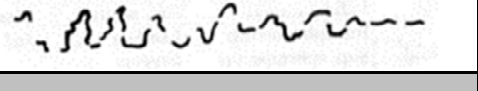

Score	Progress of suture	Sketch
0	Open/No sign of ectocranial closure	
1	Minimal closure/Any minimal to moderate closure (up to 50%)	
2	Significant closure/Marked degree of closure but some portions not completely fused	
3	Complete fusion/Obliteration	

Table 2.3: Five category cranial suture scores ^{10,26,61}

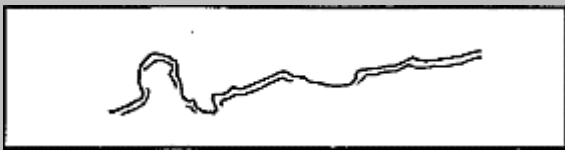
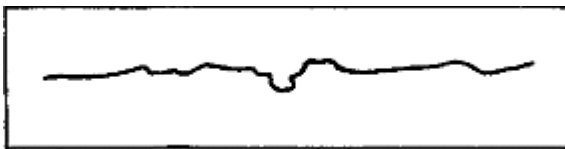
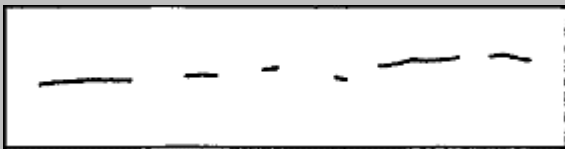
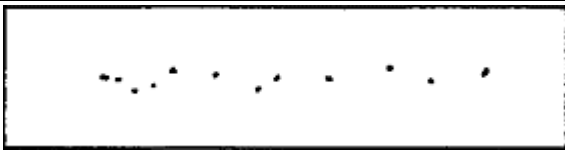

Score	Progress of suture	Alternate description	Sketch
0	Open suture	Open suture; there is still a little space left between the adjoining bones	
1	One-quarter closed	Suture is closed, but clearly visible as a continuous, zigzagging line	
2	One-half closed	Suture line becomes thinner, has less zigzags and may be interrupted by complete closure	
3	Three-quarters closed	Only pits indicate where the suture is located	
4	Completely closed	Suture completely obliterated, even its location cannot be recognised	

Table 2.4: Todd & Lyon's ²⁶ timing for endocranial suture closure in white males

Suture	Age of closure commencement (years)	Age of closure complete (years)
Vault sutures		
Sagittal	22/23	35
Coronal – pars bregmatica & complicate	24	38
Coronal – pars pterica	26	41
Lambdoid – pars lambdoidea & media	26	42
Lambdoid – pars asterica	26	47
Circummeatal sutures		
Masto-occipital – pars superior & middle	30	81
Masto-occipital – pars inferior	26	72
Spheno-temporal – pars inferior	30	67
Spheno-temporal – pars superior	31	64
Squamous	37	Never complete
Parieto-mastoid	37	81
Accessory sutures		
Spheno-parietal	29	65
Spheno-frontal – lesser wing	22	64
Spheno-frontal – greater wing	22	65

Table 2.5: Sutures rejected by Meindl & Lovejoy ⁴⁸ due to restricted value

Sutures rejected by Meindl and Lovejoy	Reason for rejection
Parietomastoid suture	Not commonly found in sample and not clearly associated with age
Squamousal point	Least amount of age-related information
Occipitomastoid point	Poor age-related information
Zygomatic & Malar points	Difficult to score creating inter-observer error and bilateral asymmetry
Frontolacrimal & Frontoethmoid points	Difficult to observe and likely damaged post-mortem

Table 2.6: Acsádi and Nemeskéri age estimation from suture closure ²⁷

Mean closure score	Average age (years)	Mean deviation (years)	Range (years)
0.4 - 1.5	28.6	13.08	15 - 40 juvenile/young adult
1.6 - 2.5	43.7	14.46	30 - 60 young adult/middle adult
2.6 - 2.9	49.1	16.40	35 - 65 young adult/middle adult
3.0 - 3.9	60.0	13.23	45 - 75 middle adult/old adult
4.0	65.4	14.05	50 - 80 middle adult/old adult

Table 2.7: Todd's pubic symphyseal phases for white males ^{1,25,62}

Phase	Age class	Age range (years)	Description
I	Post-adolescent phases	18 - 19	Symphysial surface rugged, traversed by horizontal ridges separated by well-marked grooves; no ossific (epiphyseal) nodules fusing with the surface; no definite delimiting margin; no definition of extremities
II		20 - 21	Symphysial surface still rugged, traversed by horizontal ridges, the grooves between which are, however, becoming filled near the dorsal limit with a new formation of finely textured bone. This formation begins to obscure the hinder extremities of the horizontal ridges. Ossific (epiphyseal) nodules fusing with the upper symphyseal face may occur; dorsal limiting margin begins to develop; no delimitation of extremities; foreshadowing of ventral bevel
III		22 - 24	Symphysial face shows progressive obliteration of ridge and furrow system; commencing formation of the dorsal plateau; presence of fusing ossific (epiphyseal) nodules; dorsal margin gradually becoming more defined; bevelling as a result of ventral rarefaction becoming rapidly more pronounced; no delimitation of extremities
IV	Build-up phases	25 - 26	Great increase of ventral bevelled area; corresponding diminution of ridge and furrow formation; complete definition of dorsal margin through the formation of the dorsal plateau; commencing delimitation of lower extremity
V		27 - 30	Little or no change in symphyseal face and dorsal plateau except that sporadic and premature attempts at the formation of ventral rampart occur; lower extremity, like the dorsal margin, is increasing in clearness of definition; commencing formation of upper extremity with or without the intervention of a bony (epiphysial) nodule
VI		30 - 35	Increasing definition of extremities; development and practical completion of ventral rampart; retention of granular appearance of symphyseal face and ventral aspect of pubis; absence of lipping of symphyseal margin
VII	Degenerative phases	35 - 39	Changes in symphyseal face and ventral aspect of pubis consequent upon diminishing activity; commencing bony outgrowth into attachments of tendons and ligaments, especially the gracilis tendon and sacro-tuberous ligament
VIII		39 - 44	Symphysial face generally smooth and inactive; ventral surface of pubis also inactive; oval outline complete or approximately complete; extremities clearly defined; no distinct "rim" to symphyseal face; no marked lipping of either dorsal or ventral margin
IX		45 - 50	Symphysial face presents a more or less marked rim; dorsal margin uniformly lipped; ventral margin irregularly lipped
X		50+	Symphysial face eroded and showing erratic ossification; ventral border more or less broken down; disfigurement increases with age

Table 2.8: Todd's pubic symphyseal metamorphosis for age estimation of females ²³

Phase	Age range (years)	Description
I	16+	Symphyseal surface rugged, traversed by horizontal ridges separated by well-marked grooves, there being no distinction in size between the upper and the lower ridges and the whole pattern being more delicate than the male. No bony (epiphyseal) nodules fusing with the surface. No definite delimiting margin. No definition of extremities.
II	-25	Symphyseal face still rugged. The horizontal grooves are becoming filled near their dorsal limit with new finely textured bone. Bony (epiphyseal) nodules fusing with upper symphyseal face. Dorsal delimiting margin begins to develop. No delimitation of extremities. Ventral bevel commencing.
III	25 - 26	Symphyseal face shows progressive obliteration of ridge and furrow system. Commencing formation of dorsal platform. Possible presence of bony nodules. Dorsal margin becoming more defined and sharply lipped. Ventral bevel more pronounced. Extremities not delimited.
IV	26 - 27	Great increase of ventral bevel area. Corresponding diminution of ridge and furrow formation. Complete definition of dorsal margin through the formation of the dorsal platform. Commencing delimitation of lower extremity.
V	27 - 30	Relatively small change in symphyseal face and dorsal platform except for sporadic efforts at the formation of a ventral rampart. Dorsal margin increasingly clearly defined and more sharply lipped. Lower extremity better defined. Upper extremity forming with or without the intervention of a bony (epiphyseal) nodule.
VI	30 - 36	Increasing definition of extremities. Development and practical completion of ventral rampart. Retention to a small degree of granular appearance of symphyseal face indicating that activity has not yet quite ceased. Failure of ventral aspect of pubis adjacent to ventral rampart to become transformed into a compact surface. Because of this the rampart is more or less undermined. Retention of pectinate outline of dorsal margin and in slight degree of ridge and furrow system. No lipping of ventral margin and no increased lipping of dorsal margin.
VII	36 - 40	Slight changes in symphyseal face and marked changes in ventral aspect consequent upon diminishing activity. No formation of symphyseal rim. No ossification of tendinous and ligamentous attachments. The lower age limit is approximate but the upper is more exactly defined by the material.
VIII	40 - 45	Symphyseal face and ventral aspect of pubic bone generally smooth and inactive. Oval outline complete. Extremities clearly defined. No lipping of ventral or increased lipping of dorsal margin. Development of ossification in tendinous and ligamentous attachment especially those of sacro-tuberous ligament and gracilis muscle.
IX	45 - 50	Symphyseal face presents a more or less marked rim. No lipping of ventral and no further lipping of dorsal margin. No secondary corrosion or rarefaction.
X	50+	Ventral margin eroded a greater or less extent of its length, continuing somewhat into the symphyseal face. No increased lipping. Disfigurement only occasional and slight.

Table 2.9: Acsádi-Nemeskéri pubic symphysis age estimation method ^{27,37}

Acsádi-Nemeskéri Phase	Description	Corresponding ages (years)
I	The surface is convex, traversed by horizontal ridges and furrows; curved transition in the region of the rami	18 - 45
II	The original structure of the surface begins to disappear with ridges becoming flatter and grooves shallower. Ventral and dorsal margins show rim formation; also bordering in the region of the rami	23 - 69
III	The original structure is present on the surface in granular remnants only; a continuous rim is forming on the ventral and dorsal margins; a well-defined border appears in the region of the rami	25 - 76
IV	The symphyseal face has become completely smooth; a sharp rim has developed along the ventral and dorsal margins; the inferior end of the face terminates in a ridge forming an acute angle	24 - 81
V	The completely smooth surface is partly concave, sunken inwards, porous and shrivelled. The fully developed ventral and dorsal rim rises above the surface like a crest, and surrounds it together with the sharp lower extremity	41 - 86

Table 2.10: McKern and Stewart's component stages ¹⁰

Component I – Dorsal demi-face		Component II – Ventral demi-face		Component III – Symphyseal rim	
Stage	Description	Stage	Description	Stages	Description
0	Dorsal margin absent	0	Ventral bevelling is absent	0	The symphyseal rim is absent
1	A slight margin formation first appear in the middle third of the dorsal border	1	Ventral bevelling is present only at superior extremity of ventral border	1	A partial dorsal rim is present, usually at the superior end of the dorsal margin, it is round and smooth in texture and elevated above the symphyseal surface
2	The dorsal margin extends along entire dorsal border	2	Bevel extends inferiorly along ventral border	2	The dorsal rim is complete and the ventral rim is beginning to form. There is no particular beginning site
3	Filling in of grooves and resorption of ridges to form a beginning plateau in the middle third of the dorsal demi-face	3	The ventral rampart begins by means of bony extensions from either or both of the extremities	3	The symphyseal rim is complete. The enclosed symphyseal surface is finely grained in texture and irregular of undulating in appearance
4	The plateau, still exhibiting vestiges of billowing, extends over most of the dorsal demi-face	4	The rampart is extensive but gaps are still evident along the earlier ventral border, most evident in the upper two-thirds	4	The rim begins to break down. The face becomes smooth and flat and the rim is no longer round but sharply defined. There is some evidence of lipping on the ventral edge
5	Billowing disappears completely and the surface of the entire demi-face becomes flat and slightly granulated in texture	5	The rampart is complete	5	Further breakdown of the rim (especially along the superior ventral edge) and rarefaction of the symphyseal face. There is also disintegration and erratic ossification along the ventral rim

Table 2.11: Gilbert & McKern's component stages ²³

Component I – Dorsal demi-face		Component II – Ventral rampart		Component III – Symphyseal rim	
Stage	Description	Stage	Description	Stage	Description
0	Ridges and furrows very distinct, ridges are billowed, dorsal margin undefined.	0	Ridges and furrows very distinct. The entire demi-face is bevelled up toward the dorsal demi-face.	0	The rim is absent.
1	Ridges begin to flatten, furrows to fill in, and a flat dorsal margin begins in mid-third of demi-face.	1	Beginning inferiorly, the furrows of the ventral demi-face begin to fill in, forming an expanding bevelled rampart, the lateral edge of which is a distinct, curved line extending the length of the symphysis.	1	The rim begins in the mid-third of the dorsal surface.
2	Dorsal demi-face spreads ventrally, becomes wider as flattening continues, dorsal margin extends superiorly and inferiorly.	2	Fill in of furrows and expansion of demi-face continue from both superior and inferior ends, rampart spreads laterally along its ventral edge.	2	The dorsal part of the symphyseal rim is complete.
3	Dorsal demi-face is quite smooth, margin may be narrow or indistinct from face.	3	All but about one-third of ventral demi-face is filled in with fine grained bone.	3	The rim extends from the superior and inferior ends of the symphysis until all but about one-third of the ventral aspect is complete.
4	Demi-face becomes complete and unbroken, is broad and very fine grained, may exhibit vestigial billowing.	4	The ventral rampart presents a broad, complete, fine grained surface from the pubic crest to the inferior ramus.	4	The symphyseal rim is complete.
5	Demi-face becomes pitted and irregular through rarefaction.	5	Ventral rampart may begin to break down, assuming a very pitted and perhaps cancellous appearance through rarefaction.	5	Ventral margin of dorsal demi-face may break down so that gaps appear in the rim, or it may round off so that there is no longer a clear dividing line between the dorsal demi-face and the ventral rampart.

Table 2.12: Suchey and Brook's ³⁷ phases for estimating age at death from the pubic symphysis, developed from the Todd method







Suchey-Brooks phase	Line drawings representing each phase ¹⁰¹	Unisex description of phase
I		Symphyseal face has a billowing surface (ridges and furrows) which usually extends to include the pubic tubercle. The horizontal ridges are well-marked and ventral bevelling may be commencing. Although ossific nodules may occur on the upper extremity, a key to recognition of this phase is the lack of delimitation of either extremity (upper or lower).
II		The symphyseal face may still show ridge development. The face has commencing delimitation of lower/upper extremities occurring with or without ossific nodules. The ventral rampart may be in beginning phases as an extension of the bony activity at either or both extremities.
III		Symphyseal face shows lower extremity and ventral rampart in process of completion. There can be a continuation of fusing ossific nodules forming the upper extremity and along the ventral border. Symphyseal face is smooth or can continue to show distinct ridges. Dorsal plateau is complete. Absence of lipping of symphyseal dorsal margin; no bony ligamentous outgrowths.
IV		Symphyseal face is generally fine grained although remnants of the old ridge and furrow system may still remain. Usually the oval outline is complete at this stage, but a hiatus can occur in upper ventral rim. Pubic tubercle is fully separated from the symphyseal face by definition of upper extremity. The symphyseal face may have a distinct rim. Ventrally, bony ligamentous outgrowths may occur on inferior portion of pubic bone adjacent to symphyseal face. If any lipping occurs it will be slight and located on the dorsal border.
V		Symphyseal face is completely rimmed with some slight depression of the face itself, relative to the rim. Moderate lipping is usually found on the dorsal border with more prominent ligamentous outgrowths on the ventral border. There is little or no rim erosion. Breakdown may occur on superior ventral border.
VI		Symphyseal face may show ongoing depression as rim erodes. Ventral ligamentous attachments are marked. In many individuals the pubic tubercle appears as a separate bony knob. The face may be pitted or porous, giving an appearance of disfigurement with ongoing process of erratic ossification. Crenulations may occur. The shape of the face is often irregular at this stage.

Table 2.13: Meindl *et al.*'s³¹ condensed Todd method for pubic symphyseal age estimation

Meindl <i>et al.</i> 's biological phases	Corresponding Todd stage
Pre-epiphyseal	I, II, III, IV, V
Active epiphyseal	VI
Immediate post-epiphyseal	VII
Maturing pre-degenerative	VIII
Degenerative	IX, X

Table 2.14: Description of auricular surface features⁴⁴

Surface feature	Description
Grain and density	Granulation becomes more coarse with age and is lost with old age; proceeding from fine grain to coarse grain to compact (densification)
Macroporosity	Might not present with macroporosity; general indication of age when present; covers a greater portion of surface than subchondral defects
Billowing	Not as defined as pubic billowing; rather presents as regular, transverse undulations in youth
Striations	Differ from billows only in degree; striae remain on the lower demiface after a decrease in billows
Apex	Edge of the apex sharp and distinct; after 35 years arthritic lipping broadens the margin; margin extension not an age indicator (enhanced by preauricular sulcus in females)
Retroauricular area	Smooth, undifferentiated in youth becomes increasingly porotic and osteophytic in older individuals
Transverse organisation	Antero-posterior organisation of billows and striae in youth; loses this organisation in older individuals even if billows and striae are still present

Table 2.15: Phase description for auricular surface method of age estimation ⁴⁴

Phase	Age range (years)	Description
Early post-epiphyseal phase	20 - 24	Surface displays fine granular texture and marked transverse organisation; no retro-auricular activity, apical activity or porosity; broad well-defined billows covers most of the surface with definitive transverse organisation; subchondral defects are smooth-edged and rounded; <i>billowing and fine granularity</i>
Young adult phase	25 - 29	Slight to moderate loss of billowing, replacement by striae; no apical activity, porosity or retro-auricular activity; marked transverse organisation; granulation slightly more coarse; <i>reduction of billowing, but retention of youthful appearance</i>
	30 - 34	Loss of transverse organisation on both faces; billowing much reduced, replaced by striae; more coarsely granular; no significant changes at apex; areas of microporosity; slight retroauricular activity; <i>general loss of billowing, replacement by striae and distinct coarsening of granularity</i>
Mid adult phase	35 - 39	Coarse uniformly granulated faces; reduction of billowing and striae; transverse organisation poorly defined; slight activity in retroauricular area; slight microporosity; minimal changes at apex; no macroporosity; <i>uniform coarse granularity</i>
	40 - 44	No billowing; some vague striae may persist; coarsely granular; loss of transverse organisation; partial densification; moderate activity in retroauricular area; occasional macroporosity; <i>transition from coarse granularity to dense surface, this may take part over islands of the surface of one or both demifaces</i>
Early senescent phase	45 - 49	Significant loss of granulation replaced by dense bone; no billows or striae; apex activity slight to moderate; no transverse organisation; microporosity lost; irregular margins; little or no macroporosity; moderate retroauricular activity; <i>completion of densification with complete loss of granularity</i>
	50 - 59	Marked surface irregularity; no transverse organisation; may retain some granularity; no striae or billows; inferior face becomes lipped and extends past the innominate bone; apical changes present and may be marked; irregularity of margins; macroporosity; retroauricular activity moderate to marked; <i>dense irregular surface of rugged topography and moderate to marked activity in Periauricular areas</i>
Breakdown	55 - 60	Nongranular, irregular surface; distinct signs of subchondral destruction; no transverse organisation; macroporosity present; apical activity marked; margins irregular and lipped; retroauricular surface osteophytic; <i>breakdown with marginal lipping</i>

Table 2.16: Osborne's revised auricular surface age estimation ³³

Phase	Morphological Features
1	Billowing with possible striae; mostly fine granularity with some coarse granularity possible
2	Striae; coarse granularity with residual fine granularity; retroauricular activity may be present
3	Decreased striae with transverse organization; coarse granularity; retroauricular activity present beginnings of apical change
4	Remnants of transverse organisation; coarse granularity becoming replaced by densification; retroauricular activity present; apical change; macroporosity present
5	Surface becomes irregular; surface texture is largely dense; moderate retroauricular activity; moderate apical change; macroporosity
6	Irregular surface; densification accompanied by subchondral destruction; severe retroauricular activity; severe apical change; macroporosity

Table 2.17: Stage descriptions for Buckberry and Chamberlain's method of age estimation from the auricular surface²⁹

Feature	Definition	Score description
Transverse organisation	Refers to the horizontal billows and striae that run from the medial to the lateral margins of the auricular surface	1- 90% or more of the surface is transversely organised
		2- 50 - 89% of the surface is transversely organised
		3- 25 - 49% of surface is transversely organised
		4- Transverse organisation is present on less than 25% of surface
		5- No transverse organisation is present
Surface texture	Finely grained in early life and then becoming more coarsely granular and densified. Finely granular bone is considered less than 0.5mm in diameter and coarsely granular bone is considered over 0.5mm in diameter. Dense bone refers to the surface appearance such as nodules or areas of bone that are compact and smooth	1- 90% or more of surface is finely granular
		2- 50 - 89% of surface is finely granular; replacement of finely granular bone by coarsely granular bone in some areas; no dense bone is present
		3- 50% or more of surface is coarsely granular, but no dense bone is present
		4- Dense bone is present, but occupies less than 50% of surface; this may be just one small nodule of dense bone in very early stages
		5- 50% or more of surface is occupied by dense bone
Microporosity	Porosity on the surface with a diameter less than 1mm can be localised or spread across large areas	1- No microporosity is present
		2- Microporosity is present on one demiface only
		3- Microporosity is present on both demifaces
Macroporosity	Perforations of the surface with a diameter greater than 1mm can be localised or spread across large areas; should not be confused with smooth-edged cortical defects, areas where the cortex is not complete, which can be present at any age; should not be confused with post-mortem damage, presenting with sharp, irregular edges, paler coloured with exposed trabecular bone.	1- No macroporosity present
		2- Macroporosity present on one demiface only
		3- Macroporosity present on both demifaces
Apical changes	Development of small osteophytic growths or lipping, which can alter the contour of the surface when severe	1- Apex is sharp and distinct; auricular surface may be slightly raised relative to adjacent bony surface
		2- Some lipping is present at apex, but shape of articular margin is still distinct and smooth (shape of outline of surface at apex is a continuous arc)
		3- Irregularity occurs in contours of articular surface; shape of apex is no longer a smooth arc

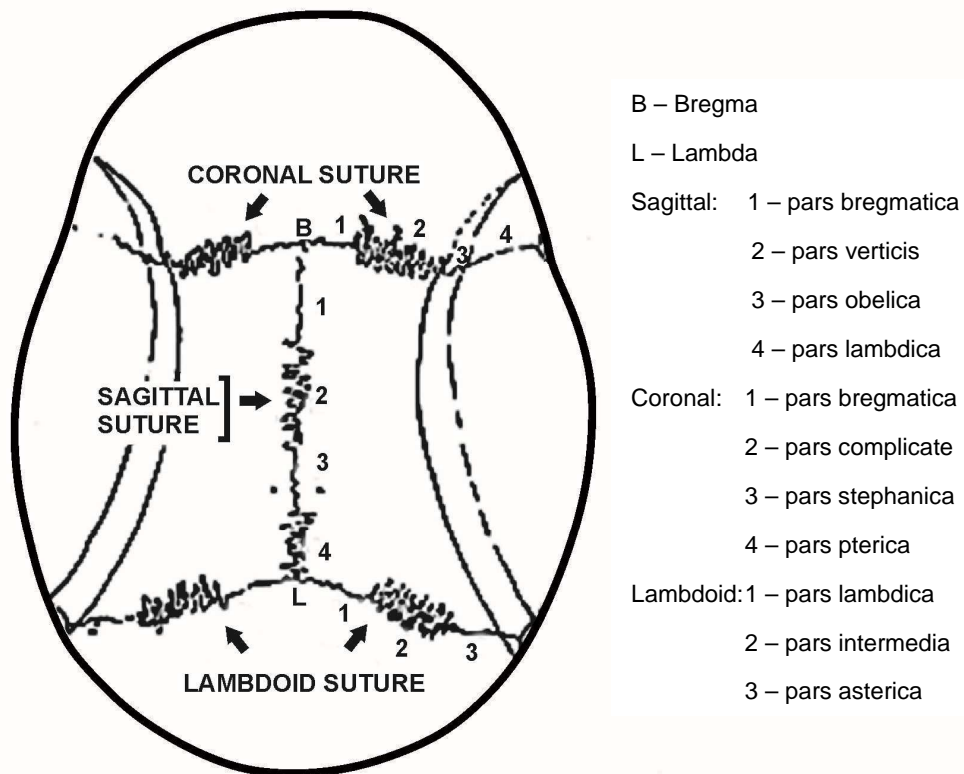


Figure 2.1: Subdivision of the vault cranial sutures used in the McKern & Stewart method ^{10,62}

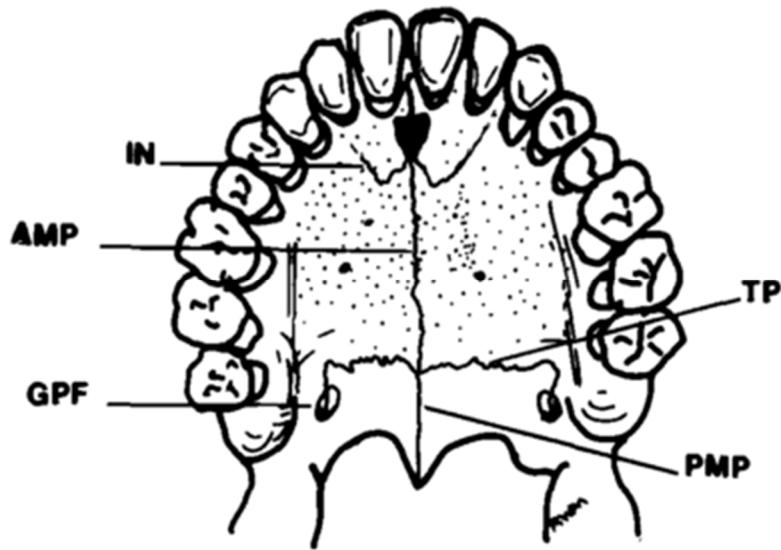


Figure 2.2: Four sutures of the bony palate used in age estimation by Mann *et al.* *Incisive suture (IN)*, *anterior median palatine suture (AMP)*, *transverse palatine suture (TP)*, *posterior median palatine suture (PMP)*, *greater palatine foramen (GPF)* ⁴³

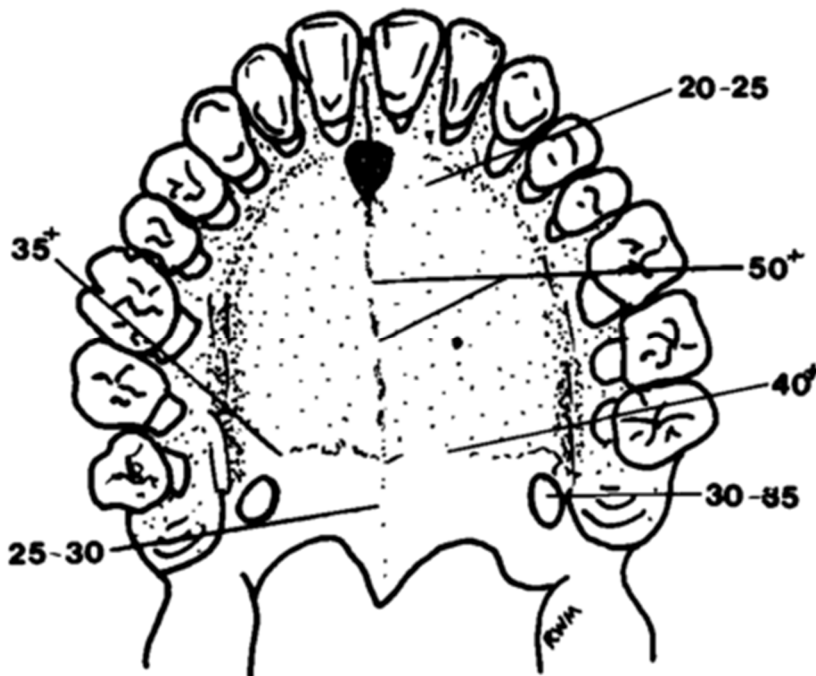


Figure 2.3: Pattern of suture obliteration for the bony palate as established by Mann *et al.* ⁴³

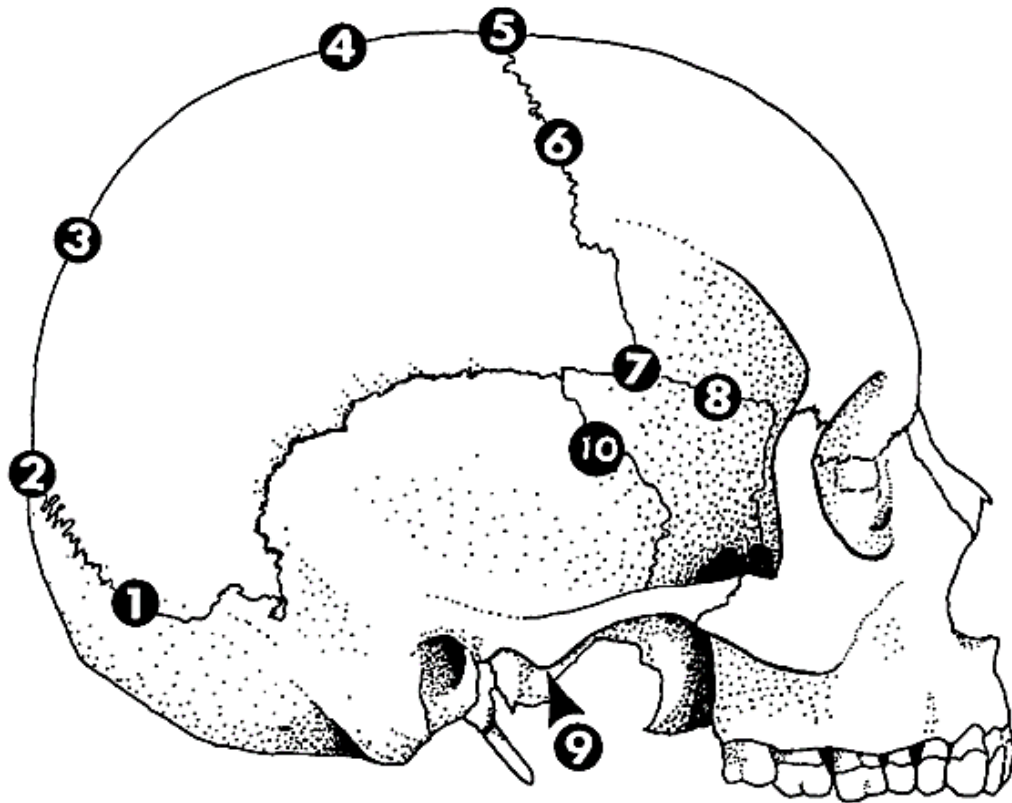


Figure 2.4: Sutures retained by Meindl & Lovejoy for their age estimation method. (1) Midlambdoid, (2) lambda, (3) obelion, (4) anterior sagittal, (5) bregma, (6) midcoronal, (7) pterion, (8) sphenofrontal, (9) inferior sphenotemporal, (10) superior sphenotemporal⁴⁸

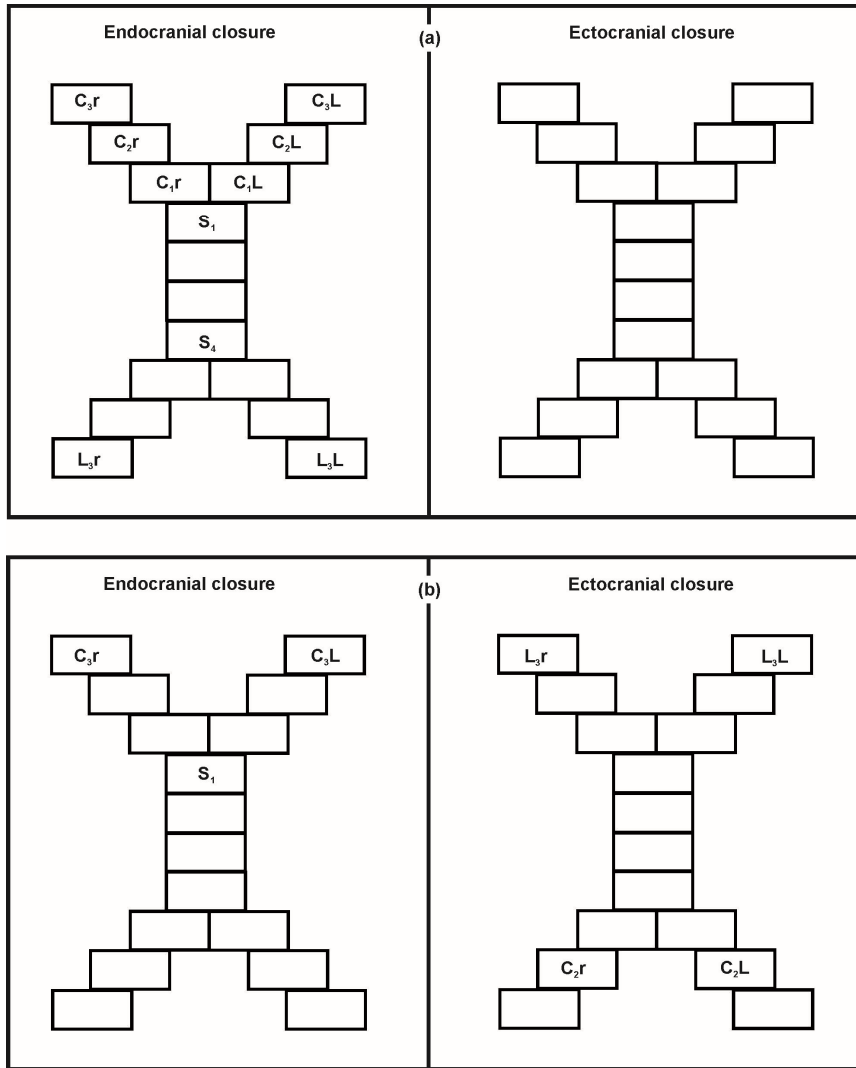


Figure 2.5: Cranial suture segments selected by Perizonius⁶¹ as relevant to indices for 20 - 49 year olds (a) and 50 - 99 year olds (b). The sutures are divided into three segments for the right coronal suture (Cr) and left coronal suture (CL) each, four segments for the sagittal suture (S) and three segments for the right lambdoid suture (Lr) and left lambdoid suture (LL) each

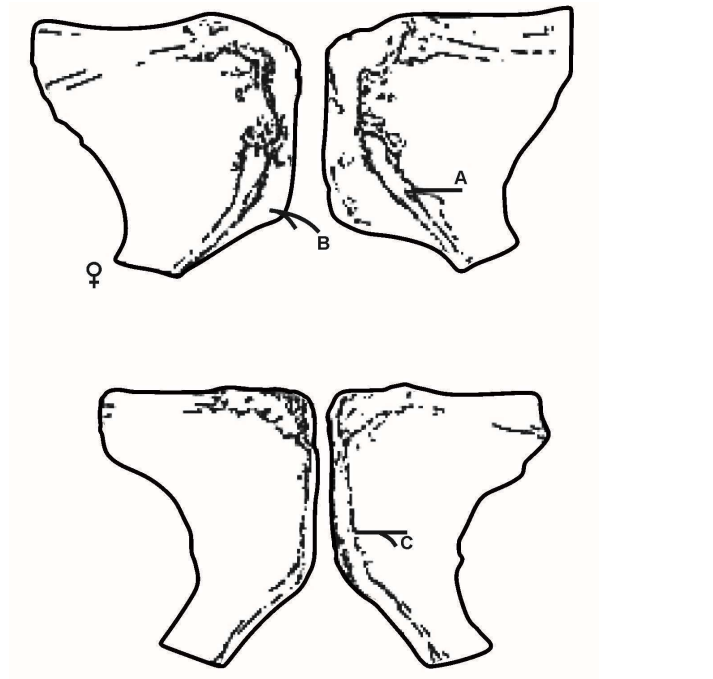


Figure 2.6: Ventral view of female pubic bones (above) compared to male (below). (A) shows the well-defined ventral arc present in females older than 25 years. The area between the ventral arc and the symphyseal rim in females (B) shows age related changes. Although males have no counterpart, a ridge parallel to the symphyseal border can be seen at (C)
78

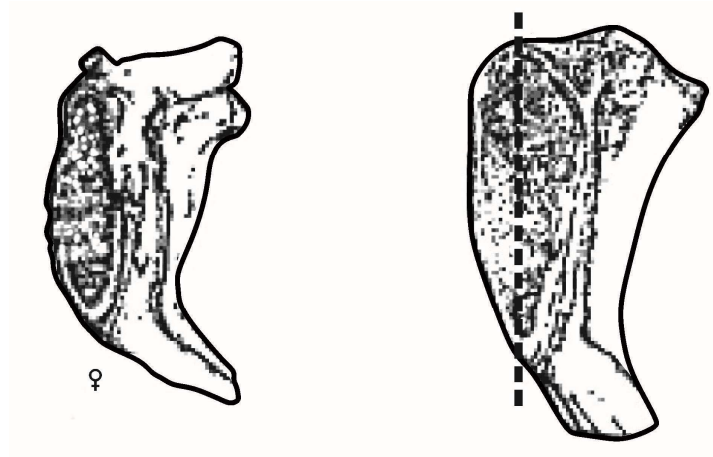


Figure 2.7: The difference of location and morphology of the ventral rampart (V) in the female (left) and the male (right). The female ventral rampart and dorsal demi-face is separated by the symphyseal rim. The male ventral rampart and dorsal demi-face are both contained within the symphyseal rim and are separated by an imaginary line⁷⁸

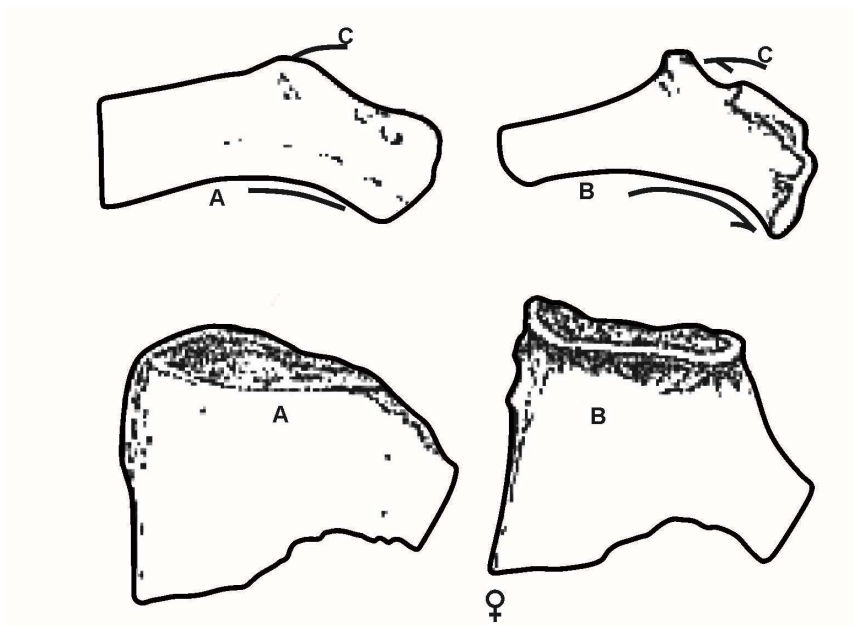


Figure 2.8: The dorsal aspect of a male pubic bone (**A**) compared to the dorsal aspect of a female pubic bone (**B**). *Pubic tubercle (C) indicated in superior view. Marked dorsal lipping is observable on the female pubic bone*⁷⁸

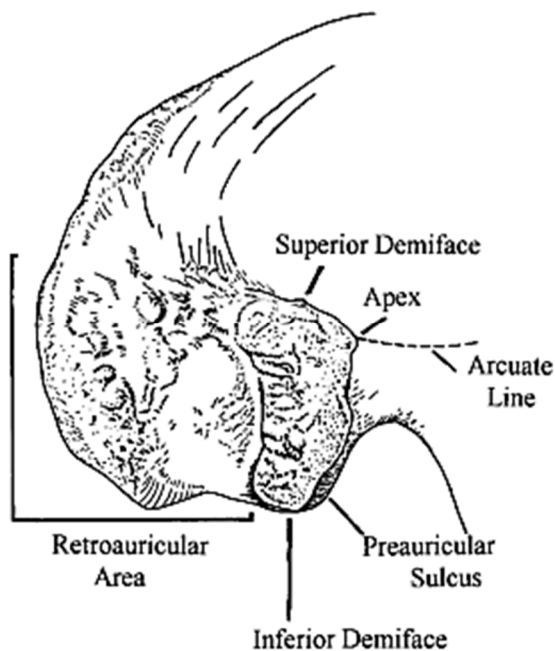


Figure 2.9: Regions of the ilium used in auricular surface age estimation^{29,44,110} **Apex:** portion of auricular surface that articulates with the posterior aspect of the arcuate line. **Superior demiface:** portion of auricular area above apex. **Inferior demiface:** portion of auricular area below apex. **Retroauricular area:** region between auricular surface and posterior inferior iliac spine.

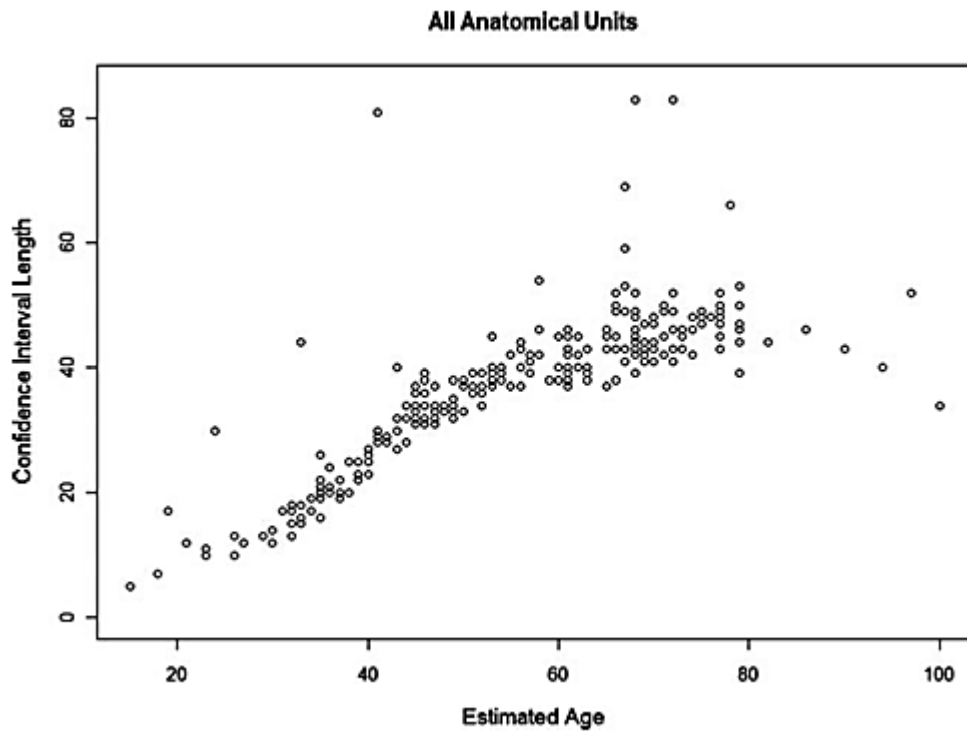


Figure 2.10: Changes in combined age estimation (uniform prior distribution) confidence interval lengths with age from Milner and Boldsen's ¹⁴ validation study

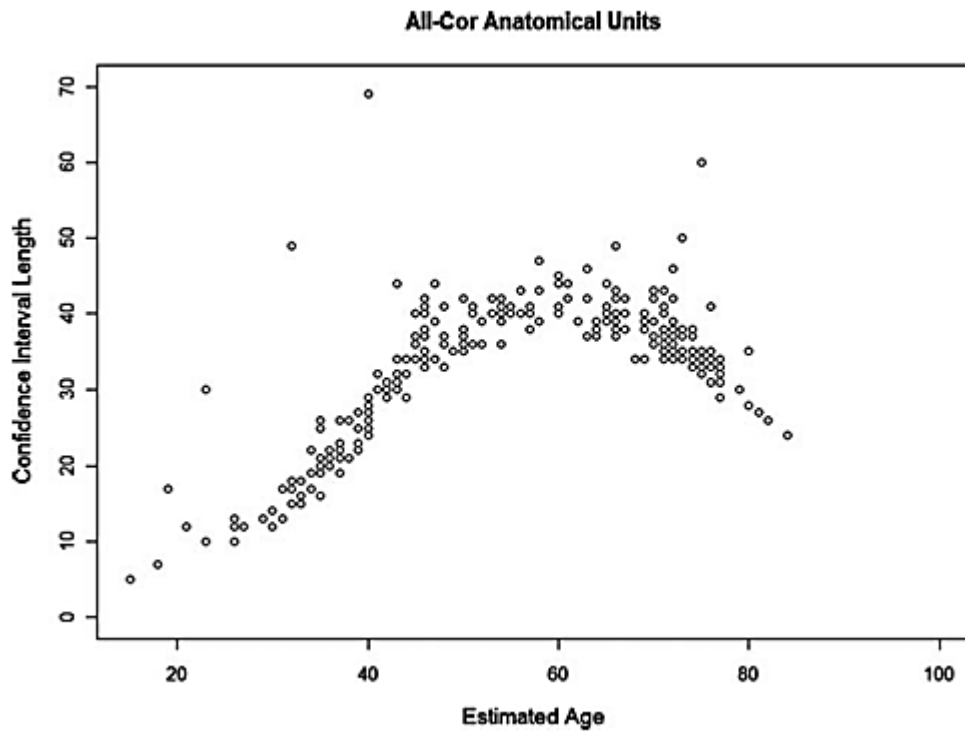


Figure 2.11: Changes in combined estimation (modified by an archaeological prior distribution) confidence interval lengths with age from Milner and Boldsen's ¹⁴ validation study

Early Modern Danish Mortality Model

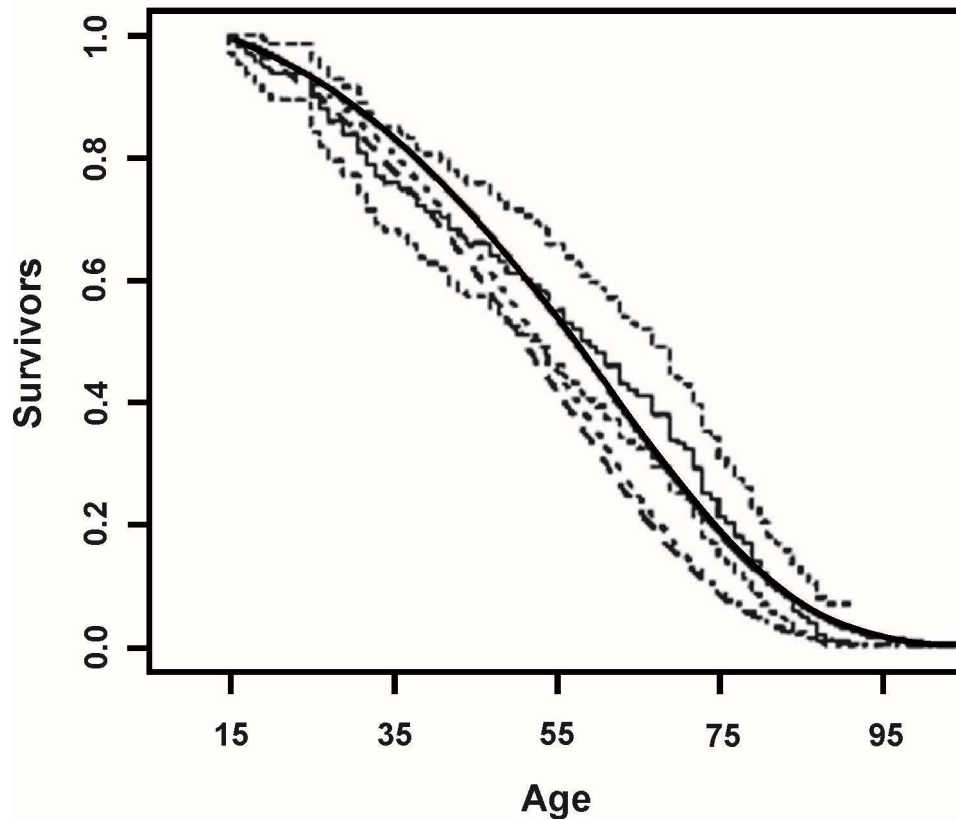


Figure 2.12: Typical prior distribution models. *The solid line represents the Gompertz mortality model from documentary information of a Danish population, the dashed line represents the Kaplan-Meier survivorship plot from the same data ¹⁴. The number of survivors per age become less likely as the age increases.*

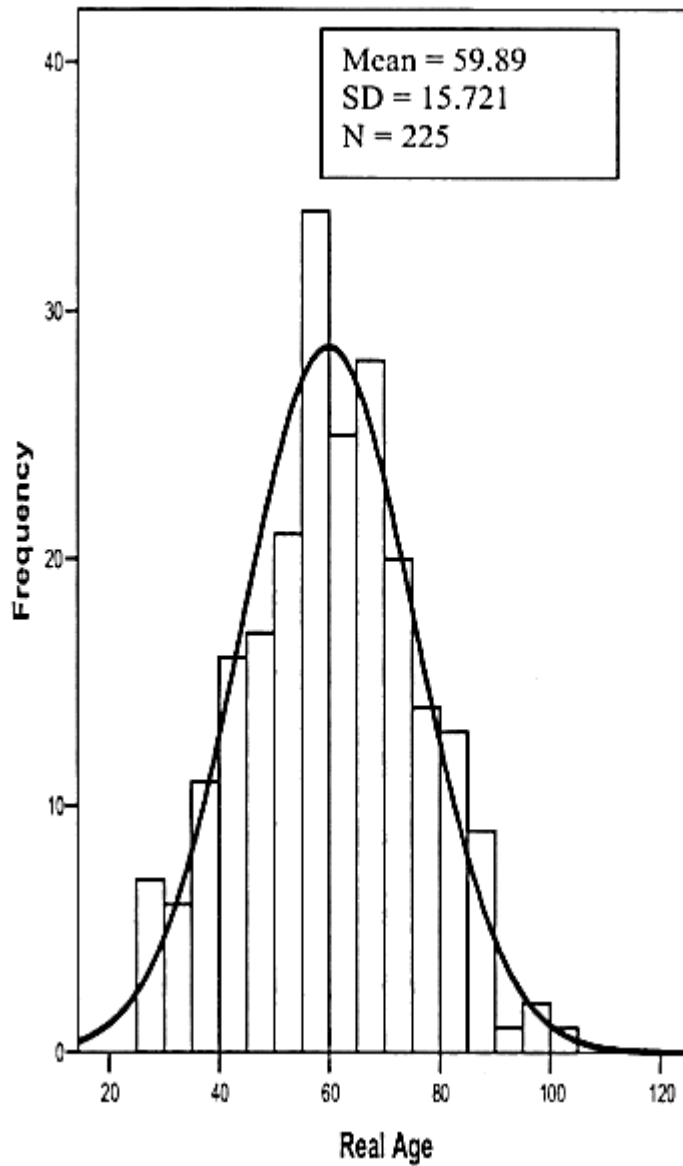


Figure 2.13: Age-at-death distribution for Bethard's ¹⁰⁶ validation study sample

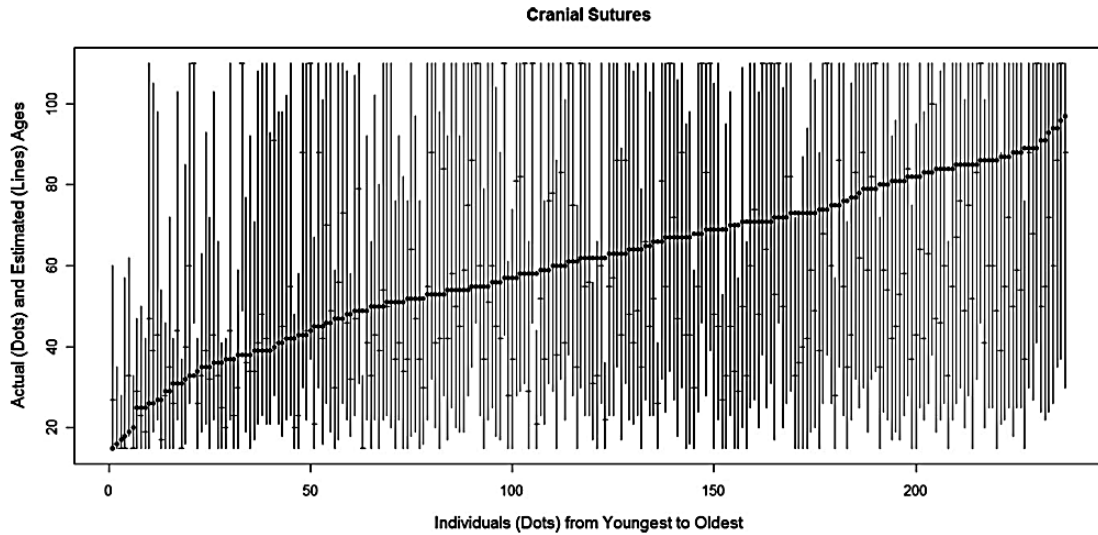


Figure 2.14: Cranial suture age estimation ranges and point values with true ages superimposed from Milner and Boldsen's ¹⁴ validation study

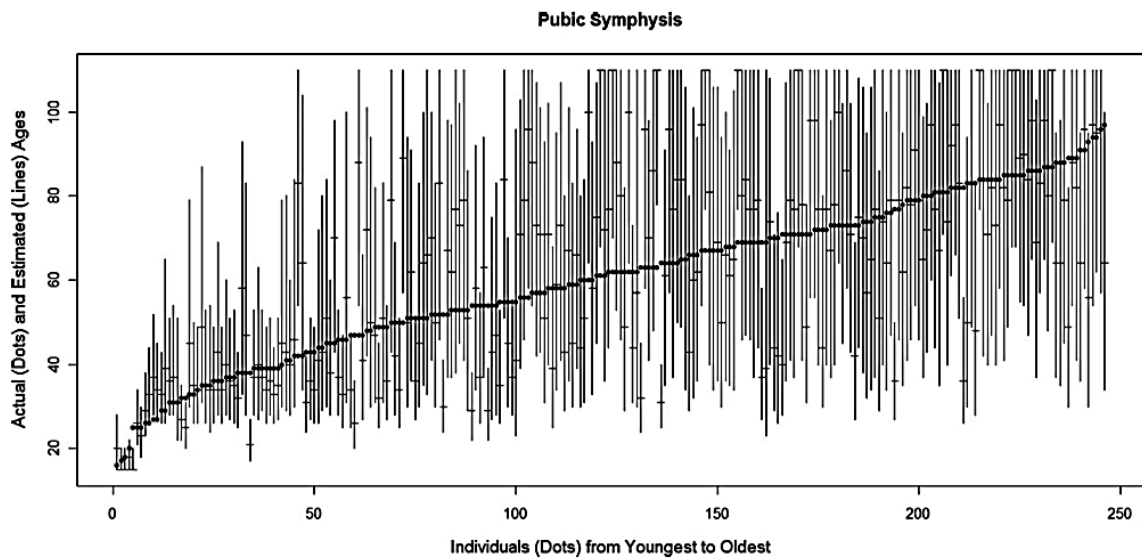


Figure 2.15: Pubic symphysis estimation age ranges and point values with true ages superimposed from Milner and Boldsen's ¹⁴ validation study

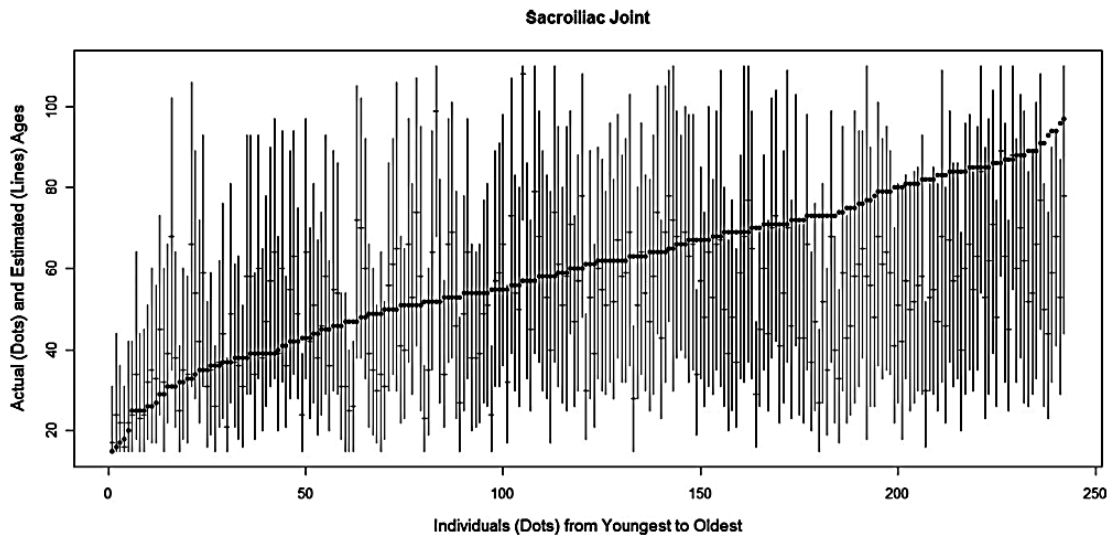


Figure 2.16: Auricular surface estimation age ranges and point values with true ages superimposed from Milner and Boldsen's ¹⁴ validation study

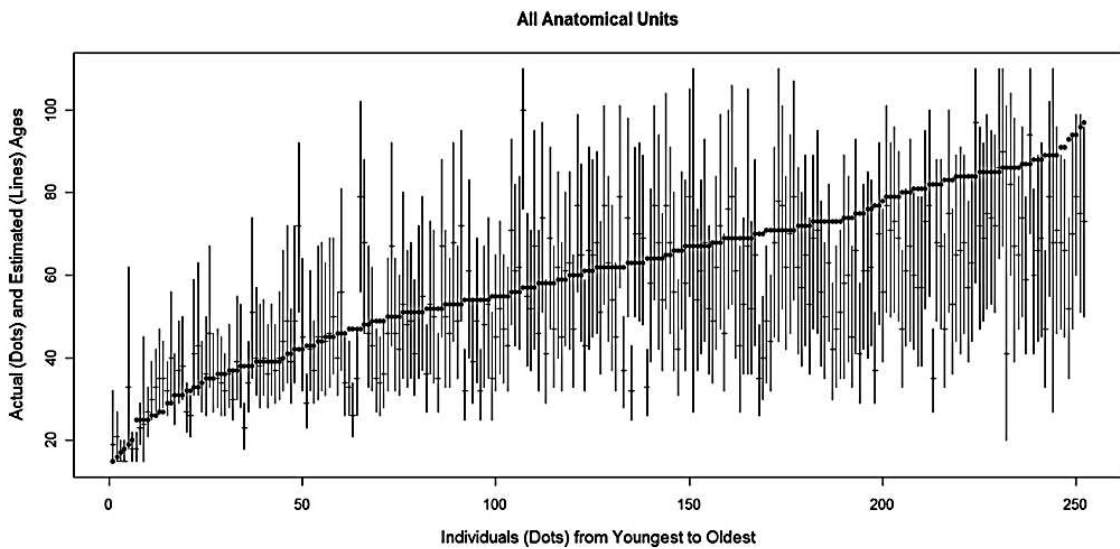


Figure 2.17: Combined estimation (uniform prior distribution) age ranges and point values with true ages superimposed from Milner and Boldsen's ¹⁴ validation study

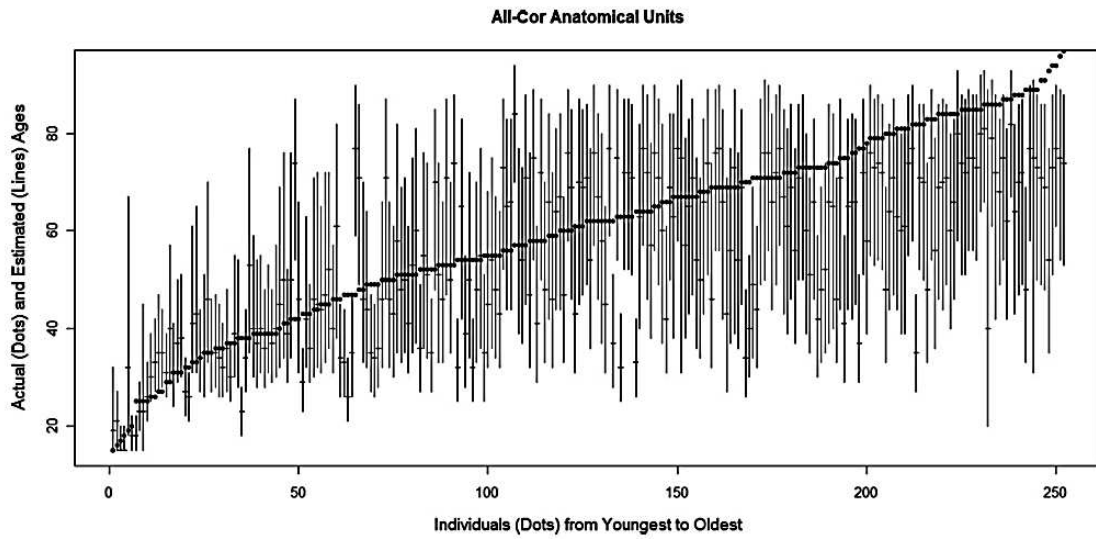


Figure 2.18: Combined estimation (modified by archaeological prior distribution) age ranges and point values with true age superimposed from Milner and Boldsen's ¹⁴ validation study

Chapter 3: Materials and Methods

3.1. Materials

The skeletal remains for this study were randomly selected from the Pretoria Bone Collection, which is a known-age, modern South African skeletal collection housed at the University of Pretoria ²¹. The Pretoria Bone Collection, as is suited to a validation study, was selected to be dissimilar to the material used in the original Boldsen *et al.* study ⁴. The Pretoria Bone Collection had its inception in 1942 in the Department of Anatomy at the University of Pretoria, South Africa. The collection is categorised according to completeness of remains including entire complete skeletons, complete skulls only, complete postcranials only and incomplete skulls or postcranials. The dissection based collection contains specimens of known age, sex and population affinity and are sourced from either donations or unclaimed bodies. There are 290 complete skeletons in the collection, of which black males (n = 168) are the most numerous, followed by white males (n = 50), black females (n = 41) and white females (n = 22). The bulk of the individuals in the collection are over 30 years of age, with a marked increase in number between 50 and 80 years of age. Only black South Africans are represented in each decade of age above 20 years. Unequal distribution of age and population affinity in the Pretoria Bone Collection is related to religion, economic circumstances, regulations of the Human Tissue Act, law no. 65 of 1983 ¹¹¹, and the willingness to donate one's remains that is influenced by cultural and religious taboos ²¹.

The skeletons were selected on the basis of age, sex and ancestry, as well as skeletal completeness, according to documentation that accompanies the collection. The black South African population group was chosen for this research as only black South Africans are represented in all adult age categories in the Pretoria Bone Collection ²¹.

Material was selected from the complete skeleton category of the collection since age-related morphological changes in both the cranium and os coxae were considered in this study. Yet, no individuals were excluded on the basis of antemortem changes that did not influence the scoring region or post-mortem

sectioning (such as the skull cap being removed from the cranial base). The skulls and os coxae were selected and separated from each other by someone other than the primary investigator in order to prevent bias.

The two sex groups within the black population group were broken down by age into groups consisting of randomly selected individuals from the 20 - 29, 30 - 39, 40 - 49, 50 - 59, 60 - 69, 70 - 79 and 80+ age-at-death categories, ensuring representation from each decade as represented in Figure 3.1. The sample was comprised of 149 South African black individuals, spread across each age category. However, it was not possible to examine an equal number of individuals in each age category because of unequal mortality distribution of ages within the Pretoria Bone Collection²¹.

3.2. Methods

The features used in transition analysis have been derived from previous descriptions of bony changes in the pelvis^{3,10,23,25,29,31,33,37,39,44,74,101} and the cranium^{26,27,34,48,67-69}, as well as modifications based on the experience of the authors who developed the method⁴. The three areas assessed were the pubic symphysis, auricular surface of the ilium and cranial sutures.

Analysis was conducted independently of the original researchers and developers of the analytical method. Each bone was analysed separately (eg. the skull and the pelvis) and separated from the rest of the skeleton by an individual other than the investigator, to ensure independent assessment. This was done to eliminate the possibility that knowledge of the stage of development from one structure might influence the assessment of another structure from the same individual. Each element was assessed without prior knowledge of the age of the individual. Seriation was not employed in this study, as it is not applicable in a forensic context.

Features that could be scored for each skeleton ranged between 19 and 36. The skeletons were for the most part complete, so the average number of traits scored – 34 – was close to what could be observed in ideal circumstances. Five characteristics were assessed on the pubic symphysis, for both the right and left sided bones (thus totalling ten scores). Nine characteristics on each of the iliac

portions of the sacroiliac joints (auricular surface) were assessed and scored. For the cranial sutures, three bilateral suture segments and two midline segments from the ectocranial surface were assessed (totalling eight scores) and each assigned a possible score. These numeral scores are subjective non-measurable quantities that are simply used as category identifiers.

Descriptions of age-related changes in the morphology of the various anatomical units, as provided by Boldsen *et al.* ⁴, are listed in Appendix A. Many of the terms used are recognisable as being derived from earlier work on morphological changes caused by age. These familiar terms were intentionally used by Boldsen *et al.* ⁴ to make classification of skeletal traits easier to understand by researchers who are familiar with existing age estimation methods. The characteristics for the pubic symphysis, sacroiliac joint and the cranial suture segments were scored separately on a scoring sheet provided for each individual as presented in Appendix B. All effort was made to score every feature. When features were obscured by post-mortem or pathological modifications, whatever remained observable was recorded as is recommended by Milner and Boldsen ³⁶. Recording all observable features, using two stage designations when encountering uncertainty, takes advantage of all information still available from the skeleton. However, when a particular feature was obscured it was designated unscorable and given the place-holder number of zero.

Some of the characteristics, in particular those of the auricular surface of the ilium, have in the past not been scored with ease and concurrence by all researchers, and therefore the repeatability of the scoring technique was assessed through intra- and inter-observer error. Inter-observer error was assessed by having an independent observer scoring 22 individuals, consisting of both males and females from each age category. These samples were also re-scored by the original observer at a later time. The two investigators gathered their data at separate times and did not discuss their evaluations with each other prior to calculation of age.

Age estimates were not generated until all data were collected. The scores for each individual were then entered into the ADBOU (Anthropological DataBase, Odense University) age estimation computer program ³⁵, in the data entering screen, which is shown in Figure 3.2. Fields for sex and ancestry were chosen by consulting accompanying documentation from the Pretoria Bone Collection. The ADBOU age

estimation computer program, developed by Boldsen, Milner and Hylleberg ³⁵, calculated age estimations from the categorical, numerical scores by using transition analysis. The program also provided approximate confidence intervals and indications of internal consistency ⁴, as well as likelihood graphs such as those illustrated in Figure 3.3. The transition analysis program has been made freely available by its developers ¹⁴.

All data entry and age estimate generation took place without knowledge of the true age. Only afterwards were data files merged so that estimated and actual ages could be compared. Separate age estimates were obtained for each of the three individual units of the skeleton (cranial sutures, pubic symphysis and auricular surface) as well as for combinations of all information. Estimates for the combined skeletal traits were obtained using both the uniform prior distribution and the prior distribution modelled on homicide data for 1996, USA and also prior distribution modelled on a 17th Century Danish population formulated from rural parish records.

3.3. Statistical analysis

Once the age of each individual in the sample was estimated using the transition analysis method, the accuracy of the age range was assessed by calculating the number of individuals for whom the known-age falls into the provided 95% confidence intervals. This was done for each of the three individual components, as well as for the combined estimates that take all three regions into account. Furthermore the accuracy of the point estimate, represented by the maximum likelihood value, was tested by assessing the mean absolute error for each of the six age estimation categories. Correlation coefficients were used to determine the relationship between the known ages and the point estimates generated by the ADBOU age estimation computer program. Graphic representations for each of the age estimation categories were generated displaying the age range with the known ages superimposed, as well as the point estimates generated with the known ages superimposed. The pattern of over- or underestimation was analysed from the graphs.

Difference in scoring between observers and for single observer repeatability was studied with relation to frequency of difference between observations, amount of

disagreement and effect of disagreement on the final age estimation. The score correlation for inter- and intra-observer error was assessed using Cohen's kappa statistics. The strength of agreement for the inter- and intra-observer scores were evaluated using categories of strength suggested by Landis and Koch ¹¹² (Table 3.1). A graph of comparison was generated for each observation for every feature that was scored. The graphs allowed visual verification of the frequency and amount of disagreement for each observation.

The correlation between the final age estimates obtained from the inter- and intra-observer scores was also assessed using a Kruskal-Wallis ANOVA analysis. The Kruskal-Wallis ANOVA analysis was used to compare the age distributions for the repeated observations in each of the six age estimation categories. Boxplots generated visual representations of the manner in which the age distribution change for scores from each observation and compared the age distribution to that of the actual ages.

Table 3.1: Landis and Koch ¹¹² strength of agreement categories

Strength of agreement category	Cohen's kappa statistic value
Poor	< 0.00
Slight	0.00 – 0.20
Fair	0.21 – 0.40
Moderate	0.41 – 0.60
Substantial	0.61 – 0.80
Almost Perfect	0.81 – 1.00

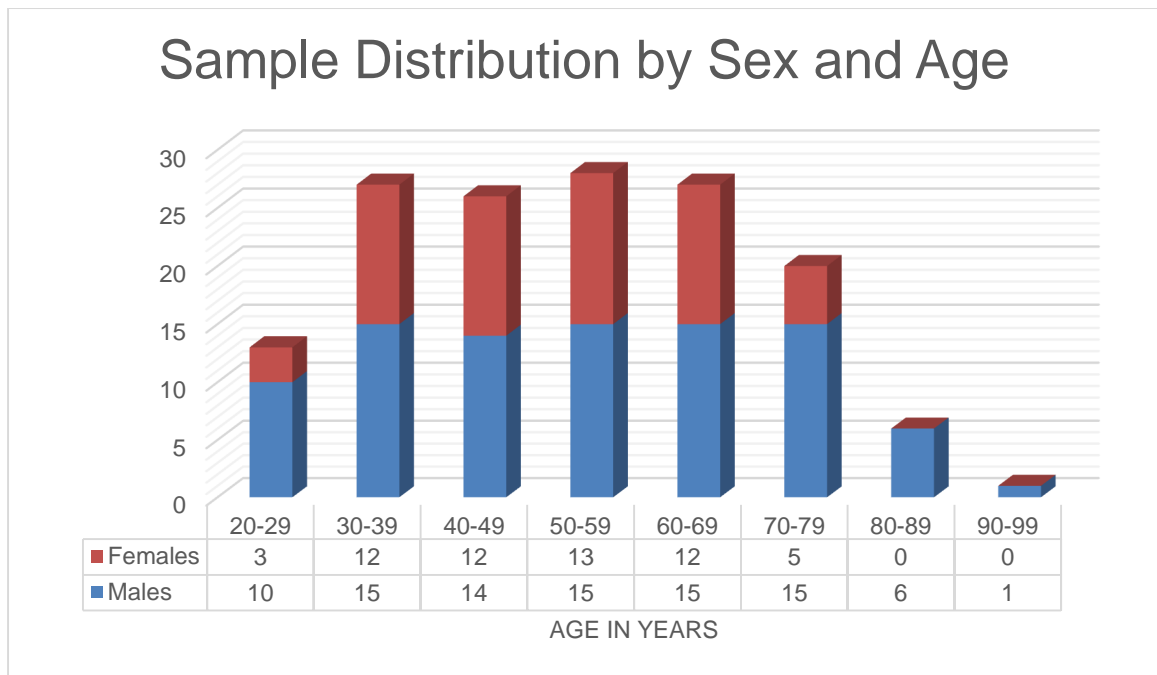


Figure 3.1: Sample distribution by sex and age

ADBOU Age estimation 2.0.056

Database form | Graph

Skeleton id-no. Find

Individual characteristic
MC08-109

Sex **Female**
Male

Group characteristic
Hazard **Archeological**
Forensic

Race **White**
Black
Unknown

Skeleton id-no.
MC07-055
Demo/test
Primer
MC-09-107
MC08-109

Cranial sutures

Coronal - pterica	5_
Sagittal - obelica	2_
Lambdoid - asterica	2_
Interpalatine suture	1_
Zygomatico-maxillary suture	1_

Pubic symphysis

Relief	Left	Right
Texture	4_	4_
Cranial ossicle	3_	3_
Ventral margin	4_	4_
Dorsal margin	5_	5_

Facies auricularis

Topography - superior	Left	Right
Topography - inferior	3_	1_
Morphology - superior	2_	2_
Morphology - apical	4_	4_
Morphology - inferior	4_	4_
Texture inferior	3_	4_
Exosteoses superior	1_	1_
Exosteoses inferior	2_	2_
Spicules	3_	3_
	1_	1_

New Skeleton Calculate Exit

Figure 3.2: Data capturing screen in the ADBOU computer program ³⁵.

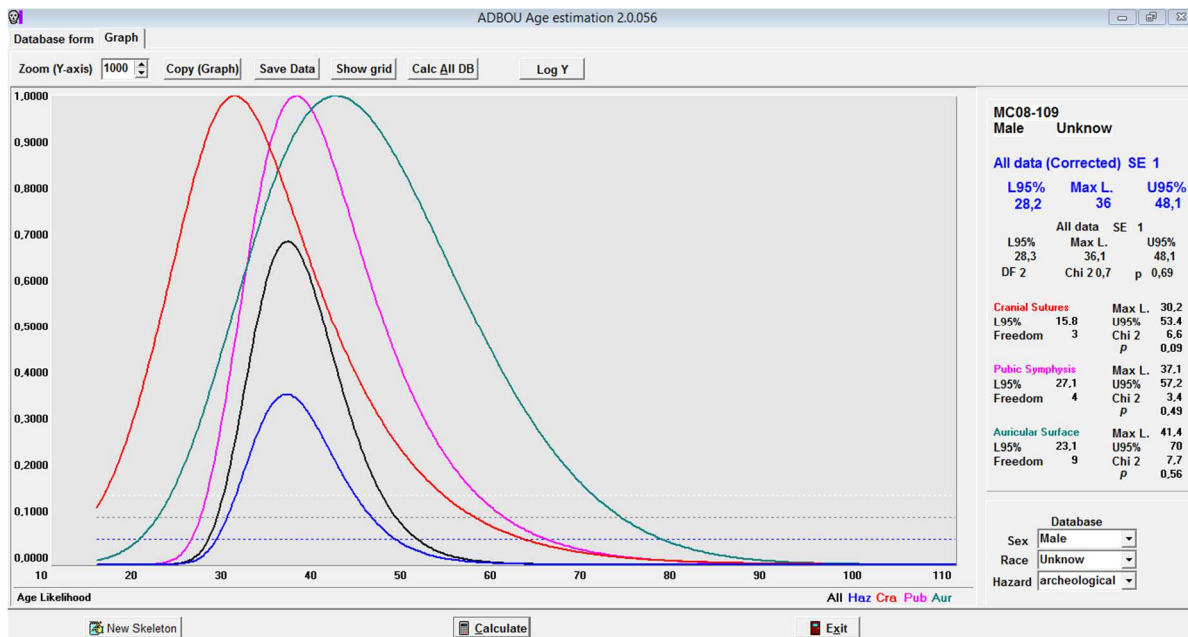


Figure 3.3: Likelihood graphs for the three separate anatomical features, pubic symphysis (**pink**), auricular surface (**green**) and cranial sutures (**red**), as well as the combined graph (**black**) generated by the ADBOU computer program ³⁵.

Chapter 4: Results

4.1. Introduction

The technique used in this study makes use of age-related morphological metamorphoses of features from the cranium and the pelvic joints in adult skeletons. Skeletons selected from the Pretoria Bone Collection needed to be adult skeletons over the age of 20 years, from a black South African population group and with both a cranium and a pelvis. A sample of 149 skeletons was selected using these criteria and although both the cranium and pelvis were present, certain scores were not possible from some individuals.

Factors preventing scoring were either post-mortem or antemortem in nature. Post-mortem factors included residual periosteum or cartilage obscuring bone features, sectioning of bone leading to the absence or masking of landmarks or portions of bone and lastly post-mortem damage translating into loss of bony landmarks or definition. The presence of serious antemortem modification due to pathology, healing trauma or anatomical variation did in some cases prevent the use of the age estimation method. However, some antemortem modifications did not obscure landmarks and features and permitted the use of the method, as advised by Milner and Boldsen in their "*Transition Analysis Age Estimation: Skeletal Scoring Manual*"³⁶. The frequency of post-mortem and antemortem factors that influenced the scoring ability and ease are listed in Table 4.1. Overall between 19 and the maximum of 36 scores could be obtained from the skeletons in the sample, with the average number of scores being 34.

The cranial sutures that were most frequently not scorable were the sagittal obelica, coronal pterica and the interpalatine as illustrated in Table 4.2. No scores could be obtained if the sagittal obelica was obscured by pitting on the cortex or by the removal of the calotte. The coronal pterica was not scored, if the suture was obscured by the removal of the calotte. If the interpalatine suture is found in a groove or on a crest, the suture is often concealed³⁶ and becomes difficult to impossible to score. The palatine bone is also a fragile bone and was sometimes lost due to post-mortem damage. Sutural bones also complicated the scoring area. The cranial

sutures where no antemortem or post-mortem obstruction of the features occurred included the lambdoid asterica and the zygomaticomaxillary sutures.

The pubic symphysis was frequently not scorable either due to cartilage obscuring the surface or post-mortem damage. The superior apex of the symphysis was the structure most often obscured. Also observed in a few cases was a normal variation of the pubic symphysis that was so narrow or tapered that visibility of the surface was affected.

The articular area of the auricular surface was sometimes obscured by remnants of cartilage or post-mortem damage as can be seen by the occasional inability to score surface morphology and texture. Another occasional occurrence at the auricular surface and iliac tuberosity location was that of synostosis to the sacrum. This normal degenerative process does allow for a score in the exostoses categories found in the iliac tuberosity area posterior to the articular area ³⁶, but this same synostosis obscures the view of the articular auricular surface and if the phenomenon is present bilaterally may even extend this obstruction to the pubic symphysis.

The area with the most features that could not be scored was the auricular surface of the ilium with a total number of 203 features from a total of 2682 features. The 203 features that could not be scored were distributed among 39 individuals. From the pubic symphysis, 90 scores of a possible 1490 scores distributed among 29 individuals could not be obtained. The least number of scores that could not be obtained were from the cranial sutures. A total of 35 features from a possible 1192 features from the cranial sutures could not be scored from 21 individuals.

4.2. Age estimations

The scores obtained for bilateral sides of the cranial sutures, pubic symphysis and auricular surface were entered into the ADBOU (Anthropological DataBase, Odense University) age estimation computer program ³⁵ for each individual skeleton and an age estimation was obtained. During calculation of the age estimation with the ADBOU age estimation program a selection of sex, ancestry and prior distribution is made. The sex and ancestry were selected according to the Pretoria Bone Collection

records. The age estimation consists of a point value of maximum likelihood and an age range composed of an upper and lower limit of the 95% confidence interval. Six separate age estimations were calculated for each individual using data from 1) only cranial suture scores, 2) only pubic symphysis scores, 3) only auricular surface scores, 4) all scores combined, 5) all scores combined and modified with a forensic prior distribution and 6) all scores combined and modified with an archaeological prior distribution. Both prior distributions are included in the ADBOU age estimation computer program.

4.2.1. Accuracy and precision of the age ranges

Evaluation of the age ranges provided by the ADBOU age estimation computer program³⁵ was approached by calculating the percentage of known ages that fell within the estimated age range for each of the six age estimation categories. When referring to the age ranges the accuracy of the technique can be said to be quite high as can be seen by the percentages of known age falling within the estimated age range (Table 4.3). From Table 4.3 it appears that the individual anatomical feature age estimation and not the combined features age estimation method is more successful with the cranial sutures achieving the highest accuracy at 92%, followed by the auricular surface (77%), the pubic symphysis (75%) and only then the estimations from the combined skeletal features. The combined estimations that appear to be more accurate are the combined estimation with uniform prior distribution with 67% known ages falling within the range and the slightly more accurate (68%) combined estimation modified by the archaeological prior distribution based on the 17th century Danish population. With regard to known age falling within the age range the estimation that performs the worst by far, at 63% inclusion, is the combined feature estimation modified by the forensic prior distribution of USA homicide data from 1996.

However, the success of an age range is not only measured by the ability of the age range to encompass the actual or known age, but also by the width of that range. A range stretching from 15 to 110 years in age, which is the case in 29 estimates making use of only cranial sutures, is practically useless as the only information garnered from this range tells the analyst that the unknown individual is not a child under 15 years of age. As seen in Table 4.4, the number of years included in the age

ranges of the six age estimation categories stretch from a minimum of 9 years to a maximum of 95 years. A relationship can be seen between the width of the age range in years and the percentage of known ages that fall within the age range. Table 4.4 illustrates that as the average number of years in the age range decreases so too does the accuracy. The average number of years in the age range decreased in the order of estimation starting with the single features namely the cranial sutures, pubic symphysis, auricular surface and continuing with the combined method modified by archaeological prior distribution, the combined method with a uniform prior distribution and lastly the combined method with a forensic prior distribution which achieved an average number of 28 years in the range.

The age range width, based on the confidence interval length, does not only differ between the age estimation methods, but also changes throughout the age continuum. This change in confidence interval length with advancing age can be visualised in Figures 4.1 to 4.6. A general trend is observed with an increase in interval length with advancing age until a plateau forms around the middle age category (approximately 40 – 60 years) where interval lengths remain constant. Interval lengths experiences a slight decrease in the older age category.

Although this general pattern is observed for the cranial suture estimation method (Figure 4.1), the plateau stage can mostly be attributed to the ADBOU-imposed upper terminal value of 110 years. The pubic symphysis estimation method (Figure 4.2) adheres to the general pattern, but a brief plateau is only reached after the 60 year mark. There is a marked decrease in interval length after 70 years. Although the auricular surface estimation method (Figure 4.3) does not experience a plateau stage, a slight decrease of interval length after approximately 70 years can be observed.

The combined estimation methods with both the uniform and forensic prior distributions (Figures 4.4 and 4.5) do not adhere to the general pattern. There is neither an obvious plateau stage nor a decrease in interval length during the older ages. However, the combined estimation method with archaeological prior distribution (Figure 4.6) displays a plateau stage from approximately 50 years and a decrease in interval length after approximately 70 years.

The age ranges for each individual, from each age estimation category, are graphically represented (Figures 4.7 to 4.12) with the known ages superimposed. From the graphic representations of the age estimation ranges, it is deduced that the upper and lower age limits for some of the age estimations fall outside the trend line for the 95% confidence interval range. Also apparent is the fact that the slope of the 95% confidence interval trend lines, for all six age estimation methods, shows very little progression with advancing age. The lack of progression with age is especially apparent in the slopes of the lower 95% confidence trend line.

Figure 4.7 displays the age ranges for each skeleton, when using the cranial suture method, with the known age superimposed. All known ages fall within the upper and lower trend lines representative of the 95% confidence interval. Graphically reinforced by this graph is the large range of the 95% confidence interval, especially apparent when looking at the trend lines.

When assessing the graph displaying the age ranges for the pubic symphysis method (Figure 4.8) it is clear that the range has narrowed for the younger individuals. Age ranges are still overly large for the older individuals. When considering the known ages in Figure 4.8, those individuals with younger ages fall below the lower 95% confidence interval trend line and were thus overestimated using the pubic symphysis method.

The age ranges using the auricular surface method, represented in Figure 4.9, is similar to what is seen with the pubic symphysis method with the narrowing of ranges. Unlike the pubic symphysis method, the narrower age ranges persist into the older ages for the auricular surface method. Known ages for the older individuals fall above the upper 95% confidence interval trend line and were thus underestimated when using the auricular surface method. The ranges had an overall trend of underestimation, inferred from the known ages that frequently appear at the upper limit of the age interval. However, this method still provided the best age ranges compared with the other single indicator methods.

A further reduction in age ranges is observed, in Figures 4.10 to 4.12, when using the combined methods compared to those seen for the individual cranial suture, pubic symphysis and auricular surface estimations. The combined method with a uniform prior distribution as well as the modified combined methods making use of

both the forensic and archaeological prior distributions overestimated the ages of the younger individuals and underestimated the ages of the older individuals as can be visualised by the known ages falling outside of the 95% confidence interval trend line. The known ages are frequently found at the lower terminal of the age range for the younger individuals and at the upper terminal of the age range for the older individuals. Using the informative prior distributions reduced the width of the age ranges even further. An overall pattern of underestimation is observed when using the forensic prior distribution, as can be seen by the presence of the known ages situated at the terminal value of the ranges for many of the older individuals (Figure 4.11).

Although the combined methods underestimate lower ages and overestimate older ages, they would still be the more suitable methods as a result of their narrower age ranges. The most suitable of the three combined methods would be the combined method with uniform prior distribution as the least amount of under- and overestimation occurs with this method.

4.2.2. Accuracy of the point value

For each of the six age estimation categories a correlation coefficient was calculated for the maximum likelihood value, which is provided as a point estimate by the ADBOU age estimation computer program ³⁵, and the known age. A correlation coefficient of one refers to a perfect correlation and is the sought value, whereas a value of zero indicates no correlation.

None of the correlations recorded in Table 4.5 for the six age estimations are above 0.50 in value. Of the three single indicator values, the cranial sutures fared the best with a correlation of 0.36, followed by the auricular surface (0.35) and the pubic symphysis (0.26).

The combined age estimates presented only slightly better values. The best correlations (0.43) were achieved by the combined method with uniform distribution and the combined method modified by a forensic prior distribution, followed closely by the combined method modified by an archaeological prior distribution (0.42).

To further clarify the relationship between the point estimate and the known age, the mean absolute error was calculated from the maximum likelihood value. The mean

absolute error measures the accuracy of the age estimation by indicating the number of years that the age estimate has either over- or underestimated the known age. A lower mean absolute error indicates a smaller amount of over- or underestimation and consequently indicates a better accuracy.

From Table 4.6 it is clear that the combined age estimation methods fare much better where the point value is concerned. The combined age estimation method modified by forensic prior distribution is the least accurate of the three combined estimations with a mean absolute error of 12.91 years, followed closely by the combined estimations with a uniform prior distribution at 12.73 years. The most accurate of the point values is the combined estimate modified by the archaeological prior distribution with a mean absolute error of 10.40 years. Inaccuracy is present in all the age estimation methods in both overestimation of the younger ages and also underestimation of the older ages represented in Figures 4.13 to 4.18. Particularly noteworthy from all the graphic representations, except those for the cranial suture age estimations, is the lack of progression with advancing age observed from the slope of the trend line representing the maximum likelihood point estimates.

In Figure 4.13 the maximum likelihood point estimates for the cranial suture estimation method is widely scattered around the known ages. The overall trend using the cranial sutures was overestimation as can be visualised by comparing the trend line to the known ages.

In Figure 4.14 the known ages tend to fall under the trend line for the point estimates from the pubic symphysis estimation method, with the overall trend being of overestimation. However, the older individuals' ages are underestimated.

In Figure 4.15 known ages predominantly fall above the trend line for the point estimates generated through the auricular surface method and the resultant overall trend is that of underestimation, which is especially true for the older individuals. Overall, the auricular surface method had point estimate values much closer to the known ages, as can be seen by the scatter pattern of the point estimates that more closely fit the superimposed known ages.

From the graphic representations of the maximum likelihood scores, with superimposed known ages (Figures 4.13 to 4.18), it is apparent that the point estimates for the combined methods are more refined and more closely represent

the known ages compared with the widely scattered point estimates for the cranial suture, pubic symphysis and auricular surface single feature methods. However, the combined estimation method modified by the forensic prior distribution does create an overall trend of underestimation, as can be seen from the point estimate trend line that falls below the known ages.

When regarding Figures 4.13, 4.14 and 4.15 for the cranial sutures method, pubic symphysis method and auricular surface method respectively, it is evident that the point estimates are occasionally represented by the terminal values of 15 years at the lower limit and 110 years at the upper limit. These upper and lower limits have been added to the ADBOU age estimation computer program as logical limits that are still inclusive of the entire adult population. As demonstrated in Table 4.7, the point estimates are represented by the lower terminal value 23 times for the cranial suture method and once for the auricular surface method. The point estimate is represented by the upper terminal value 12 times for the cranial suture method, three times for the pubic symphysis method and twice for the auricular surface method. The point values are never represented by the terminal values for the combined methods.

4.3. Observer agreement

Of the 149 skeletons scored by the primary investigator, 22 were scored again by the primary investigator as well as by a second observer, completely independent of the primary investigator. The inter- and intra-observer scores were collected separately from the original scores and no communication existed between the two observers regarding the scores.

The degree of both the intra- and the inter-observer agreement was determined by using Cohen's kappa statistics (Table 4.8) and the strength of agreement was analysed by using categories for strength suggested by Landis and Koch¹¹² and described in Table 3.1.

The scores from both observations of the primary investigator, as well as from the second observer, were used to calculate age estimations using all six possible age estimation methods. The six methods include the age estimation from the cranial

sutures only, the age estimation from the pubic symphysis only, the age estimation from the auricular surface only, the age estimation from all three features combined, a combined estimation modified by a forensic prior distribution and a combined estimation modified by an archaeological prior distribution, as before. A Kruskal-Wallis ANOVA analysis was conducted to compare the underlying age distributions as calculated from the scores of all different observations.

4.3.1. Inter- and intra-repeatability of scores

By interpreting the Cohen's kappa statistics, using the Landis and Koch ¹¹² categories, the majority (78%) of the intraobserver agreement was moderate, substantial or almost perfect with more agreement falling into the categories moderate and substantial than almost perfect. The interobserver error was mostly (83%) found to be only slight, fair or moderate with the highest overall agreement being only fair.

The bone features which had the highest agreement discernible from the Cohen's kappa statistics between the two observers were the sagittal obelica, inferior demiface topography for the left auricular surface and superior surface morphology for the right auricular surface. The Cohen's kappa statistics for these three features place them in the substantial category for the interobserver agreement, but also ranks almost perfect, substantial and moderate respectively for sagittal obelica, inferior demiface topography and superior surface morphology for the intraobserver agreement. Other bony features ranking almost perfect for intraobserver error were symphyseal relief for the right pubic symphysis, dorsal symphyseal margin from the left pubic symphysis, superior demiface topography for the left and right auricular surface and superior surface morphology for the left auricular surface. The dorsal symphyseal margin for the left pubic symphysis and the superior demiface topography for the left and right auricular surface correspond to moderate interobserver agreement ranking, but the symphyseal relief and superior surface morphology only corresponds with a ranking of fair for the interobserver agreement.

The three features that fared the poorest for interobserver agreement were the posterior exostoses for the left auricular surface and the ventral symphyseal margin for the left and right pubic symphyses. The left ventral symphyseal margin and posterior exostoses fared correspondingly poor for intraobserver agreement and

were ranked slight, however, the intraobserver agreement for the right ventral symphyseal margin was ranked moderate. Also falling into the slight category for the intraobserver agreement was the posterior exostoses for the right auricular surface.

Although some features presented with agreement that was slight or poor, especially between the two observers, p-values indicate that the level of agreement between some of these scores can likely be attributed to chance (Table 4.8). A p-value higher than 0.05 is not considered significant, as the agreement could possibly be accidental. Features with a p-value higher than 0.05 include symphyseal texture from the right pubic symphysis, the ventral symphyseal margin from the left, the superior surface morphology from the right auricular surface, the inferior surface texture from the left and the left and right posterior exostoses for the interindividual agreement.

Features that were not considered significant with regard to agreement between the observers included the interpalatine suture, the symphyseal relief for the right and left side, the symphyseal texture for the right pubic symphysis, the superior apex from the left side, the ventral symphyseal margin from the left and right side, the dorsal symphyseal margin from the right side, the inferior demiface topography from the right auricular surface, the superior surface morphology from the left, the middle surface morphology from the right, the inferior surface morphology and texture from the right and left side, the superior posterior iliac exostoses from the left and right side, the inferior iliac exostoses from the right side and the posterior exostoses from the left and right side. Although the p-values are indicative of some chance agreement, the general pattern observable from the Cohen's kappa statistics suggests that some features are problematic where repeatability is concerned.

Graphic representations, for each of the 36 traits, display the scores selected for each individual by the primary investigator and the second observer (Figures 4.19 to 4.54). The graphs demonstrate not only the number of scores chosen differently for each observation, but also the magnitude of these score differences. Table 4.9 is a summary of the total number of score differences from the original observation, regardless of which observer differed. From Table 4.9 it can be observed that in 47% of the traits, more than half the number of analysed skeletons, present with scores that are different for repeat observations. Observations differed most often, with a frequency of 0.85, for the symphyseal texture of the right pubic symphysis, right

ventral symphyseal margin and the inferior surface texture from the left auricular surface. Observations differed least, with a frequency of 0.25, for the sagittal obelica, the superior demiface topography and the inferior demiface topography from the left auricular surface.

Magnitude was also summarised from the graphic representations (Figures 4.19 to 4.54) in Table 4.9. Although features that were not scorable were represented by the numeral zero, these scores of zero were not included when magnitude of score difference was calculated from the graphs. From the graphic representations it is apparent that the scores for sagittal obelica (Figure 4.21), left and right zygomaxillary suture (Figures 4.25 and 4.26), left symphyseal relief (Figure 4.27), left and right dorsal symphyseal margin (Figures 4.35 and 4.36), right superior demiface topography (Figure 4.38), left middle surface morphology (Figure 4.43), left inferior surface morphology (Figure 4.45), left inferior surface texture (Figure 4.47) and right posterior exostoses (Figure 4.54) never differ by more than a value of one.

Similarly, scores from the left and right coronal pterica (Figures 4.19 and 4.20), left and right lambdoidal asterica (Figures 4.22 and 4.23), right symphyseal relief (Figure 4.28), left superior apex (Figure 4.31), left superior demiface topography (Figure 4.37), left and right inferior demiface topography (Figures 4.39 and 4.40), left and right superior surface morphology (Figures 4.41 and 4.42), right middle surface morphology (Figure 4.44), right inferior surface morphology (Figure 4.46), right inferior surface texture (Figure 4.48), right and left inferior posterior iliac exostoses (Figures 4.51 and 4.52) and left posterior exostoses (Figure 4.53) never differ by more than two values. The score values of the left and right symphyseal texture (Figures 4.29 and 4.30), the right superior apex (Figure 4.32) and the left and right superior posterior iliac exostoses (Figures 4.49 and 4.50) differed by up to three values. Lastly, the right and left ventral symphyseal margin (Figures 4.33 and 4.34) had a score value difference of up to four.

It is, however, not just important for observers to agree about the score value awarded to morphological features, but also as to whether the feature is visible, with enough unobscured detail, in order to reliably allocate any score. A score value of zero on the graphic representations (Figures 4.19 to 4.54) represents features which could not be scored due to a factor causing poor visibility (Table 4.1). Features

where the observers were in consensus that no score could be attributed included the right coronal pterica (Figure 4.20), the sagittal obelica (Figure 4.21), the right lambdoidal asterica (Figure 4.23), the interpalatine (Figure 4.24), the right zygomaxillary (Figure 4.26), the right superior apex (Figure 4.32), the right and left superior demiface topography (Figures 4.37 and 4.38), the right and left inferior demiface topography (Figures 4.39 and 4.40), the right and left superior surface morphology (Figures 4.41 and 4.42), the left middle surface morphology (Figure 4.43), the right and left inferior surface morphology (Figures 4.45 and 4.46), the right and left inferior surface texture (Figures 4.47 and 4.48) and the right and left inferior posterior iliac exostoses (Figures 4.51 and 4.52).

Some of the features that were slightly obscured, were still regarded by one of the observers as being satisfactorily observed to be award a score. Features where observers disagreed upon the ultimate ability to assign a score were the interpalatine (Figure 4.24), the right symphyseal relief (Figure 4.28), the right symphyseal texture (Figure 4.30), the right and left superior apex (Figures 4.31 and 4.32), the right and left ventral symphyseal margin (Figures 4.33 and 4.34), the right dorsal symphyseal margin (Figure 4.36), the right superior demiface topography (Figure 4.38), the right inferior demiface topography (Figure 4.40), the right and left superior surface morphology (Figures 4.41 and 4.42), the right middle surface morphology (Figure 4.44), the right inferior surface morphology (Figure 4.46), the right and left inferior surface texture (Figures 4.47 and 4.48), the right and left superior posterior iliac exostoses (Figures 4.49 and 4.50), the right and left inferior posterior iliac exostoses (Figures 4.51 and 4.52) and the right and left posterior exostoses (Figures 4.53 and 4.54).

Overall, cranial sutures are more frequently repeatable and scores only differ by one or two values. The pubic symphysis and auricular surface scoring system are less repeatable than the cranial sutures. Especially worrying are the symphyseal texture and ventral margin of the pubic symphysis that were not frequently repeatable and differed up to three or four score values. Scores from the articular area of the auricular surface were more repeatable with smaller score differences than the retroauricular area.

4.3.2. Effect of score repeatability on age estimates

When comparing age distributions calculated from different observations using a Kruskal-Wallis ANOVA analysis, the age distributions for all six categories were not significantly different from each other as evidenced by the p-value of greater than 0.60 (Table 4.10). The age estimation categories least effected by a change in score are the combined estimation with forensic prior distribution (p-value = 0.8911), the pubic symphysis estimation (p-value = 0.8244) and the combined method with uniform prior distribution (p-value = 0.8013).

Boxplots for each method, making use of each set of observations (from the primary investigator as well as the second observer), as well as the true age values, were used to graphically compare the age distributions. The boxplots representing the age distribution using the cranial suture method (Figure 4.55) presents a similar median line for the observations from the primary investigator and the second observer, but a lower median line for the second observation from the primary investigator. The age distribution between the 25th and 75th percentiles are more spread out for the observations of observer two, but more compressed for the two observations of the primary investigator. The age distribution for the actual age is the most compressed. The age distribution most similar to that of the actual age is that of the second observation from the primary investigator with regard to both the median line and the distribution between the 25th and 75th percentiles.

The boxplots representing the age distribution using the pubic symphysis method (Figure 4.56) presents with similar median lines for all observations. The median line for the actual age is lower than that of the estimated age distributions. The age distributions between the 25th and 75th percentiles have a more spread out distribution for observer two and a more compressed distribution for observer one's first observation. The age distribution from the primary investigator's second observation is a very close match to the distribution from the actual age, with only the median line at a higher age for observer one.

The boxplots representing the age distribution for the auricular surface method (Figure 4.57) have similar median lines for all observations. The median line for the calculated estimations is lower compared to the median line from the actual age. The age distribution between the extreme points for the auricular surface method for the

two observations of the primary investigator are more compressed than the distribution representing the actual age. The original observation for the primary investigator presents with an outlier in the auricular surface method. Overall, the least similar distribution between boxplots from investigator observations versus the actual age is seen for the auricular surface method, with the distribution for the actual age being at a higher age.

The median lines for observer age distributions are similar for the combined method with uniform prior distribution (Figure 4.58) and the combined method using the forensic prior distribution (Figure 4.59). In the case of the combined method with uniform prior distribution, the median line is also similar to that of the actual age, but the median line in the boxplot representing the actual age for the combined method modified by the forensic prior distribution is at a higher age than the median lines for the observer boxplots. The median line of the boxplot representing observer two's age distributions is higher for the combined method with an archaeological prior distribution (Figure 4.60) compared to the median lines representing distributions for the primary investigator and the actual age.

As with the auricular surface method, the boxplot representing the age distribution for the primary investigator's first observation from the combined method (Figure 4.58) presents with an outlier at a high age. The age distributions for the boxplots representing the three combined methods all present with more compressed distributions where the two observations of the primary investigator is concerned and more spread distributions for observer two. In the case of the combined method and the combined method modified with the archaeological prior distribution these more compressed age distributions, especially the distributions for the second observations, more closely represent the distribution of the actual age. The age distributions from the observer age estimations for the combined method modified by a forensic prior distribution represent distributions of much younger ages compared to the distribution representing the actual ages.

Overall, the age distributions for the second observations from the primary investigator were more refined and more closely resembled the age distributions for the actual age. The closest fit between the observer's estimation age distribution and the actual age occurred for methods using the pubic symphysis as a single indicator

and the combined method with uniform prior distribution, as well as the combined method modified by the archaeological prior distribution. Age distributions from observer estimations were younger, compared to distributions for the actual age, when using the auricular surface single indicator method and especially for the combined method modified by the forensic prior distribution.

Table 4.1: Factors influencing scoring ability and visibility

Factors	Frequency observed in sample (n = 149)
Overlying soft tissue	0.1812
Missing bone or landmark (likely due to sectioning)	0.1476
Post-mortem damage	0.1812
Antemortem modification such as pathology, pitting, synostosis, trauma with healing, osteophytes, sutural bones, new bone deposits	0.3087

Table 4.2: Number and frequency of non-scorable features (n = 149)

	Bone feature	Number not scorable	Frequency not scorable
Cranial sutures	Coronal Pterica Left	4	0.027
	Coronal Pterica Right	8	0.054
	Sagittal Obelica	13	0.087
	Lambdoidal Asterica Left	0	0
	Lambdoidal Asterica Right	1	0.007
	Interpalatine	6	0.040
	Zygomaxillary Left	0	0
	Zygomaxillary Right	3	0.020
	TOTAL	35 scores (from 21 individuals)	
Pubic symphysis	Symphyseal Relief Left	9	0.060
	Symphyseal Relief Right	4	0.027
	Symphyseal Texture Left	13	0.087
	Symphyseal Texture Right	6	0.040
	Superior Apex Left	15	0.101
	Superior Apex Right	13	0.087
	Ventral Symphyseal Margin Left	8	0.054
	Ventral Symphyseal Margin Right	7	0.047
	Dorsal Symphyseal Margin Left	10	0.067
	Dorsal Symphyseal Margin Right	5	0.034
		TOTAL	90 scores (from 29 individuals)
Auricular surface	Superior Demiface Topography Left	12	0.081
	Superior Demiface Topography Right	6	0.040
	Inferior Demiface Topography Left	11	0.074
	Inferior Demiface Topography Right	6	0.040
	Superior Surface Morphology Left	21	0.141
	Superior Surface Morphology Right	11	0.074
	Middle Surface Morphology Left	17	0.114
	Middle Surface Morphology Right	12	0.081
	Inferior Surface Morphology Left	18	0.121
	Inferior Surface Morphology Right	12	0.081
	Inferior Surface Texture Left	20	0.134
	Inferior Surface Texture Right	15	0.101
	Superior Posterior Iliac Exostoses Left	5	0.034
	Superior Posterior Iliac Exostoses Right	4	0.027
	Inferior Posterior Iliac Exostoses Left	12	0.081
	Inferior Posterior Iliac Exostoses Right	9	0.061
	Posterior Exostoses Left	7	0.047
Posterior Exostoses Right	5	0.034	
	TOTAL	203 scores (from 39 individuals)	

Table 4.3: Number and percentage of known ages within estimated age range (n = 149)

Age estimation category	Number of known ages within range	Percentage of known ages within range
Cranial suture estimation	137	92%
Pubic symphysis estimation	112	75%
Auricular surface estimation	114	77%
Combined estimation	100	67%
Combined estimation modified by forensic prior distribution	94	63%
Combined estimation modified by archaeological prior distribution	102	68%

Table 4.4: Range width

Age estimation category	Minimum number of years in range	Maximum number of years in range	Average number of years in range
Cranial suture estimation	30	95	74
Pubic symphysis estimation	9	90	51
Auricular surface estimation	16	85	44
Combined estimation	9	60	32
Combined estimation modified by forensic prior distribution	9	53	28
Combined estimation modified by archaeological prior distribution	9	48	31

Table 4.5: Correlation between point value and known age

Age estimation category	Correlation coefficient
Cranial suture estimation	0.360164771
Pubic symphysis estimation	0.262350037
Auricular surface estimation	0.349834816
Combined estimation	0.425487736
Combined estimation modified by forensic prior distribution	0.427763866
Combined estimation modified by archaeological prior distribution	0.42082774

Table 4.6: Mean absolute error for point value

Age estimation category	Mean absolute error
Cranial suture estimation	23.48188
Pubic symphysis estimation	17.59799
Auricular surface estimation	15.54161
Combined estimation	12.72886
Combined estimation modified by forensic prior distribution	12.91409
Combined estimation modified by archaeological prior distribution	10.39933

Table 4.7: Number and frequency of point estimate values represented by upper or lower terminal values

Age estimation category	Low terminal value	High terminal value	Frequency of low terminal value	Frequency of high terminal value
Cranial suture estimation	23	12	0.154	0.080
Pubic symphysis estimation	0	3	0	0.020
Auricular surface estimation	1	2	0.007	0.013
Combined estimation with uniform distribution	0	0	0	0
Combined estimation modified by forensic prior distribution	0	0	0	0
Combined estimation modified by archaeological prior distribution	0	0	0	0

Table 4.8: Cohen's kappa statistics for determining intra- and interobserver agreement strength

	Bone feature	Intraobserver agreement	p-value	Landis and Koch ¹¹² strength category	Interobserver agreement	p-value	Landis and Koch ¹¹² strength category
Cranial sutures	Coronal Pterica L	0.503106	0.0002	Moderate	0.455782	0.0003	Moderate
	Coronal Pterica R	0.753846	0.0000	Substantial	0.55836	0.0000	Moderate
	Sagittal Obelica	0.866221	0.0000	Almost Perfect	0.744409	0.0000	Substantial
	Lambdoidal Asterica L	0.418182	0.0154	Moderate	0.453925	0.0024	Moderate
	Lambdoidal Asterica R	0.725086	0.0000	Substantial	0.537954	0.0001	Moderate
	Interpalatine	0.475655	0.0018	Moderate	0.219858	0.1439	Fair
	Zygomaxillary L	0.781022	0.0000	Substantial	0.395973	0.0119	Fair
	Zygomaxillary R	0.701493	0.0000	Substantial	0.391892	0.0130	Fair
Pubic symphysis	Symphyseal Relief L	0.354839	0.0428	Fair	0.52381	0.0064	Moderate
	Symphyseal Relief R	0.837398	0.0000	Almost Perfect	0.298246	0.0734	Fair
	Symphyseal Texture L	0.350181	0.0387	Fair	0.297125	0.0749	Fair
	Symphyseal Texture R	0.256198	0.0814	Fair	0.082569	0.6933	Slight
	Superior Apex L	0.365079	0.0302	Fair	0.083969	0.7824	Slight
	Superior Apex R	0.792746	0.0000	Substantial	0.363057	0.0461	Fair
	Ventral Symphyseal Margin L	0.117647	0.3827	Slight	-0.18812	0.5778	Poor
	Ventral Symphyseal Margin R	0.545455	0.0007	Moderate	-0.20301	0.1250	Poor
	Dorsal Symphyseal Margin L	0.834711	0.0000	Almost Perfect	0.447005	0.0449	Moderate
	Dorsal Symphyseal Margin R	0.565217	0.0039	Moderate	0.285714	0.2817	Fair
Auricular surface	Superior Demiface Topography L	0.831224	0.0000	Almost Perfect	0.5671	0.0004	Moderate
	Superior Demiface Topography R	0.807692	0.0000	Substantial	0.473684	0.0175	Moderate
	Inferior Demiface Topography L	0.767442	0.0000	Substantial	0.693487	0.0000	Substantial
	Inferior Demiface Topography R	0.779412	0.0000	Substantial	0.267399	0.0908	Fair
	Superior Surface Morphology L	0.865772	0.0000	Almost Perfect	0.282511	0.0975	Fair
	Superior Surface Morphology R	0.43662	0.0907	Moderate	0.633028	0.0014	Substantial
	Middle Surface Morphology L	0.669421	0.0001	Substantial	0.372822	0.0156	Fair
	Middle Surface Morphology R	0.347826	0.0442	Fair	0.130435	0.4258	Slight
	Inferior Surface Morphology L	0.689922	0.0000	Substantial	0.338235	0.0600	Fair
	Inferior Surface Morphology R	0.553903	0.0004	Moderate	0.139785	0.3089	Slight
	Inferior Surface Texture L	0.417476	0.0511	Moderate	0.178082	0.5877	Slight
	Inferior Surface Texture R	0.622642	0.0042	Substantial	0.085714	0.7821	Slight
	Superior Posterior Iliac Exostoses L	0.459459	0.0042	Moderate	0.233227	0.0598	Fair
	Superior Posterior Iliac Exostoses R	0.545455	0.0000	Moderate	0.136213	0.5058	Slight
	Inferior Posterior Iliac Exostoses L	0.732441	0.0000	Substantial	0.281046	0.0371	Fair
	Inferior Posterior Iliac Exostoses R	0.503546	0.0003	Moderate	0.157088	0.2775	Slight
	Posterior Exostoses L	0	1.0000	Slight	-0.06195	0.8304	Poor
Posterior Exostoses R	0	1.0000	Slight	0	1.0000	Slight	

Table 4.9: Number and magnitude of observer differences by features

	Bone feature	Number of overall observer differences	Frequency of observer differences	Maximum score difference; not including unscorable = 0
Cranial sutures	Coronal Pterica L	11	0.55	2
	Coronal Pterica R	8	0.4	2
	Sagittal Obelica	5	0.25	1
	Lambdoidal Asterica L	9	0.45	1
	Lambdoidal Asterica R	8	0.4	2
	Interpalatine	14	0.7	2
	Zygomaxillary L	10	0.5	1
	Zygomaxillary R	11	0.55	1
Pubic symphysis	Symphyseal Relief L	7	0.35	1
	Symphyseal Relief R	6	0.3	2
	Symphyseal Texture L	15	0.75	3
	Symphyseal Texture R	17	0.85	3
	Superior Apex L	8	0.4	2
	Superior Apex R	6	0.3	2
	Ventral Symphyseal Margin L	17	0.85	4
	Ventral Symphyseal Margin R	12	0.6	4
	Dorsal Symphyseal Margin L	6	0.3	1
	Dorsal Symphyseal Margin R	9	0.45	1
Auricular surface	Superior Demiface Topography L	5	0.25	2
	Superior Demiface Topography R	6	0.3	1
	Inferior Demiface Topography L	5	0.25	2
	Inferior Demiface Topography R	11	0.55	2
	Superior Surface Morphology L	8	0.4	2
	Superior Surface Morphology R	5	0.25	2
	Middle Surface Morphology L	11	0.55	1
	Middle Surface Morphology R	10	0.5	2
	Inferior Surface Morphology L	9	0.45	1
	Inferior Surface Morphology R	12	0.6	2
	Inferior Surface Texture L	17	0.85	1
	Inferior Surface Texture R	16	0.8	2
	Superior Posterior Iliac Exostoses L	14	0.7	3
	Superior Posterior Iliac Exostoses R	13	0.65	3
	Inferior Posterior Iliac Exostoses L	11	0.55	2
Inferior Posterior Iliac Exostoses R	13	0.65	2	
Posterior Exostoses L	12	0.6	2	
Posterior Exostoses R	9	0.45	2	

Table 4.10: p-value from Kruskal-Wallis ANOVA indicating no significant difference in age estimation during different observations

Age estimation method	p-value from Kruskal-Wallis ANOVA
Cranial sutures age estimation	0.6845
Pubic symphysis age estimation	0.8244
Auricular surface age estimation	0.6288
Combined age estimation	0.8013
Combined age estimation modified with forensic prior distribution	0.8911
Combined age estimation modified with archaeological prior distribution	0.6388

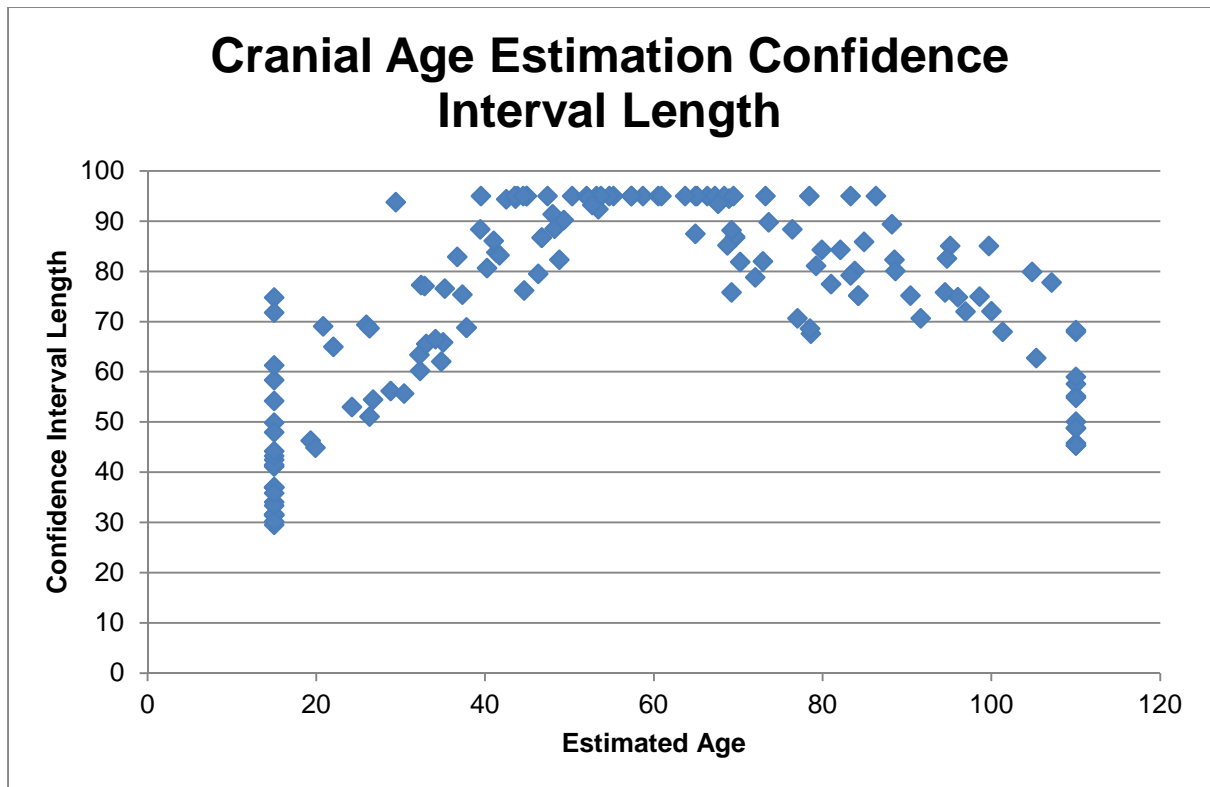


Figure 4.1: Changes in cranial age estimation confidence interval length with age

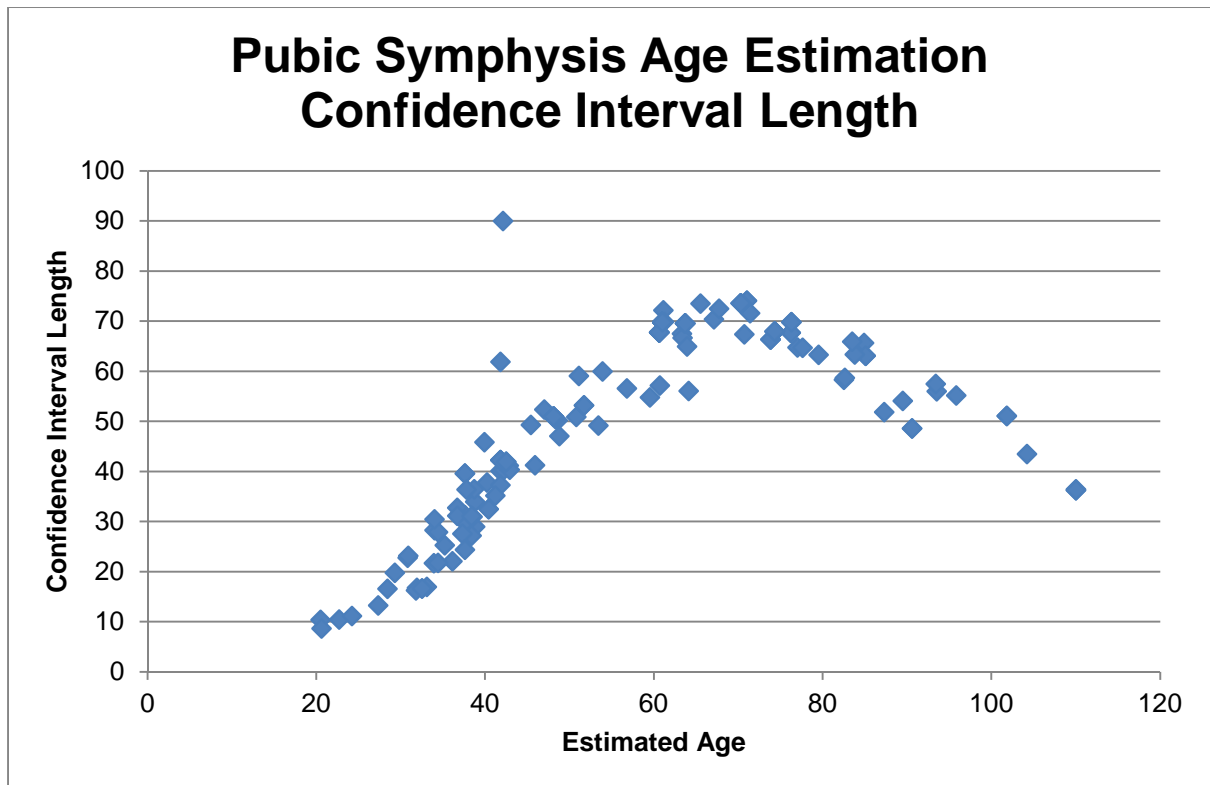


Figure 4.2: Changes in pubic symphysis age estimation confidence interval length with age

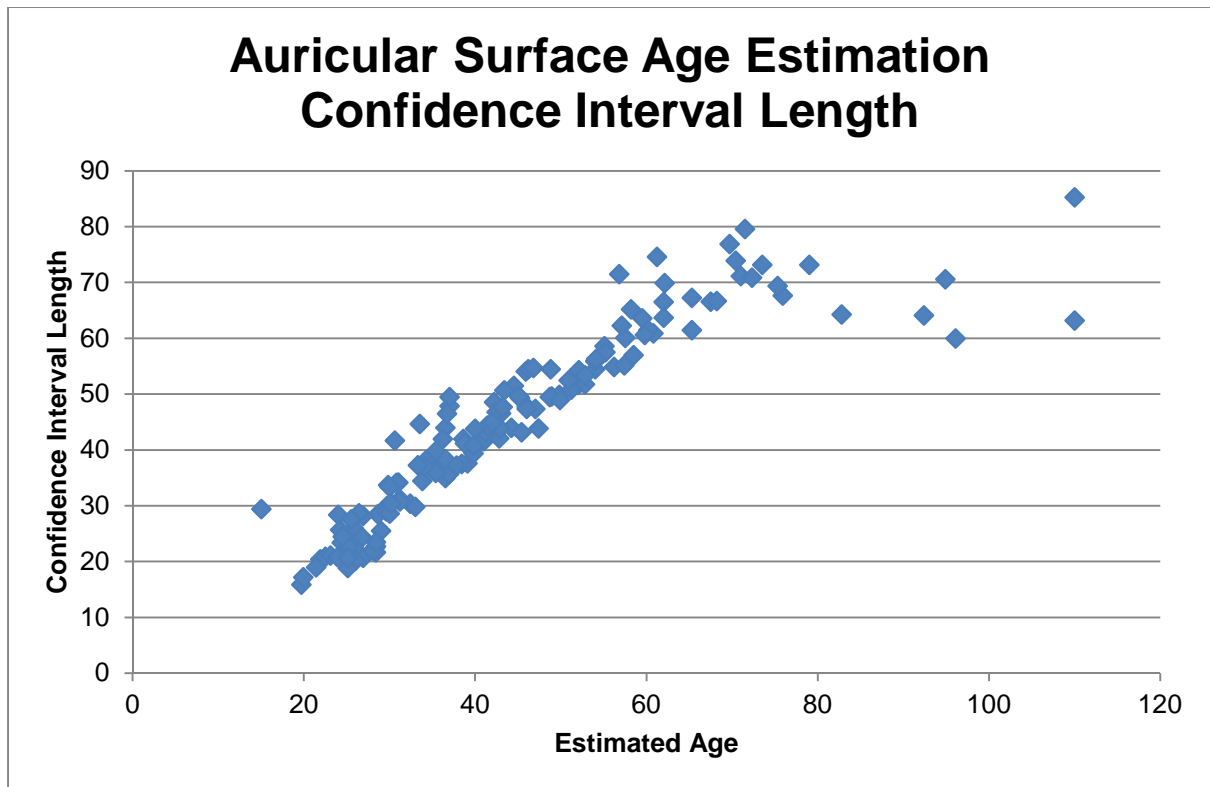


Figure 4.3: Changes in auricular surface age estimation confidence interval length with age

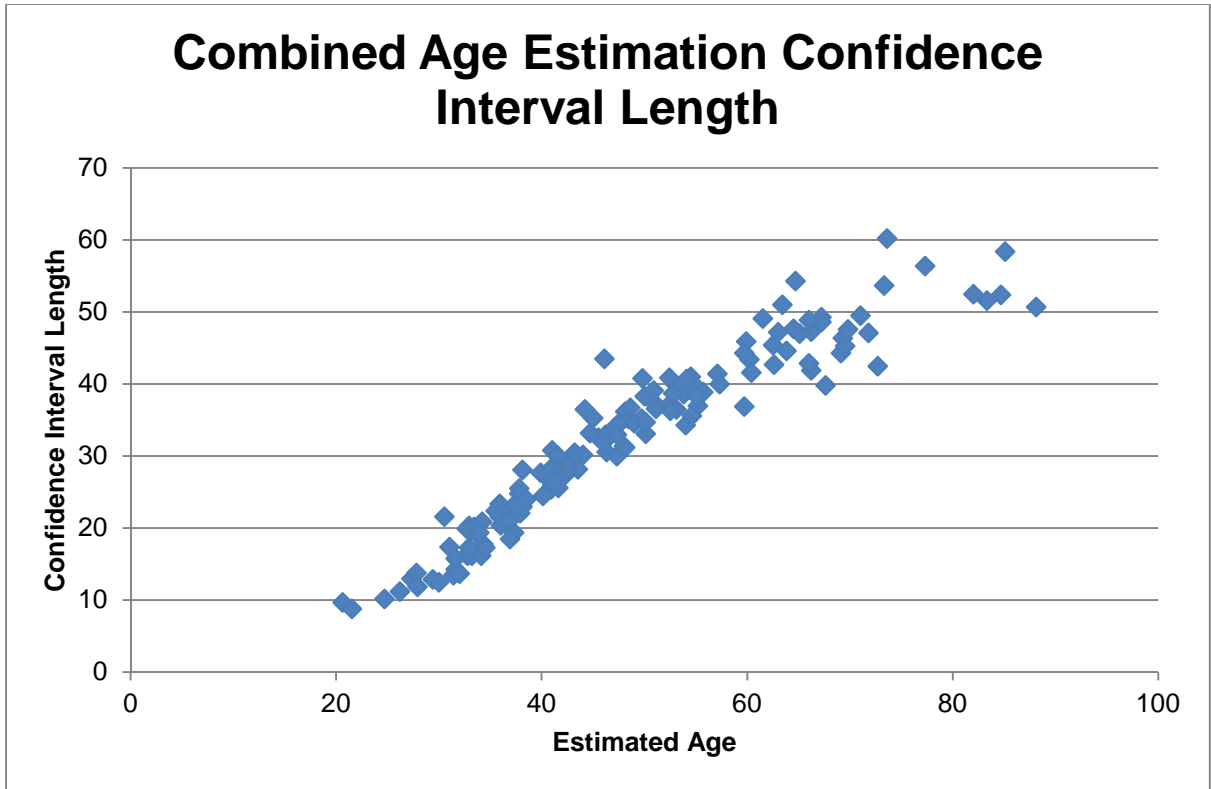


Figure 4.4: Changes in combined age estimation (uniform prior distribution) confidence interval lengths with age

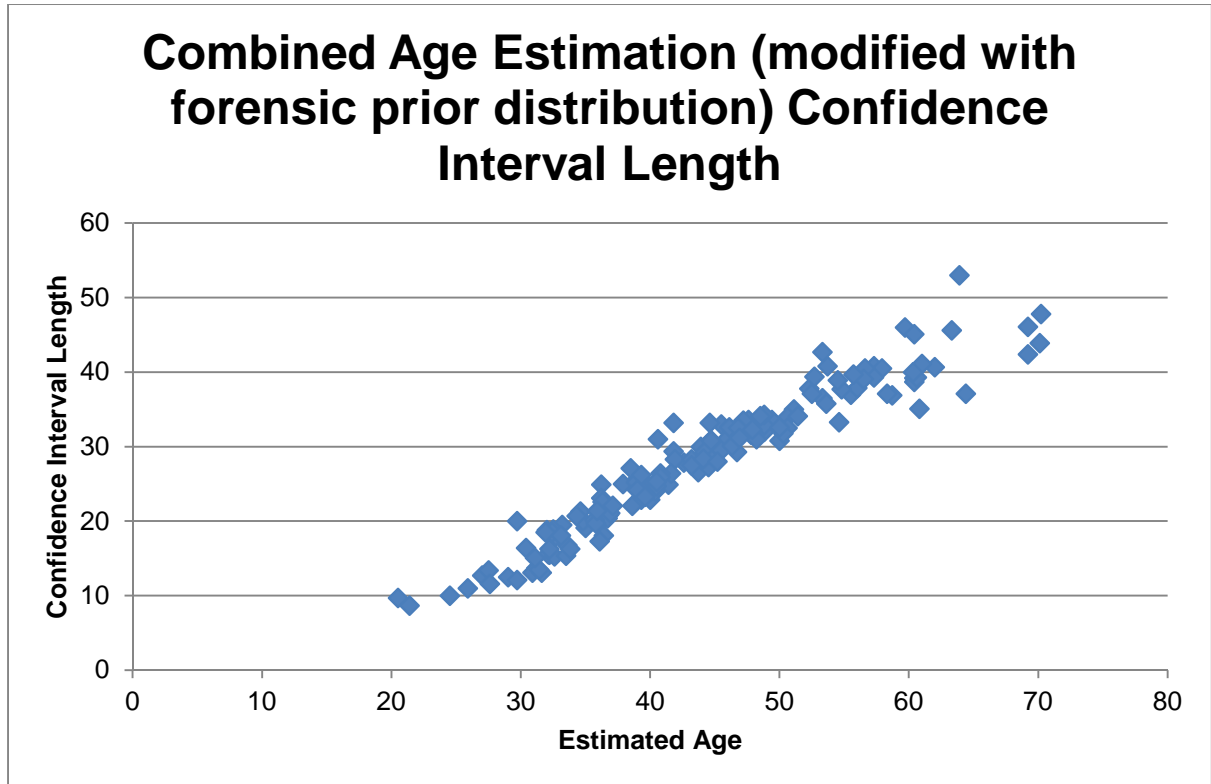


Figure 4.5: Changes in combined age estimation (modified with forensic prior distribution) confidence interval lengths with age

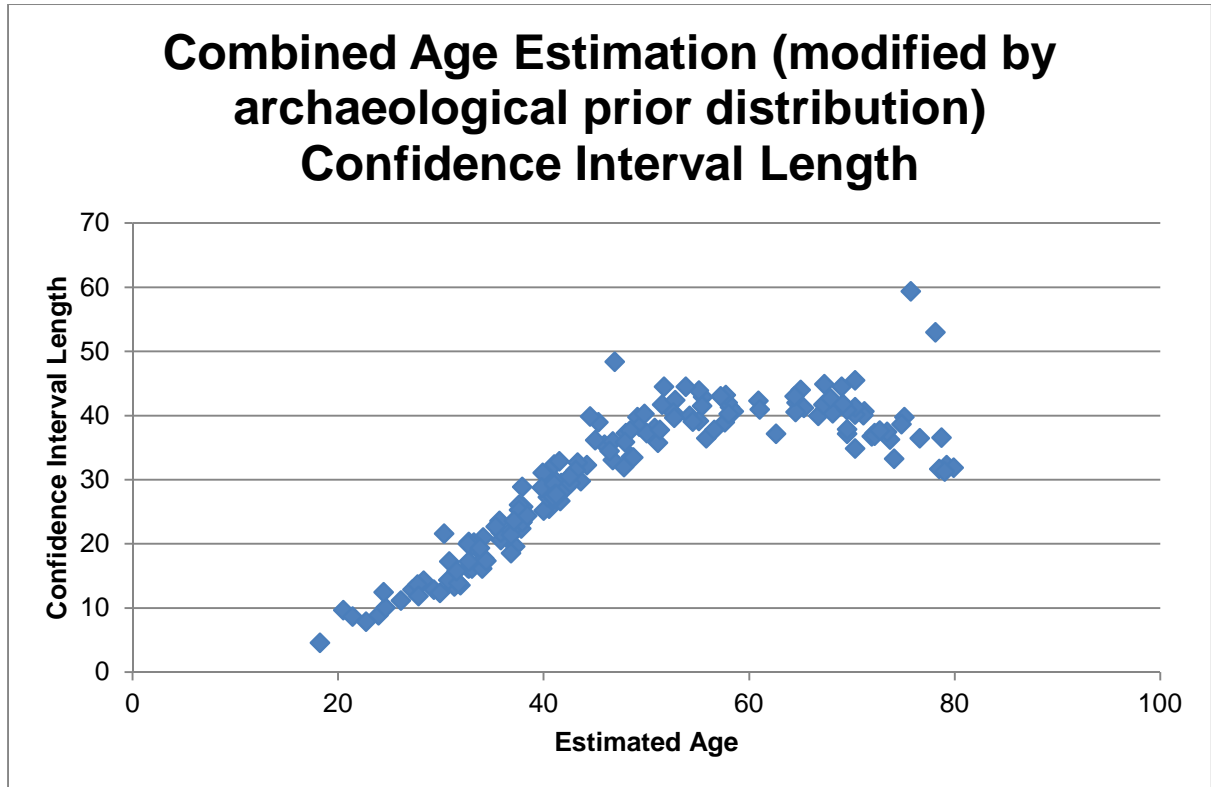


Figure 4.6: Changes in combined age estimation (modified with an archaeological prior distribution) confidence interval lengths with age

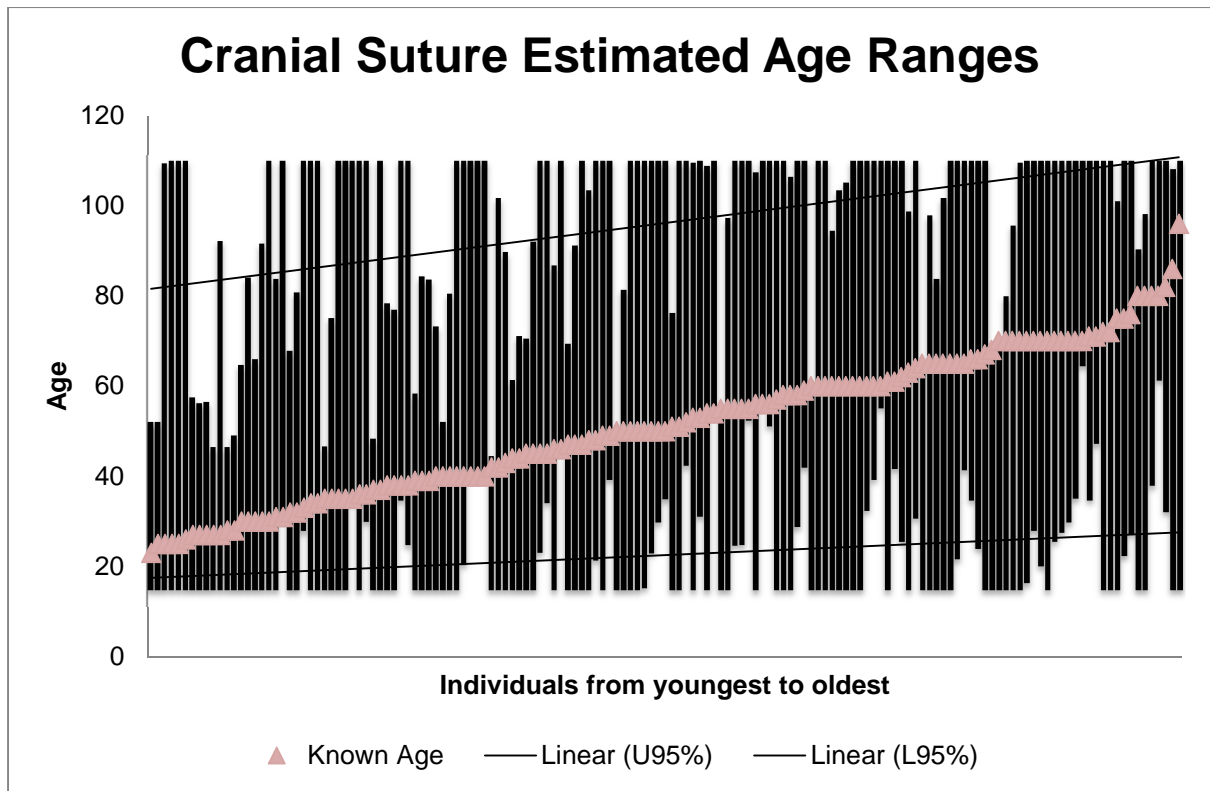


Figure 4.7: Cranial suture estimated age ranges

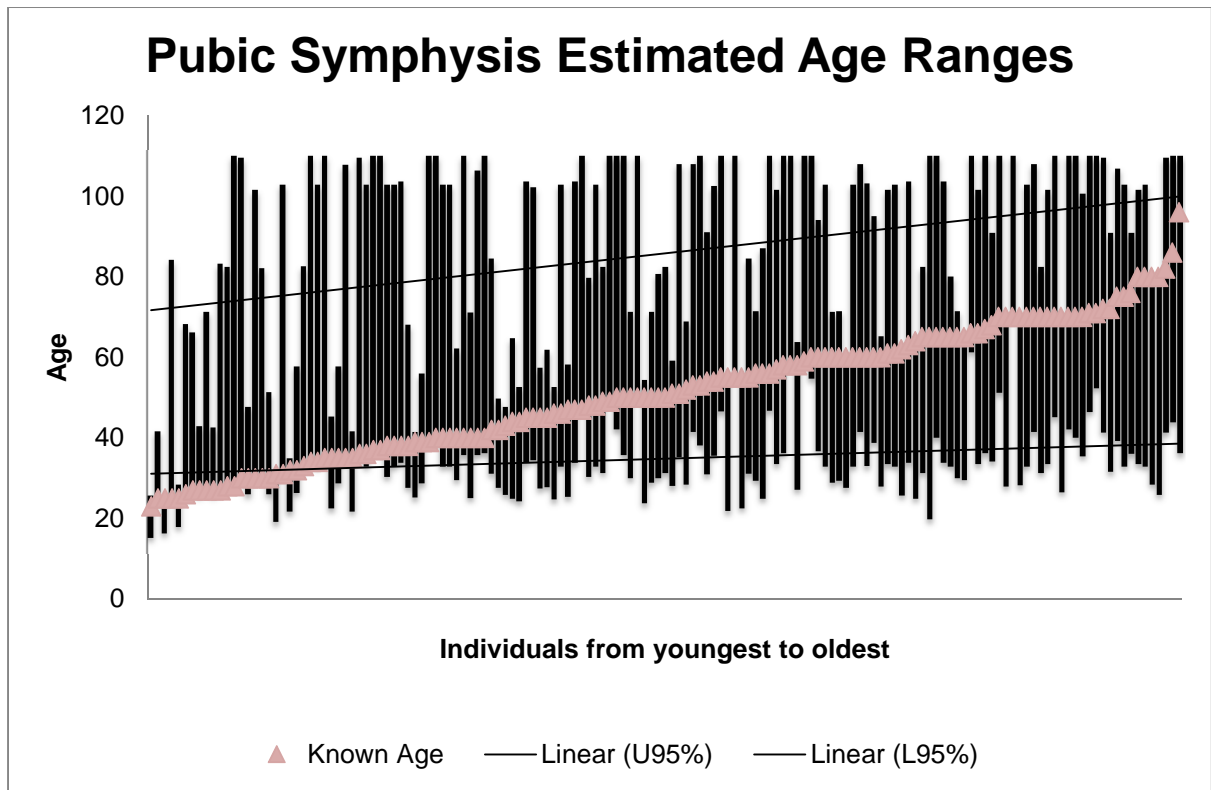


Figure 4.8: Pubic symphysis estimated age ranges

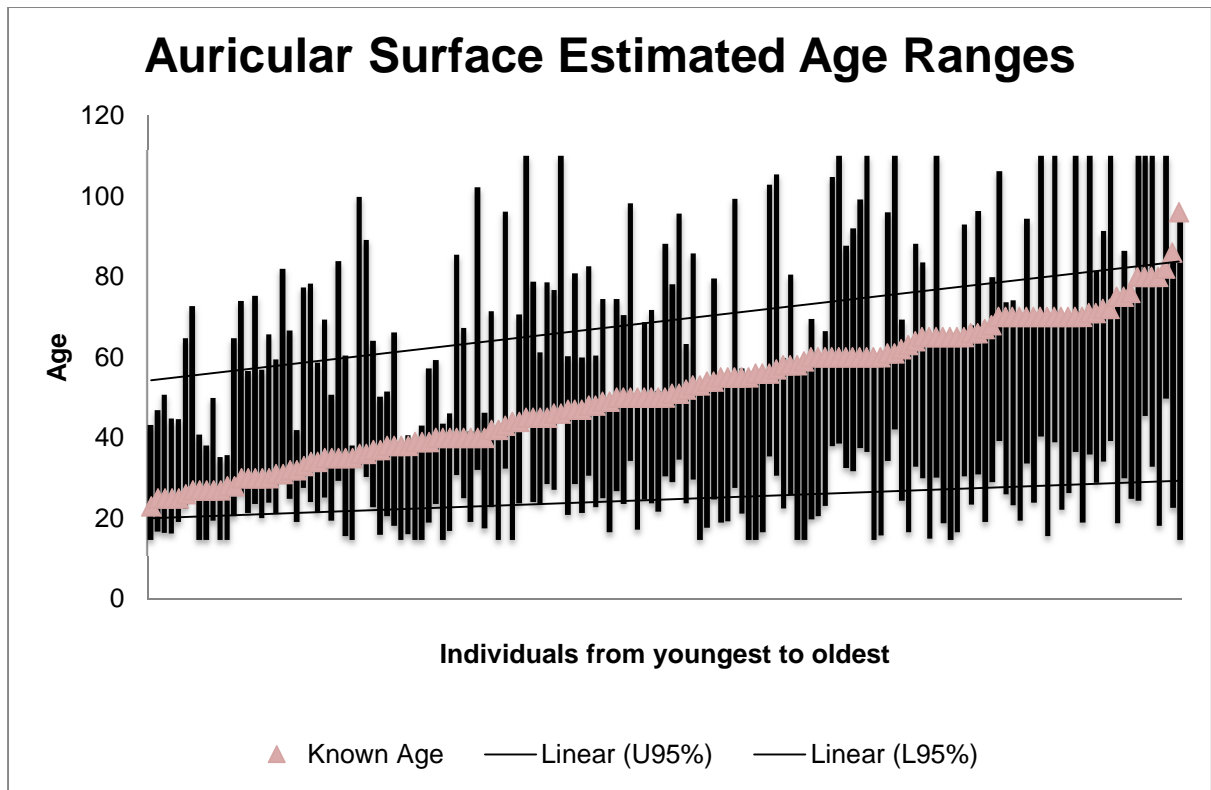


Figure 4.9: Auricular surface estimated age ranges

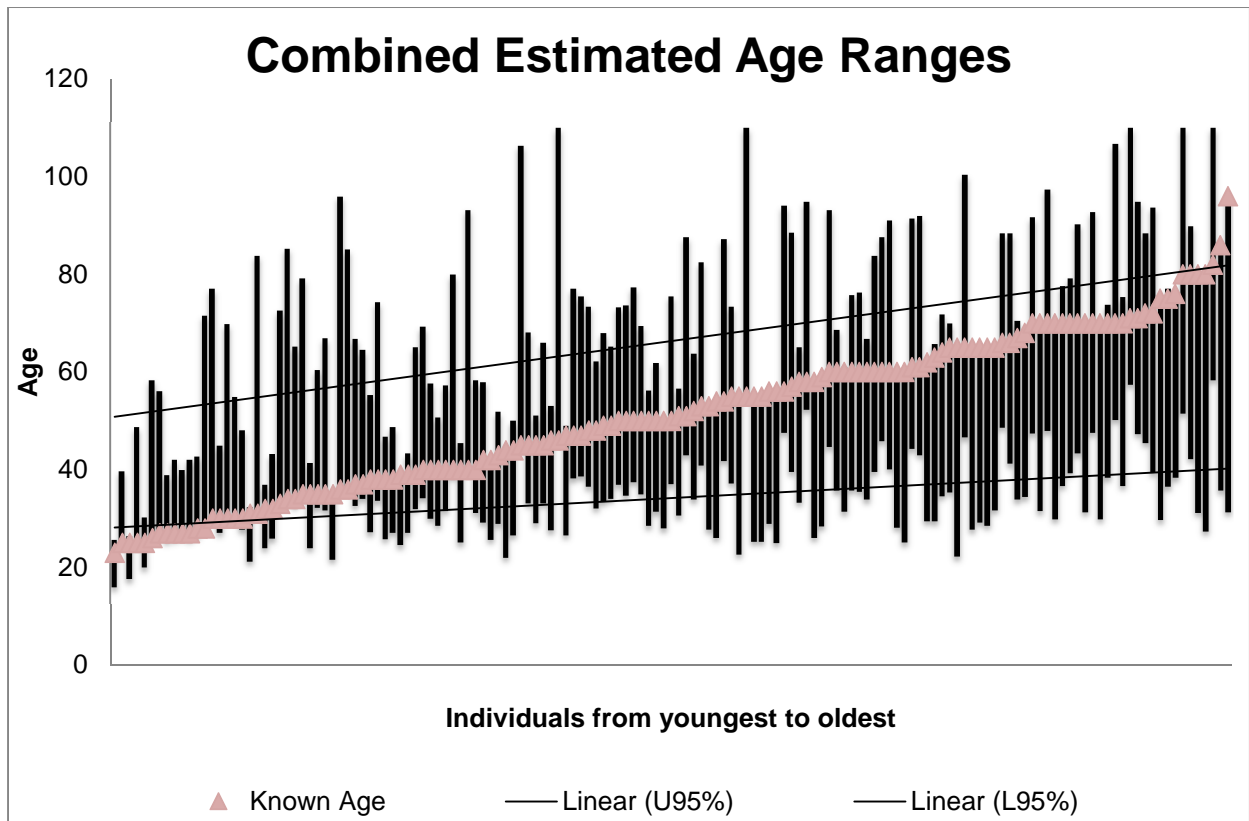


Figure 4.10: Combined estimated age ranges (uniform prior distribution)

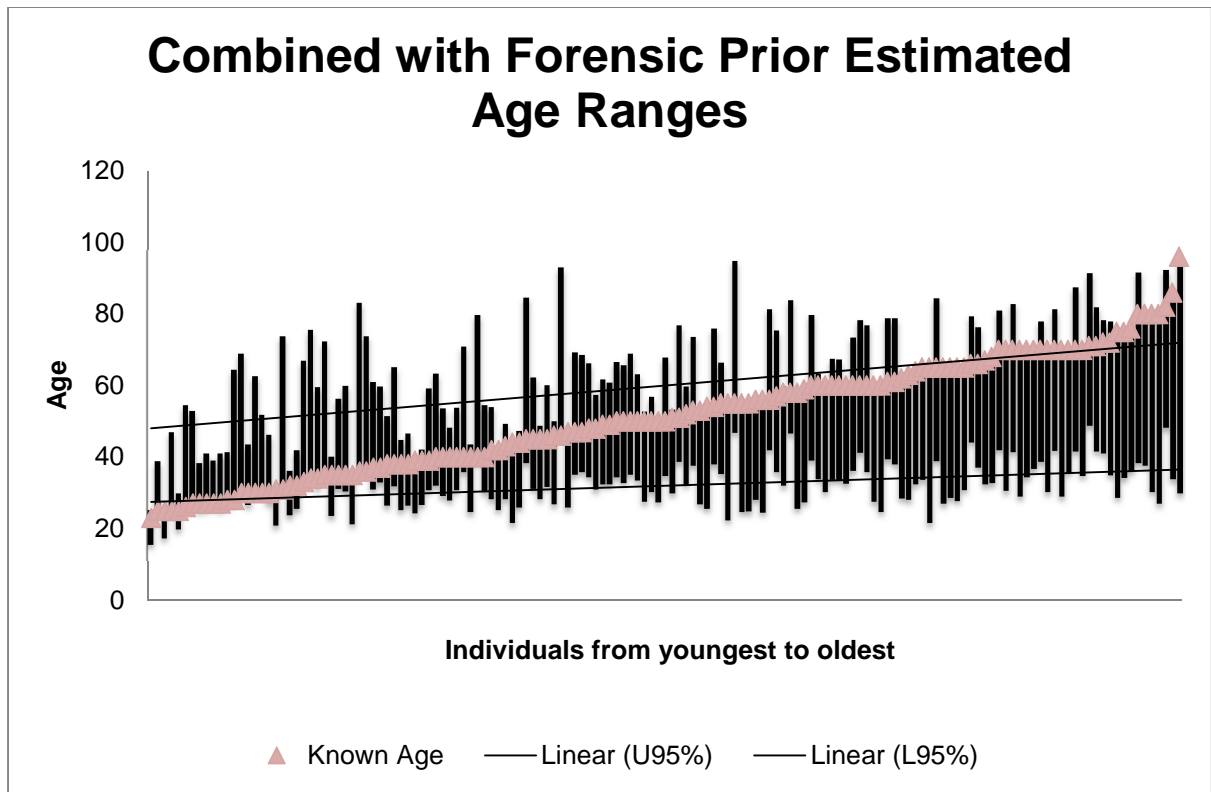


Figure 4.11: Combined estimated age ranges (forensic prior distribution)

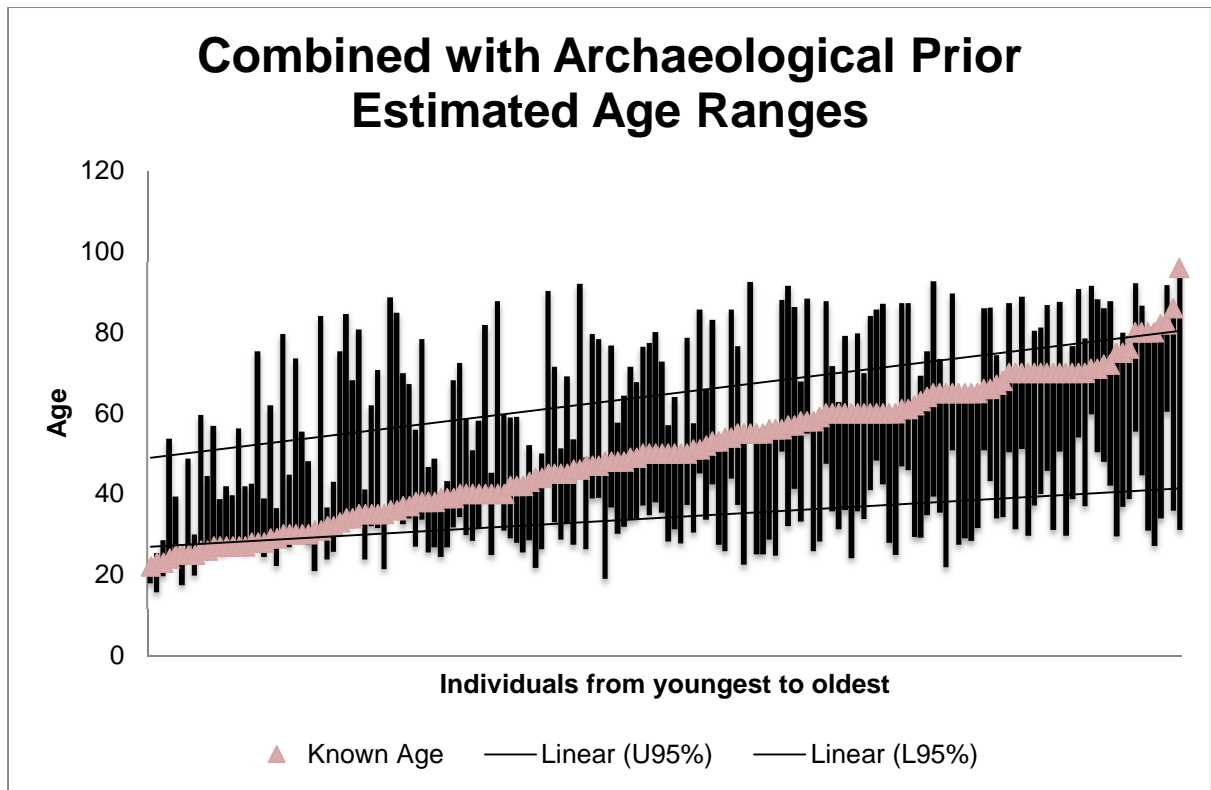


Figure 4.12: Combined estimated age ranges (archaeological prior distribution)

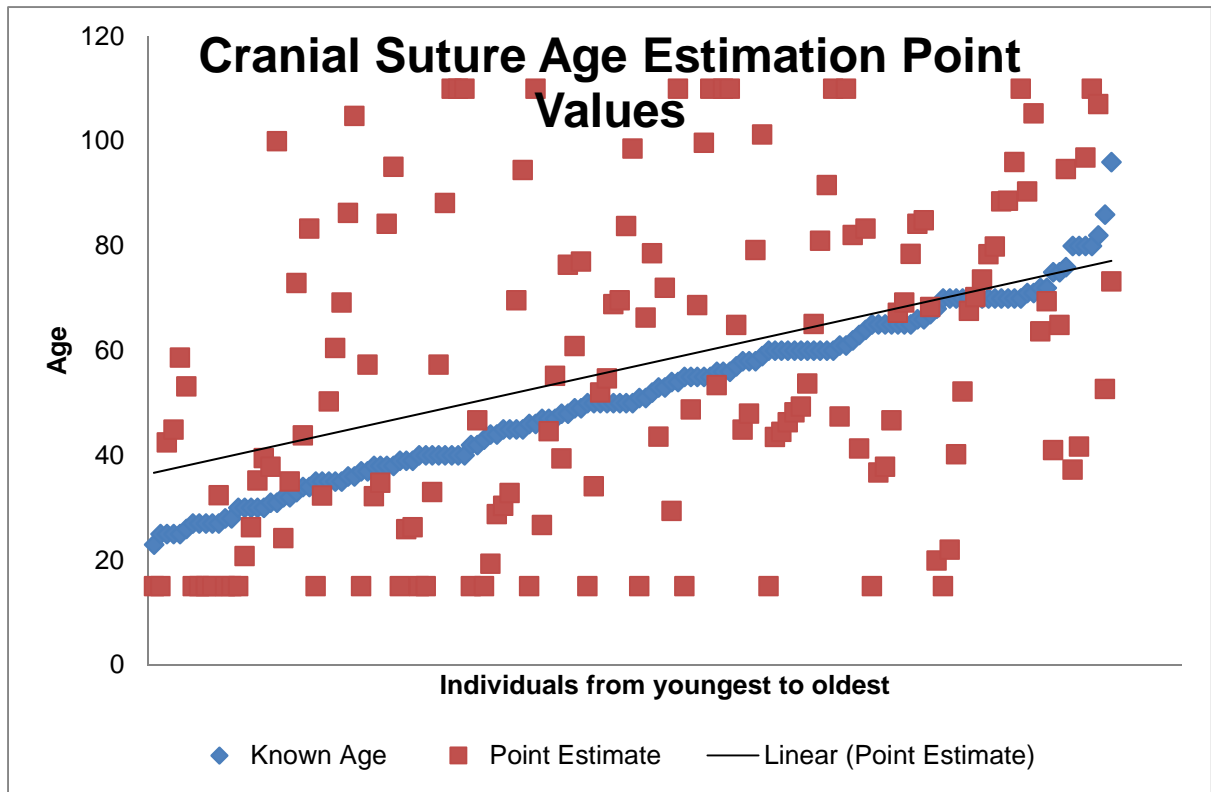


Figure 4.13: Cranial suture age estimation point values

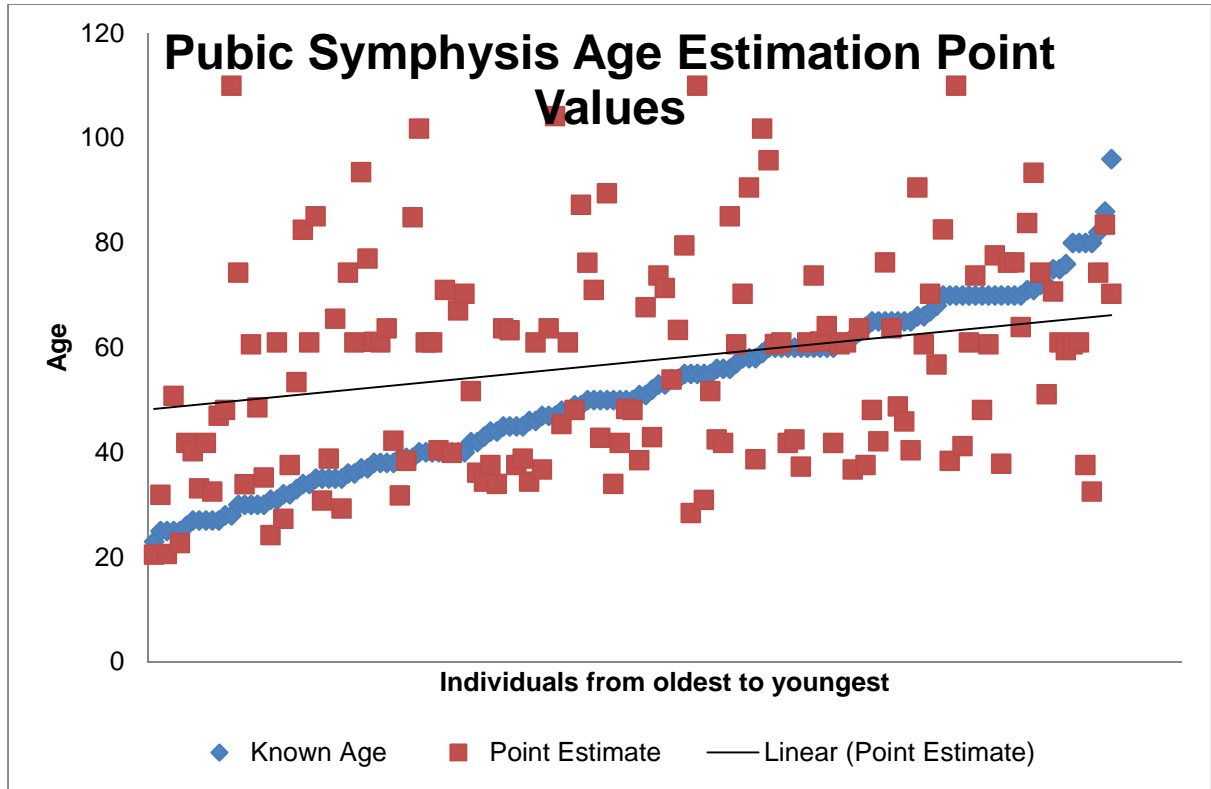


Figure 4.14: Pubic symphysis age estimation point values

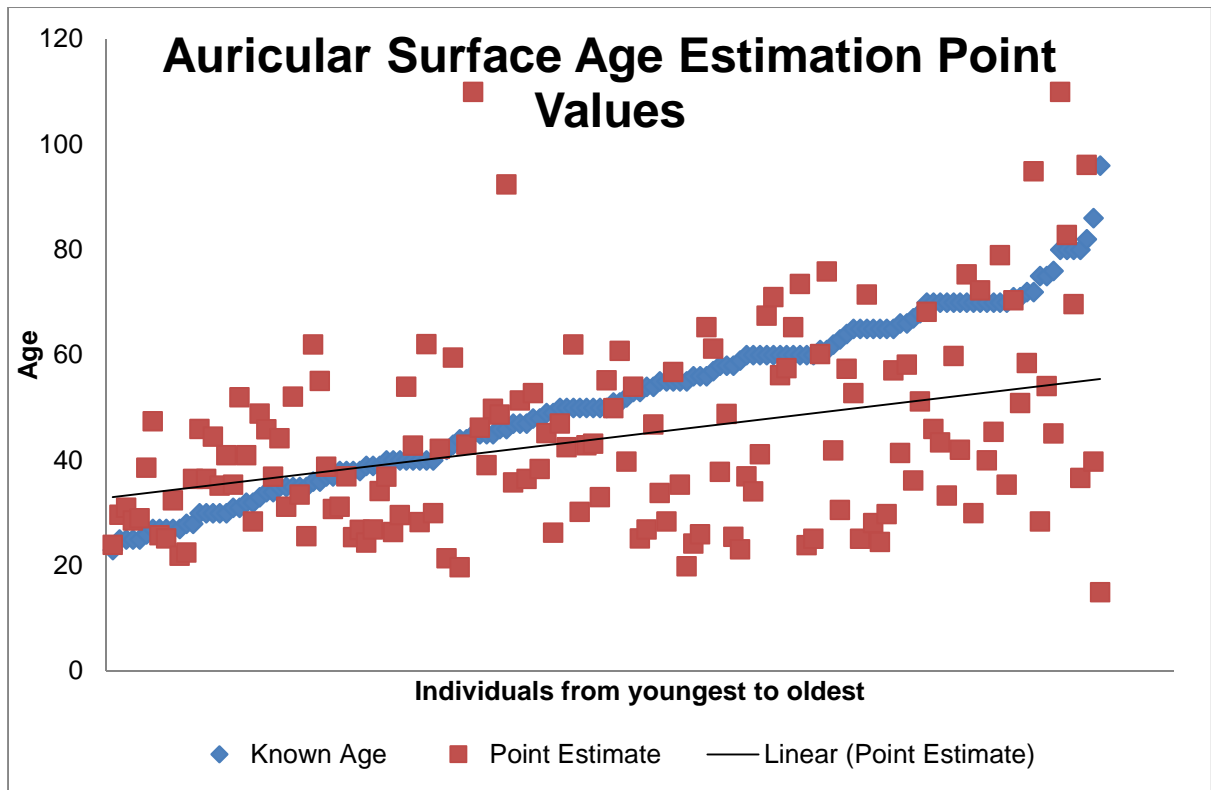


Figure 4.15: Auricular surface age estimation point values

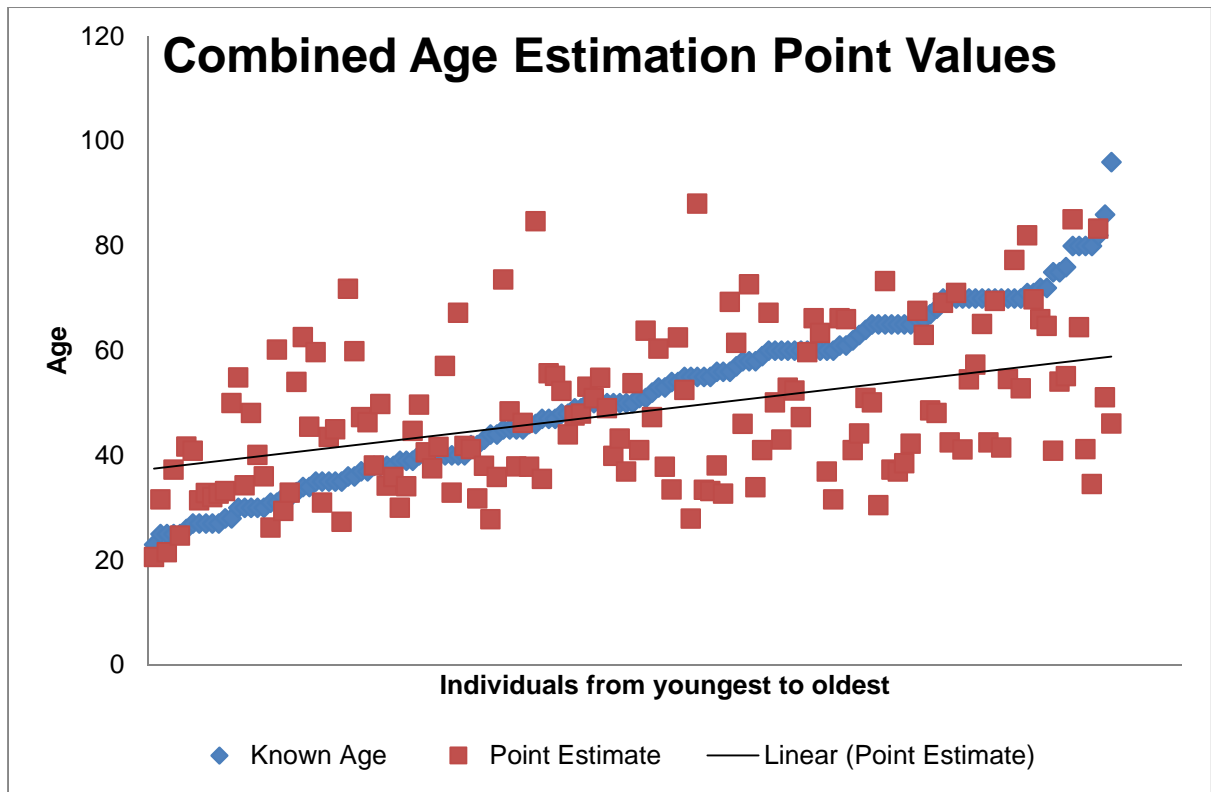


Figure 4.16: Combined age estimation (uniform prior distribution) point values

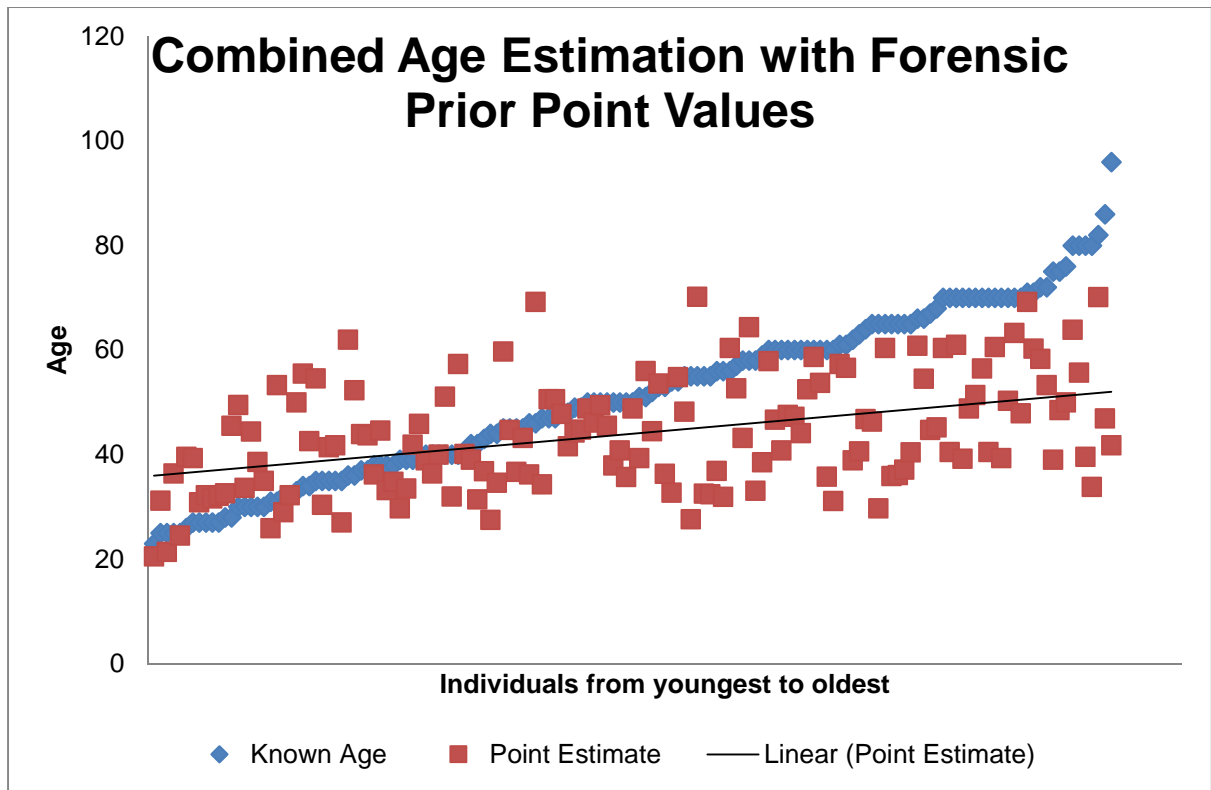


Figure 4.17: Combined age estimation (forensic prior distribution) point values

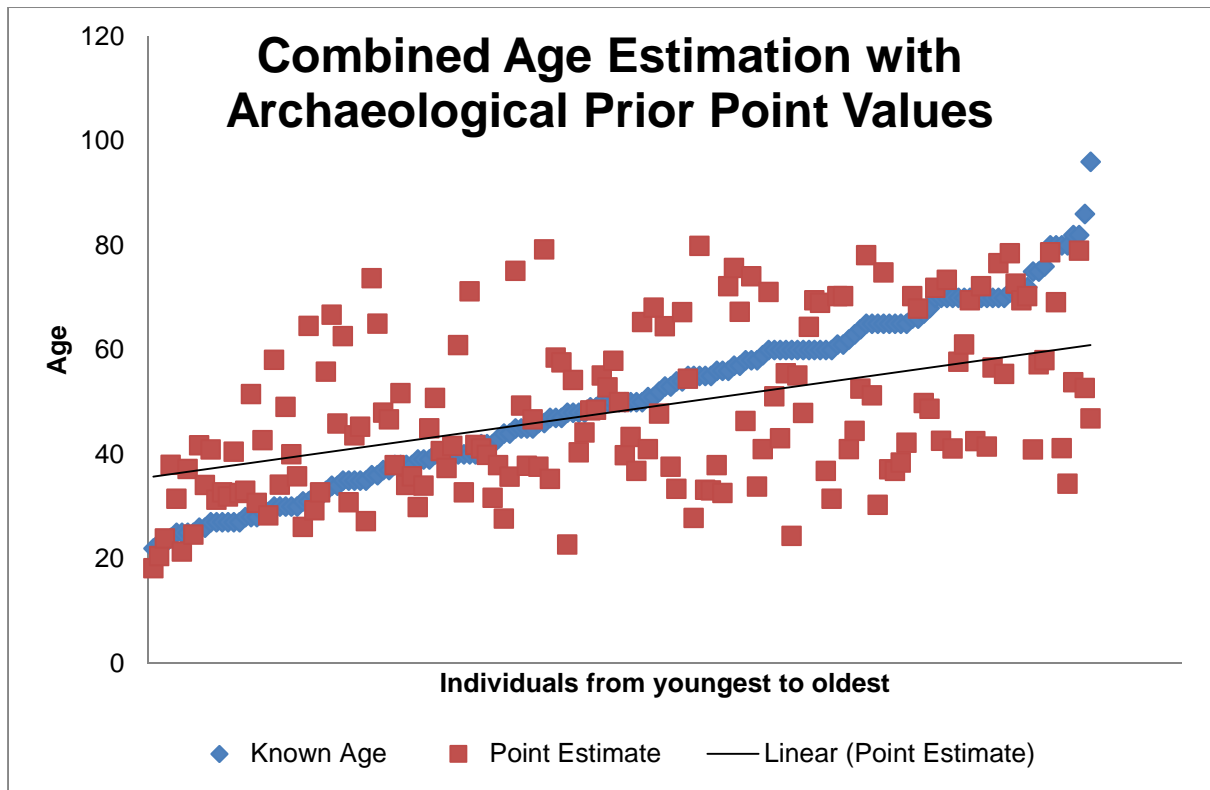


Figure 4.18: Combined age estimation (archaeological prior distribution) point values

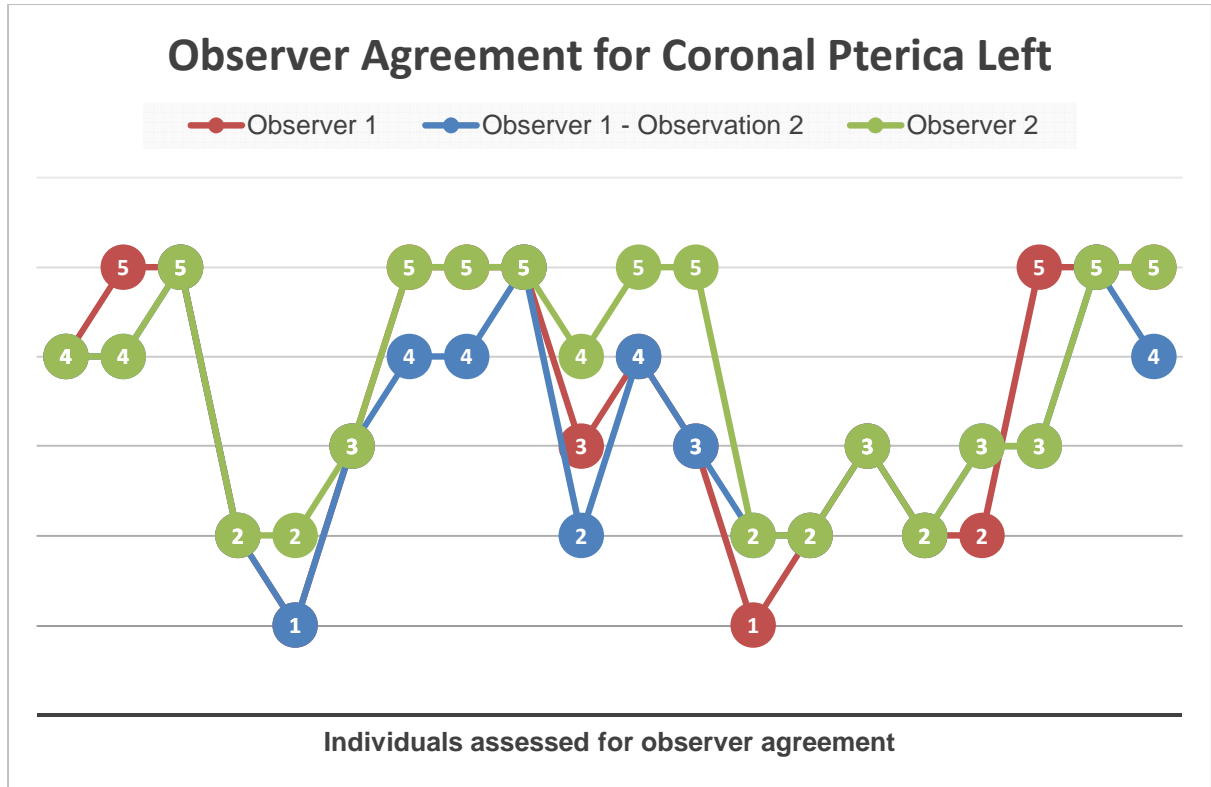


Figure 4.19: Observer agreement for coronal pterica left. (0) No score, (1) open, (2) juxtaposed, (3) partially obliterated, (4) punctuated, (5) obliterated

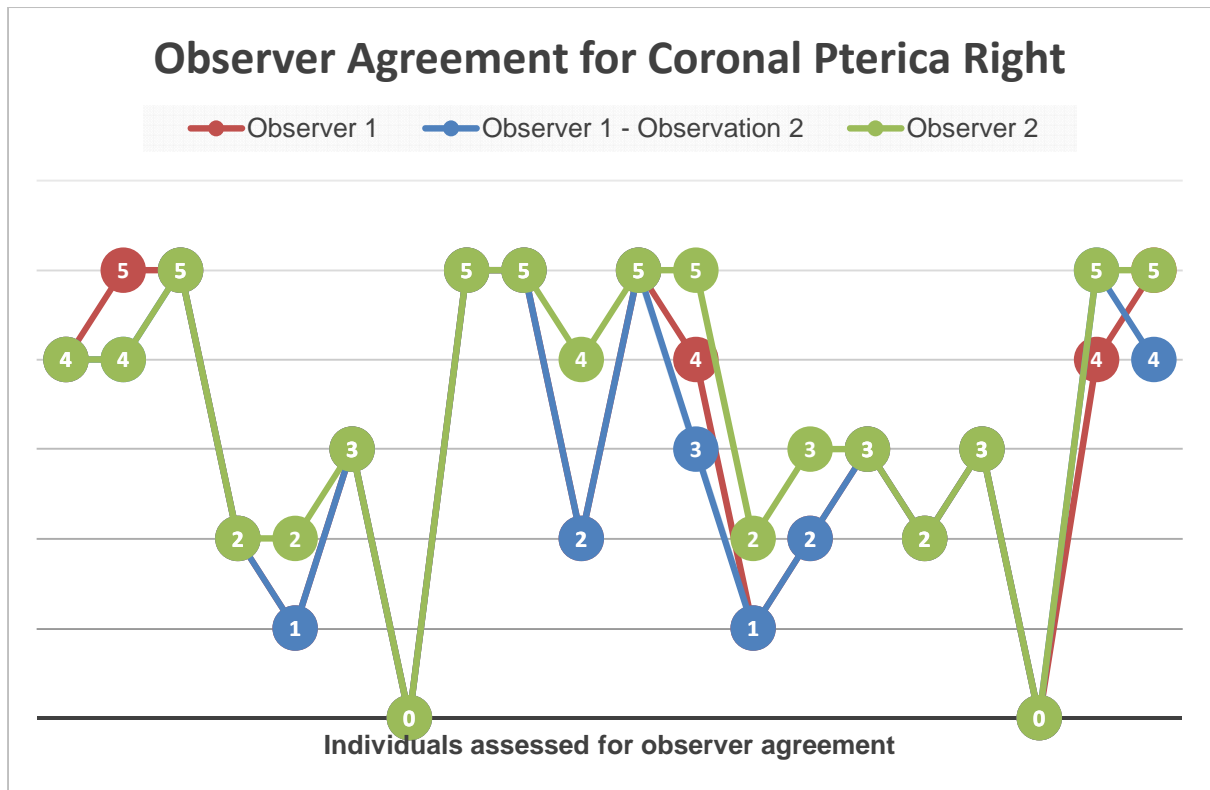


Figure 4.20: Observer agreement for coronal pterica right. (0) No score, (1) open, (2) juxtaposed, (3) partially obliterated, (4) punctuated, (5) obliterated

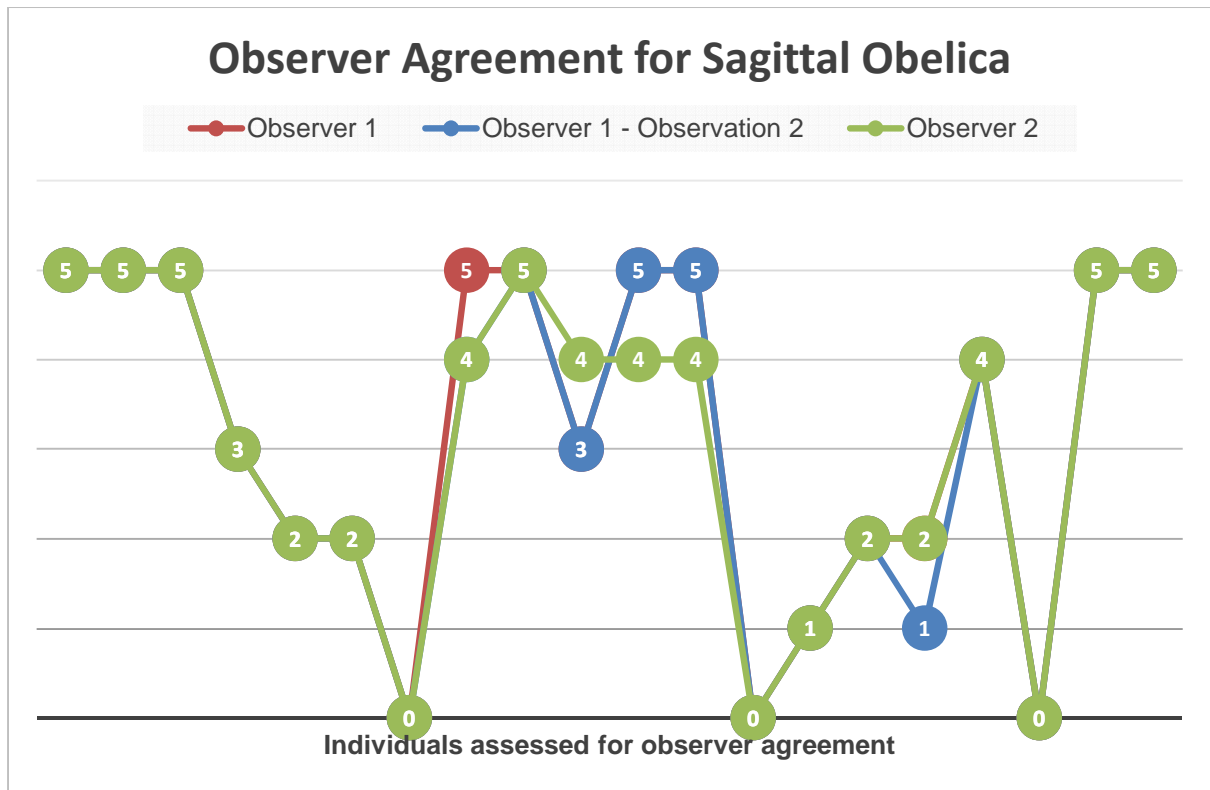


Figure 4.21: Observer agreement for sagittal obelica. (0) No score, (1) open, (2) juxtaposed, (3) partially obliterated, (4) punctuated, (5) obliterated

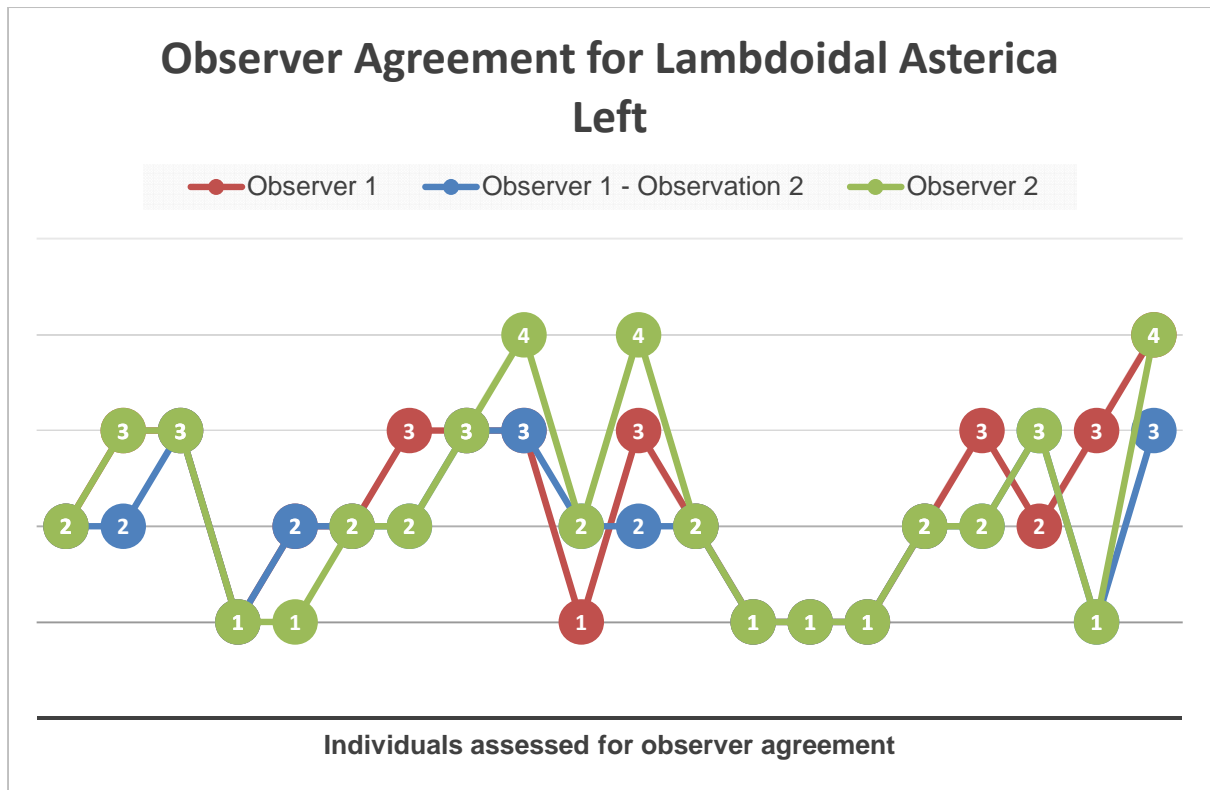


Figure 4.22: Observer agreement for lambdoidal asterica left. (0) No score, (1) open, (2) juxtaposed, (3) partially obliterated, (4) punctuated, (5) obliterated

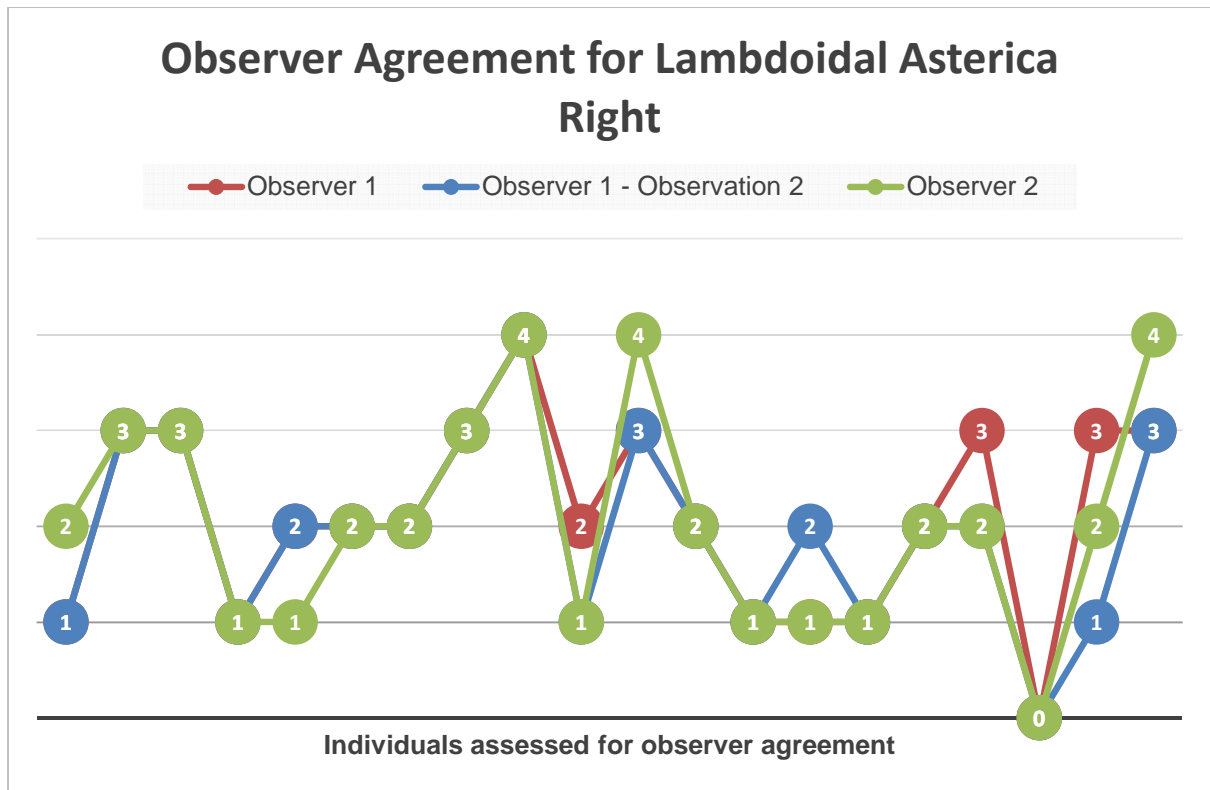


Figure 4.23: Observer agreement for lambdoidal asterica right. (0) No score, (1) open, (2) juxtaposed, (3) partially obliterated, (4) punctuated, (5) obliterated

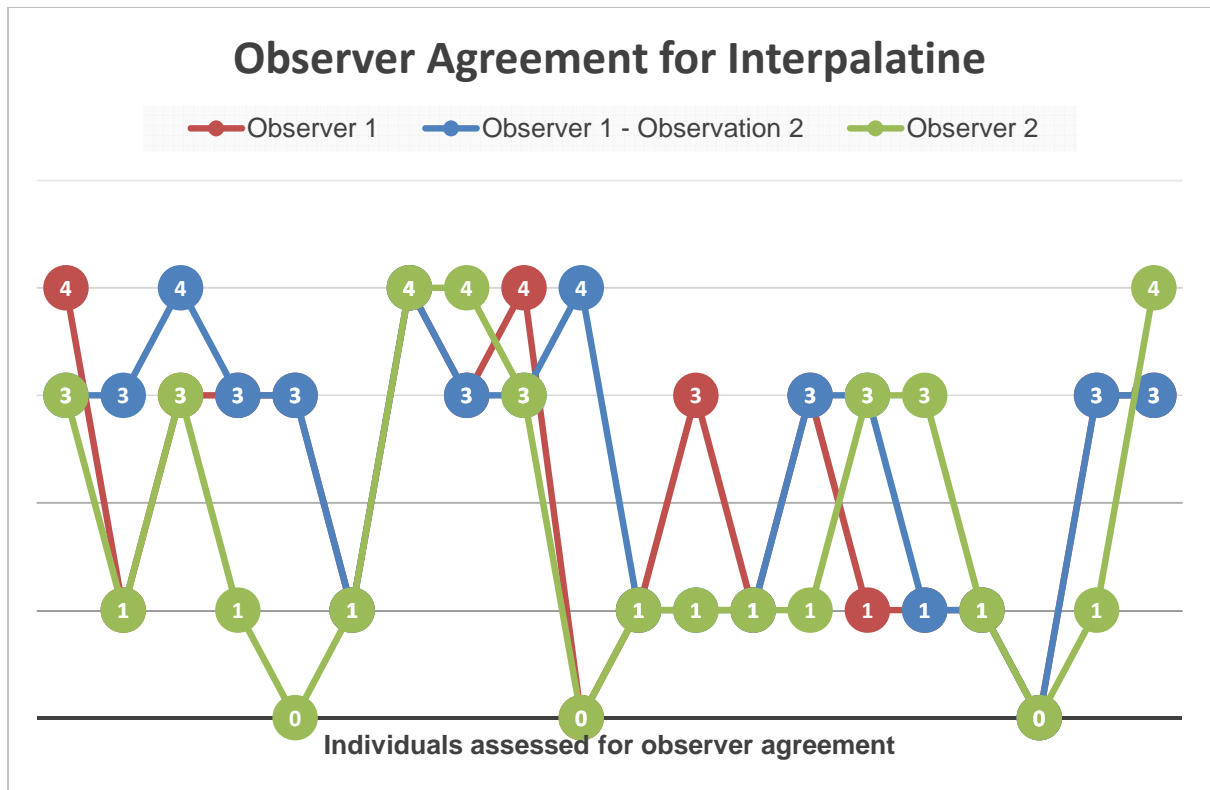


Figure 4.24: Observer agreement for interpalatine. (0) No score, (1) open/juxtaposed, (3) partially obliterated, (4) punctuated, (5) obliterated

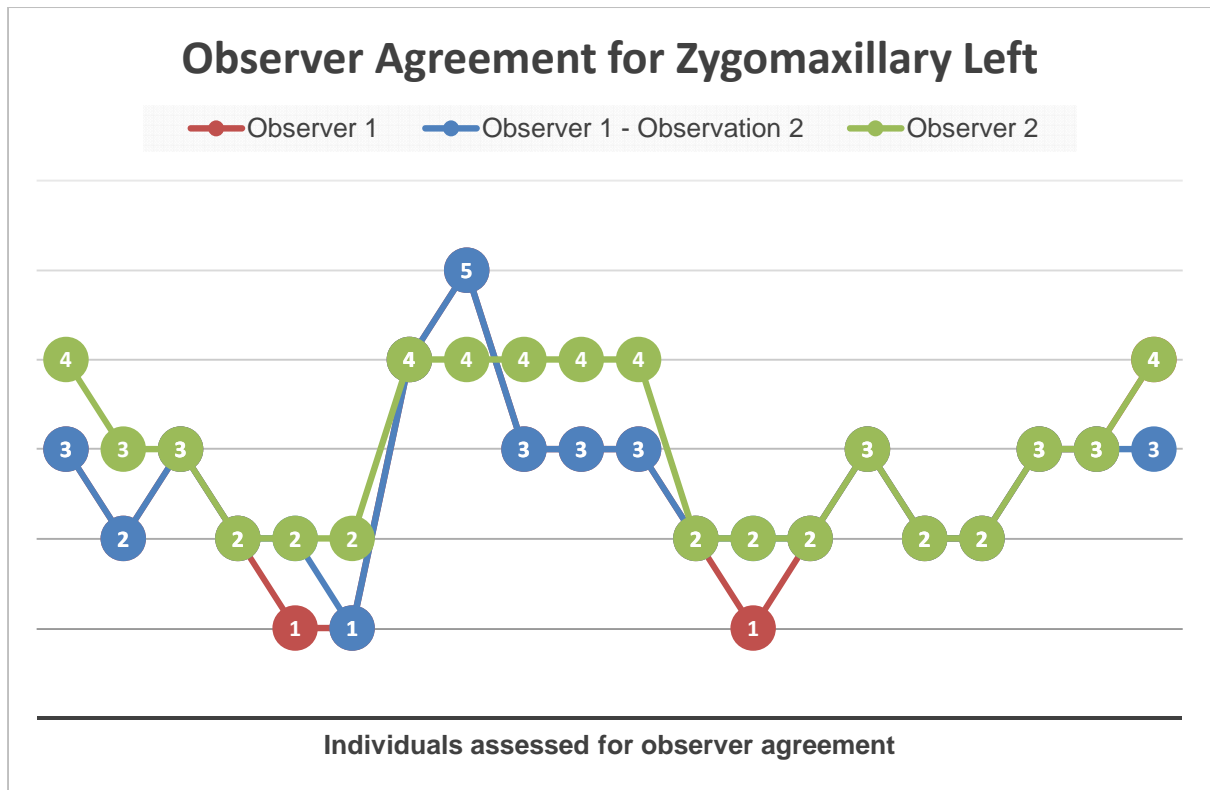


Figure 4.25: Observer agreement for zygomaxillary left. (0) No score, (1) open, (2) juxtaposed, (3) partially obliterated, (4) punctuated, (5) obliterated

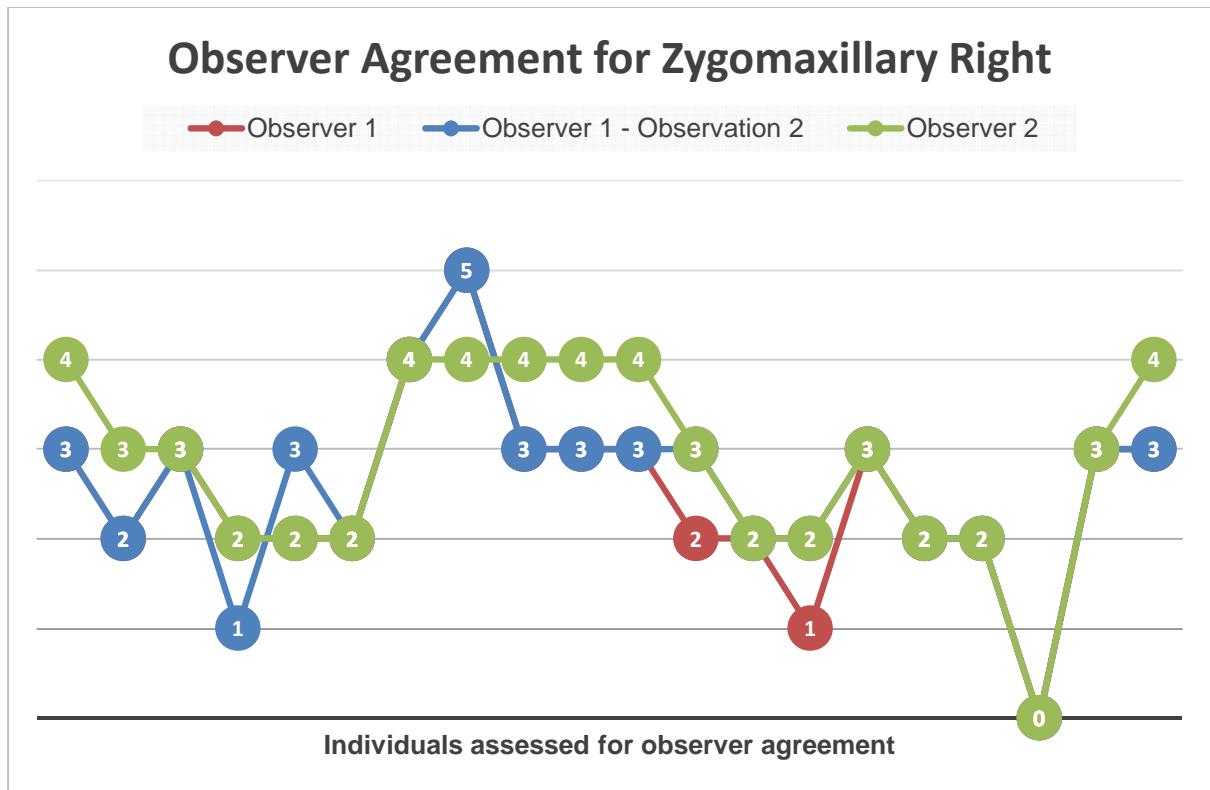


Figure 4.26: Observer agreement for zygomaxillary right. (0) No score, (1) open, (2) juxtaposed, (3) partially obliterated, (4) punctuated, (5) obliterated

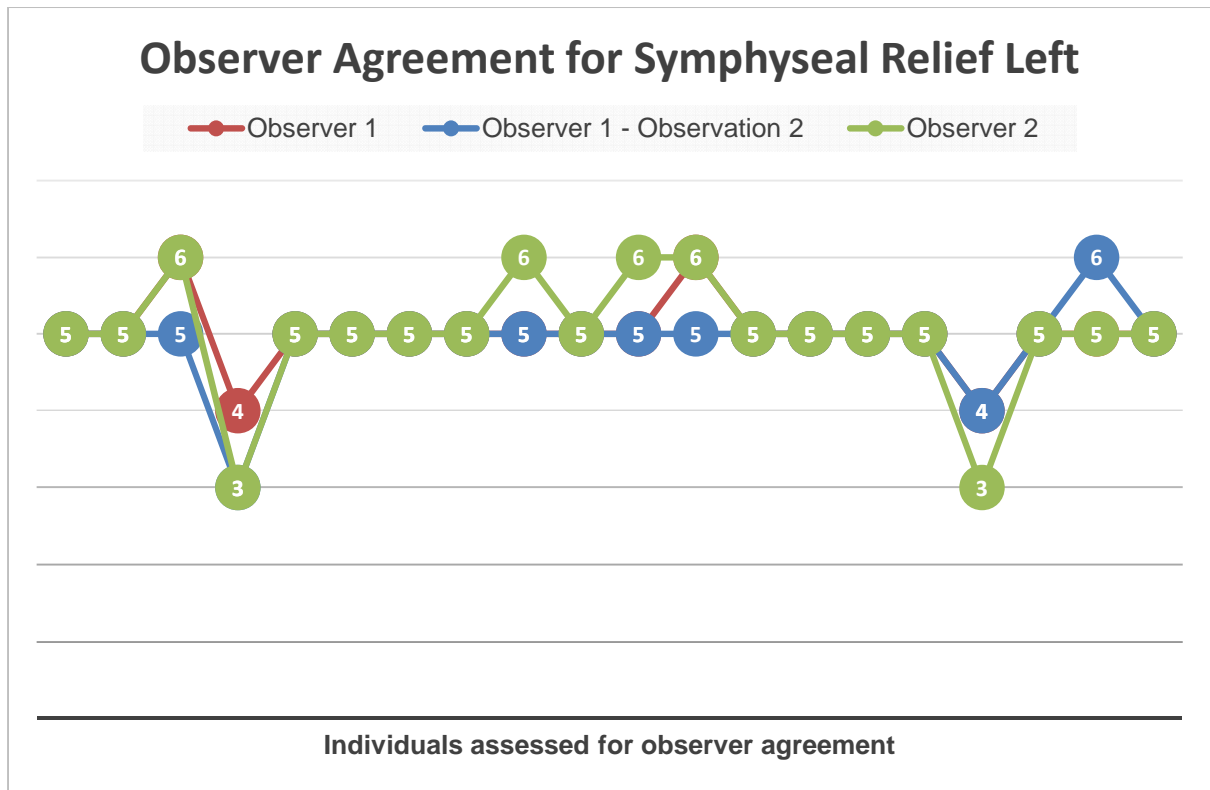


Figure 4.27: Observer agreement for symphyseal relief left. (0) No score, (1) sharp billowing, (2) soft, deep billowing, (3) soft, shallow billowing, (4) residual billowing, (5) flat, (6) irregular

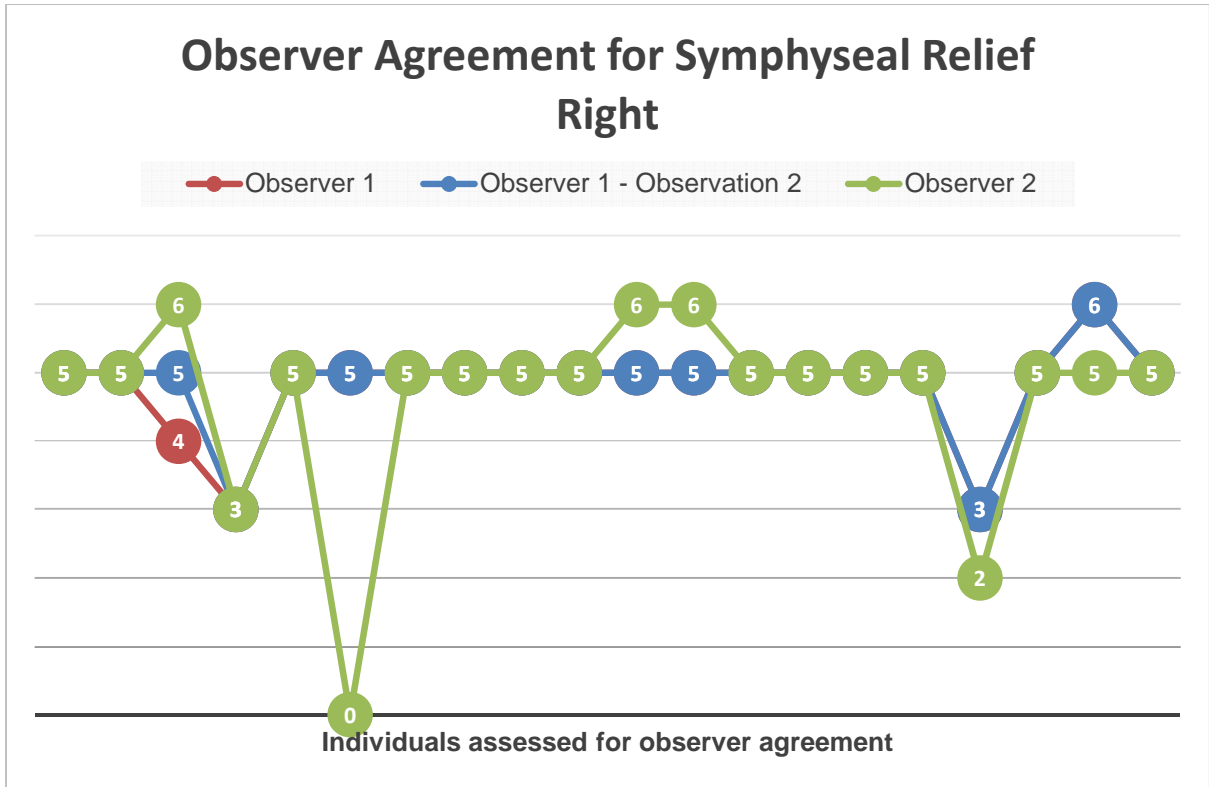


Figure 4.28: Observer agreement for symphyseal relief right. (0) No score, (1) sharp billowing, (2) soft, deep billowing, (3) soft, shallow billowing, (4) residual billowing, (5) flat, (6) irregular

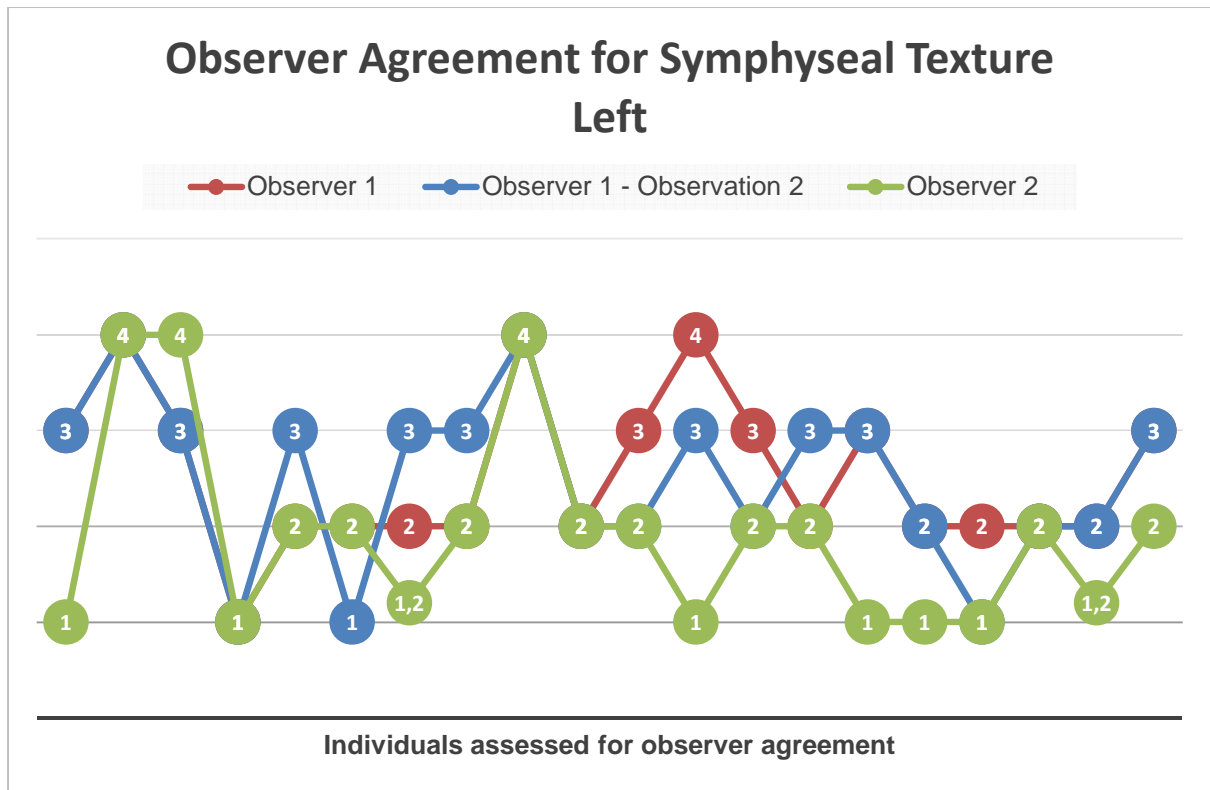


Figure 4.29: Observer agreement for symphyseal texture left. (0) No score, (1) smooth/fine grained, (2) coarse grained, (3) microporosity, (4) macroporosity

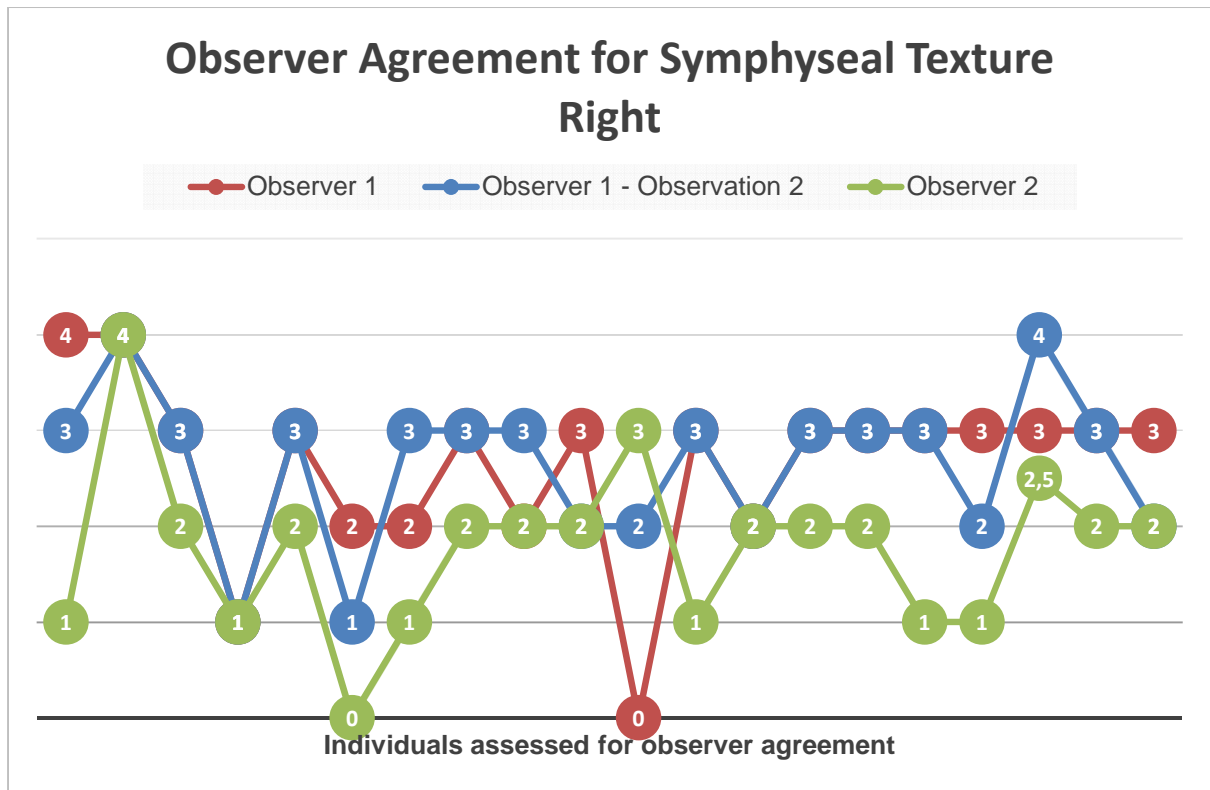


Figure 4.30: Observer agreement for symphyseal texture right. (0) No score, (1) smooth/fine grained, (2) coarse grained, (3) microporosity, (4) macroporosity

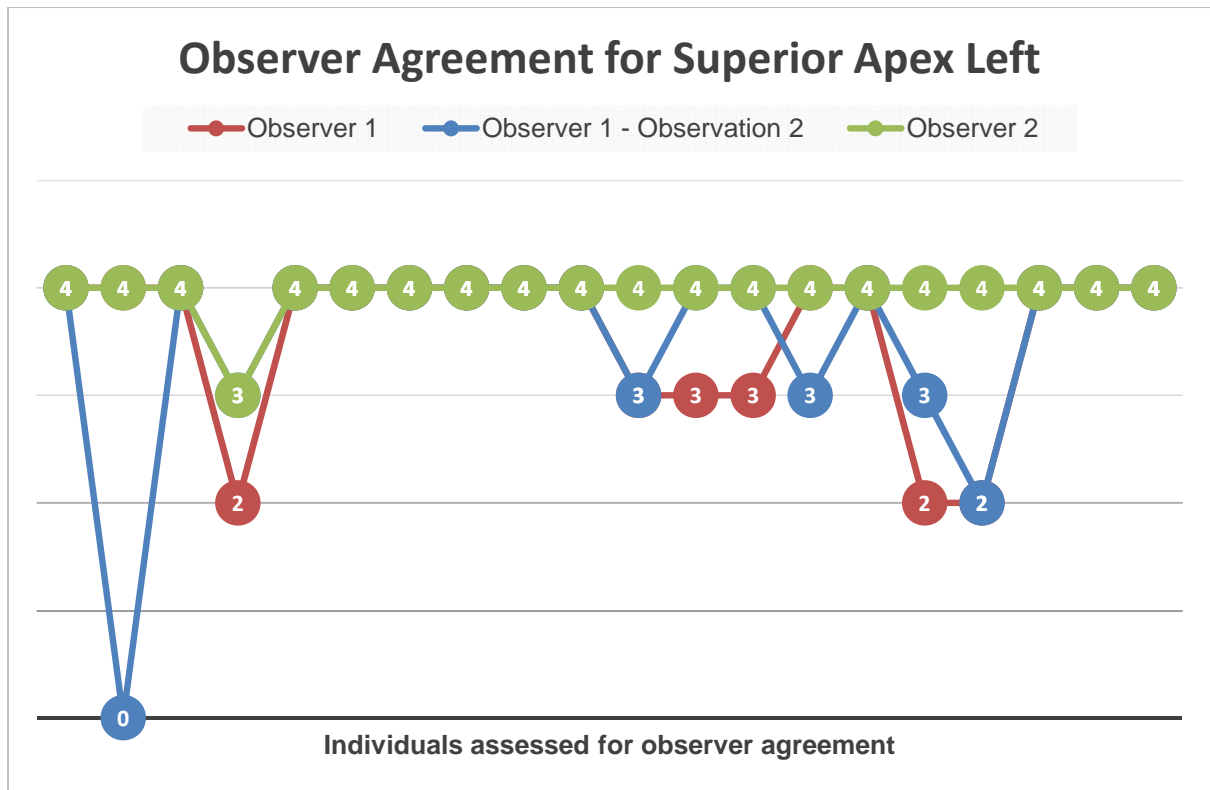


Figure 4.31: Observer agreement for superior apex left. (0) No score, (1) no protuberance, (2) early protuberance, (3) late protuberance, (4) integrated

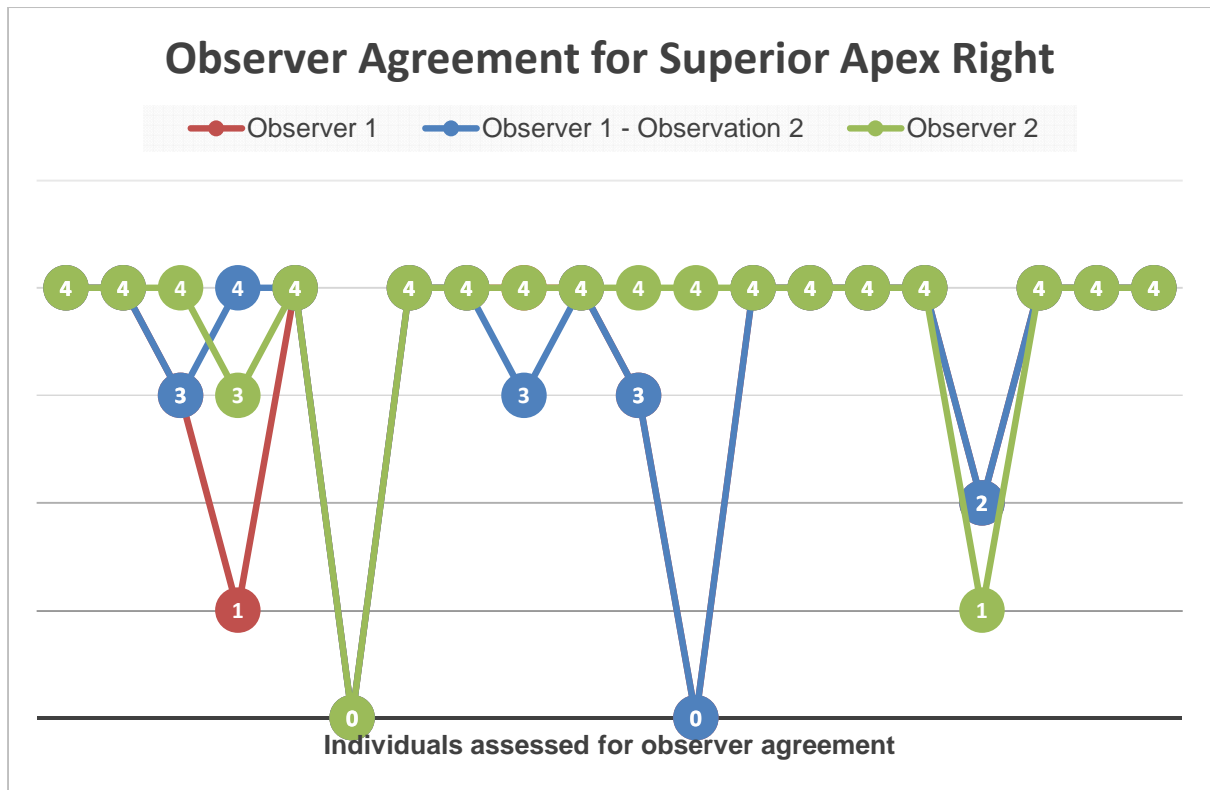


Figure 4.32: Observer agreement for superior apex right. (0) No score, (1) no protuberance, (2) early protuberance, (3) late protuberance, (4) integrated

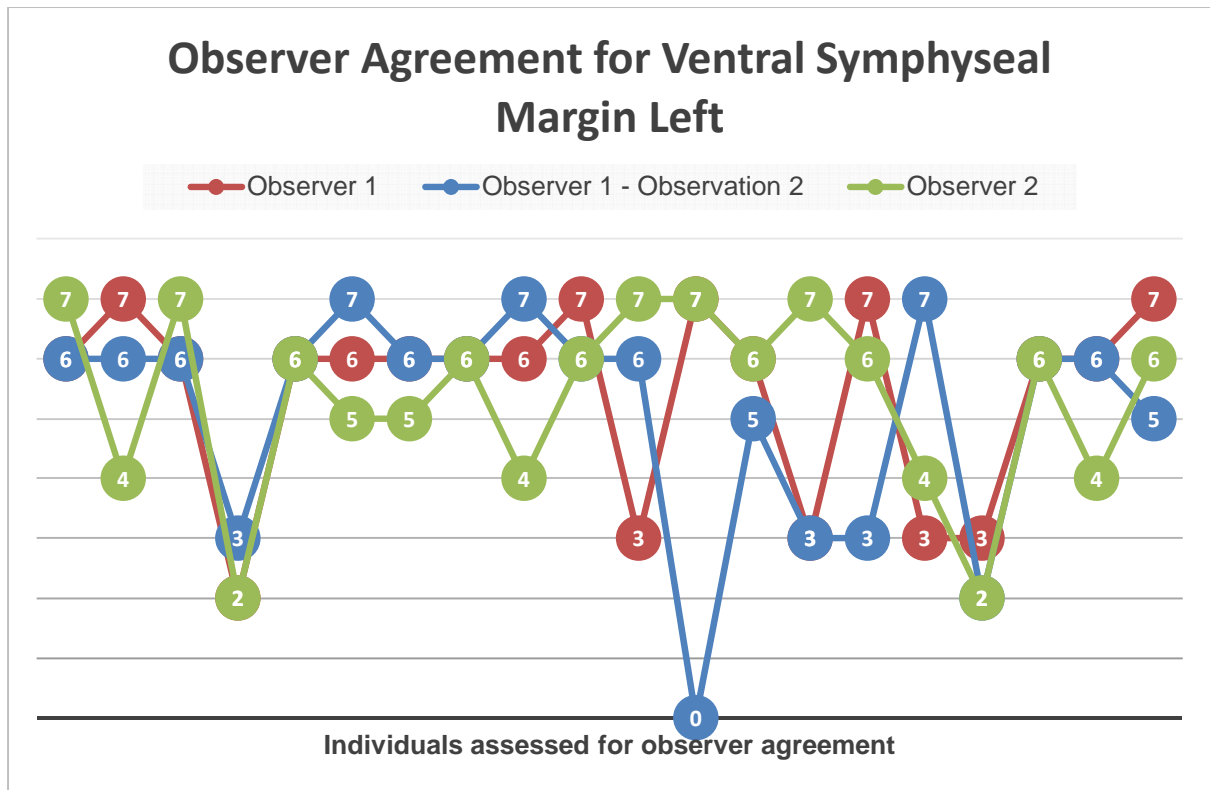


Figure 4.33: Observer agreement for ventral symphyseal margin left. (0) No score, (1) serrated, (2) bevelling, (3) rampart formation, (4) rampart completion I, (5) rampart completion II, (6) rim, (7) breakdown

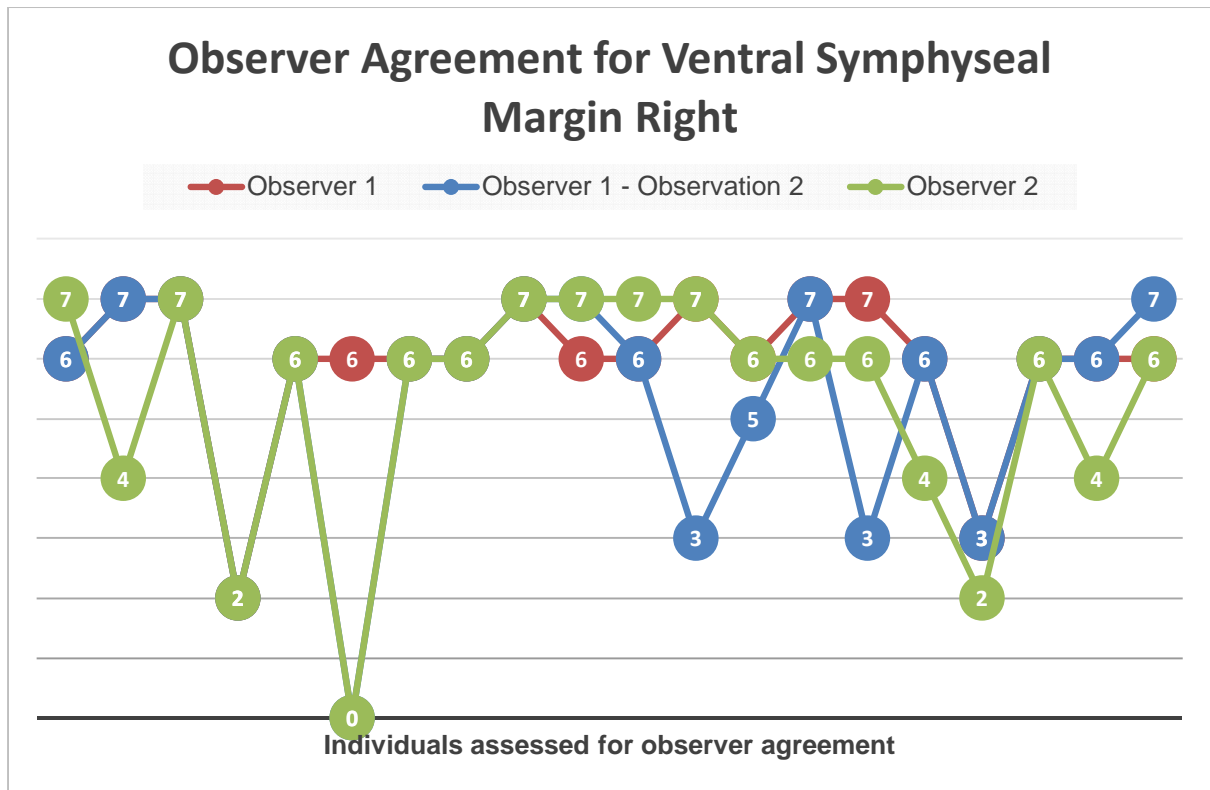


Figure 4.34: Observer agreement for ventral symphyseal margin right. (0) No score, (1) serrated, (2) bevelling, (3) rampart formation, (4) rampart completion I, (5) rampart completion II, (6) rim, (7) breakdown

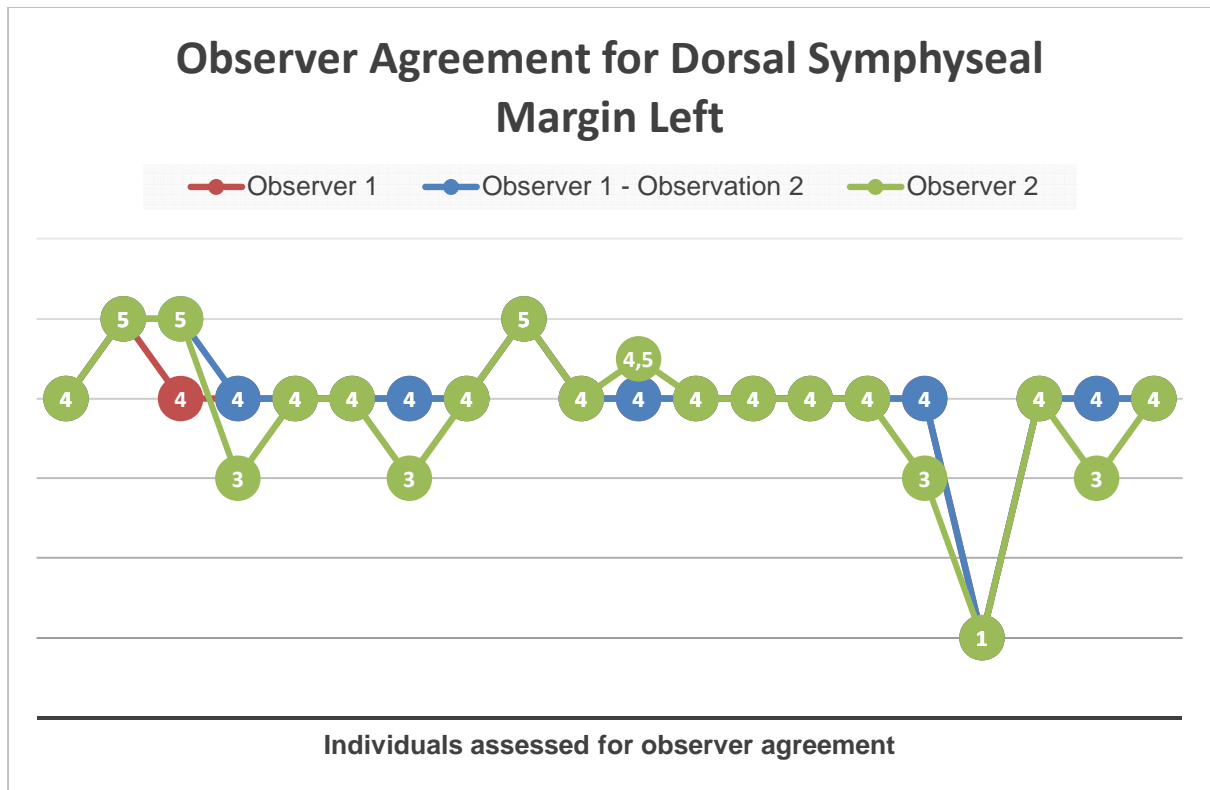


Figure 4.35: Observer agreement for dorsal symphyseal margin left. (0) No score, (1) serrated, (2) flattening incomplete, (3) flattening complete, (4) rim, (5) breakdown

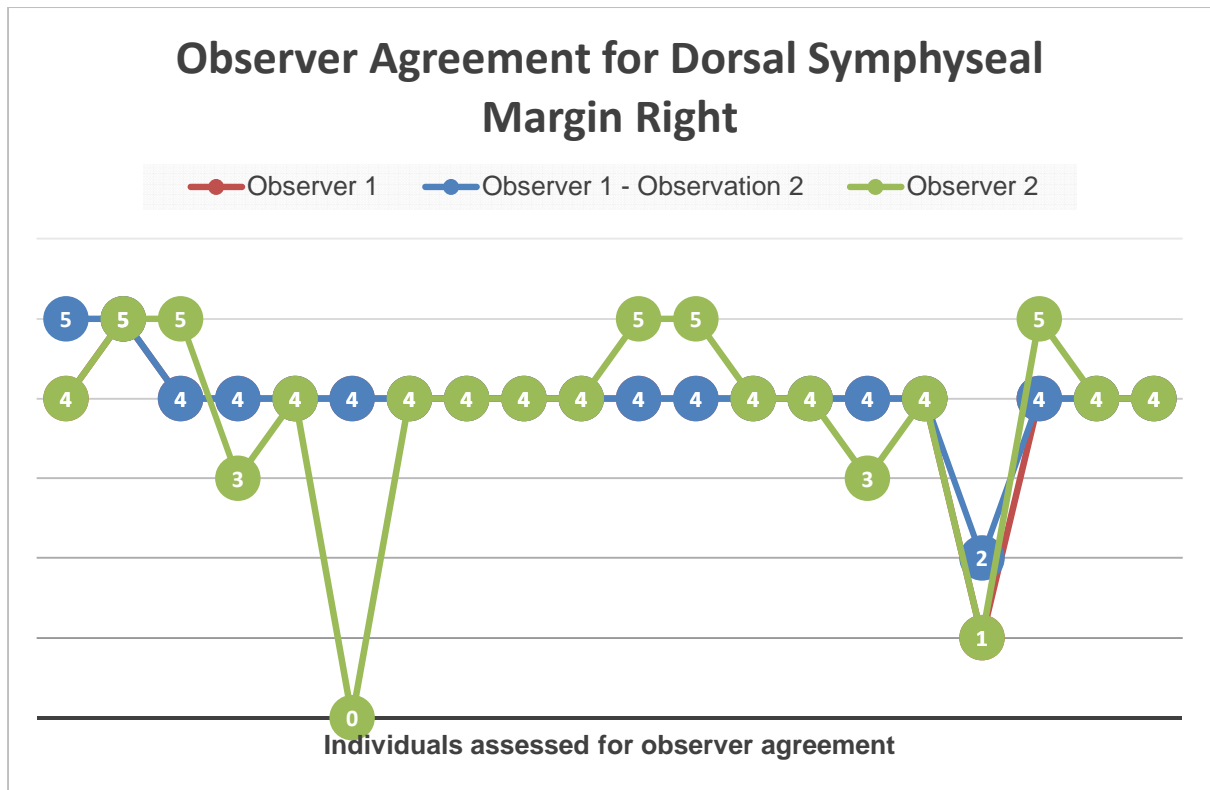


Figure 4.36: Observer agreement for dorsal symphyseal margin right. (0) No score, (1) serrated, (2) flattening incomplete, (3) flattening complete, (4) rim, (5) breakdown

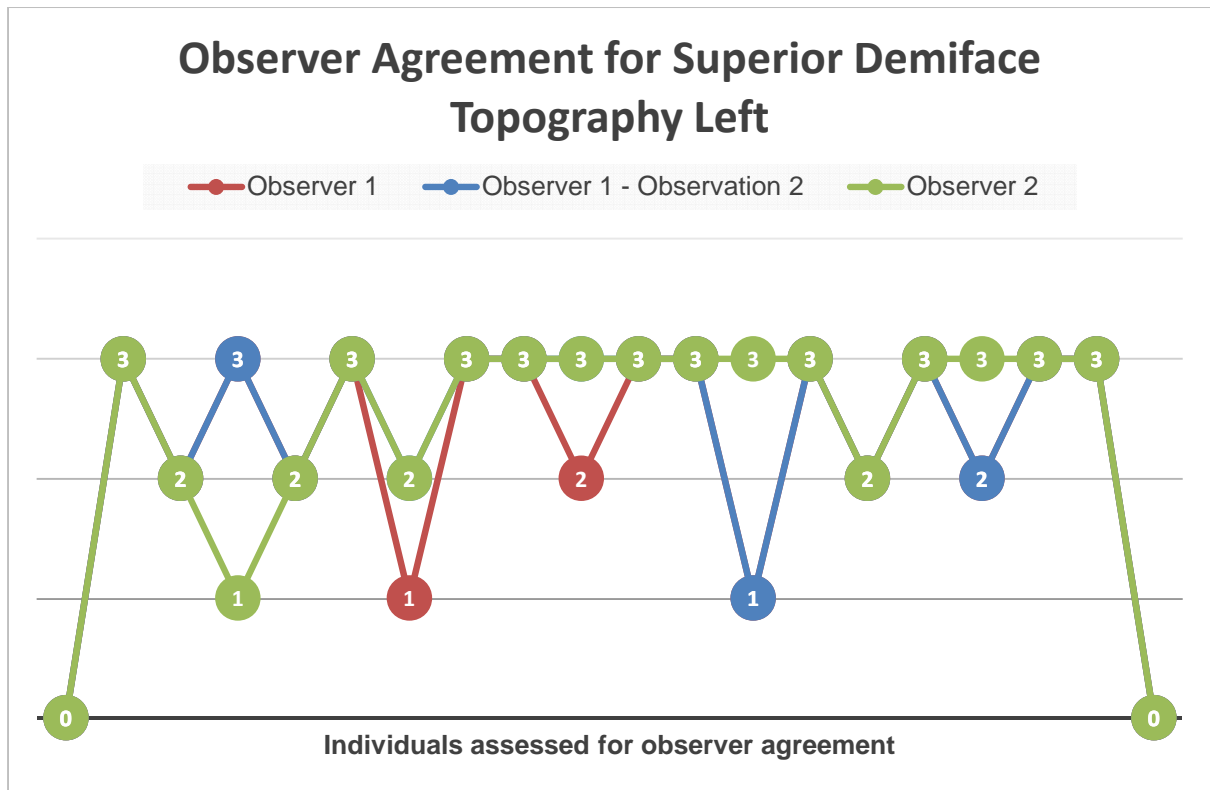


Figure 4.37: Observer agreement for superior demiface topography left. (0) No score, (1) undulating, (2) median elevation, (3) flat/irregular

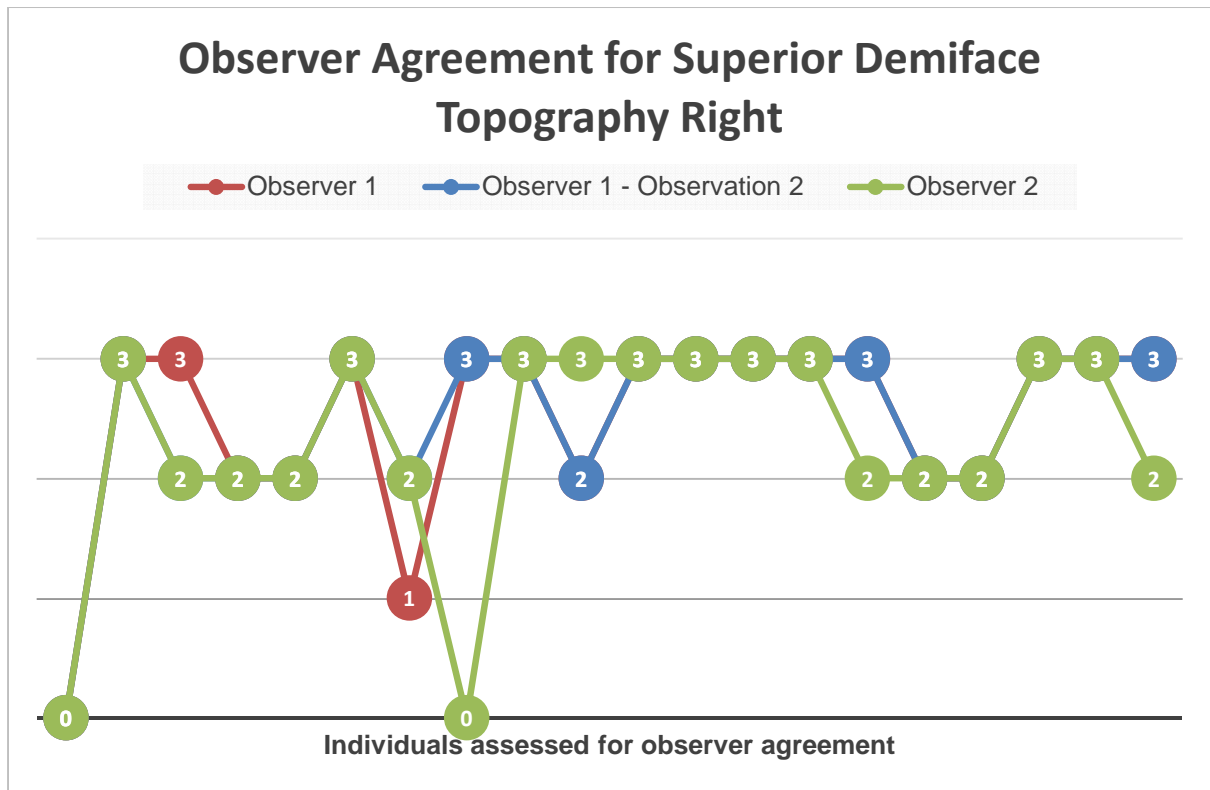


Figure 4.38: Observer agreement for superior demiface topography right.
(0) No score, (1) undulating, (2) median elevation, (3) flat/irregular

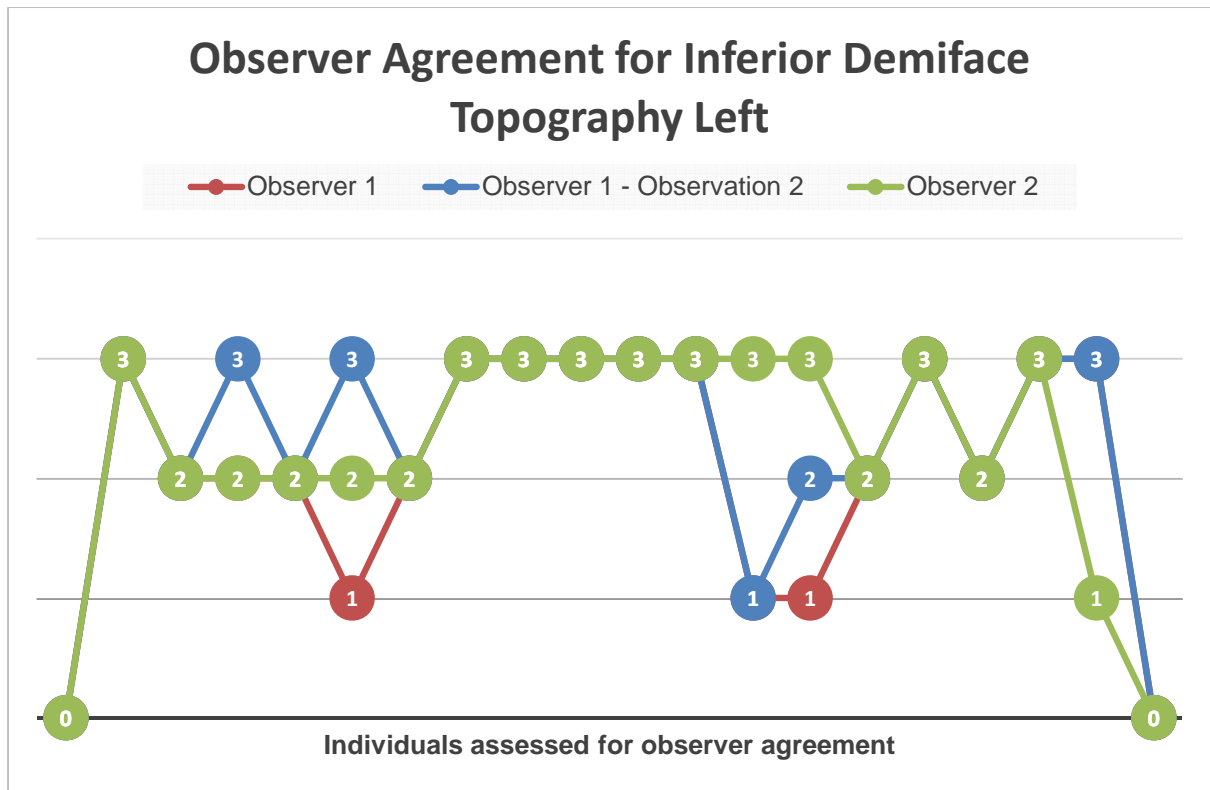


Figure 4.39: Observer agreement for inferior demiface topography left. (0) No score, (1) undulating, (2) median elevation, (3) flat/irregular

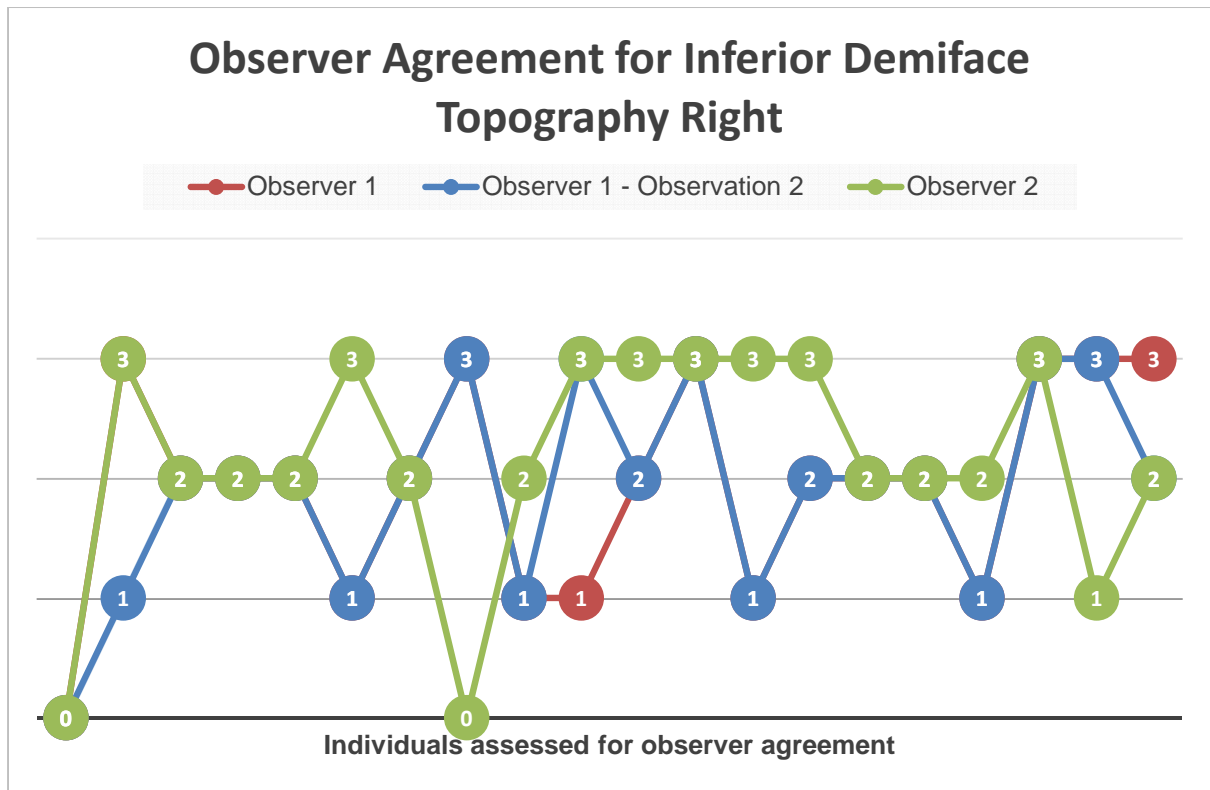


Figure 4.40: Observer agreement for inferior demiface topography right. (0) No score, (1) undulating, (2) median elevation (3) flat/irregular

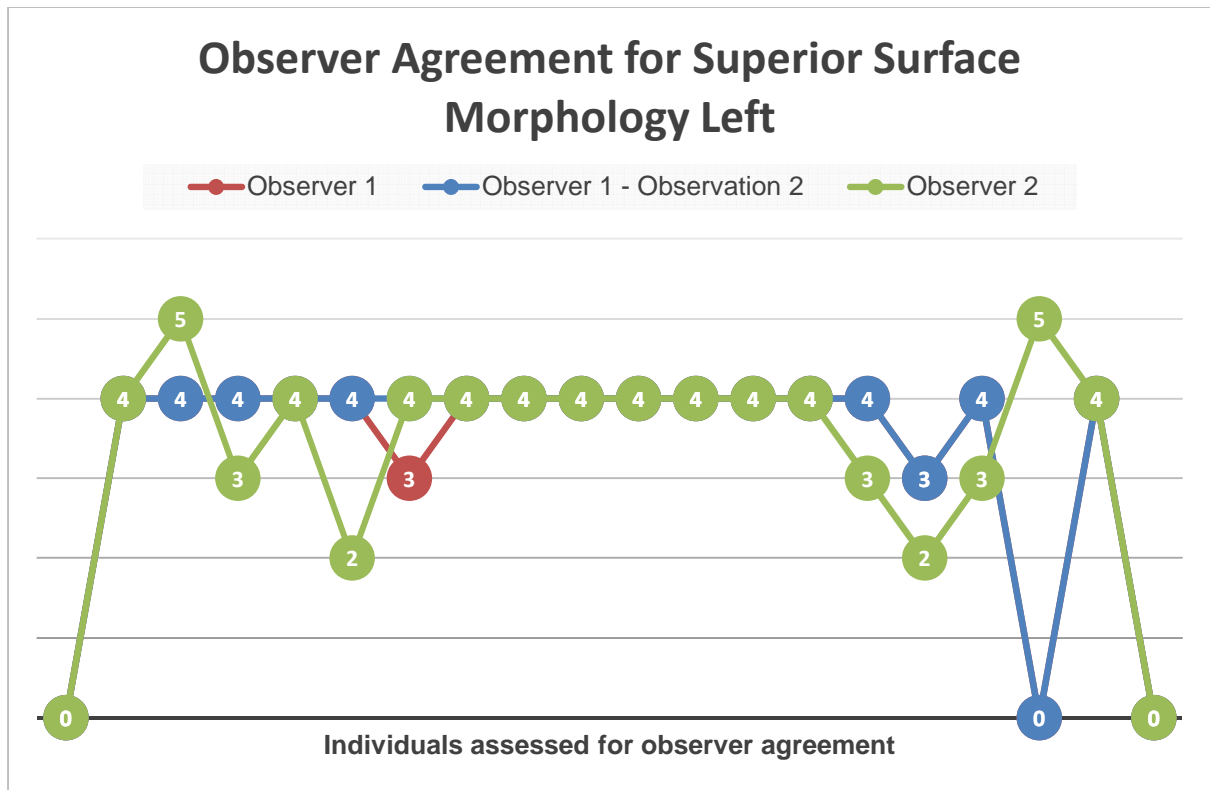


Figure 4.41: Observer agreement for superior surface morphology left. (0) No score, (1) >2/3 covered by billows, (2) 1/3 – 2/3 covered by billows, (3) <1/3 covered by billows, (4) flat/no billows, (5) bumps

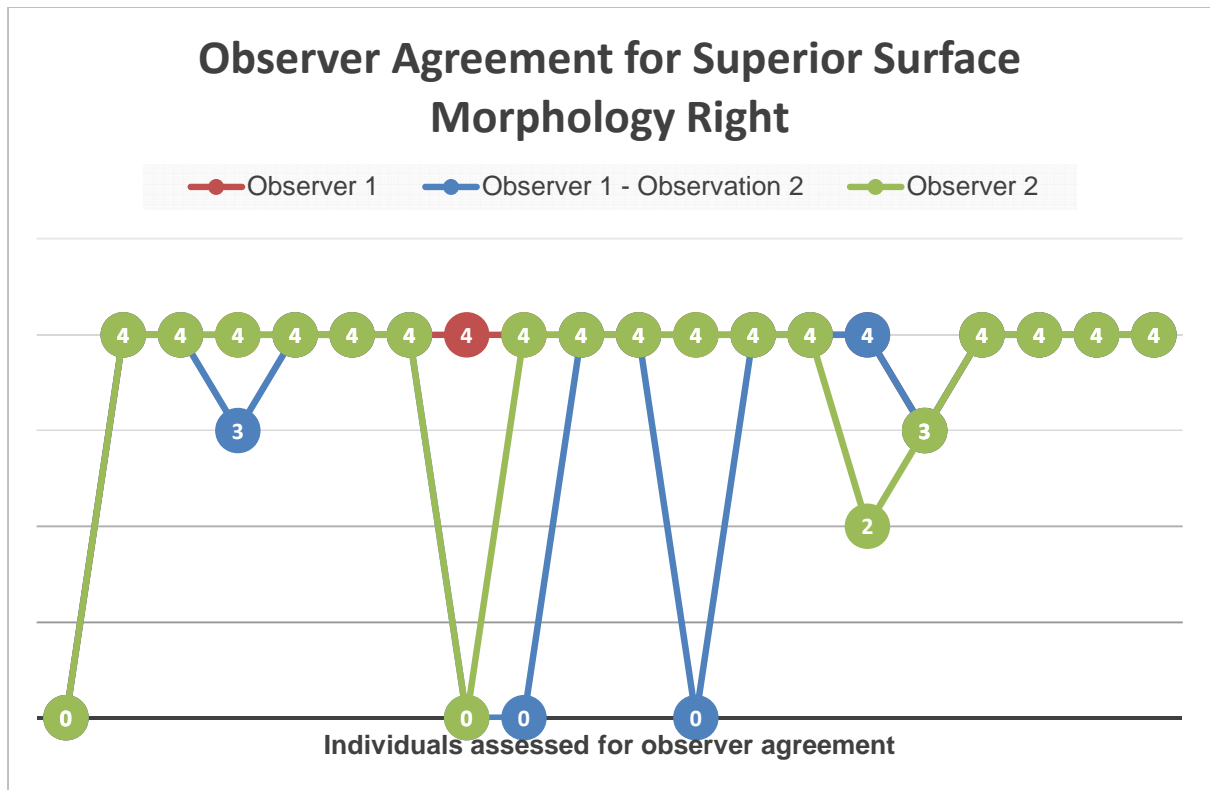


Figure 4.42: Observer agreement for superior surface morphology right. (0) No score, (1) >2/3 covered by billows, (2) 1/3 – 2/3 covered by billows, (3) <1/3 covered by billows, (4) flat/no billows, (5) bumps

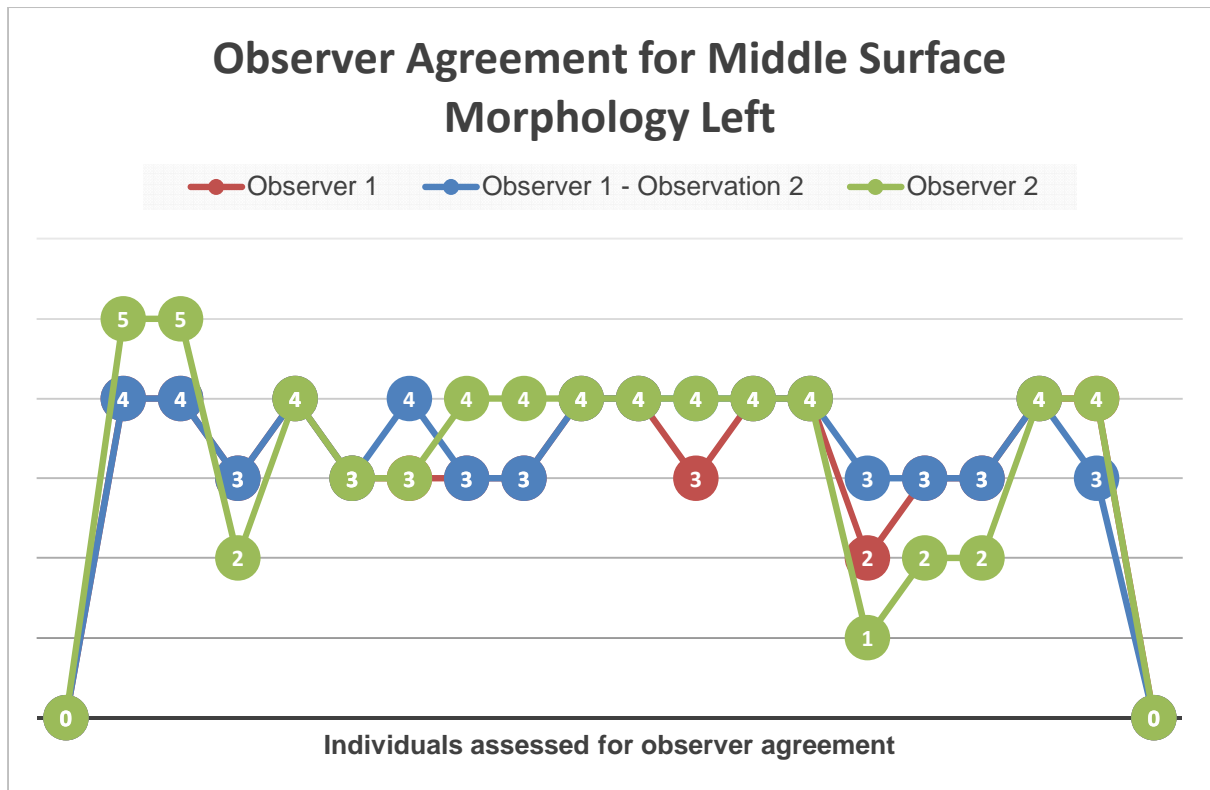


Figure 4.43: Observer agreement for middle surface morphology left. (0) No score, (1) >2/3 covered by billows, (2) 1/3 – 2/3 covered by billows, (3) <1/3 covered by billows, (4) flat/no billows, (5) bumps

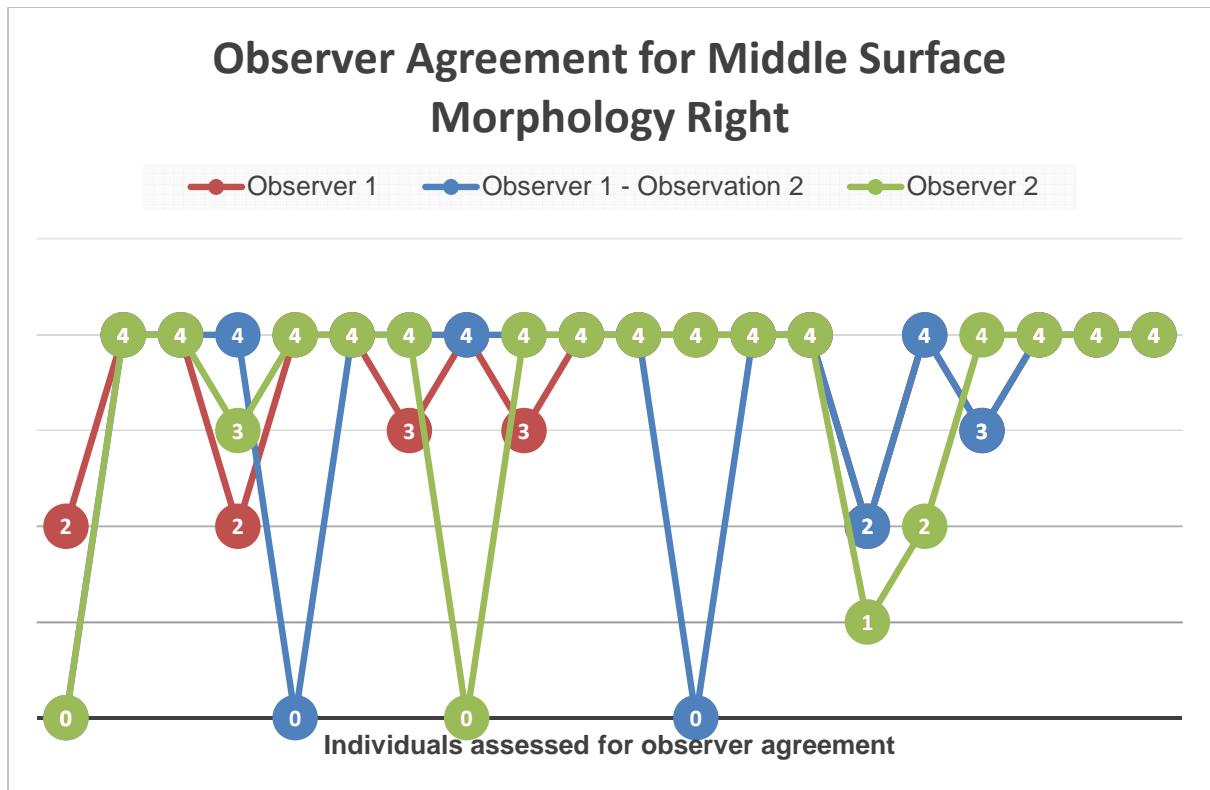


Figure 4.44: Observer agreement for middle surface morphology right. (0) No score, (1) >2/3 covered by billows, (2) 1/3 – 2/3 covered by billows, (3) <1/3 covered by billows, (4) flat/no billows, (5) bumps

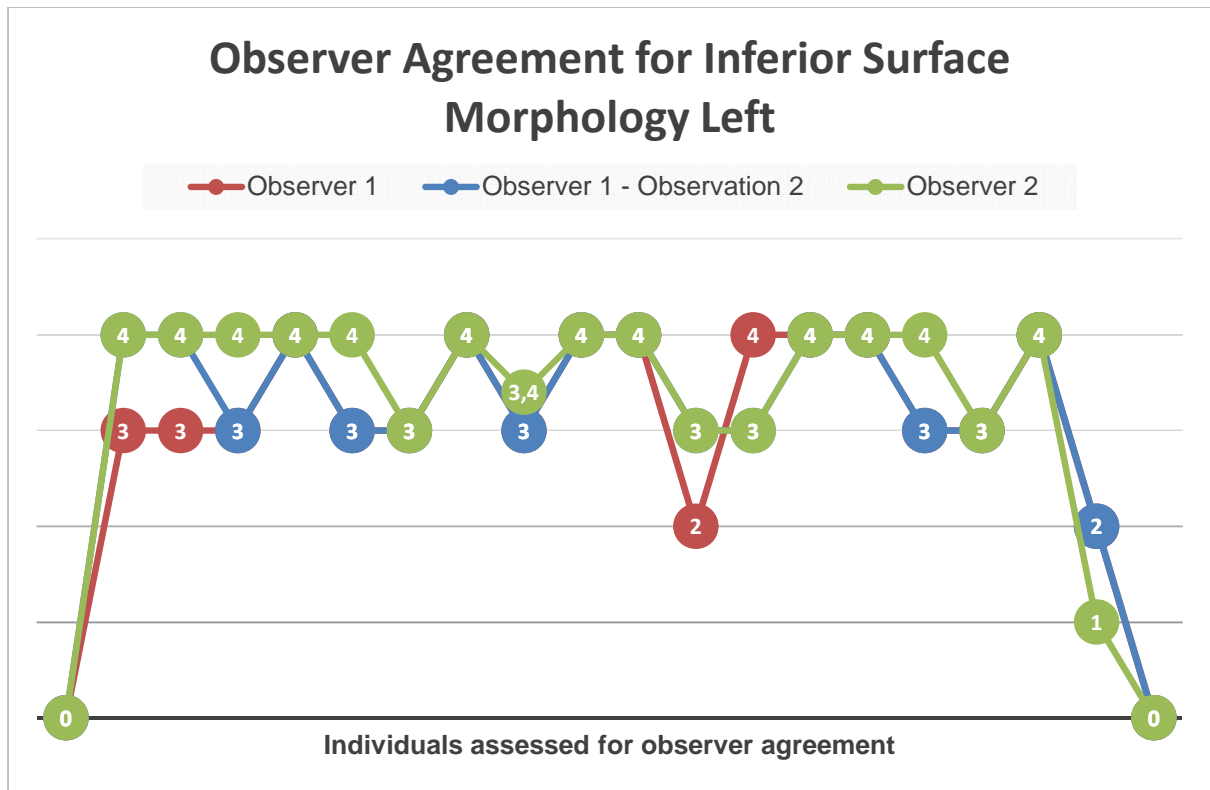


Figure 4.45: Observer agreement for inferior surface morphology left. (0) No score, (1) >2/3 covered by billows, (2) 1/3 – 2/3 covered by billows, (3) <1/3 covered by billows, (4) flat/no billows, (5) bumps

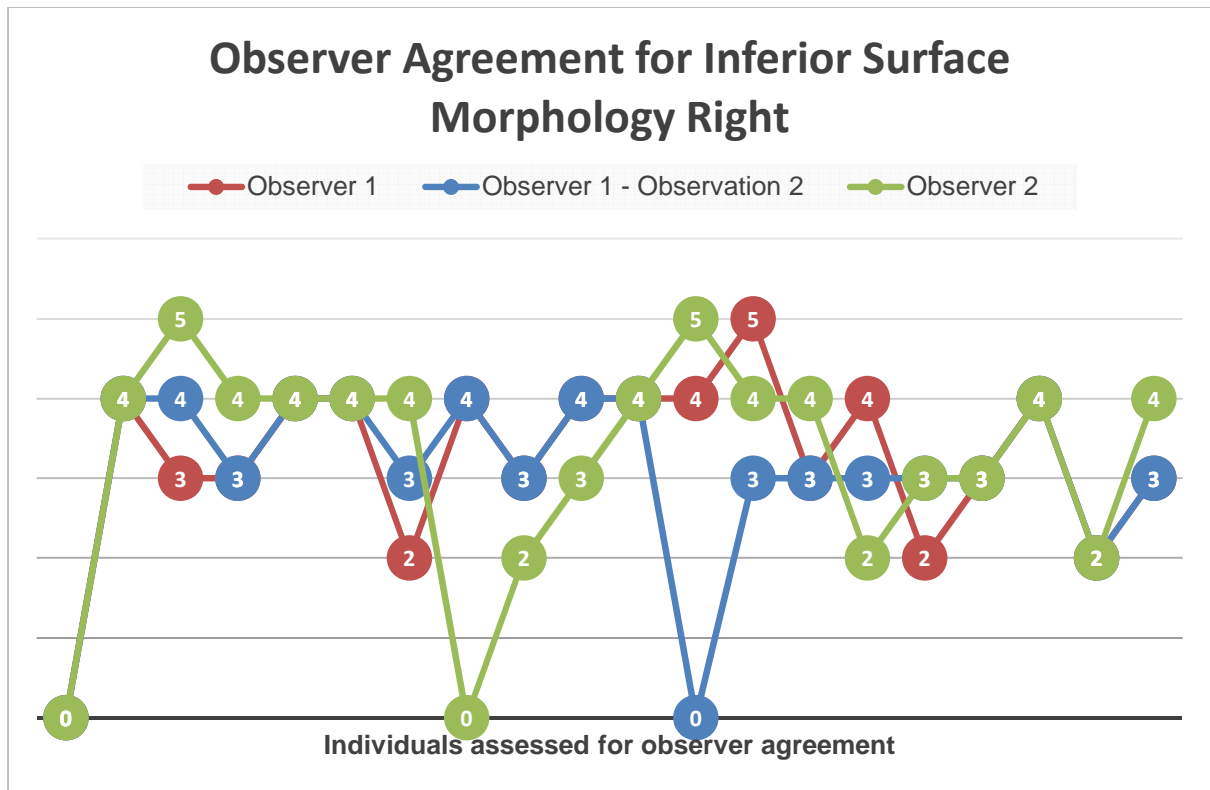


Figure 4.46: Observer agreement for inferior surface morphology right. (0) No score, (1) >2/3 covered by billows, (2) 1/3 – 2/3 covered by billows, (3) <1/3 covered by billows, (4) flat/no billows, (5) bumps

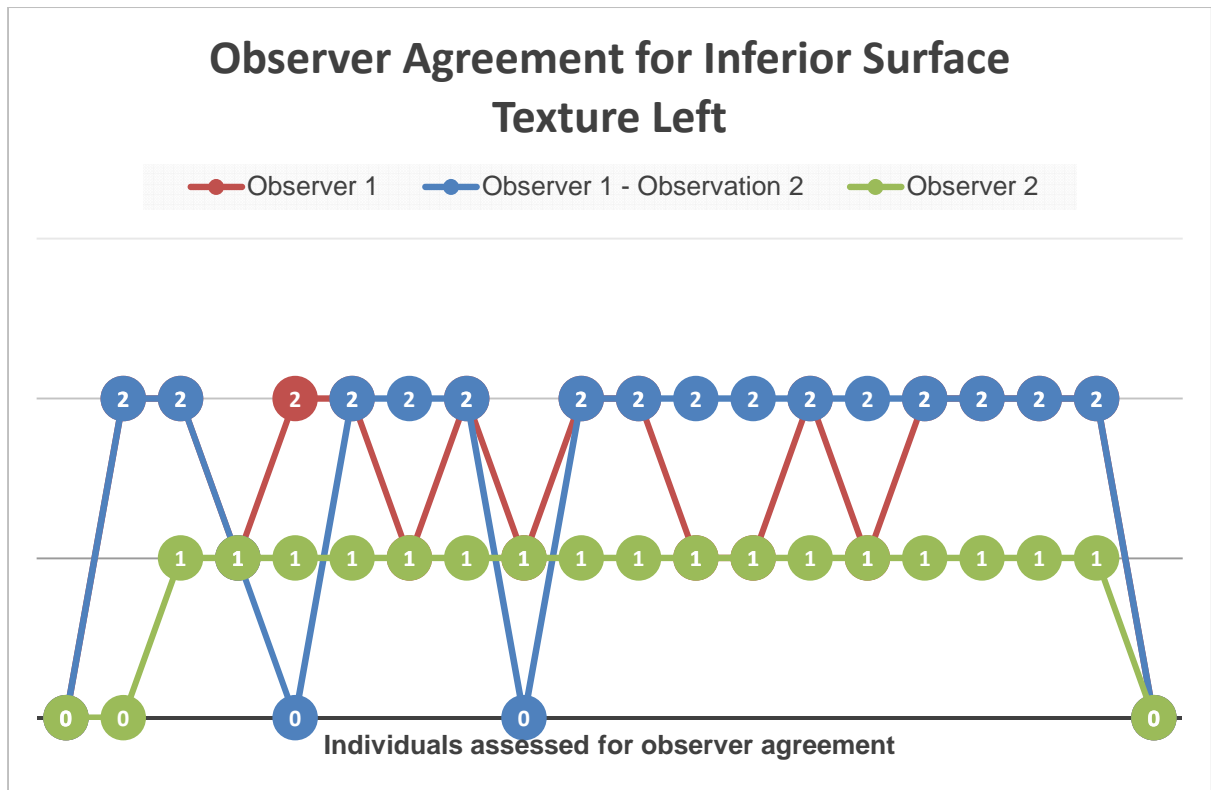


Figure 4.47: Observer agreement for inferior surface texture left. (0) No score, (1) smooth, (2) microporosity, (3) macroporosity

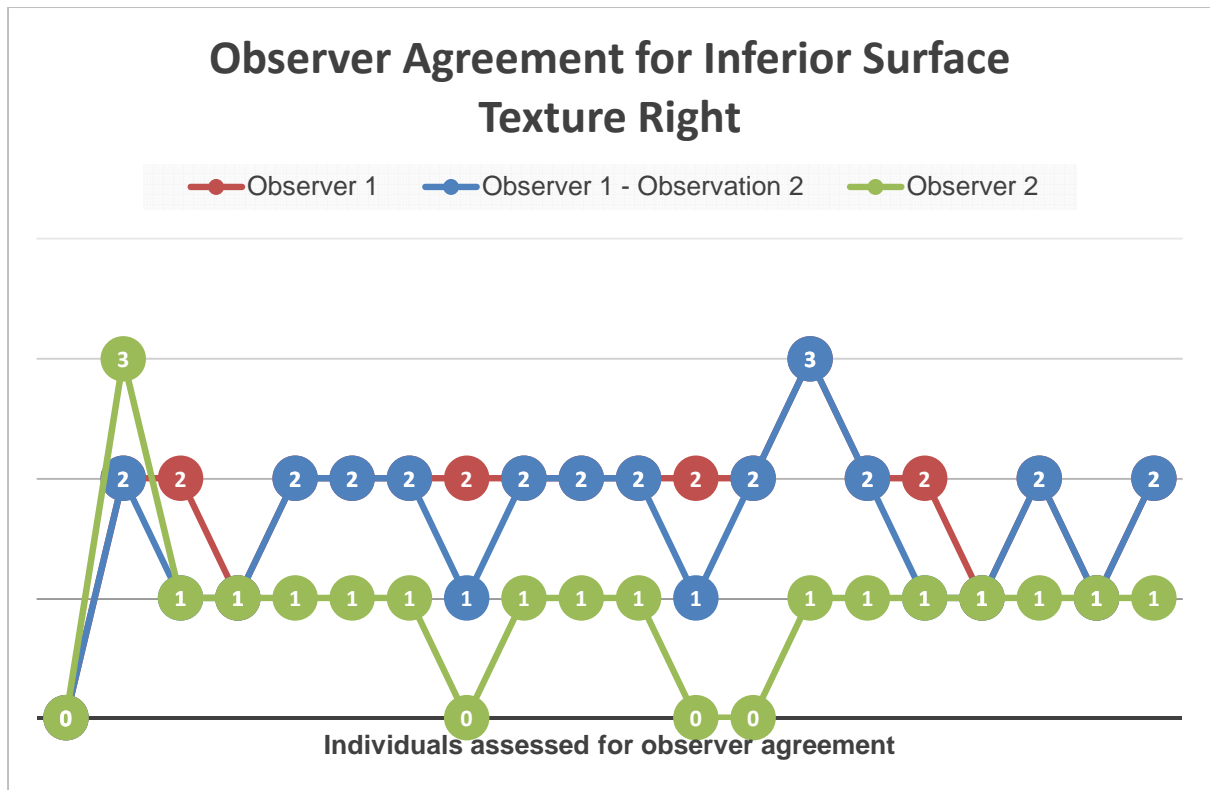


Figure 4.48: Observer agreement for inferior surface texture right. (0) No score, (1) smooth, (2) microporosity, (3) macroporosity

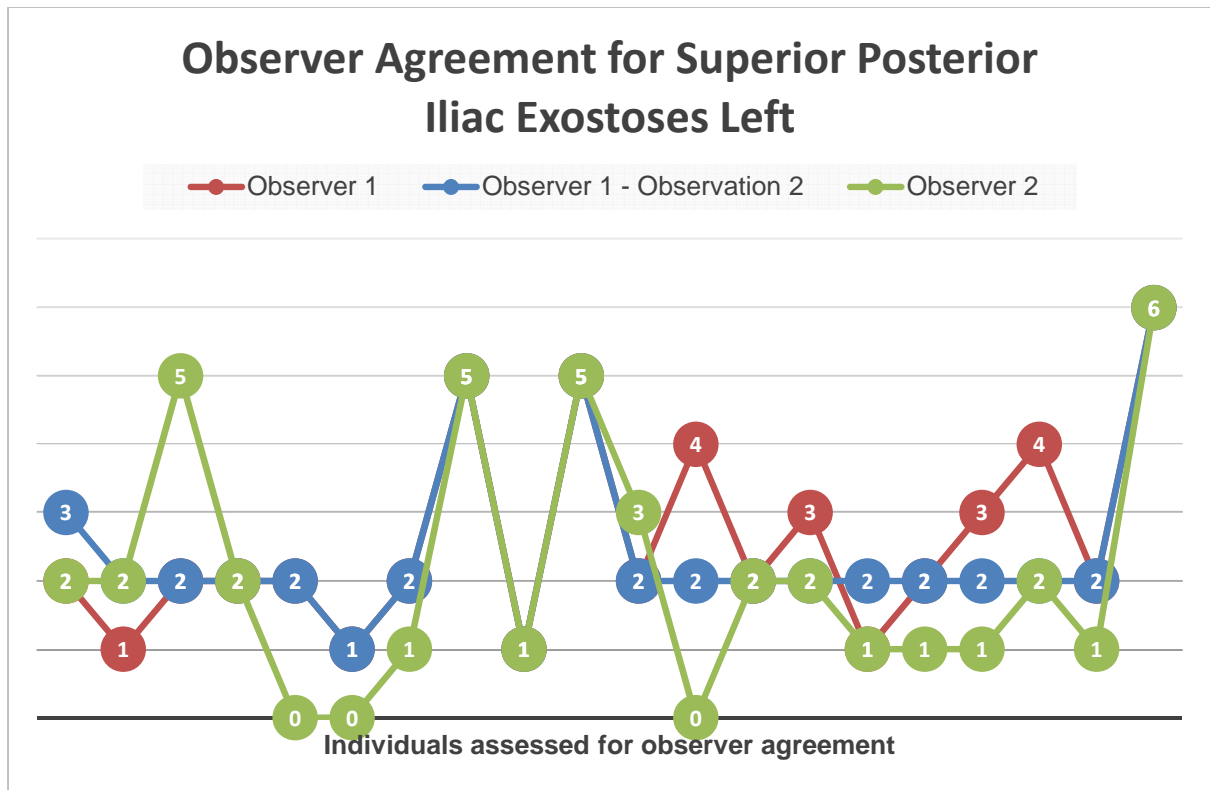


Figure 4.49: Observer agreement for superior posterior iliac exostoses left. (0) No score, (1) smooth, (2) rounded bony elevations, (3) pointed exostoses, (4) jagged exostoses, (5) touching exostoses, (6) fusion

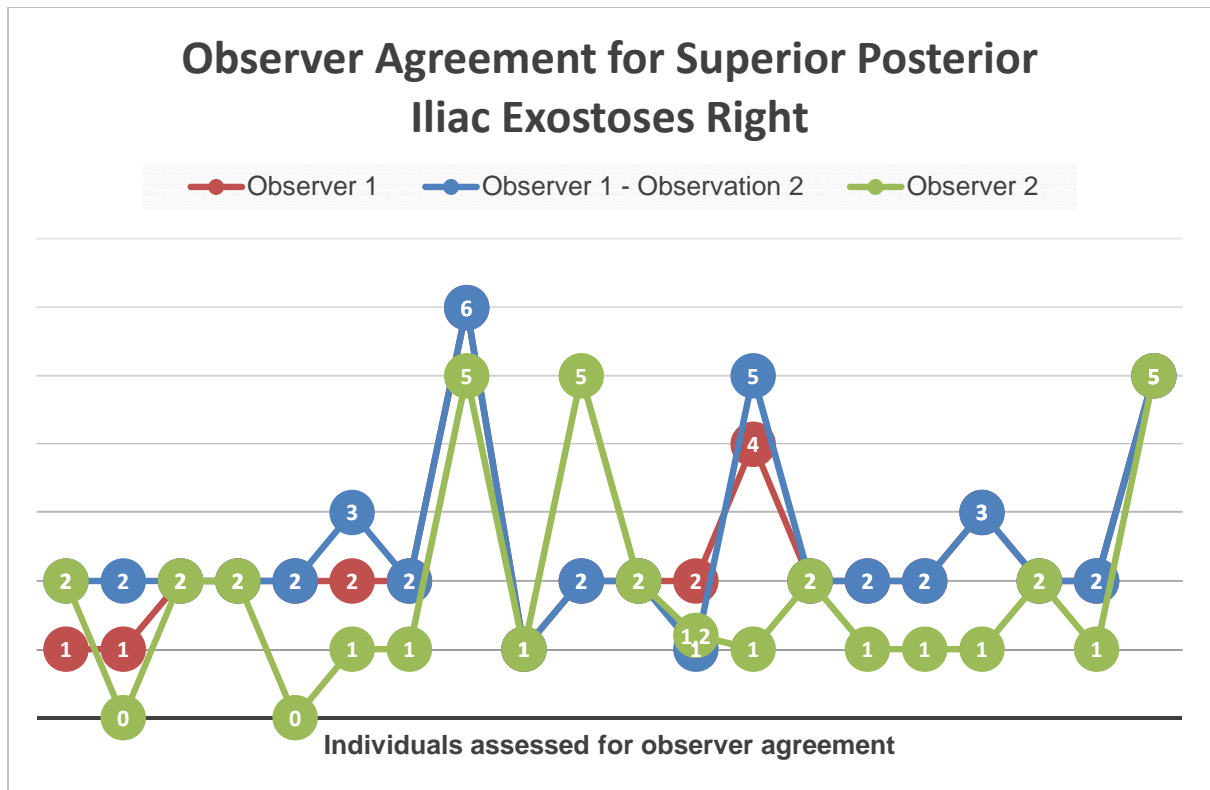


Figure 4.50: Observer agreement for superior posterior iliac exostoses right. (0) No score, (1) smooth, (2) rounded bony elevations, (3) pointed exostoses, (4) jagged exostoses, (5) touching exostoses, (6) fusion

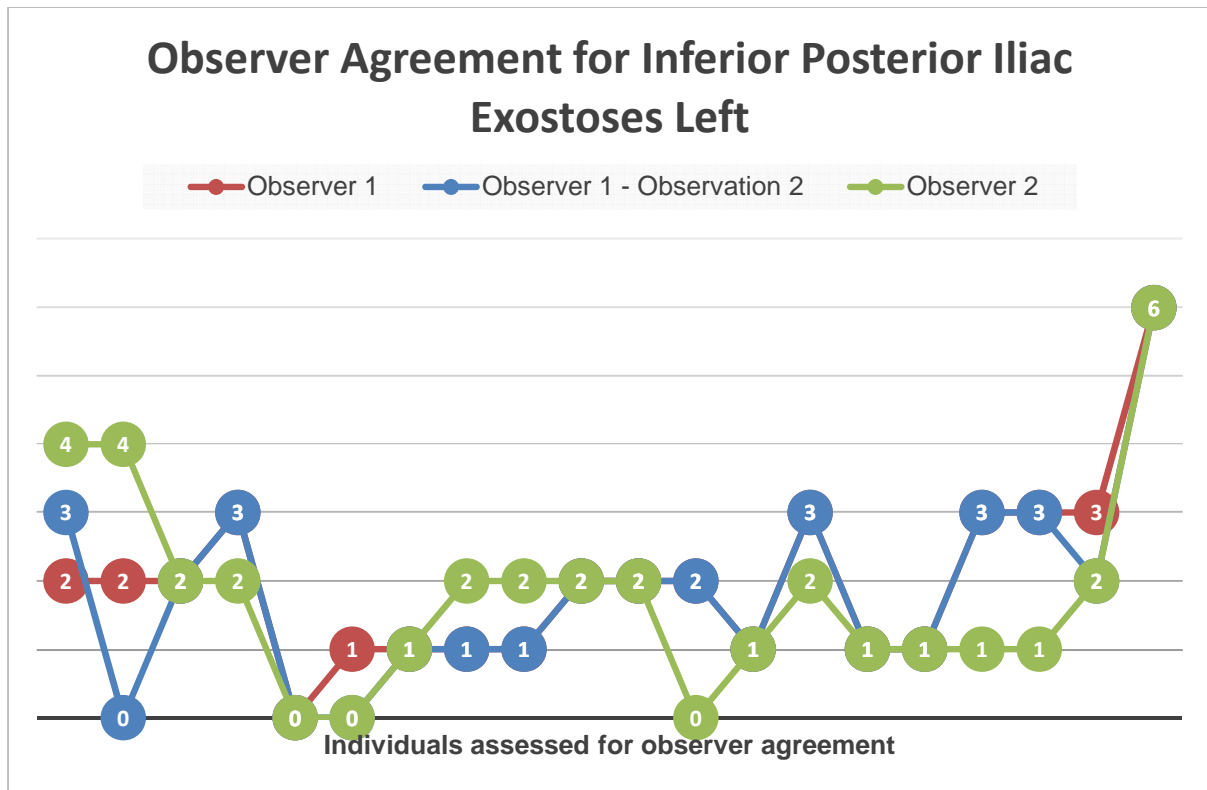


Figure 4.51: Observer agreement for inferior posterior iliac exostoses. (0) No score, (1) smooth, (2) rounded bony elevations, (3) pointed exostoses, (4) jagged exostoses, (5) touching exostoses, (6) fusion

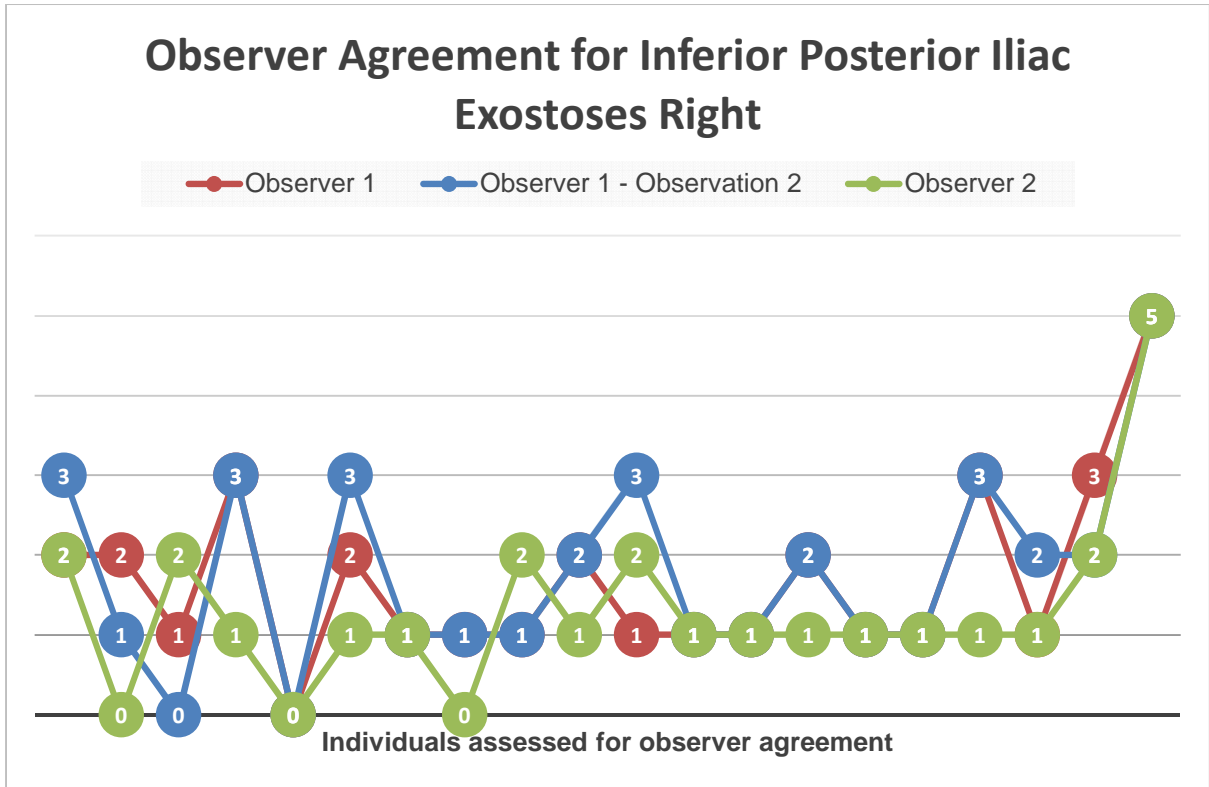


Figure 4.52: Observer agreement for inferior posterior iliac exostoses right. (0) No score, (1) smooth, (2) rounded bony elevations, (3) pointed exostoses, (4) jagged exostoses, (5) touching exostoses, (6) fusion

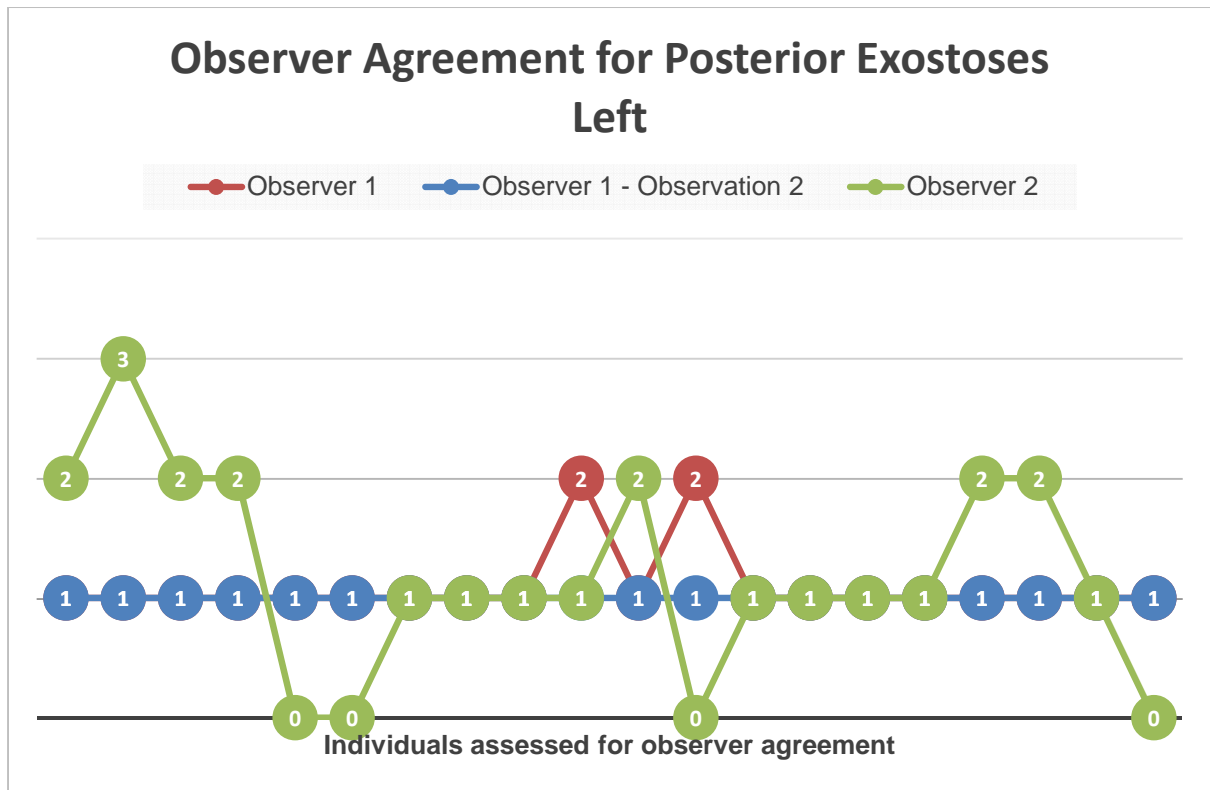


Figure 4.53: Observer agreement for posterior exostoses left. (0) No score, (1) smooth/no exostoses, (2) rounded exostoses, (3) pointed exostoses

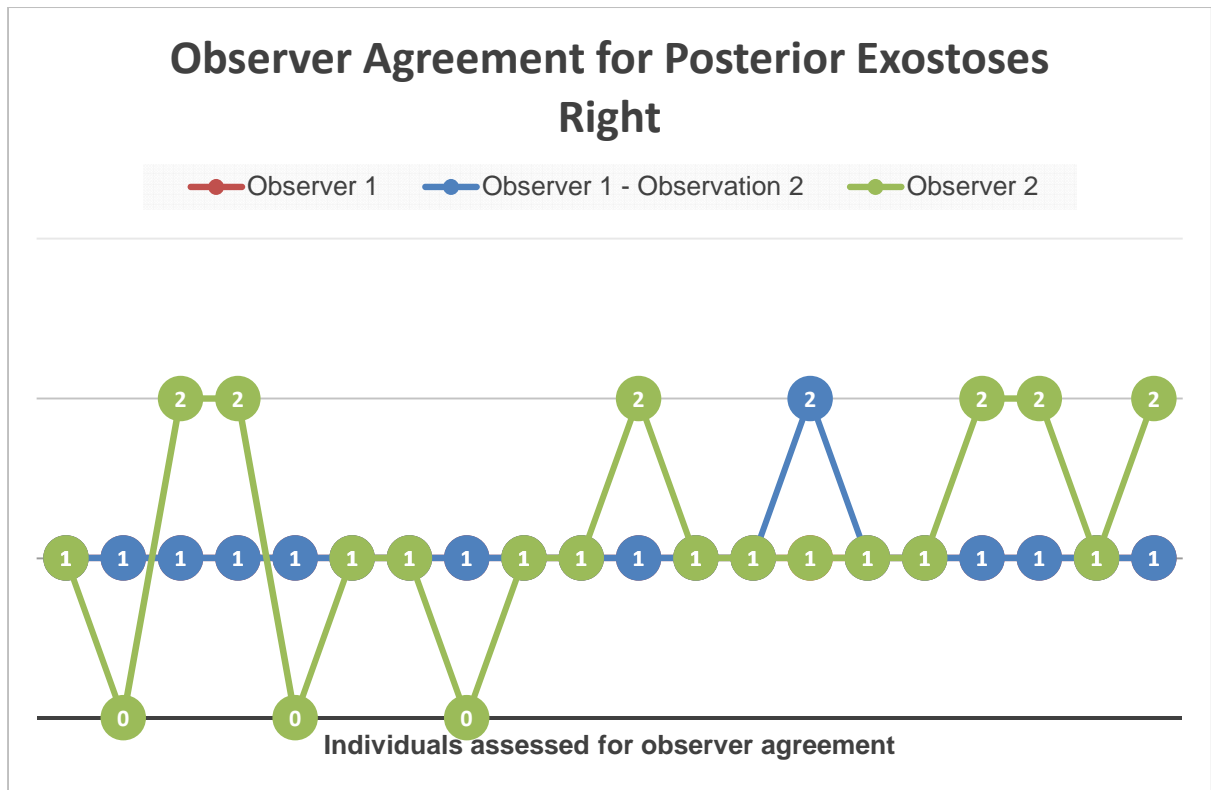


Figure 4.54: Observer agreement for posterior exostoses right. (0) No score, (1) smooth/no exostoses, (2) rounded exostoses, (3) pointed exostoses

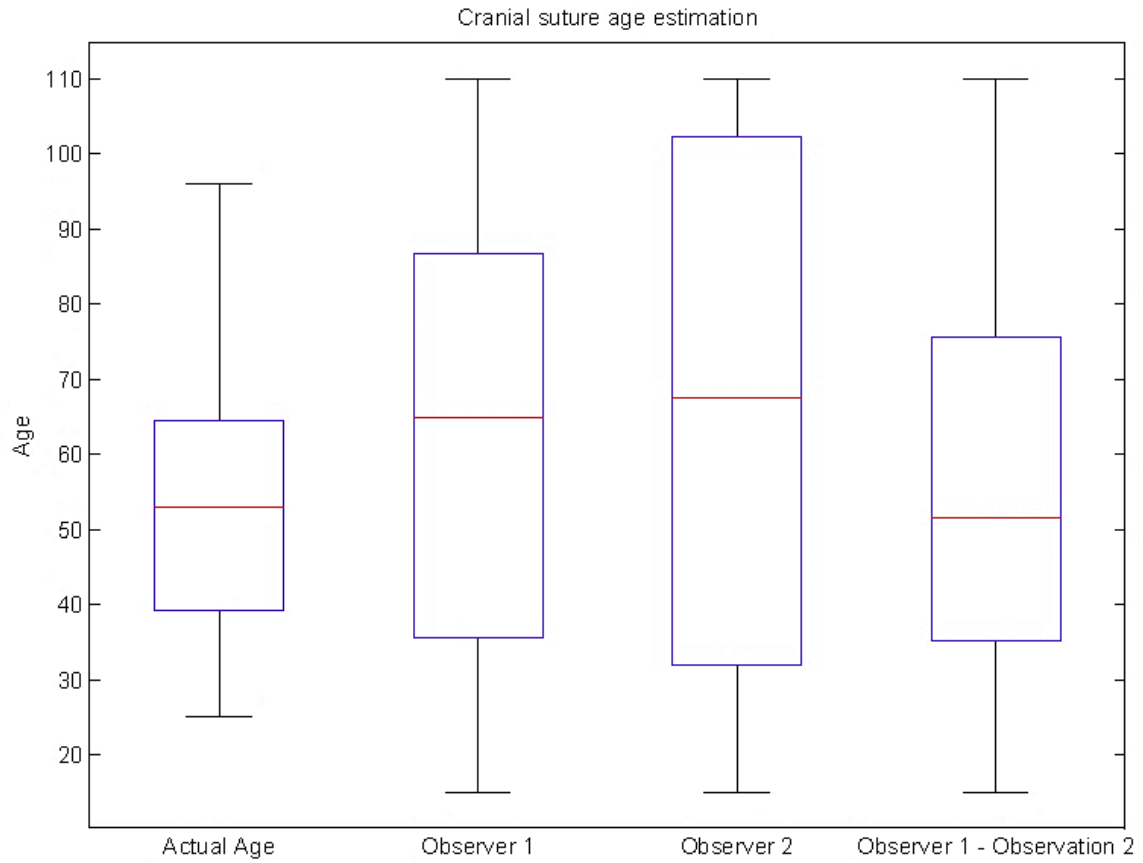


Figure 4.55: Comparison of age distributions using inter- and intra-observer scores for cranial suture age estimation

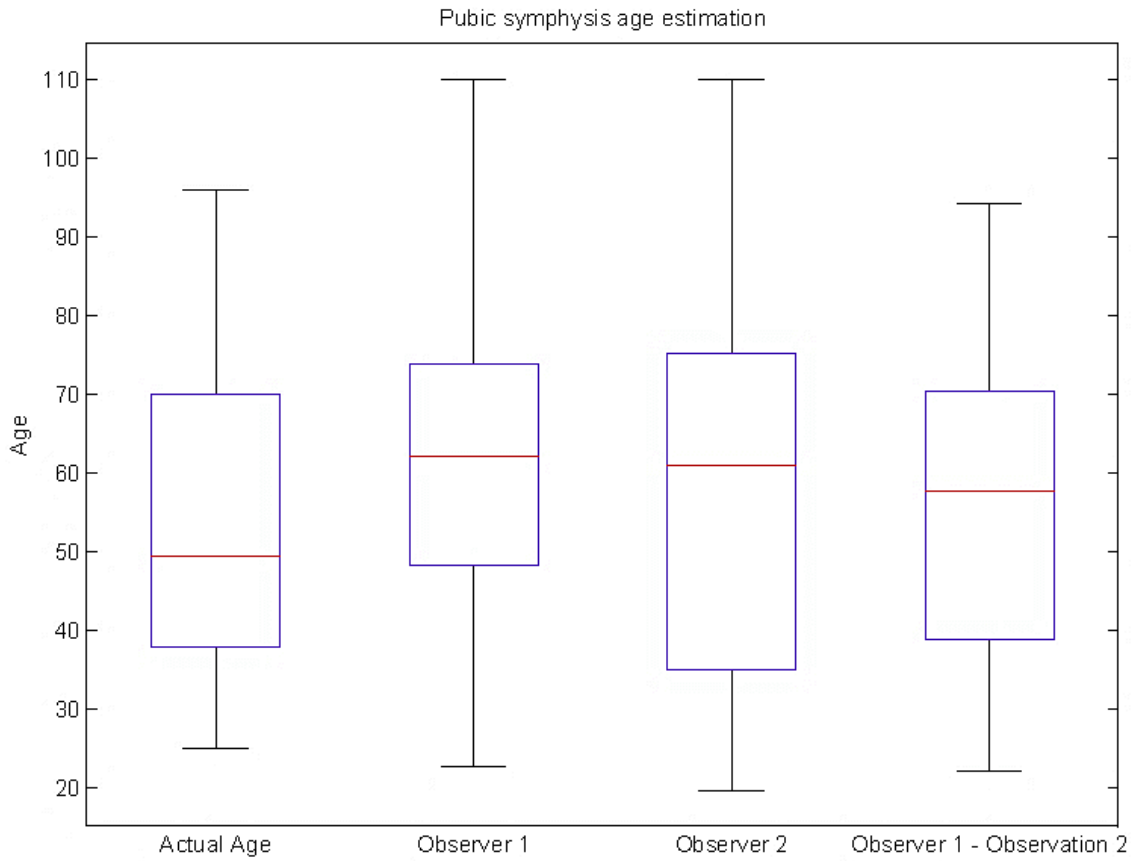


Figure 4.56: Comparison of age distributions using inter- and intra-observer scores for pubic symphysis age estimation

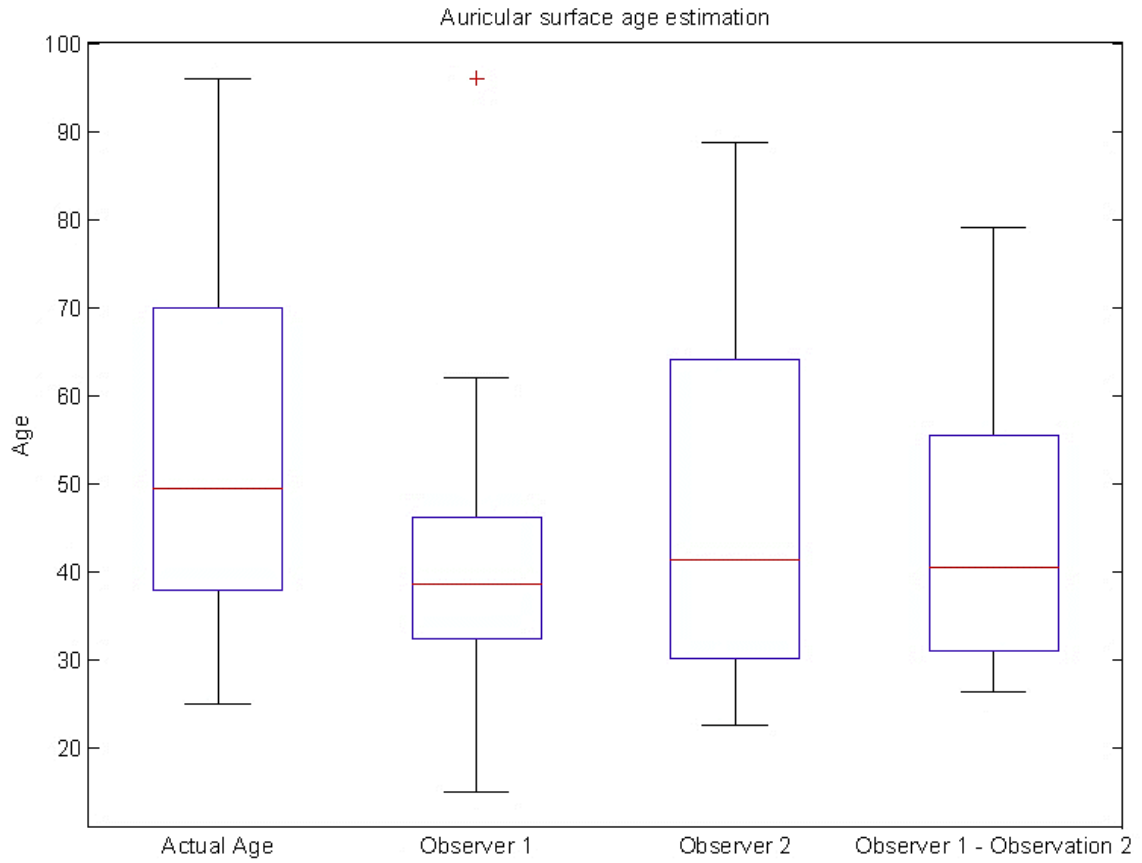


Figure 4.57: Comparison of age distributions using inter- and intra-observer scores for auricular surface age estimation

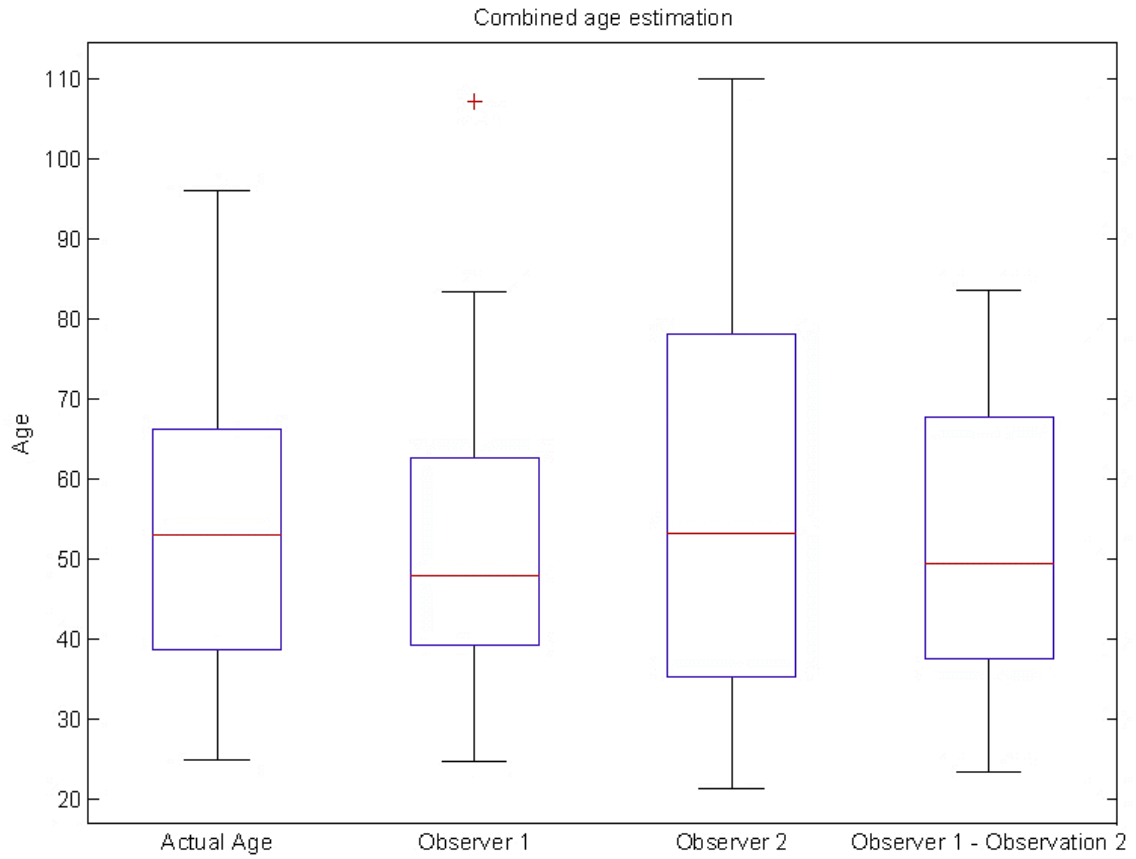


Figure 4.58: Comparison of age distributions using inter- and intra-observer scores for uniform combined age estimation

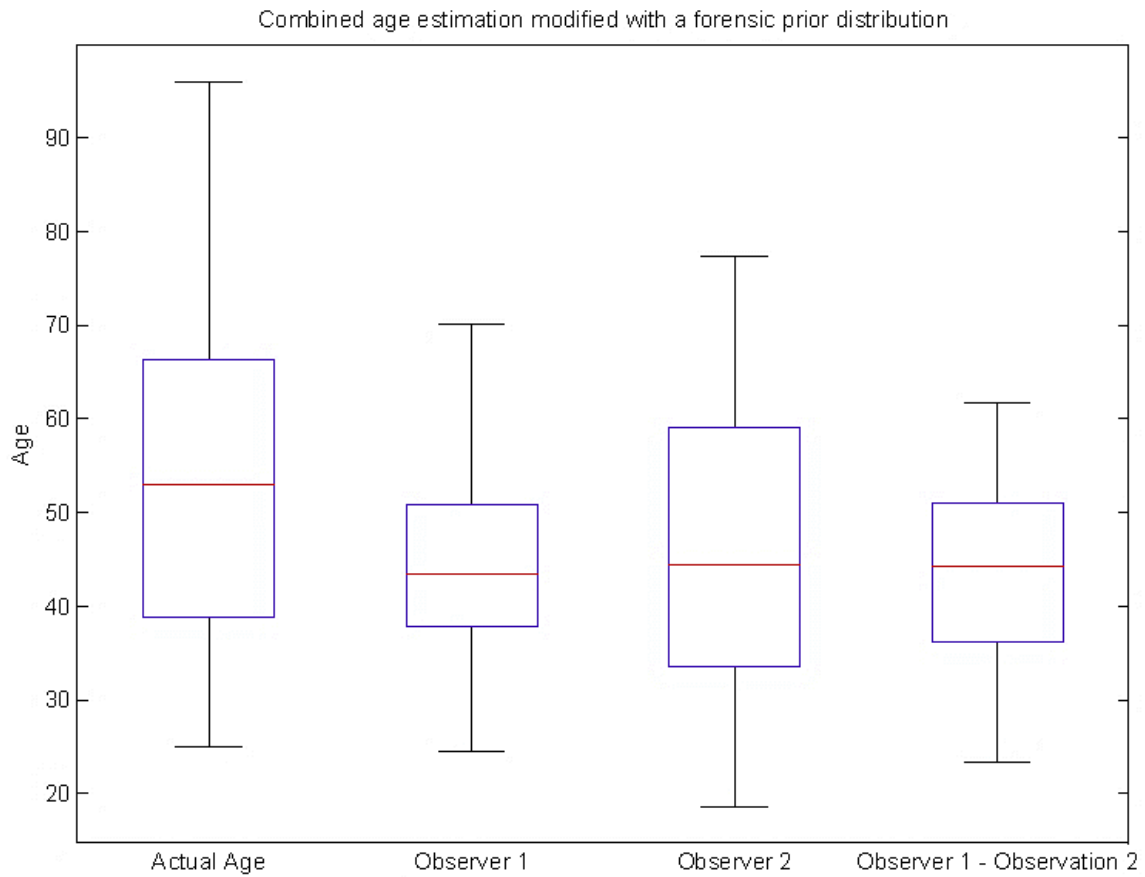


Figure 4.59: Comparison of age distributions using inter- and intra-observer scores for combined age estimation modified with a forensic prior distribution

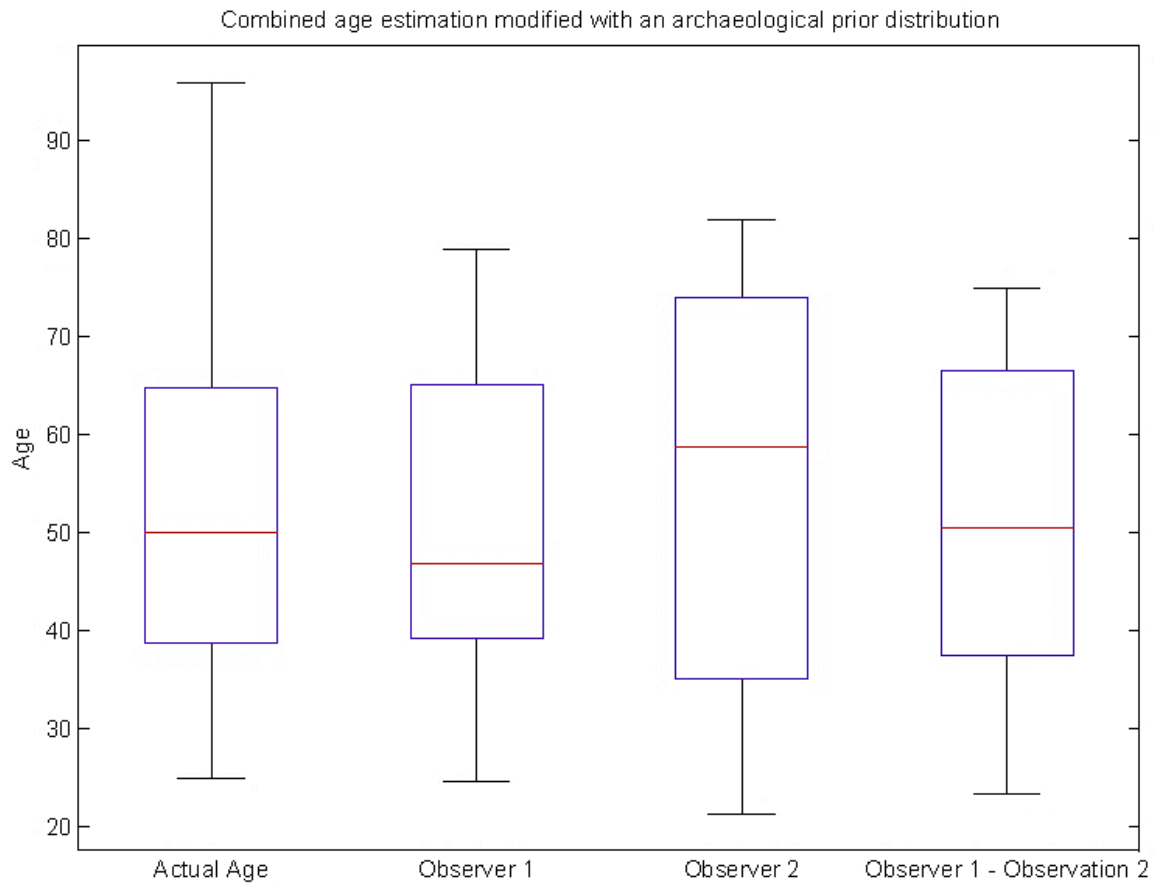


Figure 4.60: Comparison of age distributions using inter- and intra-observer scores for combined age estimation modified with an archaeological prior distribution

Chapter 5: Discussion

5.1. Introduction

The transition analysis method by Boldsen *et al.*⁴ was developed to improve four age estimation difficulties, namely 1) to best present unavoidable uncertainty, 2) to avoid mimicry of the reference sample distribution, 3) to best combine multiple skeletal indicators of age and 4) to best score anatomical traits in order to capture maximum morphological variation with age. This study aimed to validate transition analysis in a South African sample with regard to the accuracy of both the point estimate, attained from the maximum likelihood function, and the age range, attained from the 95% confidence interval. The precision of the age range was also assessed. In addition, the reliability of transition analysis was also assessed through inter- and intra-observer score agreement using Cohen's kappa statistics. The overall effect of observer disagreement on the final age estimation was assessed using Kruskal-Wallis ANOVA statistics and boxplots to compare the age distributions calculated from different observations.

5.2. The scoring procedure

Using the scoring system developed by Boldsen *et al.*⁴ and described in the transition analysis scoring manual³⁶ (Appendix A), 94% of scores could be scored in the current sample. The majority of the scores that could not be obtained were due to post-mortem damage or the processing of the remains. Only 35/1192 scores from 21 individuals were not possible from the skull (Table 4.2), making it the component that most often had a full set of features to score, which corresponds with literature^{3,4,14}. Differing from literature, however, is the fact that the more robust auricular surface did not possess a complete set of features, more often than the fragile pubic symphysis, with 203/2682 scores from 39 individuals not possible for the auricular surface compared to 90/1490 scores from 29 individuals for the pubic symphysis^{10,12,25,44,95}.

Specific landmarks were occasionally not scorable due to normal anatomical variation. These variations are also found in the literature and include landmarks

such as the interpalatine suture that was either found in a groove or a crest³⁶ and a narrow pubic symphysis^{3,25,72–74,78} that made distinguishing features difficult. Other landmarks could produce a score, but obscured surrounding landmarks rendering them impossible to score. Such a landmark is the exostoses related to the retroauricular surface of the ilium which can fuse to the sacrum with advancing age in males specifically^{31,44,97}. The fusion of the exostoses is considered a scorable feature by Boldsen *et al.*⁴, but the state of fusion obscures the view of the auricular surface and sometimes even the pubic symphysis, if present bilaterally. These landmarks will possibly prove more useful if protocols are developed for use in situations where these variations are present.

The characteristic that makes the transition analysis method exceedingly useful is the fact that all the age indicator features are not necessary for the ADBOU age estimation computer program to calculate an age estimation, but the presence of all landmarks refines the age estimation^{4,14}.

5.3. Age estimations

Success of the age estimation is measured by the accuracy and precision of the estimation. For the age range, calculated from the 95% confidence interval, the accuracy was determined by the percentage of the known ages that was encompassed by the age range. Precision of the range was also evaluated with regard to the range width and the frequency of the occurrence of terminal values imposed by the ADBOU age estimation computer program³⁵.

The relationship between the calculated point estimates and the known ages were determined by the correlation coefficient. The accuracy of the point estimate was evaluated by the mean absolute error which quantifies the amount of under- and overestimation.

5.3.1. Accuracy and precision of the age ranges

The accuracy of the 95% confidence interval age ranges, measured by the percentage of known ages falling within the age range, was between 75% and 92% for the single indicator methods and between 63% and 68% for the combined estimation methods (Table 4.3). When comparing the accuracy of the age range with

the width (precision) of the 95% confidence interval, an increase of accuracy was observed with an increase of range width. The relationship of range width with accuracy is expected, as a larger range width increases the number of ages encompassed by the range and thus the likelihood of the known age being included within the range. Thus, a high percentage of inclusion within the age range is an unrealistic indication of success, unless the range width is narrow enough to be of practical value. As the single indicator methods have especially large age ranges, the values of inclusion achieved by the combined estimation methods are the preferred indication of accuracy.

These results correspond to the accuracy of the age ranges attained by Bethard¹⁰⁶ in his test of transition analysis as compared in Table 5.1. The accuracy for the range is very similar for both studies, with single indicators, especially the cranial sutures, having higher accuracies. Interestingly, Bethard's accuracy for the combined method modified with forensic prior distribution (72.4%) is higher than that for the combined method with a uniform prior distribution (64.8%). This contrasts with the current study, which had a decreasing accuracy from the combined method with archaeological prior distribution (68%), combined method with uniform prior distribution (67%) and lastly the combined method with forensic prior distribution (63%). Unfortunately Bethard¹⁰⁶ did not test the combined method modified with the archaeological prior distribution, but his improved accuracy when using the forensic prior distribution could be indicative of the need for prior distributions to be specific to the population for which the method is being used. As the forensic prior distribution is modelled on homicide data, it represents a younger age-at-death distribution, as is often seen with victims of homicide, suicide and accident²⁴ and is thus suited to Bethard's¹⁰⁶ sample which has a younger age-at-death distribution (Figure 2.13). The archaeological age-at-death distribution which is modelled on an older age-at-death distribution seen with natural causes, was more suited to the older sample used in the current validation study (Figure 3.1).

Although Milner and Boldsen's¹⁴ graphs (Figures 2.14 to 2.18), generated as part of their validation of transition analysis, also show the success of the 95% confidence interval in encompassing the true age (consistent with the findings of Bethard¹⁰⁶ and the current study), they specifically noted the overly large age ranges. These large impractical age ranges are observed in the results of the current study with ranges

sometimes stretching from the ADBOU-imposed minimum terminal value of 15 years to the maximum terminal value of 110 years. Similar wide age ranges were also noted by Bethard ¹⁰⁶.

A visual comparison of the age ranges for the cranial sutures, between Milner and Boldsen's ¹⁴ validation study (Figure 2.14) and the current study (Figure 4.7), attest to equally large ranges. The pubic symphysis and the auricular surface both produce narrower age ranges. While Milner and Boldsen ¹⁴ found the pubic symphysis produced the narrowest ranges (Figure 2.15 compared to Figure 2.16) of the three single indicator methods, the current method found that the auricular surface method produced narrower age ranges (Figure 4.8 compared to Figure 4.9).

Again similar to the current results (Figures 4.10 and 4.12), Milner and Boldsen's ¹⁴ combined age estimation with uniform prior distribution (Figure 2.17) and modified by archaeological prior distribution (Figure 2.18) possessed much narrower age ranges. Milner and Boldsen ¹⁴ did not test the combined method modified by the forensic prior distribution.

It is already a well-established fact that age intervals do not have an equal length throughout the continuum of age, but become less precise (broader) after adulthood and especially so with accumulating variation as time progresses ^{1,2,4,11,14,33,37,38,41,43}. However, Milner and Boldsen ¹⁴ revealed that the age intervals do not just increase in a linear manner with advancing age, but after an initial increase reaches a plateau at around 70 years, followed by a decrease in the age interval lengths. Milner and Boldsen ¹⁴ illustrated this relationship between confidence interval length and advancing age using the combined method with uniform prior distribution (Figure 2.10) and modified by archaeological prior distribution (Figure 2.11).

For the combined estimation method with a uniform prior distribution the confidence interval lengths show an overall trend towards increase with increasing age, with no obvious plateau forming (Figure 4.4). This does not correspond to findings by Milner and Boldsen ¹⁴ that show a clear plateau being reached at around 60 years and a decrease in confidence interval length at around 80 years for the combined estimation method (Figure 2.10). The combined estimation method with a forensic prior distribution (Figure 4.5) yielded a similar pattern in the current study. When comparing the changes in confidence interval length with age for the combined

method with archaeological prior distribution, however, a very similar pattern is seen. Both the Milner and Boldsen ¹⁴ results (Figure 2.11) and the current study's results (Figure 4.6) show a clear plateau being reached at around 50 years and a marked decrease in confidence interval length at around 70 years. A plateau and slight decrease in confidence interval length with advancing age is also observed for the single indicator methods in the current study. However, the plateau that is reached for the cranial suture age estimation is very likely due to the maximum interval length being reached when the range stretches from the upper terminal value (110 years) to the lower terminal value (15 years).

Milner and Boldsen ¹⁴ attribute the decrease in confidence interval length with older ages to two reasons. Firstly, they state that old age indicators, namely the dorsal margin of the pubic symphysis and the posterior exostoses of the sacroiliac joint improve precision for these ages. Secondly, the archaeological prior distribution modifies the age ranges of the older individuals as old ages are expected to be less predominant due to selective mortality ¹⁴. The marked reduction in confidence interval length in the older ages for the pubic symphysis and auricular surface estimation method does give credence to those old age markers. However, as no marked decrease was observed in older ages' confidence interval lengths for the combined estimate in the current study, the addition of the cranial sutures could likely negate the effects of these old age markers. Consequently, the effect of the archaeological prior distribution is in all likelihood more responsible for the decrease in confidence interval lengths with older ages for the combined estimation.

Overall, the three tests of transition analysis concur that although a large number of known ages fall within the age range (good accuracy), the age range width is too large to be of practical use (precision). The key to refining the precision possibly lies with adding other age-indicative features to the method as suggested by Boldsen *et al.* ⁴ and Milner and Boldsen ¹⁴. Although confidence interval length does increase with advancing age, the archaeological prior distribution is successful in decreasing interval length in older individuals (over 70 years).

5.3.2. Accuracy and precision of the point estimate

In their original study, Boldsen *et al.* ⁴ had great success with the point estimates (maximum likelihood values) generated by their transition analysis method. The

quality of the age estimates they were able to produce was measured by a correlation coefficient which varied from 0.66 to 0.88, depending on the feature(s) used. During a test of the method Bethard¹⁰⁶ had less success applying the transition analysis method and only generated correlation coefficients between 0.17 and 0.51. Correlation data from the current study (Table 4.5) more closely match the values obtained by Bethard¹⁰⁶ (Table 5.2).

Bethard¹⁰⁶ attributed the weak relationship between the actual age and the estimated age to either a weak relationship between age and the skeletal traits used, or the method with regard to scoring being difficult or impossible to replicate or population dependence of the method. A weak relationship between age and the skeletal traits is a possibility concerning features from the cranium. The usefulness of cranial sutures as a single indicator for age estimation has long been debated^{3,25,26,48,66,71}. However, the relationship between age and the features of, especially the pubic symphysis, is a well-established fact^{1,10,25,31}. This leaves the possibility of the difficulty grade of the scoring method, which is to be discussed with observer consistency, or the population dependence of the method. Transition analysis was specifically designed to incorporate an entire spectrum of variation in order to nullify the effect of the reference sample distribution on the method through use of Bayes' theorem and prior distributions. However, Milner and Boldsen³⁶ does caution against certain features which are not comparable between Native American populations and the original reference sample. This population variation may also hold true for South African populations.

The mean absolute error calculated for the point value (maximum likelihood value) showed inaccuracy ranging from 10.40 to 12.48 years (Table 4.6). As expected, larger inaccuracy was present for the single indicator methods and less inaccuracy for the combined methods. This inaccuracy is similar to the values calculated by Nawrocki³⁴ for the cranial sutures, Meindl *et al.*³¹ for the pubic symphysis and Osborne *et al.*³³ for the auricular surface. A graphic representation of the inaccuracy shows widely scattered point estimates for cranial sutures (Figure 4.13), pubic symphysis (Figure 4.14) and auricular surface (Figure 4.15) with the point estimate occasionally represented by the ADBOU-imposed terminal values of 15 years and 110 years. Very little progression with age could be observed from the slope of the trend line. The lack of progression could possibly be attributed to the overestimation

of the younger ages and the underestimation of the older ages. Although this under- and overestimation is usually attributed to a tendency to mimic the reference sample population, the possibility exists that the age indicator stages do not sufficiently represent the progression of age. Thus, insufficient correlation between the indicator stages and age could possibly result in a more gradual slope of the trend line.

In their validation study of transition analysis, Milner and Boldsen¹⁴ also found the point estimates for especially the single indicator methods to be inaccurate and thus widely spread around the known ages (Figures 2.14 to 2.16). They found that the sacroiliac joint underestimated ages above 60 years (Figure 2.16), whereas the current study found overall underestimation from the auricular surface method especially predominant after 40 years (Figure 4.15). Underestimations of ages over 40 years are also the trend observed with traditional auricular surface age estimation³³. Milner and Boldsen¹⁴ found the pubic symphysis to fare best overall, whereas the current study found the pubic symphysis to generally overestimate age, especially over 65 years (Figure 4.14). Where Milner and Boldsen¹⁴ found the pubic symphysis to fare the best of the single indicator methods, the current study found the auricular surface method to include point estimates that more closely matched the known ages compared to the other single indicator methods.

Also of significance in the Milner and Boldsen¹⁴ study is the tendency for the point value to be the upper terminal value (110 years), especially in the case of the cranial suture method. Milner and Boldsen¹⁴ attribute this to individuals with very few features available for scoring and most features appearing in the terminal stage. In the current study neither a lack of scorable features, nor an excessive amount of features in the terminal state were observed for the instances where terminal values represented the point values for the cranial sutures. However, many of the features were indeed not scorable for the instances where the terminal values represented the point values for the pubic symphysis and the auricular surface.

Milner and Boldsen¹⁴ found the combined estimation methods, with uniform and archaeological prior distribution, to improve accuracy of the point estimates, but both estimation methods had a tendency to underestimate age over 70 years. The current study concurs that these combined estimation methods improve the accuracy of the

point estimates, but found that their tendency to underestimate ages begin earlier, at approximately 50 years.

Overall, the point estimates are plagued with much inaccuracy in the form of under- and over-estimation. This is most likely due to osteological indicators that do not have a strong enough relationship to age, in order to estimate maximum likelihood accurately, in which case more age indicative features should be added to the method to be inclusive of all information from the skeleton. The relationship of the osteological indicators to age could possibly be influenced by population variation. The applicability of these features should be tested in a South African population.

5.4. Observer agreement

The primary investigator scored 22 individuals during two separate observations. These same 22 individuals were also scored by a second observer. The degree of inter- and intra-observer agreement was calculated using Cohen's kappa statistics and analysed with categories of strength by Landis and Koch ¹¹² (Table 3.1). The significance of the influence of observer disagreement on the overall age estimation was evaluated using a Kruskal-Wallis ANOVA analysis. Boxplots were utilised to compare age distributions calculated from scores selected by each observer to the age distribution for the actual age.

5.4.1. Inter- and intra-repeatability of scores

Intra-observer agreement was much stronger, compared to interobserver agreement, with the majority of traits having moderate, substantial or almost perfect agreement (Table 4.8). Interobserver agreement was weaker with the majority of traits having only slight, fair or moderate agreement.

Bone features that showed strong agreement based on the Cohen's kappa scores, for both inter- and intra-observer repeatability, included the sagittal obelica, inferior demiface topography for the left auricular surface and superior surface morphology for the right auricular surface, the dorsal symphyseal margin for the left pubic symphysis and the superior demiface topography for both left and right auricular surfaces. These easily repeatable features all share the condition of a clearly defined and understandable scoring area and distinct stages that are not easily confused.

These conditions also hold true for all the cranial sutures in the absence of accessory bones.

Very poor agreement was found for the ventral symphyseal margin and posterior exostoses features. The difficulty with scoring the ventral rampart has been noted by previous researchers ^{25,37} and is depicted in the many overlapping and confusing stages, described in Milner and Boldsen's ³⁶ scoring manual (Appendix A), for this region. From the scoring manual it also appears that the ventral rampart can exhibit variation, for example the presence of a hiatus, at an individual and population level, which encumbers the feature even more. Similarly, the description of the stages are confusing for the posterior exostoses even though it is composed of only three stages. Distinguishing between rounded and sharp exostoses would definitely benefit from a cast system where the different stages can clearly be observed by sight as well as touch. However, the feature of the posterior exostoses that is most uncertain is its exact location, as the description of the area where the posterior exostoses can be found is unclear.

Both these features would benefit from clearer descriptions accompanied by photographs of model stages and possible variations, as well as cast models. A reduction in the number of stages, especially those which seem to closely compare such as rampart complete I and II in the case of the ventral rampart, would possibly also be beneficial. Features such as texture, which cannot be readily observed on photographic material, would also possibly benefit from cast models.

The poor agreement of these features might explain the overestimation of the younger ages noticed for the pubic symphysis (Figures 4.8 and 4.14), as the ventral margin is an age indicator associated with younger ages ²⁵. Similarly the poor agreement for the posterior exostoses may explain the underestimation of older ages for the auricular surface estimation method (Figures 4.9 and 4.15), as this feature is an old age indicator ^{4,14}. The lack of agreement for this old age indicator may also explain the mere marginal decrease in confidence level interval length with age (Figure 4.3).

Although many of the scores differed with repeat observations (Table 4.9), most scores only differed by one or two stages. However, the left and right symphyseal texture, the right superior apex and the left and right superior posterior exostoses

differed by up to three stages and the right and left ventral symphyseal margin sometimes differed by up to four stages. It is evident that the largest uncertainty, with regard to attributing scores, lie with the pubic symphysis and auricular surface. This corresponds to statements made by Brooks and Suchey³⁷ concerning the difficulty of attributing score values to the pubic symphysis when the feature is treated as separate components. Similar difficulty with assigning stages to the auricular surface have been noted^{29,33}, regardless of whether the feature is treated as a whole or separate components. As scores for the retroauricular area were more often not repeatable, the removal of these features may benefit the method, as previously undertaken by Buckberry and Chamberlain²⁹.

Another inconsistency between observers was the uncertainty of whether enough of a feature was represented in order to accurately attribute a score. This is denoted by the differences in scores, where one of the scores is represented by zero. This inconsistency can easily be remedied by an inclusion in the scoring manual of an exact amount of the feature that needs to be visible in order to classify a stage. For instance, if 1cm of microporosity can be viewed on the dorsal surface of the pubic symphysis, the score can be confidently attributed.

5.4.2. Effect of score repeatability on age estimates

When assessing the effect of score changes on the age estimations generated, age distributions calculated by a Kruskal-Wallis ANOVA analysis were not significantly different (Table 4.10). The relationship between the age distributions can be better visualised by boxplots (Figures 4.55 to 4.60).

None of the age distributions, from the three different observer estimations, for cranial sutures (Figure 4.55) correspond to the actual age distribution. The overly wide distributions for the estimations correspond to what is known from literature, namely that cranial sutures can only estimate age in the broadest of sense^{3,25,26,48,66,71}.

The age distributions, representing the three different observer estimations, for the pubic symphysis is a much closer match to actual age (Figure 4.56) than the age distributions seen for the cranial sutures. Although the initial observations from the primary investigator generated a smaller age distribution, the second observation's

age distribution was much closer to that of the actual age. This may indicate that some experience and practice with the method is necessary to achieve optimal results, as is the general suggestion by Katz and Suchey³⁹ and Baccino *et al.*⁹⁹.

All observer-estimated age distributions for the auricular surface are much narrower and provide a younger distribution than the age distribution for the actual age (Figure 4.57). The outlier observed in the age distribution boxplot for the first observation of observer one is a consequence of a fused sacroiliac joint that results in only the superior posterior iliac exostoses and the inferior posterior iliac exostoses being scorable. This outlier in the age distribution for the estimations from observer one still corresponds to the age distribution of the actual age and may be indicative of the auricular surface's ability to more accurately estimate older ages.

When combining all features (Figure 4.58), the observer estimation age distributions become much more similar to the distributions of the actual age, especially so for observer one's second observations, essentially decreasing the effect of observer disagreement. This illustrates the value of combining skeletal features into a single statistically sound method, not only to improve accuracy, but also to increase reliability of the method. However, the effect of observer disagreement is only decreased with the combined estimation when an appropriate prior distribution is chosen. The effect of the forensic prior distribution on the age distribution is to decrease the overall age, making it less similar to the actual age distribution (Figure 4.59). Whereas the archaeological prior distribution increases the similarity between the observer-estimated age distributions and that of actual age distribution (Figure 4.60).

The outlier noticed in the age distribution for observer one, for the combined estimation method, is once again attributed to the lack of availability of a full set of features to score. The outlier present in the first observation for observer one corresponds to the higher extreme values of observer two, this alludes to the possibility that the method's reliability is not problematic but that an increase in components are needed to negate those lost through post-mortem or antemortem modification and further increase accuracy and precision.

Thus, some features could not be consistently scored, with the least agreement seen for the ventral symphyseal margin and the posterior exostoses. Most scores

disagreed by only one or two stages, but the ventral symphyseal margin was particularly concerning as the scores sometimes differed by up to four stages. However, the effect of disagreement on the final age estimation could possibly be decreased by using a full set of features, combining additional components into the combined estimation method and using a suitable prior distribution. The most important factor that seemed to decrease the effect of disagreement on the final age estimation was familiarity with the method, which could possibly be achieved by either good descriptions of the features' stages, accompanied by photographic or cast models and practical training with the method.

5.5. The success of transition analysis in a South African population

Even though good accuracy was achieved with the 95% confidence interval age ranges, the ranges were much too wide to be of practical use. Ranges were sometimes narrowed by the combined methods, but were still too wide to be usable. The archaeological prior distribution seems promising in decreasing confidence interval lengths of older individuals, however, a South African age-at-death population distribution would most likely be more beneficial. These findings are consistent with that of Bethard ¹⁰⁶ and Milner and Boldsen ¹⁴.

A very poor relationship between estimated age and actual age was indicated by low correlation coefficients. This concurs with findings from Bethard ¹⁰⁶, but not with those of Boldsen *et al.* ⁴. The correlation is also much lower than would be expected from previous age estimation methods making use of these same anatomical features, which indicates a need for further testing of these features in a South African population. Once again, an improvement was seen with the combined estimation method and also with use of the archaeological prior distribution.

Some features have proven to have very low repeatability, such as the ventral symphyseal margin and the posterior exostoses, and should either be redefined and possibly condensed to contain fewer stages or completely removed from the method. Reliability does appear to improve with the combination of all features, especially if a full set of features are available. Hence, the addition of components to the combined

estimation method could possibly improve the reliability, in addition to the accuracy and precision of the method. Reliability achieved when using the archaeological prior distribution is promising and could possibly be improved with a South African prior distribution. The factor most likely to improve reliability is practical training with the method and the use of photographic and cast models.

5.6. Future research in transition analysis

Although Boldsen *et al.*⁴ developed a commendable method for adult age estimation, which is especially notable for presenting unavoidable uncertainty, avoiding reference sample mimicry, combining multiple skeletal indicators and capturing morphological variation with age, much further research is proposed.

A correlation existed between the ages estimated from the single skeletal indicators (cranial sutures, pubic symphysis and auricular surface) and the actual age. This correlation was increased by combining these skeletal components into a single method, indicating the possibility that a higher correlation could be achieved by adding age-indicative skeletal components to the existing method. As the correlation coefficients were much lower for the study in a South African population compared to Boldsen *et al.*'s⁴ population, correlation could possibly be improved by using scoring criteria developed using a South African population.

The effect of adding skeletal information and accounting for population variation could possibly include an increase in accuracy and precision of the method. The narrowing of age ranges is particularly important, as the current range widths were too wide and impractical. Especially concerning are the width of the ranges for the decades between 40 – 60 years, which may never be improved if skeletal material indicative of age changes in these decades is not forthcoming.

The use of prior distributions were very promising with regard to narrowing age ranges and should be further researched with regard to population specificity. A population specific prior distribution could possibly optimise transition analysis for use in populations outside the United States of America and Denmark.

The allocation of scores were quite repeatable and with the addition of visual aids, such as photographs and cast models, the repeatability should be even further

improved. Some scores that proved difficult to replicate such as those for the ventral margin of the pubic symphysis and the posterior exostoses of the sacroiliac joint, would possibly benefit from redefining the descriptions. Any overlapping morphology between stages would possibly benefit by reducing the number of stages. Multiple stages for each features might be too complex and may need to be simplified to a binary (present-absent) scoring system.

An important revelation regarding observer agreement was that a small score difference does not significantly influence the overall age distribution, but that practice and familiarity with the method does improve the results. Conveying future improvements to the method through practical training may significantly improve results achieved.

Adult age estimation has always been imprecise and problematic as it is by nature a measure of degeneration, which can be influenced by many factors other than age. Transition analysis does serve to improve age estimation, but can only do so if further advances can be made with the age-related information generated from the skeletal material. Thus, improving age-related data generated from skeletal material should be the focus of future research.

Table 5.1: Comparison of the accuracy of the age range between Bethard's ¹⁰⁶ validation study and the current validation study

Age estimation category	Bethard's ¹⁰⁶ validation study		Current validation study	
	Number of known ages within range	Percentage of known ages within range	Number of known ages within range (n = 149)	Percentage of known ages within range
Cranial suture estimation	177/215	82.3%	137	92%
Pubic symphysis estimation	160/215	74.4%	112	75%
Auricular surface estimation	159/223	71.3%	114	77%
Combined estimation	146/225	64.8%	100	67%
Combined estimation modified by forensic prior distribution	163/225	72.4%	94	63%
Combined estimation modified by archaeological prior distribution	Not tested		102	68%

Table 5.2: Comparison of correlation between estimated age and actual age from different researchers

Age estimation category	Correlation coefficients		
	Boldsen <i>et al.</i> 's ⁴ original study	Bethard's ¹⁰⁶ validation study	Current validation study
Cranial suture estimation	0.66	0.17	0.36
Pubic symphysis estimation	0.86	0.41	0.26
Auricular surface estimation	0.82	0.41	0.35
Combined estimation	0.88	0.51	0.43
Combined estimation modified by forensic prior distribution	Not tested	0.50	0.43
Combined estimation modified by archaeological prior distribution	Not tested	Not tested	0.42

Chapter 6: Conclusion

The aim of this study was to validate the accuracy and repeatability of transition analysis as a method for age estimation in a South African population. The effect of observer variation on the final age estimation was also assessed. It was concluded that:

1. The level of accuracy for the 95% confidence interval for all six age estimation categories of transition analysis corresponds with results from previous research.
2. The range of the 95% confidence interval is impractically large, especially for the single indicator age estimation categories, which spanned up to 95 years in some cases.
3. The range of the 95% confidence interval does not increase linearly with increasing age, but instead starts to decrease at around 70 years of age. This decrease in confidence interval width is facilitated by the archaeological prior distribution. This indicates that age estimation is least successful for the middle age ranges, between 40 – 60 years.
4. The maximum likelihood point estimations are least accurate for the single indicator methods, but does improve when using combined estimation methods and is particularly promising when using the archaeological prior distribution.
5. The ventral margin of the pubic symphysis and the posterior exostoses of the auricular surface were the least repeatable features. Simplifying these features by using better descriptions, accompanied by photographs or cast models, and reducing the number of stages would be beneficial.
6. Small score differences between observers did not significantly influence the overall population distributions, but practice using the method improved the results achieved.
7. Not only did the archaeological prior distribution improve accuracy and precision of the age estimation, but the effect of observer disagreement on the population distribution was also moderated. Use of a South African population prior distribution could possibly improve results even further.
8. Future research should include the addition of more good quality age indicators to the combination method and accounting for population variation in the skeletal material and the prior distribution.

References

1. White TD, Folkens PA. *The Human Bone Manual*. Burlington: Elsevier Academic Press; 2005.
2. Scheuer L, Black S. *Developmental Juvenile Osteology*. Bath: Elsevier Academic Press; 2000.
3. Brooks ST. Skeletal age at death: The reliability of cranial and pubic age indicators. *Am J Phys Anthropol* 1955;13:567–97.
4. Boldsen JL, Milner GR, Konigsberg LW, Wood JW. Transition analysis: A new method for estimating age from skeletons. In: Hoppa RD, Vaupel JW, editors. *Paleodemography: Age Distributions from Skeletal Samples*. New York: Cambridge University Press; 2002. page 73–106.
5. Dirkmaat DC, editor. *A Companion to Forensic Anthropology*. West Sussex (UK): Blackwell Publishing Ltd; 2012.
6. Ousley SD, Hollinger RE. The pervasiveness of Daubert. In: Dirkmaat D, editor. *A Companion to Forensic Anthropology*. John Wiley & Sons; 2012. page 654–65.
7. Grivas CR, Komar DA. Kumho, Daubert and the nature of scientific inquiry: Implications for forensic anthropology. *J Forensic Sci* 2008;53:771–6.
8. Hoppa RD, Vaupel JW. The Rostock Manifesto for paleodemography: The way from stage to age. In: Hoppa RD, Vaupel JW, editors. *Paleodemography: Age Distributions from Skeletal Samples*. Cambridge University Press; 2002. page 1–8.
9. Christensen AM, Crowder CM. Evidentiary standards for forensic anthropology. *J Forensic Sci* 2009;54:1211–6.
10. McKern TW, Stewart TD. *Skeletal age changes in young American males*. Natick: 1957.
11. Hoppa RD. Population variation in osteological aging criteria: An example from the pubic symphysis. *Am J Phys Anthropol* 2000;111:185–91.
12. DiGangi EA, Bethard JD, Kimmerle EH, Konigsberg LW. A new method for estimating age-at-death from the first rib. *Am J Phys Anthropol* 2009;138:164–76.
13. Hunt DR, Albanese J. History and demographic composition of the Robert J. Terry anatomical collection. *Am J Phys Anthropol* 2005;127:406–17.
14. Milner GR, Boldsen JL. Transition analysis: A validation study with known-age modern American skeletons. *Am J Phys Anthropol* 2012;148:98–110.

15. Usher BM. Reference samples: The first step in linking biology and age in the human skeleton. In: Hoppa RD, Vaupel JW, editors. *Paleodemography: Age Distributions from Skeletal Samples*. New York: Cambridge University Press; 2002. page 29–47.
16. Molleson T, Cox M, Waldron H, Whittaker DK. *The Spitalfields Project Volume 2. The Anthropology: The Middling Sort*. York, United Kingdom: Council for British Archaeology; 1993.
17. Cardoso HF V. Brief communication: The collection of identified human skeletons housed at the Bocage Museum (National Museum of Natural History), Lisbon, Portugal. *Am J Phys Anthropol* 2006;129:173–6.
18. Giraudi R, Fissore F, Giacobini G. The collection of human skulls and postcranial skeletons at the Department of Human Anatomy of the University of Torino (Italy). *Am J Phys Anthropol* 1984;65:105–7.
19. Dayal MR, Kegley ADT, Strkalj G, Bidmos M a, Kuykendall KL. The history and composition of the Raymond A. Dart Collection of Human Skeletons at the University of the Witwatersrand, Johannesburg, South Africa. *Am J Phys Anthropol* 2009;140:324–35.
20. Tal H, Tau S. Statistical survey of the human skulls in the Raymond Dart Collection of Skeletons. *S Afr J Sci* 1983;79:215–7.
21. L'Abbé EN, Loots M, Meiring JH. The Pretoria Bone Collection: A modern South African skeletal sample. *HOMO - J Comp Hum Biol* 2005;56:197–205.
22. Galera V, Ubelaker DH, Hayek LA. Comparison of macroscopic cranial methods of age estimation applied to skeletons from the Terry Collection. *J Forensic Sci* 1998;43:933–9.
23. Gilbert BM, McKern TW. A method for aging the female os pubis. *Am. J. Phys. Anthropol.* 1973;38:31–8.
24. Konigsberg LW, Herrmann NP, Wescott DJ, Kimmerle EH. Estimation and evidence in forensic anthropology: Age-at-death. *J Forensic Sci* 2008;53:541–57.
25. Todd TW. Age changes in the pubic bone: I. The male white pubis. *Am J Phys Anthropol* 1920;3:285–339.
26. Todd TW, Lyon DW. Endocranial suture closure: Its progress and age relationship. Part I. Adult males of white stock. *Am J Phys Anthropol* 1924;7:325–84.
27. Acsádi GY, Nemeskéri J. *History of Human Life Span and Mortality*. Budapest: Akadémiai Kiadó; 1970.

28. Klepinger LL, Katz D, Micozzi MS, Carroll L. Evaluation of cast methods for estimating age from the os pubis. *J Forensic Sci* 1992;37:763–70.
29. Buckberry JL, Chamberlain AT. Age estimation from the auricular surface of the ilium: A revised method. *Am J Phys Anthropol* 2002;119:231–9.
30. Lampl M, Johnston FE. Problems in the aging of skeletal juveniles: Perspectives from maturation assessments of living children. *Am J Phys Anthropol* 1996;101:345–55.
31. Meindl RS, Lovejoy CO, Mensforth RP, Walker RA. A revised method of age determination using the os pubis, with a review and tests of accuracy of other current methods of pubic symphyseal aging. *Am J Phys Anthropol* 1985;68:29–45.
32. Mensforth RP, Lovejoy CO. Anatomical, physiological and epidemiological correlates of the aging process: A confirmation of multifactorial age determination in the Libben Skeletal Population. *Am J Phys Anthropol* 1985;68:87–106.
33. Osborne DL, Simmons TL, Nawrocki SP. Reconsidering the auricular surface as an indicator of age at death. *J Forensic Sci* 2004;49:905-11.
34. Nawrocki SP. Regression formulae for estimating age at death from cranial suture closure. In: Reichs KJ, editor. *Forensic Osteology: Advances in the Identification of Human Remains*. Springfield, Illinois: Charles C Thomas; 1998. page 276–93.
35. Boldsen JL, Milner GR, Hylleberg R. ADBOU. 2002.
36. Milner GR, Boldsen JL. *Transition Analysis Age Estimation: Skeletal Scoring Manual*; 2012.
37. Brooks S, Suchey JM. Skeletal age determination based on the os pubis: A comparison of the Acsadi-Nemeskeri and Suchey-Brooks methods. *Hum Evol* 1990;5:227–38.
38. Lampl M, Veldhuis JD, Johnson ML. Saltation and stasis: A model of human growth. *Science* 1992;258:801–3.
39. Katz D, Suchey JM. Age Determination of the male os pubis. *Am J Phys Anthropol* 1985;69:427–35.
40. Ubelaker DH. Estimating age at death from immature human skeletons: An overview. *J Forensic Sci* 1987;32:1254–63.
41. Mulhern DM, Jones EB. Test of revised method of age estimation from the auricular surface of the ilium. *Am J Phys Anthropol* 2005;126:61–5.

42. Falys C, Lewis M. Proposing a way forward: A review of standardisation in the use of age categories and ageing techniques in osteological analysis (2004-2009). *Int J Osteoarchaeol* 2011;21:704–16.
43. Mann RW, Jantz RL, Bass WM, Willey PS. Maxillary suture obliteration: A visual method for estimating skeletal age. *J Forensic Sci* 1991;36:781–91.
44. Lovejoy CO, Meindl RS, Pryzbeck TR, Mensforth RP. Chronological metamorphosis of the auricular surface of the ilium: A new method for the determination of adult skeletal age at death. *Am J Phys Anthropol* 1985;68:15–28.
45. İşcan MY, Loth SR, Wright RK. Metamorphosis at the sternal rib end: A new method to estimate age at death in white males. *Am J Phys Anthropol* 1984;65:147–56.
46. İşcan MY, Loth SR, Wright RK. Age estimation from the rib by phase analysis: White males. *J Forensic Sci* 1984;29:1094–104.
47. İşcan MY, Loth SR, Wright RK. Age estimation from the rib by phase analysis: White females. *J Forensic Sci* 1985;30:853–63.
48. Meindl RS, Lovejoy CO. Ectocranial suture closure: A revised method for the determination of skeletal age at death based on the lateral-anterior sutures. *Am J Phys Anthropol* 1985;68:57–66.
49. Langley-Shirley N, Jantz RL. A Bayesian approach to age estimation in modern Americans from the clavicle. *J Forensic Sci* 2010;55:571–83.
50. Kunos C, Simpson S, Russel K, Hershkovitz I. First rib metamorphosis: Its possible utility for human age-at-death estimation. *Am J Phys Anthropol* 1999;110:303–23.
51. Lamendin H, Baccino E, Humbert JF, Tavenier J, Nossintchouk RM, Zerille A. A simple technique for age estimation in adult corpses: The two criteria dental method. *J Forensic Sci* 1992;37:1373–9.
52. Wittwer-Backofen U, Gampe J, Vaupel JW. Tooth cementum annulation for age estimation: Results from a large known-age validation study. *Am J Phys Anthropol* 2004;123:119–29.
53. Maat GJR, Gerretsen RRR, Aarents MJ. Improving the visibility of tooth cementum annulations by adjustment of the cutting angle of microscopic sections. *Forensic Sci Int* 2006;159:S95–S99.
54. Gustafson G. Age determination of teeth. *J Am Dent Assoc* 1950;41:45–54.
55. Kerley ER. The microscopic determination of age in human bone. *Am J Phys Anthropol* 1965;23:149–63.

56. Kerley ER, Ubelaker DH. Revision in the microscopic method of estimating age at death in human cortical bone. *Am J Phys Anthropol* 1978;49:545–6.
57. Ericksen MF. Histological examination of age at death using the anterior cortex of the femur. *Am J Phys Anthropol* 1991;84:171–9.
58. Stout SD. The use of histomorphology to estimate age. *J Forensic Sci* 1988;33:121–5.
59. Stewart TD. The rate of development of vertebral osteoarthritis in American whites and its significance in skeletal age identification. *Leech* 1958;28:144–51.
60. Aiello LC, Molleson T. Are microscopic ageing techniques more accurate than macroscopic ageing techniques? *J Archaeol Sci* 1993;20:689–704.
61. Perizonius WRK. Closing and non-closing sutures in 256 crania of known age and sex from Amsterdam (A.D. 1883-1909). *J Hum Evol* 1984;13:201–16.
62. Krogman WM, İşcan MY. *The Human Skeleton in Forensic Medicine*. 2nd ed. Springfield: Charles C Thomas; 1986.
63. Shirley NR, Jantz RL. Spheno-occipital synchondrosis fusion in modern Americans. *J Forensic Sci* 2011;56:580–5.
64. Bassed RB, Briggs C, Drummer OH. Analysis of time of closure of the spheno-occipital synchondrosis using computed tomography. *Forensic Sci Int* 2010;200:161–4.
65. Williams PL, Bannister LH, Berry MM, Collins P, Dyson M, Dussek JE. *Gray's Anatomy*. New York, NY: Churchill Livingstone; 1995.
66. Key CA, Aiello LC, Molleson T. Cranial suture closure and its implications for age estimation. *Int J Osteoarchaeol* 1994;4:193–207.
67. Todd TW, Lyon DW. Cranial suture closure: Its progress and age relationship. Part II. Ectocranial closure in adult males of white stock. *Am J Phys Anthropol* 1925;8:23–45.
68. Todd TW, Lyon DW. Suture closure: Its progress and age relationship. Part IV. Ectocranial closure in adult males of negro stock. *Am J Phys Anthropol* 1925;8:149–68.
69. Todd TW, Lyon DW. Cranial suture closure: Its progress and age relationship. Part III. Endocranial closure in adult males of negro stock. *Am J Phys Anthropol* 1925;8:47–71.
70. Bass WM, Ph D, Mann R, Obliteration MS. Maxillary suture obliteration : Aging the human skeleton based on intact or fragmentary maxilla. *J Forensic Sci* 1987;32:148-57.

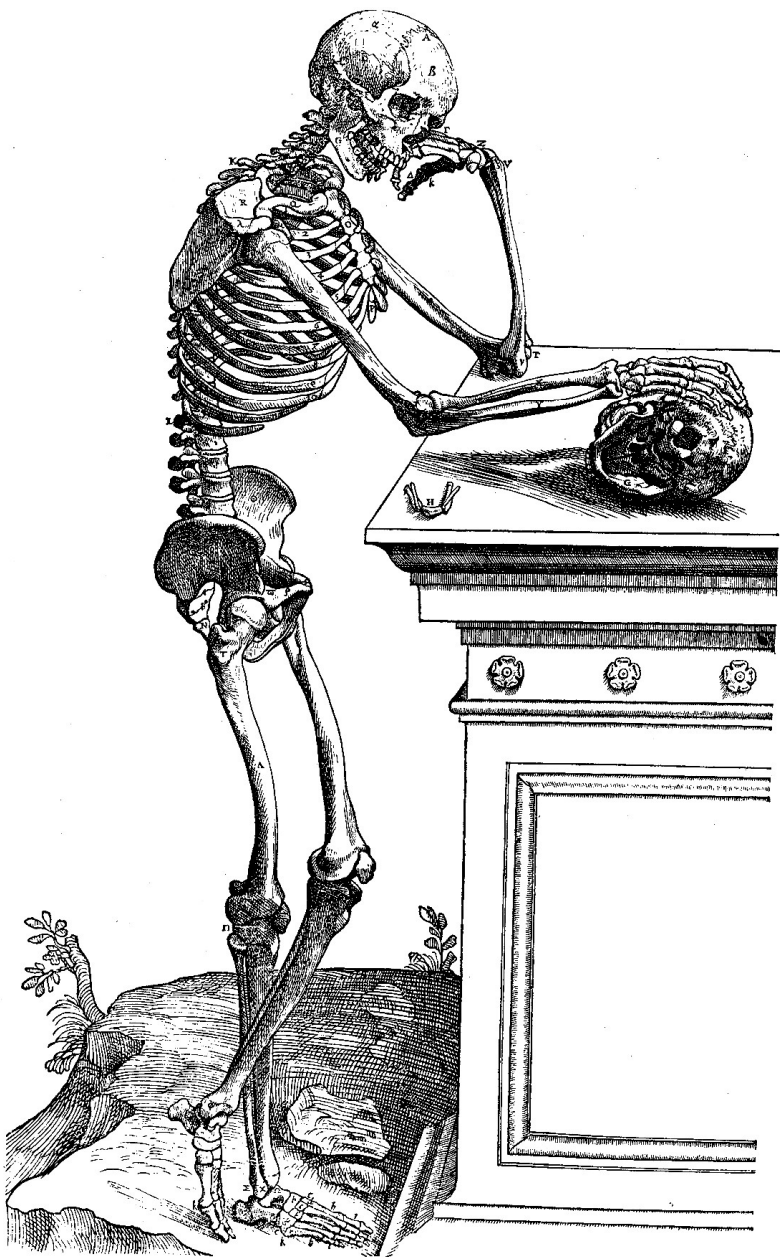
71. Singer R. Estimation of age from cranial suture closure. *J Forensic Med* 1953;1:52–9.
72. Berg GE. Pubic bone age estimation in adult women. *J Forensic Sci* 2008;53:569–77.
73. Todd TW. Age changes in the pubic symphysis: VII. The anthropoid strain in human pubic symphyses of the third decade. *J Anat* 1923;57:274–94.
74. Todd TW. Age changes in the pubic bone: Part II, III and IV. *Am J Phys Anthropol* 1921;4:1–70.
75. Todd TW. Age changes in the pubic bone: VI. The interpretation of variations in the symphyseal area. *Am J Phys Anthropol* 1921;4:407–24.
76. Todd TW. Age changes in the pubic bone: VIII. Roentgenographic differentiation. *Am J Phys Anthropol* 1930;14:255–71.
77. Snow CC. Equations for estimating age at death from the pubic symphysis: A modification of the McKern-Stewart method. *J Forensic Sci* 1983;28:864–70.
78. Suchey JM, Katz D. Applications of pubic age determination in a forensic setting. In: Reichs KJ, editor. *Forensic Osteology: Advances in the Identification of Human Remains*. Springfield: Charles C Thomas; 1998. page 204–36.
79. Chen X, Zhang Z, Zhu G, Tao L. Determining the age at death of females in the Chinese Han population: Using quantitative variables and statistical analysis from pubic bones. *Forensic Sci Int* 2011;210:278.e1–278.e8.
80. Chen X, Zhang Z, Tao L. Determination of male age at death in Chinese Han population: Using quantitative variables statistical analysis from pubic bones. *Forensic Sci Int* 2008;175:36–43.
81. Hanihara K, Suzuki T. Estimation of age from the pubic symphysis by means of multiple regression analysis. *Am J Phys Anthropol* 1978;48:233–40.
82. Schmitt a. Age-at-death assessment using the os pubis and the auricular surface of the ilium: A test on an identified Asian sample. *Int J Osteoarchaeol* 2004;14:1–6.
83. Stewart TD. Distortion of the pubic symphyseal surface in females and its effect on age determination. *Am J Phys Anthropol* 1957;15:9–18.
84. Tague RG. Bone resorption of the pubis and preauricular area in humans and nonhuman mammals. *Am. J. Phys. Anthropol.* 1988;76:251–67.
85. Snodgrass JJ, Galloway A. Technical Note: Utility of dorsal pits and pubic tubercle height in parity assessment. *J Forensic Sci* 2003;48:1226–30.

86. Sutherland LD, Suchey JM. Use of the ventral arc in pubic sex determination. *J Forensic Sci* 1991;36:501–11.
87. Budinoff LC, Tague RG. Anatomical and developmental bases for the ventral arc of the human pubis. *Am J Phys Anthropol* 1990;82:73–9.
88. Anderson BE. Ventral arc of the os pubis: Anatomical and developmental considerations. *Am J Phys Anthropol* 1990;83:449–58.
89. Kelley MA. Parturition and pelvic changes. *Am J Phys Anthropol* 1979;51:541–6.
90. Suchey JM, Wiseley D V, Green RF, Noguchi TT. Analysis of dorsal pitting in the os pubis in an extensive sample of modern American females. *Am J Phys Anthropol* 1979;51:517–40.
91. Sashin D. A critical analysis of the anatomy and the pathological changes of the sacro-iliac joints. *J Bone Jt Surg* 1930;12:891–910.
92. Bowen V, Cassidy JD. Macroscopic and microscopic anatomy of the sacroiliac joint from embryonic life until the eighth decade. *Spine (Phila Pa 1976)* 1981;6:620–8.
93. Stewart TD. Pathological changes in aging sacroiliac joints: A study of dissecting-room skeletons. *Clin Orthop Relat Res* 1984;183:188–96.
94. Schmitt A. A new method to assess adult age at death from the iliac sacro-pelvic surface. *Bull Mem Soc Anthropol Paris* 2005;17:89–101.
95. Murray KA, Murray T. A test of the auricular surface aging technique. *J Forensic Sci* 1991;36:1162–9.
96. Igarashi Y, Uesu K, Wakebe T, Kanazawa E. New method for estimation of adult skeletal age at death from the morphology of the auricular surface of the ilium. *Am J Phys Anthropol* 2005;128:324–39.
97. Brooke R. The sacro-iliac joint. *J Anat* 1924;58:299–305.
98. Rougé-Maillart C, Telmon N, Rissech C, Malgosa A, Rougé D. The determination of male adult age at death by central and posterior coxal analysis - A preliminary study. *J Forensic Sci* 2004;49:208–14.
99. Baccino E, Ubelaker DH, Hayek LA, Zerilli A. Evaluation of seven methods of estimating age at death from mature human skeletal remains. *J Forensic Sci* 1999;44:931–6.
100. Lovejoy CO, Meindl RS, Mensforth RP, Barton TJ. Multifactorial determination of skeletal age at death: A method and blind tests of its accuracy. *Am J Phys Anthropol* 1985;68:1–14.

101. Katz D, Suchey JM. Race differences in pubic symphyseal aging patterns in the male. *Am J Phys Anthropol* 1989;80:167–72.
102. King CA, İşcan MY, Loth SR. Metric and comparative analysis of sexual dimorphism in the Thai femur. *J Forensic Sci* 1998;43:954–8.
103. Boldsen JL. Transitional analysis: A method for unbiased age estimations from skeletal traits. In: American Association of Physical Anthropologists. St. Louis, Missouri: 1997. page 79.
104. Milner GR. Age at death determination using revised scoring procedures for age-progressive skeletal traits. In: American Association of Physical Anthropologists. St. Louis, Missouri: 1997. page 170.
105. Gompertz B. On the nature of the function expressive of the law of human mortality, and on a new mode of determining the value of life contingencies. *Philos Trans R Soc London* 1825;115:513–83.
106. Bethard JD. A Test of the Transition Analysis Method for Estimation of Age-at-Death in Adult Human Skeletal Remains. MA thesis, University of Tennessee, Knoxville, TN; 2005.
107. Bullock M, Márquez L, Hernández P, Ruíz F. Paleodemographic age-at-death distributions of two Mexican skeletal collections: A comparison of transition analysis and traditional aging methods. *Am J Phys Anthropol* 2013;152:67–78.
108. Poulsen LW, Qvesel D, Brixen K, Vesterby a, Boldsen JL. Low bone mineral density in the femoral neck of medieval women: A result of multiparity? *Bone* 2001;28:454–8.
109. Boldsen JL. Early childhood stress and adult age mortality — A study of dental enamel hypoplasia in the medieval Danish village of Tirup. *Am J Phys Anthropol* 2007;132:59–66.
110. Buikstra JE, Ubelaker DH. Standards for data collection from human skeletal remains. Fayetteville: Arkansas Archaeological Survey; 1994.
111. Human Tissue Act, 1983. Republic of South Africa Government Gazette, vol. 216, pp. 1–34.
112. Landis JR, Koch GG. The measurement of observer agreement for categorical data. *Biometrics* 1977;33:159–74.

Appendix A

TRANSITION ANALYSIS AGE ESTIMATION: SKELETAL SCORING MANUAL



George R. Milner¹

and

Jesper L. Boldsen²

¹ The Pennsylvania State University
University Park, PA USA

² Syddansk Universitet
Odense, DK

Abbreviated Scoring Formats

Pubic Symphysis

Symphyseal Relief

Location

Entire surface

Characteristics

1. Sharp billowing
2. Soft, deep billowing
3. Soft, shallow billowing
4. Residual billowing
5. Flat
6. Irregular

4. Rampart completion I
5. Rampart completion II
6. Rim
7. Breakdown

Symphyseal Texture

Location

Dorsal demiface

Characteristics

1. Smooth (fine grained)
2. Coarse grained
3. Microporosity
4. Macroporosity

Superior Apex

Location

Superior end of the symphyseal face

Characteristics

1. No protuberance
2. Early protuberance
3. Late protuberance
4. Integrated

Ventral Symphyseal Margin

Location

Ventral demiface

Characteristics

1. Serrated
2. Beveling
3. Rampart formation

Dorsal Symphyseal Margin

Location

Dorsal demiface

Characteristics

1. Serrated
2. Flattening incomplete
3. Flattening complete
4. Rim
5. Breakdown

Iliac Auricular Surface

Superior demiface topography

Location

Superior demiface

Characteristics

1. Undulating
2. Median elevation
3. Flat to irregular

Inferior demiface topography

Location

Inferior demiface

Characteristics

1. Undulating
2. Median elevation
3. Flat to irregular

Superior surface morphology

Location

Superior part of the auricular surface

Characteristics

1. >2/3 covered by billows
2. 1/3-2/3 covered by billows
3. <1/3 covered by billows
4. Flat (no billows)
5. Bumps

5. Touching exostoses
6. Fusion

Apical (Middle) surface morphology

Location

Apical (middle) part of the auricular surface

Characteristics

1. >2/3 covered by billows
2. 1/3-2/3 covered by billows
3. <1/3 covered by billows
4. Flat (no billows)
5. Bumps

Inferior posterior iliac exostoses

Location

Inferior part of the posterior ilium

Characteristics

1. Smooth
2. Rounded bony elevations
3. Pointed exostoses
4. Jagged exostoses
5. Touching exostoses
6. Fusion

Inferior surface morphology

Location

Inferior part of the auricular surface

Characteristics

1. >2/3 covered by billows
2. 1/3-2/3 covered by billows
3. <1/3 covered by billows
4. Flat (no billows)
5. Bumps

Posterior exostoses (or spicules)

Location

Posterior to the sacroiliac joint

Characteristics

1. Smooth (no exostoses or spicules)
2. Rounded exostoses
3. Pointed exostoses

Inferior surface texture

Location

Inferior angle

Characteristics

1. Smooth
2. Microporosity
3. Macroporosity

Coronal Pterica (left)

Characteristics

1. Open
2. Juxtaposed
3. Partially obliterated
4. Punctuated
5. Obliterated

Superior posterior iliac exostoses

Location

Superior part of the posterior ilium

Characteristics

1. Smooth
2. Rounded bony elevations
3. Pointed exostoses
4. Jagged exostoses

Sagittal Obelica

Characteristics

1. Open
2. Juxtaposed
3. Partially obliterated
4. Punctuated
5. Obliterated

Lambdoidal Asterica (left)

Characteristics

1. Open
2. Juxtaposed
3. Partially obliterated
4. Punctuated
5. Obliterated

2. Juxtaposed
3. Partially obliterated
4. Punctuated
5. Obliterated

Zygomaticomaxillary suture (left)

Characteristics

1. Open

Interpalatine (median palatine, posterior portion)

Characteristics

1. Open (open and juxtaposed)
3. Partially obliterated
4. Punctuated
5. Obliterated

Introduction

This manual covers how to record three skeletal features – the pubic symphysis, the iliac auricular area, and cranial sutures – used to estimate the ages of adults with the Transition Analysis computer program. When developing the procedure, beginning in 1996, we designed new scoring systems for age-progressive changes in bony morphology and examined two known age-at-death skeletal collections (Terry and Coimbra) to estimate the age distribution associated with each of the various stages that were defined. The program calculates an estimated age (maximum likelihood) and confidence intervals for archaeological or forensic skeletons. Further explanation of the procedure can be found in Boldsen et al. (2002).

One does not have to observe all skeletal traits to generate an age estimate. That is, the procedure was designed to accommodate the possibility – in many archaeological or forensic settings, bordering on a certainty – that only a partial skeleton is available.

Ambiguous skeletal features

Occasionally it is difficult or impossible to distinguish between sequential stages in one or more components. Skeletal features might be altered by pathological processes or eroded after burial. There is still information, however, in such characters.

Osteologists should record whatever is observable, using a two or more stage designation as appropriate (e.g., Stages 3-4). Doing so allows one to take full advantage of the meager information that might be available in the bony structure that is being scored.

When a particular component cannot be observed it should be coded as unscorable. Usually such situations arise when there is postmortem damage. But sometimes that can happen as a result of antemortem alterations to normal skeletal structures. For example, large parity pits can eat deeply into the dorsal demiface of the pubic symphysis of females, eliminating features that otherwise could be scored.

There is no substitute for becoming thoroughly familiar with age-related changes in the skeleton before scoring unknown-age individuals.

That is especially true of the pubic symphysis and sacroiliac joint, as the procedures used here are not the same as those of conventional methods.

Pubic Symphysis

Five separate components are examined for the pubic symphysis. The various features are based on previous descriptions of bony changes in the pubic bone, especially those of Todd (1920) and McKern and Stewart (1957), supplemented by observations of numerous North American and Danish archaeological skeletons. Many terms used here are derived from this earlier work.

Users of Transition Analysis can gain experience with the changes that take place in the pubic symphysis by closely examining the excellent casts in the McKern-Stewart and SucheyBrooks pubic bone sets. For sake of convenience, the several parts of the roughly oval symphyseal face are described as superior, inferior, ventral (anterior), and dorsal (posterior), even though such terms are not entirely accurate when the bone is oriented in proper anatomical position.

Left and right sides are scored separately in Transition Analysis, using the codes associated with the stage descriptions (1, 2, 3, etc.). Opposing pubic bones generally resemble one another, although they often differ in some respects. The Transition Analysis program accommodates such variation as each pubic symphysis is scored separately.

Symphyseal Relief

Location

The entire face is of interest, and the terms generally follow those of McKern and Stewart (1957). Often the features distinguished here, especially billowing, are most clearly seen in the dorsal half of the symphyseal face. In fact, low ridges of bone, the billowing, can be entirely absent from the ventral symphyseal face, beginning as early as the ventral beveling stage.

Characteristics

1. Sharp billowing
2. Soft, deep billowing
3. Soft, shallow billowing
4. Residual billowing
5. Flat
6. Irregular

Definitions

1. *Sharp billowing*: Sharply crested ridges of bone cover at least half of the surface. Deep furrows that extend completely across the symphyseal face separate distinct ridges. The deepest furrows cut into the ventral and dorsal margins of the symphyseal face, interrupting the edge of the bone and giving it a jagged appearance. The distance between the high and low points of adjacent ridges and furrows can often be 3 mm or more. Occasionally, round instead of sharp crests occur on the high ridges in specimens that otherwise have deep furrows exceeding 3 mm. Such specimens are also considered examples of Sharp Billowing. Sharp Billowing has only been seen in teenagers.

2. *Soft, deep billowing*: Softly crested to low billows separated by deep furrows extend across at least half of the surface, typically the dorsal demiface. The furrows do not appear as if they have been filled in with bone. The distance between high and low points of adjacent ridges and furrows is 3 mm or less.

3. *Soft, shallow billowing*: Low but clearly visible and discrete billows separated by shallow furrows are present on at least half of the dorsal demiface. The remnants of an earlier ridge and furrow system dominate the dorsal demiface, and the furrows look as if they were partially filled with bone. Billows extend most or all of the way across the dorsal demiface, and in some individuals they reach the ventral margin.

4. *Residual billowing*: Billows are barely elevated above the symphyseal face, and they blend into one another to form low and indistinct raised areas that lack clearly defined furrows between them. The slightly raised areas, however, are still an important element of the surface, and they almost invariably occur on the inferior half of the face, often in the dorsal demiface. Individual billows usually cross only part of the symphyseal face, typically less than one-half its width. There must be two or more adjacent raised areas corresponding to billows to qualify as Residual Billowing. A single isolated bony elevation is not sufficient to be classified as Residual Billowing; instead, such specimens are considered Flat.

5. *Flat*: More than one-half of the symphyseal face within well-defined margins is flat or slightly recessed, especially if surrounded by a welldeveloped Rim (see below). Occasionally small, flat, pillows of bone give the surface a pebbly appearance. The remainder of the symphyseal face does not conform to Residual Billowing (i.e., there is no more than one discrete low raised area). Sometimes there is a gap where the ventral rampart has failed to extend along the entire ventral edge of the pubis (see below); when that occurs, the surface within the gap does not receive a score.

6. *Irregular*: Pitting, which can be deep, covers more than one-half of the symphyseal face, giving it an irregular and disfigured appearance. The pits can be accompanied by small, sharp exostoses scattered across the face. Occasionally, in old people an otherwise flat face is thickly covered by rounded sharp exostoses of bone. Pitting in such specimens might be minor, but the bone is still classified as Irregular. Similar to the Flat category, the scored part of the symphyseal face does not include the ventral gap, if present. In Irregular specimens, the margins of the symphyseal face are typically defined by the Rim and Breakdown stages of the Ventral and Dorsal Margin components.

Symphyseal Texture

Location

The dorsal demiface surface is examined³.

The ventral part of the bone, when ventral beveling is present, is often pitted, giving it the appearance of microporosity. A porous appearing ventral demiface should not be confused with whatever is happening in the dorsal demiface.

Characteristics

1. Smooth (fine grained)
2. Coarse grained
3. Microporosity
4. Macroporosity

Definitions

1. *Smooth (fine grained)*: Smooth to finegrained bone extends across most, or all, of the dorsal demiface.

2. *Coarse grained (little net)*: Coarse-textured bone covers over one-third of the dorsal demiface. The surface looks like packed fine sand, similar to fine-grained sandpaper.

3. *Microporosity*: Porous bone covers over one-third of the dorsal demiface. It looks as if the surface was pierced by closely packed pin pricks.

4. *Macroporosity*: Deep pits cover over onethird of the dorsal demiface, giving it an irregular appearance. The pits are at least 0.5 mm in diameter, and are generally spaced close together. Sometimes the symphyseal surface is so irregular from pitting that it resembles the edge of a sponge.

³ It is our impression that prehistoric Native American skeletons have microporosity more often and at an earlier age than medieval Scandinavians. More importantly, they differ from modern people in the Terry and Coimbra collections used to generate the transition curves used to estimate age. Therefore, it is best not to rely heavily on this component when examining Native American skeletons. In fact, it is prudent to record Symphyseal Texture stages for Native Americans, but treat them as missing data.

Superior Apex

Location

A distinct knob of bone or, later, an elevated area is visible on the superior part of some pubic symphyses. Otherwise, this part of the symphyseal face resembles the rest of it.

Characteristics

1. No protuberance
2. Early protuberance
3. Late protuberance
4. Integrated

Definitions

1. No protuberance: Deep to shallow billowing is present in the superior part of the symphyseal face. There are no signs of a bony protuberance. In young individuals, this part of the symphyseal face can be poorly differentiated from the non-articular portion of the pubis immediately lateral to the joint.

2. Early protuberance: A distinct bony knob of variable dimensions with well-defined margins is visible in the superior part of the symphyseal face. It projects above the plane(s) defined by the immediately adjacent symphyseal face (i.e., the superior portions of the dorsal and ventral demifaces, where the latter can be characterized by ventral beveling). The surface of the bony protuberance is typically smooth to fine grained. The bony knob often reminds one of a lentil or pea stuck on the bone.

3. Late protuberance: The superior part of the symphyseal face is raised somewhat above the rest of the articulation surface. The elevated area is typically located on the ventral side of the midline.⁴ The margins of the slightly raised area tend to be poorly defined. Thus the Late Protuberance is more completely integrated with the rest of the symphyseal face than the distinctly knob-like Early Protuberance. Integration is partly a result of ventral rampart formation. Late Protuberance should not be confused with a narrow raised rim that can border the cranial end of the symphyseal face in many specimens. For a Late Protuberance to be scored as present, the slightly raised area must extend onto the symphyseal face; that is, it is not restricted to the margin that can feature a pronounced rim. Occasionally, the superior part of the symphyseal face can be isolated by marked pitting of the middle symphyseal surface, but these specimens should not be considered as a Late Protuberance stage. For Late Protuberance to be present, the slightly raised area must be visible on a rather smooth symphyseal face.

4. Integrated: The symphyseal face's superior end displays no signs of a low bony elevation. The area where the protuberance was formerly present is fully integrated with the rest of the symphyseal face. That is, the smooth to irregular (usually pitted) symphyseal face is essentially flat.

⁴ Occasionally, a gap exists in the superior one-half of the ventral margin, but the ventral rampart is otherwise completely formed. In that case the presence of a protuberance is not scored as the appearance of the bone can be confusing.

Ventral Symphyseal Margin

Location

The ventral part of the pubic symphysis is scored separately from the rest of the bone.

Characteristics

1. Serrated
2. Beveling
3. Rampart formation
4. Rampart completion I
5. Rampart completion II
6. Rim
7. Breakdown

Definitions

1. Serrated: Ridges and furrows typical of Sharp or Soft Deep Billowing extend uninterrupted across the ventral part of the symphyseal face, producing a serrated or jagged ventral margin.

2. Beveling: Billows are flattened in the ventral demiface, a process that generally starts at the superior end. The flattening, or beveling, must extend along at least one-third of the ventral margin to be scored as present. There is generally a well-defined margin where the ventral surface of the pubis (the beveled part) meets the articular surface located immediately posterior to it.

3. Rampart incomplete: The ventral rampart, following McKern and Stewart (1957), refers to a distinct outgrowth of bone that ultimately forms the ventral aspect of the symphyseal face. The rampart extends from one or both ends of the symphysis, and it often resembles a roll of well-chewed gum stuck on the ventral edge of the symphyseal face. The rampart does not extend along the entire ventral edge, and often some elements of a youthful symphyseal surface can be followed uninterrupted to the ventral edge of the symphysis. In the superior part of the ventral margin, the rampart forms on the Beveled surface. In the inferior part of the margin, remnants of the original irregular surface can often be seen dipping below a partially formed rampart, which looks as if it was lying on a shallowly furrowed surface. An incomplete rampart frequently extends inferiorly from the bony protuberance defining the cranial end of the face, sometimes forming a bony elevation that resembles a comma, with the rampart being the tail.⁵ A rampart can also extend superiorly from the inferior end of the symphysis. Bony extensions from the superior and inferior ends of the symphysis, if both are present, typically leave a gap in the middle one-third of the ventral margin. An early Rampart Incomplete stage can consist of one or more bony knobs, commonly located in the middle one-third of the ventral margin. The knobs can occur with, or without, the formation of a bony rampart extending from the superior and inferior ends of the symphysis. If the rampart is more than two-thirds complete

⁵ A well-developed bony protuberance at the cranial end of the face that lacks a distinct inferiorly projecting ventral rampart should not be coded as Ventral Rampart Formation; that is, the mere existence of a cranially located bony knob without bone being laid down along the ventral margin is not sufficient to score the ventral rampart as present.

but there is a gap in the superior part of it, you should consider the possibility that the specimen is in the Rampart Complete I or II stages. Occasionally a rampart never completely forms along the ventral margin (see below).

4. Rampart complete I: Here the ventral rampart is complete, but there is a shallow sulcus extending along much of the length of the ventral pubis immediately lateral to the symphysis (often more pronounced inferiorly). The groove is a residual feature related to rampart formation along the ventral margin. A reasonably flat symphyseal surface extends uninterrupted from the dorsal to ventral margins, so the face is unlike the somewhat furrowed appearance of many Rampart Incomplete specimens where there is a shallow groove just dorsal to an incomplete ventral rampart. Occasionally a gap exists in the ventral margin, usually in its superior half; the ventral rampart is otherwise completely formed.⁶

5. Rampart complete II: Here the ventral rampart is complete, and there is no shallow sulcus as described in Rampart Complete I. A reasonably flat symphyseal surface extends uninterrupted from its dorsal to ventral margins, so the face is unlike the somewhat furrowed appearance of many Rampart Incomplete specimens where there is also a shallow groove just dorsal to the incomplete ventral rampart. Occasionally there is a gap in the superior half of the ventral margin, but the ventral rampart is otherwise complete. These specimens should be classified as Rampart Complete. With regard to Rampart Complete I and II, most specimens are in the later (II) stage.⁵

6. Rim: A narrow, bony rim defining the ventral margin of the symphysis, perched on top of the ventral rampart, demarcates a usually flat or irregular face. The rim does not have to be complete, but it must be at least 1 cm long and readily visible as a raised ridge adjacent to a slightly recessed symphyseal face. The rim can be either a continuous ridge of bone or several segments, as long as 1 cm of an elevated border is present. The rim's crest can be low and rounded, or narrow and sharp. A ventral rim is always formed on top of a ventral rampart. Odd rim-like bone formations on gaps in a rampart or formed with no rampart at all are *not* scored as a ventral rim.

7. Breakdown: The ventral margin of the symphyseal face has begun to break down, as indicated by pitting and an erosion of the Rim. The breakdown of the ventral margin must exceed 1 cm (either in one spot, or when two or more areas of erosion are combined) to be scored as present. Care must be taken to distinguish antemortem degeneration – that is, true Breakdown – from postmortem damage. The latter, of course, can render the bone unscorable if it is extensive enough.

⁶ The gap in the ventral margin that occurs in some individuals was noted by McKern and Stewart (1957: 77, Fig. 40), who called it the “ventral hiatus.” Gaps, when present, usually occur in the superior half of the pubic symphysis. In most instances, they are readily distinguishable from incomplete rampart formation because the remainder of the ventral rampart appears complete. That is, the ventral margin elsewhere has a rounded to angular edge, an anterior sulcus is typically absent, and a rim might have developed on the part of the rampart that is present. In addition, the symphyseal surface extends uninterrupted from the dorsal to ventral margins, and it is often flat. The appearance of the symphyseal face contrasts sharply with what is present in the typical Rampart Incomplete stage. In the earlier Rampart Incomplete stage, a shallow depression is often present immediately dorsal to the newly formed and still rather narrow rampart, and much of the rest of the symphyseal face is marked by remnants of the original ridges and furrows.⁵ It is our impression that the Rampart Complete I variant – the one with the narrow ventrally located sulcus immediately lateral to the ventral symphyseal margin – is more commonly found on Native American skeletons than on medieval and modern Europeans. But even in Native American skeletons, it is not often encountered.

Dorsal Symphyseal Margin

Location

The dorsal part of the pubic symphysis is scored separately from the ventral margin. In females, dorsally located characteristics can be partly or entirely obscured by large postpartum, or parity, pits. Occasionally, such specimens cannot be scored properly.

Characteristics

1. Serrated
2. Flattening incomplete
3. Flattening complete
4. Rim
5. Breakdown

Definitions

1. Serrated: The dorsal margin of the symphyseal face is irregular because ridges and furrows typical of pronounced billowing extend uninterrupted to the edge of the bone.

2. Flattening incomplete: A well-defined flattened area at least 1 cm long is present where the symphyseal face meets the dorsal margin.

Flattening usually starts in the superior part of the dorsal demiface. Billowing is also present on the dorsal demiface, and it typically produces an undulating edge to the pubic symphysis, although it is not as extreme as what is found in Serrated specimens. The undulating edge usually occurs in the inferior part of the symphyseal face.

3. Flattening complete: There is a rather obvious area of flattening that completely (or almost entirely) covers the symphyseal face where it meets the dorsal margin. This flattening seemingly occurs partly through a coalescence of billows. A small area at the inferior end of the dorsal margin occasionally retains an undulating appearance.

4. Rim: An elevated bony rim demarcates a flat or, infrequently, an irregular face. The rim projects slightly above the symphyseal face, and its crest can be blunt or sharp. The rim does not have to extend along the entire dorsal margin to be scored as present, but it must be at least 1 cm long. The 1 cm rule pertains to either a continuous rim or discontinuous segments that together sum to that length. A rim typically develops first along the superior part of the dorsal margin. It can, however, occur anywhere along the dorsal margin.

5. Breakdown: The dorsal margin where the Rim is located shows evidence of breakdown, specifically a pitting and erosion of the edge of the pubic symphysis. The breakdown must exceed 1 cm in length either in one spot or when two or more areas of erosion are combined. Care must be taken to differentiate antemortem degeneration of the margin from postmortem damage, which is of no concern. Antemortem destruction attributable to large parity pits in females that can undercut the

dorsal margin is not considered breakdown in the sense of the term as used here. It might not be possible to score those specimens; when that occurs, the component is simply missing data.

Sacroiliac Joint

Four aspects of the sacroiliac joint area on the ilium are examined: the entire surface topography; surface morphology; surface texture; and marginal bony proliferation (exostoses on the posterior ilium facing the sacrum). Anatomical features and terms follow those of Lovejoy and colleagues (1985) where possible. Different parts of the joint (auricular) surface are scored for the same morphological features because bony changes do not change in lockstep in all places.

Superior Demiface Topography

Location

The superior demiface is examined. The two demifaces are divided by a line extending posteriorly from the most anterior point of the apex to the posterior joint margin.

Characteristics

1. Undulating
2. Median elevation
3. Flat to Irregular

Definitions

1. Undulating: The surface is undulating, particularly in a superior to inferior direction. There is no centrally located and linear area of elevated bone (Median Elevation). When the entire articulation surface is viewed in aggregate, the overall effect is of two or three low waves proceeding lengthwise along the joint.

2. Median elevation: In the middle to posterior part of the demiface there is a broad raised area where the joint surface is elevated slightly above the rest of the joint. The elevation is flanked anteriorly, posteriorly, or both by one or two long low areas. The elevated area takes the form of an elongated ridge with the long axis paralleling the main orientation of the demiface. Occasionally the elevated area is restricted to a noticeable raised area, especially in the inferior portion of the superior demiface. The elevated area occupies as much as one-third of the joint surface.

3. Flat to irregular: The surface is essentially flat or recessed, a result of marginal lipping, or it is irregular from degeneration of the joint or the formation of low pillow-like exostoses.

Inferior Demiface Topography

Location

The inferior demiface is examined. The superior and inferior demifaces are divided by a line extending posteriorly from the most anterior point of the apex to the posterior border of the joint.

Characteristics

1. Undulating
2. Median elevation
3. Flat to Irregular

Definitions

1. Undulating: The surface is undulating, particularly in a superior to inferior direction. There is no centrally located area of elevated bone (Median Elevation). When the entire articulation surface is viewed in aggregate, the overall effect is of two or three low waves proceeding lengthwise along the joint.

2. Median elevation: In the middle to posterior part of the demiface there is a broad raised area where the joint surface is elevated slightly above the rest of the joint. The elevation is flanked anteriorly, posteriorly, or both by one or two long low areas. The elevated area takes the form of an elongated ridge – it is particularly apparent in the inferior demiface, in contrast with the superior one – with the long axis paralleling the main orientation of the demiface. The ridge occupies as much as one-third of the joint surface.

3. Flat to irregular: The surface is essentially flat or recessed, a result of marginal lipping, or it is irregular, from degeneration of the joint or the formation of low pillow-like exostoses.

Superior Surface Morphology

Location

The superior part of the face is examined. The joint surface is divided into superior, apical (middle), and inferior segments.

Characteristics

1. >2/3 covered by billows
2. 1/3-2/3 covered by billows
3. <1/3 covered by billows

4. Flat (no billows)
5. Bumps

Definitions

1. *Billows cover >2/3 of the surface*: Low rounded ridges separated by furrows, which have distinctly rounded bases, are clearly identifiable. The ridge surfaces are curved from the depths of the furrows completely across their crests. Most or all of the billowing is oriented roughly anterior to posterior, and furrows generally run across much, or all, of the face. Billowing covers most (>2/3) of the joint surface (i.e., it is a dominant element of the surface).

2. *Billows cover 1/3-2/3 of the surface*: About one-half of the surface is covered by billows.

3. *Billows cover <1/3 of the surface*: Billows are a noticeable, but minor, component of the joint surface. The rest of the surface is flat or bumpy.

4. *Flat (no billows)*: The joint surface is flat.

5. *Bumps*: Most, or all, of the joint surface is covered by low, rounded bony exostoses, much like little irregular pillows. Part of the surface may be flat, but over one-half of it is bumpy.

Unscorable: If pitting is so extensive it obscures much of the face, the joint surface is considered unscorable.

Apical Surface Morphology

Location

The apical (middle) part of the face is examined. The joint surface is divided into the superior, apical (middle), and inferior segments.

Characteristics

1. >2/3 covered by billows
2. 1/3-2/3 covered by billows
3. <1/3 covered by billows
4. Flat (no billows)
5. Bumps

Definitions

1. *Billows cover >2/3 of the surface*: Low rounded ridges separated by furrows, which have distinctly rounded bases, are clearly identifiable. The ridge surfaces are curved from the depths of the furrows completely across their crests. Most or all of the billowing is oriented roughly anterior to posterior, and furrows generally run across much, or all, of the face. Billowing covers most (>2/3) of the joint surface (i.e., it is a dominant element of the surface).

2. *Billows cover 1/3-2/3 of the surface*: About one-half of the surface is covered by billows.

3. *Billows cover <1/3 of the surface*: Billows are a noticeable, but minor, component of the joint surface. The rest of the surface is flat or bumpy.

4. *Flat (no billows)*: The joint surface is flat.

5. *Bumps*: Most, or all, of the joint surface is covered by low, rounded bony exostoses, much like little irregular pillows. Part of the surface may be flat, but over one-half of it is bumpy.

Unscorable: If pitting is so extensive it obscures much of the face, the joint surface is considered unscorable.

Inferior Surface Morphology

Location

The inferior part of the face is examined. The joint surface is divided into the superior, apical (middle), and inferior segments.

Characteristics

1. >2/3 covered by billows
2. 1/3-2/3 covered by billows
3. <1/3 covered by billows
4. Flat (no billows)
5. Bumps

Definitions

1. *Billows cover >2/3 of the surface*: Low rounded ridges separated by furrows, which have distinctly rounded bases, are clearly identifiable. The ridge surfaces are curved from the depths of the furrows completely across their crests. Most or all of the billowing is oriented roughly anterior to posterior, and

furrows generally run across much, or all, of the face. Billowing covers most ($>2/3$) of the joint surface (i.e., it is a dominant element of the surface).

2. *Billows cover 1/3-2/3 of the surface*: About one-half of the surface is covered by billows.

3. *Billows cover $<1/3$ of the surface*: Billows are a noticeable, but minor, component of the joint surface. The rest of the surface is flat or bumpy.

4. *Flat (no billows)*: The joint surface is flat.

5. *Bumps*: Most, or all, of the joint surface is covered by low, rounded bony exostoses, much like little irregular pillows. Part of the surface may be flat, but over one-half of it is bumpy.

Unscorable: If pitting is so extensive it obscures much of the face, the joint surface is considered unscorable.

Inferior Surface Texture

Location

Only one part of the joint surface – the inferior area – is scored for texture. This part of the joint is 1 cm long, as measured in a superior to inferior direction. Its lowermost point is a line defined by the margin of the greater sciatic notch on either side of the joint surface. Do not score the part that can extend well beyond the margin of the notch as defined above. Elongated joint surfaces commonly occur in females, and they are often characterized by macroporosity and marginal lipping. The pitting and lipping in these skeletons frequently differs markedly from the appearance of the rest of the joint.

Characteristics

1. Smooth
2. Microporosity
3. Macroporosity

Definitions

1. *Smooth*: Most, or all, of the joint surface appears to be smooth to slightly granular.

2. *Microporosity*: At least one-half of the surface has a porous appearance with apertures less than 0.5 mm in diameter. The symphyseal face looks as if it is covered by many closely spaced pinpricks.

3. *Macroporosity*: At least one-half of the surface is porous, with most, or all, of the apertures exceeding 0.5 mm in diameter.

Superior Posterior Iliac Exostoses

Location

Superior posterior iliac exostoses are scored. This area refers to the superior part of the medial surface of the posterior ilium where ligaments attach. It is located superior to the sacroiliac joint surface; that is, to a line that passes from the anterior superior iliac spine, to the most superior point of the joint surface (the superior angle), and on through the posterior part of the ilium. In some individuals, the bone is distinctly raised in this area. So care must be taken to differentiate jagged (or high) exostoses from rounded or pointed ones perched on top of a raised elevation of bone.

Characteristics

1. Smooth
2. Rounded bony elevations
3. Pointed exostoses
4. Jagged exostoses
5. Touching exostoses
6. Fusion

Definitions

1. *Smooth*: The surface is often elevated in this area, but shows no evidence of discrete bony elevations. At most there are a few isolated small exostoses projecting from the bone surface.

2. *Rounded bony elevations*: Definite raised areas of bone with rounded crests dominate the scoring area.

3. *Pointed exostoses*: Over one-half of the rough area where ligaments attach is dominated by sharply pointed elevations of bone.

4. *Jagged exostoses*: The raised areas of bone have a jagged appearance, and round or sharp exostoses dominate the rough area where ligaments attach in life.

5. *Touching exostoses*: There is a pronounced growth of bone with a relatively flat top, usually roughly oval, where exostoses touch the sacrum.

6. *Fusion*: The ilium and sacrum are fused by exostoses in this area.

Inferior Posterior Iliac Exostoses

Location

The inferior posterior iliac exostoses are scored. This area refers to the inferior part of the medial surface of the posterior ilium where ligaments attach. It is located inferior to a line that passes from the anterior superior iliac spine, to the most superior point of the sacroiliac joint surface (the superior angle), and on through the posterior part of the ilium. This area is located immediately posterior to the middle of the sacroiliac joint; that is, it lies behind the most anteriorly projecting part of the posterior margin of the joint. In some individuals, the bone is distinctly raised in this area. So care must be taken to differentiate jagged (or high) exostoses from rounded or pointed ones perched on top of a raised elevation of bone.

Characteristics

1. Smooth
2. Rounded bony elevations
3. Pointed exostoses
4. Jagged exostoses
5. Touching exostoses
6. Fusion

Definitions

1. *Smooth*: The surface is often elevated in this area, but shows no evidence of discrete bony elevations. At most there are a few isolated small exostoses projecting from the bone surface.

2. *Rounded bony elevations*: Definite raised areas of bone with rounded crests dominate the scoring area.

3. *Pointed exostoses*: Over one-half of the rough area where ligaments attach is dominated by sharply pointed elevations of bone.

4. *Jagged exostoses*: The raised areas of bone have a jagged appearance, and round or sharp exostoses dominate the rough area where ligaments attach in life.

5. *Touching exostoses*: There is a pronounced growth of bone with a relatively flat top, usually roughly oval, where exostoses touch the sacrum.

6. *Fusion*: The ilium and sacrum are fused by exostoses in this area.

Posterior Exostoses

Location

The posterior iliac area between the Superior and Inferior Posterior Iliac Exostoses, as defined above, are scored. The area where the exostoses occur is on the medial side of the ilium bordered posteriorly by the iliac crest, anteriorly by the sacroiliac joint surface, superiorly by a slightly raised area often surmounted by bony exostoses (Superior Posterior Iliac Exostoses), and inferiorly by a similar area (Inferior Posterior Iliac Exostoses). Most individuals are Smooth as defined below. The feature is best considered an old-age trait.

Characteristics

1. Smooth (no exostoses)
2. Rounded exostoses
3. Pointed exostoses

Definitions

1. Smooth: The area posterior to the sacroiliac joint is smooth, except for the two areas scored separately as Superior and Inferior Posterior Iliac Exostoses.

2. Rounded exostoses: Low, rounded exostoses (or spicules) cover the *entire* bone surface posterior to the sacroiliac joint, except for a ca. 0.5 cm band of smooth bone immediately adjacent to the posterior edge of the joint. The exostoses are normally lower than the Superior and Inferior Posterior Iliac Exostoses. The low exostoses give the normally smooth iliac surface a rough appearance. It looks as if the surface is covered by coarse (construction) sand.

3. Pointed exostoses: Low, pointed exostoses (or spicules) cover the *entire* bone surface posterior to the sacroiliac joint, except for a ca. 0.5 cm band of smooth bone immediately adjacent to the posterior edge of the joint. The exostoses are normally lower than the Superior and Inferior Posterior Iliac Exostoses. The sharp exostoses give the normally smooth iliac surface a rough appearance. It looks as if the surface is covered by coarse (construction) sand.

Cranial Sutures

The suture closure scores are similar to what osteologists have used for over a century. As far as the vault is concerned, ectocranial suture closure is recorded because it is often difficult to examine the interiors of archaeological crania, which can be dirty. Suture segment names conform to those commonly used by osteologists. Palatal sutures are included largely because they have been shown to be of some use in age estimation, even though they are often damaged (Mann et al. 1987). For sake of completeness, it is a good practice to record the closure of both the left and right coronal, lambdoidal, and zygomaticomaxillary sutures, if present.

Coronal Suture

Location

Score the most inferior section of the coronal suture, a relatively straight part without a meandering appearance.

Characteristics

1. Open
2. Juxtaposed
3. Partially obliterated
4. Punctuated
5. Obliterated

Definitions

1. *Open*: The suture is visible along its entire length, and there is a noticeable gap between the bones.

2. *Juxtaposed*: The suture is visible along its entire length, but the suture is narrow because the bones are tightly juxtaposed. If there are any bony bridges they are rare and small, sometimes with a trace of the original suture still evident.

3. *Partially obliterated*: The suture is partially obscured. There is no trace of the original suture in the bony bridges.

4. *Punctuated*: Only remnants of the suture are present. They appear as scattered small points or grooves each no more than two millimeters long.

5. *Obliterated*: There is no evidence of a suture.

Sagittal Suture

Location

Score the relatively straight part of the posterior sagittal suture near the parietal foramina.

Characteristics

1. Open
2. Juxtaposed
3. Partially obliterated
4. Punctuated
5. Obliterated

Definitions

1. *Open*: The suture is visible along its entire length, and there is a noticeable gap between the bones.

2. *Juxtaposed*: The suture is visible along its entire length, but the suture is narrow because the bones are tightly juxtaposed. If there are any bony bridges they are rare and small, sometimes with a trace of the original suture still evident.

3. *Partially obliterated*: The suture is partially obscured. There is no trace of the original suture in the bony bridges.

4. *Punctuated*: Only remnants of the suture are present. They appear as scattered small points or grooves each no more than two millimetres long.

5. *Obliterated*: There is no evidence of a suture.

Lambdoidal Asterica

Location

The most inferior part of the lambdoidal suture is scored. It is adjacent to asterion, and extends about one-quarter of the way up to lambda.

Characteristics

1. Open
2. Juxtaposed
3. Partially obliterated
4. Punctuated
5. Obliterated

Definitions

1. *Open*: The suture is visible along its entire length, and there is a noticeable gap between the bones.
2. *Juxtaposed*: The suture is visible along its entire length, but the suture is narrow because the bones are tightly juxtaposed. If there are any bony bridges they are rare and small, sometimes with a trace of the original suture still evident.
3. *Partially obliterated*: The suture is partially obscured. There is no trace of the original suture in the bony bridges.
4. *Punctuated*: Only remnants of the suture are present. They appear as scattered small points or grooves each no more than two millimeters long.
5. *Obliterated*: There is no evidence of a suture.

Zygomaticomaxillary

Location

The facial, or anterior, part of the zygomaticomaxillary suture is scored.

Characteristics

1. Open
2. Juxtaposed
3. Partially obliterated
4. Punctuated
5. Obliterated

Definitions

1. *Open*: The suture is visible along its entire length, and there is a noticeable gap between the bones.
2. *Juxtaposed*: The suture is visible along its entire length, but the suture is narrow because the bones are tightly juxtaposed. If there are any bony bridges they are rare and small, sometimes with a trace of the original suture still evident.
3. *Partially obliterated*: The suture is partially obscured. There is no trace of the original suture in the bony bridges.

4. *Punctuated*: Only remnants of the suture are present. They appear as scattered small points or grooves each no more than two millimeters long.

5. *Obliterated*: There is no evidence of a suture.

Interpalatine (Median Palatine, Posterior Portion)

Location

The suture located between the two opposing palatine bones is of interest. The Open (1) and Juxtaposed (2) distinction is not important here because it is difficult to impossible to differentiate the two categories consistently. Note that to keep scoring consistent across all sutures, the Juxtaposed (2) category is simply eliminated. A small bony crest that often forms along the midline of the palate can make it difficult to record the extent of suture closure. In other specimens, the suture is barely visible in the depths of a deep and narrow groove. Both the ridge and groove make it hard or impossible to score the suture.

Characteristics

1. Open (open and juxtaposed)
3. Partially obliterated
4. Punctuated
5. Obliterated

Definitions:

1. *Open (and juxtaposed)*: The suture is visible along its entire length, and there is a noticeable gap between the bones.

3. *Partially obliterated*: The suture is partially obscured. There is no trace of the original suture in the bony bridges.

4. *Punctuated*: Only remnants of the suture are present. They appear as scattered small points or grooves each no more than two millimeters long.

5. *Obliterated*: There is no evidence of a suture.

References

Boldsen JL, Milner GR, Konigsberg LW, Wood JW

2002 Transition Analysis: A New Method for Estimating Age from Skeletons. In *Paleodemography: Age Distributions from Skeletal Samples*. Hoppa RD and Vaupel JW (eds), pp. 73-106. Cambridge University Press, Cambridge.

Lovejoy CO, Meindl RS, Pryzbeck TR, Mensforth RP

1985 Chronological Metamorphosis of the Auricular Surface of the Ilium: A New Method for the Determination of Adult Skeletal Age at Death. *American Journal of Physical Anthropology* 68:15-28.

Mann RW, Symes SA, Bass WM

1987 Maxillary Suture Obliteration: Aging the Human Skeleton Based on Intact or Fragmentary Maxilla. *Journal of Forensic Sciences* 32:148-157.

McKern TW, Stewart TD

1957 *Skeletal Age Changes in Young American Males*. Technical Report EP-45. Quartermaster Research and Development Center, US Army, Natick, Massachusetts.

Appendix B

Project: _____

Site or Collection: _____ Skeleton: _____

Sex: _____ Age: ____/____/____ Height: _____ Weight: ____/____/____

Cranial Sutures	Left	Right
Coronal Pterica	- 1 2 3 4 5	- 1 2 3 4 5
Sagittal Obelica (midline)	- 1 2 3 4 5	
Lambdoidal Asterica	- 1 2 3 4 5	- 1 2 3 4 5
Interpalatine (midline)	- 1 3 4 5	
Zygomaticomaxillary	- 1 2 3 4 5	- 1 2 3 4 5

Pubic Symphysals	Left	Right
Symphyseal Relief	- 1 2 3 4 5 6	- 1 2 3 4 5 6
Symphyseal Texture	- 1 2 3 4	- 1 2 3 4
Superior Apex	- 1 2 3 4	- 1 2 3 4
Ventral Symphyseal Margin	- 1 2 3 4 5 6 7	- 1 2 3 4 5 6 7
Dorsal Symphyseal Margin	- 1 2 3 4 5	- 1 2 3 4 5

Iliac Auricular Surface	Left	Right
Superior Demiface Topography	- 1 2 3	- 1 2 3
Inferior Demiface Topography	- 1 2 3	- 1 2 3
Superior Surface Morphology	- 1 2 3 4 5	- 1 2 3 4 5
Middle Surface Morphology	- 1 2 3 4 5	- 1 2 3 4 5
Inferior Surface Morphology	- 1 2 3 4 5	- 1 2 3 4 5
Inferior Surface Texture	- 1 2 3	- 1 2 3
Superior Posterior Iliac Exostoses	- 1 2 3 4 5 6	- 1 2 3 4 5 6
Inferior Posterior Iliac Exostoses	- 1 2 3 4 5 6	- 1 2 3 4 5 6
Posterior Exostoses	- 1 2 3	- 1 2 3

Codes: - (Missing or Not Observable), 1-7 (defined in Transition Analysis manual)
